Boundary symmetries and strong coupling dualities

Oling, G.W.J.

BOUNDARY SYMMETRIES AND STRONG COUPLING DUALITIES

Gerben Oling

Boundary Symmetries
and Strong Coupling Dualities

NW𝒲O | Institutes

Cover: absolute value of the $43^{\rm rd}$ and the $47^{\rm th}$ eigenfunctions of the Laplacian on a disk with Dirichlet boundary conditions. Layout by Naomi Nota.

Boundary Symmetries
and Strong Coupling Dualities

ACADEMISCH PROEFSCHRIFT

ter verkrijging van de graad van doctor

aan de Universiteit van Amsterdam

op gezag van de Rector Magnificus

prof. dr. ir. K.I.J. Maex

ten overstaan van een door het College voor Promoties ingestelde commissie,

in het openbaar te verdedigen in de Agnietenkapel

op dinsdag 2 oktober 2018, te 12:00 uur

door

Gerben Wilhelmus Jacobus Oling

geboren te Velsen

Promotiecommissie

Promotor:	prof. dr. E.P. Verlinde	Universiteit van Amsterdam
Copromotor:	dr. D.M. Hofman	Universiteit van Amsterdam
Overige leden:	prof. dr. J. de Boer	Universiteit van Amsterdam
	dr. A. Castro Anich	Universiteit van Amsterdam
	dr. C.N. Cheng	Universiteit van Amsterdam
	prof. dr. N.A.J. Obers	University of Copenhagen
	prof. dr. S.J.G. Vandoren	Universiteit Utrecht

Faculteit der Natuurwetenschappen, Wiskunde en Informatica

Preface

This thesis presents part of the research I conducted over the last four years at the Institute for Theoretical Physics of the University of Amsterdam, which resulted in the publications listed on page iii. A large part of theoretical physics is inherently collaborative, and all my research was done in the context of collaborations. For this reason, all but a few pages of this thesis are written using the pronoun 'we' to do justice to the involvement and the influence of others. (Apart from this preface, the only exception to this rule is page iii, where I outline my individual contributions to the publications on which this thesis is based.)

My research focuses on dualities that arise from string theory. To motivate the utility of these dualities and to illustrate their context, I first give a general introduction in Chapter 1. Section 1.1 is presented at a level that should be accessible to the interested lay reader. Here, I first illustrate the overwhelming success of the perturbative approach to quantum field theory by means of the computation of the magnetic moment of the electron. I then motivate the study of nonperturbative and strong coupling effects using dualities. Starting from Section 1.2, the technical level of the discussion increases gradually. The rest of Chapter 1 introduces the holographic principle, its realization in the AdS/CFT correspondence and several elements of the AdS/CFT dictionary. I also motivate the importance of nonperturbative effects using a simple quantum-mechanical model and explain the idea behind electromagnetic duality in gauge theory. Finally, in Section 1.6, I give an overview of the other chapters of this thesis, and explain how they are related to the introduction.

A large part of my research is related to boundary symmetries. Chapter 2 gives a detailed introduction to this topic. There, I first introduce the Chern-Simons formulation of three-dimensional gravity. After analyzing its boundary symmetries, I explain how Drinfeld–Sokolov reduction leads to interesting asymptotic symmetry algebras. The techniques introduced in Chapter 2 are used extensively in Chapter 3 and are an important part of the motivation underlying Chapter 4. To give a coherent presentation of these techniques, I have incorporated parts of the publications on which Chapters 3 and 4 are based in Chapter 2. Finally, Chapter 5 presents an investigation of the evolution of entanglement entropy following a quantum quench using the AdS/CFT dictionary. This thesis concludes with a technical summary and outlook in English on page 145 and a non-technical summary in Dutch on page 171.

List of publications

Here I list the publications on which this thesis is based and describe my personal contributions to them. All publications arose out of collaborations with others, and the intellectual work underlying them as well as the actual writing was very much a joint effort. Note that authors are sorted alphabetically in theoretical high-energy physics, so the order in which they appear does not necessarily reflect the extent of their contribution to the publication.

[1] **Chapter 3:** *Zooming in on AdS_3/CFT_2 near a BPS bound*,
J. Hartong, Y. Lei, N. A. Obers and G. Oling,
JHEP **05** (2018) 016, [`1712.05794`].

Responsible for the Drinfeld–Sokolov approach to the asymptotic symmetry algebra and the invariant current perspective on its contraction. Different forms of the algebra contraction were proposed by all members of the collaboration, but I worked out the sl_2 form which is presented in the publication. Wrote the majority of Sections 3.2.1, 3.3.1 and 3.4 as well as the appendices, which have been absorbed in Chapter 2 here.

[2] **Chapter 4:** *Generalized Toda theory from six dimensions and the conifold*,
S. van Leuven and G. Oling,
JHEP **12** (2017) 050, [`1708.07840`].

Suggested looking at general $sl_2 \subset sl_N$ embeddings in the context of the AGT correspondence. Worked out the geometry of the generalized conifold. Made all illustrations and wrote the majority of Sections 4.1.1, 4.2.2 (mostly moved to Section 2.5.2 here), 4.3.2 and Appendix 4.A. Section 4.4, which is the core of the publication, was a joint effort. Wrote up the majority of Section 4.4.2.

[3] **Chapter 5:** *Linear response of entanglement entropy from holography*,
S. F. Lokhande, G. W. J. Oling and J. F. Pedraza,
JHEP **10** (2017) 104, [`1705.10324`].

Performed many of the analytic and *Mathematica* computations, made plots and illustrations. Worked out the linear and periodic quench examples, wrote a previous version of the draft, parts of the conclusion and the majority of Section 5.3.3. Contributed to all conceptual discussions.

Contents

Chapter 1

Introduction

The research presented in this thesis investigates dualities that arise from string theory. This chapter introduces a selection of the ideas that led to these dualities and explores several of their features.

We start off gently in Section 1.1 by introducing perturbative expansions in quantum field theory. Using the famous calculation of the anomalous magnetic moment of the electron as an example, we point out two possible problems with perturbation theory: strong coupling and nonperturbative phenomena.

The first problem motivates the idea of dualities. In Section 1.2, we introduce the holographic principle and explain how it is realized by the AdS/CFT correspondence. The second problem leads us to instantons and magnetic monopoles in Section 1.3. We then use these nonperturbative objects to describe electromagnetic duality. Next, we demonstrate several entries in the AdS/CFT dictionary in more detail. We study symmetries in Section 1.4, where the three-dimensional case gets particular emphasis. Section 1.5 then introduces correlators, Wilson loops and entanglement entropy as probes of holography. Finally, in Section 1.6, we summarize the remaining chapters and explain their relation to this introduction.

1.1 The trouble with perturbation theory

In everyday life, objects move in a very definite way. When you play a game of pool, the balls will move along the exact same trajectory every time you hit them at the same angle and with the same force. The same is true for larger objects: this way, we can predict when the sun will rise and when it will set.

In fact, already hundreds of years ago, scientists have developed models of gravity that allow us to predict the motion of the planets in our solar system in great detail. They have been continuously improved. Our current understanding of gravity was developed by Einstein and is known as *general relativity*. It allows us to describe many aspects of our universe at *large* scales, including the formations of galaxies and even the beginning of time itself at the Big Bang. For all these diverse processes, general relativity allows us to make very definite predictions.

On the other hand, one of the great surprises of 20th century physics has been that smaller objects, such as molecules and atoms, move in a rather different way. *Quantum* physics tells us that such objects can actually be found along *all* trajectories, and it associates a certain probability to every possible outcome. Quantum physics has proven to be an extremely accurate description of a particular part of our universe. While general relativity focuses on large scales, quantum physics allows us to describe the physics of *small* scales. The fundamental insights it provides have been essential in developing many new technologies such as lasers, atom clocks and the microprocessors used in computers.

Although general relativity and quantum physics describe rather different aspects of our universe, they should ultimately be two different sides of the same coin. *String theory* allows us to describe both general relativity and quantum mechanics in a consistent way. As the name suggests, it describes particles and gravity in terms of vibrations of a string. Although many aspects of string theory remain to be understood, it has suggested some remarkable and unexpected connections between quantum physics and gravity.

This thesis consists of several attempts to extend, understand and apply such connections, which are also known as *dualities*. In the remainder of this section, we will motivate two such dualities from the point of view of quantum physics. Starting from Section 1.2, the discussion will gradually become more technical. An accessible lay summary (in Dutch) is provided on page 171.

When we study the motion of relatively large objects, such as those involved in a game of pool or in our solar system, one trajectory dominates overwhelmingly and reproduces the definite motion we are used to. However, as one approaches the length scales of atoms, quantum physics tells us that we also need to take other trajectories into account. To illustrate this, let us look at the motion of an electron, as depicted in Figure 1.1.

$$e^- \longrightarrow e^-$$

Figure 1.1: An electron e^- moving through space and time.

In quantum physics, the motion of an electron is described by a *wave*, whose frequency is determined by the mass of the electron. Such waves can *interact*, and these interactions manifest themselves as *forces* in our everyday world. For example, the electric force is modeled by the interaction of the electron with a *photon*, which is depicted in Figure 1.2a. There, a photon (wavy line) is absorbed by the electron (straight line) as it moves forward in time. The strength of this force is parametrized by the charge e of the electron.

In fact, the process in Figure 1.2a corresponds to a particular physical effect: it measures the ratio between the electron's intrinsic spin and its magnetic moment. This ratio is often called g, and the process in Figure 1.2a corresponds to $g = 2$. However, this is not the final answer. More complicated trajectories are also possible, such as the one depicted in Figure 1.2b. Following the rules of quantum physics, we should take *both* of the trajectories in Figure 1.2 into account!
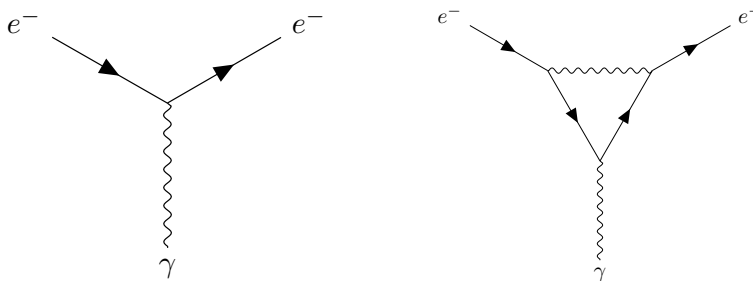
(a) Single interaction with a photon γ. (b) More complicated interaction.

Figure 1.2: Diagrams contributing to the magnetic moment g of the electron.

The trajectory depicted in Figure 1.2b requires two *additional* interactions between the electron and a photon. This means that it should be weighted with a factor of e^2 compared to the trajectory in Figure 1.2a. Conventionally, the weights associated to these diagrams are expressed using what is known as the *fine structure constant*

$$\alpha = \frac{e^2}{4\pi} \approx \frac{1}{137}. \tag{1.1}$$

This dimensionless number quantifies the strength of the interaction between the photon and the electron. Since α is rather small, diagrams with more interactions carry less weight. Concretely, this means that the diagram in Figure 1.2b will modify the result from the diagram in Figure 1.2a, but *only slightly*. In other words, we can compute the answer *perturbatively*, including higher order corrections at each step. The correction associated to the diagram in Figure 1.2b corresponds to the first term in this perturbative result. It was first computed by Schwinger [4,5], who obtained

$$\frac{g-2}{2} = \frac{\alpha}{2\pi} \approx 0.0011614. \tag{1.2}$$

Back in 1948, when Schwinger announced this result, experiments had long shown that g was slightly larger than 2. Explaining this difference was one of the first major successes of quantum field theory.

Of course, more complicated diagrams are also possible. They will come with higher powers of α and correspond to even smaller corrections. Today, seventy years after Schwinger's result, the correction to g is currently known numerically [6] up to α^5:

$$\frac{g-2}{2} = 0.00115965218178(77). \tag{1.3}$$

On the other hand, it has been found experimentally that [7]

$$\frac{g-2}{2} = 0.00115965218073(28). \tag{1.4}$$

Using this iterative method, which is known as *perturbation theory*, quantum field theory allows us to make unfathomably precise predictions. Moreover, these predictions agree wonderfully with experiment!

In practice, performing these computations quickly becomes extremely difficult. For one, the number of diagrams that go into each additional correction grows rapidly: to obtain the most subleading contribution to (1.3), a whopping 12672 diagrams had to be calculated. Needless to say, we will have little to contribute to these results in this thesis. However, apart from its computational difficulty, perturbation theory has several *inherent* shortcomings. We discuss two such shortcomings in the remainder of this section. First, for some problems, there are no small coupling constants that we can use to iterate our way to an answer. Second, even if a perturbative expansion is possible, it may not tell us about several important effects. This thesis is an attempt to expand and apply several ideas that have been raised to tackle these problems.

1.1.1 Strong coupling and duality

The first problem with perturbation theory comes from the fact that most coupling constants, such as α, are in fact *not* constant. Rather, their value depends on the energy scale at which we perform our experiments. In our previous example, this energy scale could be set by the total energy contained in the mass and the momentum of the electron in Figure 1.2. If the momentum of the electron is small compared to its mass, the value of the coupling constant in equation (1.1) is approximately correct. If we increase the energy scale μ of the experiment, for example by accelerating the electron, it turns out that the value of the coupling constant increases as well. This is illustrated in Figure 1.3a.

In some theories, a coupling constant that is initially small may increase to be much larger than one. At that point, we say that the theory is *strongly coupled.* Since higher powers of the coupling constant then contribute *more*, we cannot obtain useful results using perturbation theory. This is not a very pressing problem when we are studying the magnetic moment of the electron since α is small at all reasonable energy scales, and we can still use our perturbative methods. On the other hand, the situation is much worse for the nuclear force, where the coupling constant is *large* at low energies and small at high energies, as in Figure 1.3b.

(a) Electromagnetic coupling α (b) Nuclear force coupling g_{YM}
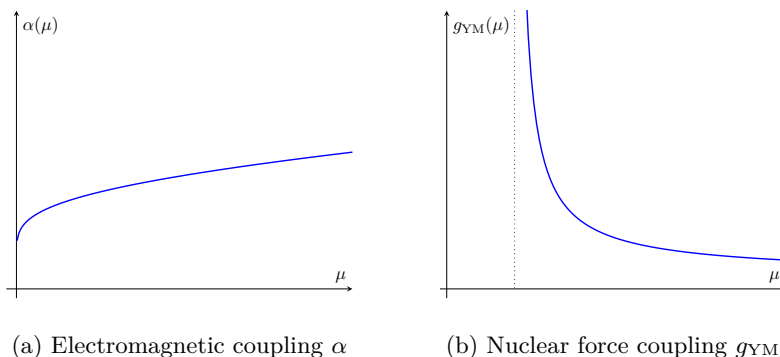
Figure 1.3: Coupling constants as a function of energy μ.

This phenomenon is known as *asymptotic freedom* and was discovered by Gross, Wilczek and Politzer [8,9]. It is one of the reasons that the Large Hadron Collider exists: we need to collide nucleons with high energy to enter a regime where they are no longer bound together, so that we can test our perturbative computations. However, although this program has been very successful, these high-energy perturbative results tell us little about the strong-coupling behavior that determines nuclear physics at low energy.

So what are we to do if we insist on studying the strong-coupling physics of, for example, the nuclear force? We can hope for a miracle. In rare cases, it has been discovered that such strongly-coupled systems have a *dual* description. This dual description may involve completely different physics and, if we're lucky, it can sometimes be easier to solve. Twenty years ago, Maldacena discovered the *AdS/CFT correspondence* [10]. It allows us to describe strongly-coupled quantum field theories in terms of a seemingly unrelated system involving *gravity*. This correspondence is a realization of a more general idea about the nature of quantum gravity, known as the *holographic principle*. We will introduce both in Section 1.2.

1.1.2 Divergence of perturbation expansion

Now let us return to the case of the electron magnetic moment g. Since the fine structure constant is small at reasonable energy scales, we are free to continue doing perturbation theory. Imagine that some day, a brave physicist manages to compute the 1000th order correction to g. Would this be an improvement?

Surprisingly, no! As was first pointed out by Dyson [11], the perturbative expansion in quantum field theory is generally *asymptotic*: at some point, the subsequent corrections become *larger* rather than smaller.

In fact, Dyson gave a good physical argument for why we should have expected this failure. Let's say we're using perturbation theory to compute a quantity $F(\alpha)$ which depends on the value of the coupling constant, such as g. If we're doing a perturbative computation, we expand $F(\alpha)$ around $\alpha = 0$. This can only work if the result also makes sense for small but *negative* values of α. But recall that α quantifies the electric force, so $\alpha < 0$ means that equally charged particles *attract* instead of repel! This would trigger so many instabilities that the question of the electron's magnetic moment would quickly become a very ill-posed one.

That being said, we should emphasize that the divergence of a perturbation expansion is not a failure of physics, but a failure of our *methods*. It means that we are missing essential physical phenomena if we only do perturbation theory. Such phenomena are collectively known as *nonperturbative effects*, and we will illustrate them using a simple model in Section 1.3.

1.2 The holographic principle and AdS/CFT

Einstein's theory of general relativity tells us that gravity can be understood as the curvature of space and time. One of the most intriguing aspects of this
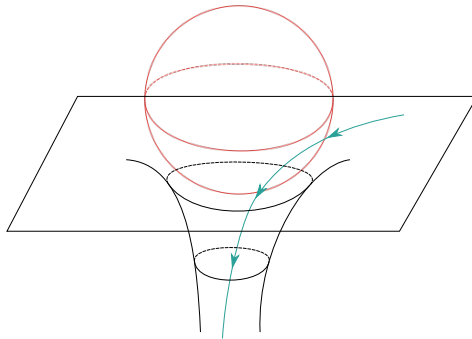
Figure 1.4: Black hole with spherical horizon at $r = r_0$ and infalling observer.

theory is the appearance of *black hole* solutions, such as the four-dimensional Schwarzschild metric:

$$ds^2 = -\left(1 - \frac{2GM}{r}\right) dt^2 + \frac{dr^2}{1 - 2GM/r} + r^2 d\Omega_2^2. \tag{1.5}$$

Here, G is Newton's constant and $d\Omega_2^2$ is the metric on the round two-sphere. The metric in equation (1.5) is a solution of the vacuum Einstein equations: it is purely gravitational and requires no matter to exist. We can still assign a mass M to it, which corresponds to the gravitational pull one would feel at a large distance away from the black hole. The apparent singularity at $r = r_0 = 2GM$ is merely an artifact of the coordinates. However, at that point, the sign of the temporal and radial components of the metric is exchanged. After coming closer than r_0 to a black hole, an ill-fated observer—who has to travel forward in the direction with negative sign—is then forced to move *inward* along the radial direction and can never return to $r > r_0$. Therefore, $r = r_0$ parametrizes what is known as an *event horizon*. This is illustrated in Figure 1.4. For the black hole in (1.5), the event horizon is a sphere of area $A = 4\pi r_0^2 = 16G^2M^2$.

Many beautiful mathematical results are known about the dynamics of black holes in Einstein gravity. For example, Hawking [12] showed that if two black holes merge, their total horizon area is *nondecreasing*:

$$A_{\text{final}} \geq A_{\text{initial}}. \tag{1.6}$$

Bardeen, Carter and Hawking [13] related an infinitesimal change in the mass of a black hole to an infinitesimal change of its area:

$$\delta M = \frac{\kappa}{8\pi} \delta A. \tag{1.7}$$

Here, κ is the surface gravity of the black hole. While we have restricted ourselves to spherically symmetric black holes, similar results still hold if rotating

and charged black holes are included. Remarkably, if one interprets κ as a temperature and A as an entropy, equations (1.7) and (1.6) are similar to the first and second law of thermodynamics, respectively. At first, this appears to be a purely mathematical analogy. Since black holes can exist in a vacuum, there seems to be nothing that can have an actual temperature. However, as pointed out by Bekenstein [14], we are *forced* to take this analogy seriously!

Black holes can be formed by gravitational collapse. If a spherically symmetric matter distribution of total mass M gravitates to be contained within a sphere of radius r_0, it will eventually be described by the metric (1.5). At least on the level of classical physics, all information about the composition of the initial matter distribution is then lost to an outside observer. From $r > r_0$, there is no way to tell if the black hole was formed by the collapse of, say, red bricks or blue balloons. In fact, assuming spacetime is asymptotically flat, Birkhoff's theorem [15] shows that that the Schwarzschild solution is actually the *only* spherically symmetric solution of Einstein gravity.

But then we are in trouble. If only *one* black hole can be formed by such a collapse, the final entropy is *zero*. Since our initial matter shell certainly has nonzero entropy, this appears to be a blatant violation of the second law!

In an effort to resolve such paradoxes, Bekenstein [14] made the radical proposal to take the analogy between black holes and thermodynamics seriously. As suggested by equations (1.6) and (1.7), we can assign an entropy to the black hole *itself*, proportional to its area. Taking this entropy into account, thermodynamics is properly described by the *generalized second law*:

$$d\left(S_{\text{matter}} + S_{\text{BH}}\right) \geq 0. \tag{1.8}$$

Hawking then found that a scalar field that is in a vacuum state near the horizon is actually *at finite temperature* $T_H = \kappa/2\pi$ far away from the black hole. This fixes the constant of proportionality between the black hole entropy and area:

$$\boxed{S_{\text{BH}} = \frac{A}{4G}.} \tag{1.9}$$

This is known as the *Bekenstein-Hawking* entropy of a black hole. This raises one immediate question: If $S = k \log \Omega$ and only a very finite class of black hole solutions exist in gravity, then what does the degeneracy Ω count? Remarkably, for special classes of black holes, string theory can answer this question! As Strominger and Vafa [16] showed, the string theory construction corresponding to these black holes has a degeneracy which precisely reproduces (1.9).

1.2.1 The holographic principle

Although string theory provides a precise interpretation of the black hole degrees of freedom, it only does so for a very limited class of black holes. However, there are good reasons to believe that the idea of associating degrees of freedom to a

horizon holds more generally. This is known as the *holographic principle.* Following the review [17] by Bousso, we now repeat an argument due to Susskind [18] and 't Hooft [19].

Suppose we start with a collection of matter which is contained in a sphere of area A. Assume that it is approximately static, so it does not collapse into a black hole of its own accord. This means that the total energy E of the matter must be less than the mass M of the black hole corresponding to a sphere of area A. If it were equal to or larger than that mass, it would effectively be a black hole already. We can then *force* a collapse by throwing in an additional shell of mass $M - E$. For an outside observer, the result is a black hole of mass M. Since the shell we threw in has nonzero entropy, the generalized second law (1.8) leads to

$$S_{\text{matter}} < S_{\text{matter}} + S_{\text{shell}} \leq S_{\text{BH}} = \frac{A}{4G}. \tag{1.10}$$

This gives us a bound on the entropy of the initial matter in terms of the *area* of a sphere enclosing it. But this is very peculiar! For normal matter, one would expect the entropy to scale like the *volume.* For example, a two-state system on a three-dimensional lattice with spacing a would have approximately $2^{V/a^3}$ degrees of freedom, which would violate the bound (1.10) if the system is large enough. This means that at some point, the degrees of freedom in a theory including gravity behave differently than what we are used to. On the other hand, if we believe (1.10), it is conceivable that a *regular* but *lower-dimensional* description exists! Said differently, at some point the degrees of freedom of a system including gravity become *nonlocal*, but they can then be described by a non-gravitational system on its *boundary.* This is known as the *holographic principle.*

1.2.2 The AdS/CFT correspondence

String theory is a theory of quantum gravity. It *unifies* particle physics and gravity by describing both in terms of excitations of strings. In addition to strings, the theory contains nonperturbative objects known as *D-branes*, which can extend in several dimensions. See Figure 1.5 for a sketch.

Gravity is contained in the excitations of *closed* strings. They feel the presence of D-branes as heavy objects which create a gravitational potential. If one stacks sufficiently many D-branes on top of each other, they can be used to create black holes. It turns out that a large number of D-brane configurations lead to black holes with the same macroscopic properties such as charge and mass. As we mentioned earlier, Strominger and Vafa [16] showed that in certain cases, this degeneracy *agrees exactly* with the horizon area of the corresponding black hole.

In addition to their gravitational interpretation, D-branes play another role in string theory: they are objects on which *open* strings can end. Just like the closed string spectrum contains gravitons, the first excitations of the open string describe Yang–Mills gauge fields—similar to those that appear in the Standard Model. In some cases, these gauge theories are *conformal*: they are insensitive to any change in the metric that preserves angles.
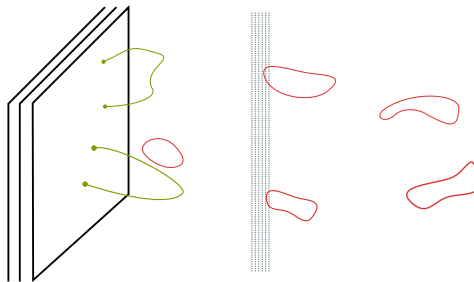
Figure 1.5: D-branes with open and closed strings and a horizon.

Maldacena [10] realized that it is possible to take a particular low-energy limit of this setup which retains nontrivial degrees of freedom from both an open and closed string perspective. First consider closed strings, which see the D-branes as a black hole background. Since the light cone collapses near the horizon, strings moving close to it experience an infinite redshift. In fact, for the *extremal* black holes that D-branes produce, the region of infinite redshift turns out to have infinite volume itself. This region, which is described by an *anti-de Sitter* geometry, is effectively decoupled from the rest of the black hole spacetime. All string excitations on the near-horizon anti-de Sitter (AdS) geometry are of zero energy from the point of view of an outside observer. Thus, the low-energy excitations of closed strings near a large number of D-branes corresponds to closed strings on AdS.

On the other hand, the low-energy excitations of open strings produce a conformal field theory which does *not* contain gravity. If we believe that the low-energy degrees of freedom of the open and closed strings give an equivalent description of the low-energy degrees of freedom of the D-brane system, this implies a relation which is known as the *AdS/CFT correspondence*. It relates a gravitational theory of closed strings on AdS_{d+1} to a non-gravitational conformal field theory (CFT) on a d-dimensional manifold. As such, it provides a concrete realization of the holographic correspondence outlined in Section 1.2.1.

The best-understood incarnation of this correspondence arises from the low-energy limit of N D3 branes. From the point of view of the closed strings, a large number of D3 branes produce a black hole whose horizon stretches along four spacetime dimensions. Its near-horizon geometry is $\mathrm{AdS}_5 \times S^5$. Given the amount of supersymmetry that the D3 branes preserve, their four-dimensional low-energy open string description is fully determined: it is $\mathcal{N} = 4$ supersymmetric $SU(N)$ Yang–Mills theory, which is a CFT. Then the AdS/CFT correspondence states that

$$\text{IIB string theory on } \mathrm{AdS}_5 \times S^5$$
$$\Updownarrow \tag{1.11}$$
$$\text{four-dimensional } \mathcal{N} = 4 \text{ super-Yang–Mills theory.}$$

This is an amazing result. However, although it strokes with our intuition from the holographic principle, it is also confusing. First, these theories are formulated

in different dimensions. Second, their *variables* are at first sight also very different. To make sense of the correspondence between these two seemingly unrelated languages, we need a dictionary to translate between them. Developing and understanding a precise dictionary has been a major effort in string theory since Maldacena first made his discovery. We will only be able to touch upon a small part of the literature, see for example [20–23] for more general reviews.

Parameters of the duality   As a first entry in this dictionary, let us discuss the relation between the various coupling constants involved. The gauge theory has a coupling constant which we denote by g_{YM}. Furthermore, the rank N of the gauge group corresponds to the number of D-branes. As first discovered by 't Hooft [24], it is useful to combine both parameters in a new coupling constant[1]

$$\lambda = g_{\mathrm{YM}}^2 N. \tag{1.12}$$

In the closed string picture, the strings have a length scale l_s and a coupling constant g_s. In addition, the AdS_5 and S^5 spaces have an (equal) radius of curvature, which we will denote by ℓ. The Einstein equation then imposes the relation

$$\ell^4 = 4\pi l_s^4 g_s N = l_s^4 g_{\mathrm{YM}}^2 N. \tag{1.13}$$

For the last equality, we have used the relation between open and closed strings, which prescribes that $4\pi g_s = g_{\mathrm{YM}}^2$. In terms of the 't Hooft parameter (1.12), we can write this as

$$\left(\frac{\ell}{l_s}\right)^4 = \lambda. \tag{1.14}$$

Then sending $N \to \infty$ at fixed $\lambda = 4\pi g_s N$ corresponds to sending the string coupling g_s to zero. This means that the duality is now between

$$\text{classical IIB strings on } \mathrm{AdS}_5 \times S^5$$
$$\Updownarrow \tag{1.15}$$
$$\text{planar } \mathcal{N} = 4 \text{ super-Yang–Mills theory.}$$

This is already much better: now we have some hope of calculation! In field theory, $\lambda \ll 1$ allows us to do perturbation theory, but that comes at the cost of having the string length much larger than the AdS radius, which complicates even classical string computations. One can study this regime using integrability (see [25] for a review) but we will not discuss it here.

On the AdS side, a simpler limit is $\lambda \to \infty$. In that case, the string length is small compared to the AdS radius. In this limit, string theory is well approximated

---

[1]If we send $N \to \infty$ while keeping λ fixed, all gauge theory diagrams that are topologically nontrivial are suppressed: only *planar* diagrams survive. This drastically simplifies the perturbative expansion in the new coupling constant λ. Higher genus diagrams are subleading terms in a $1/N$ expansion.

by classical supergravity. This brings us to perhaps the most frequently used limit of the AdS/CFT correspondence:

$$\text{classical IIB AdS}_5 \times S^5 \text{ supergravity}$$
$$\Updownarrow \tag{1.16}$$
$$\text{planar } \mathcal{N} = 4 \text{ super-Yang–Mills theory at \textit{strong} coupling.}$$

Generalizations So far, we have mainly studied the concrete realization of the AdS/CFT correspondence which arises from the low-energy excitations of N D3 branes. However, it turns out that several aspects of the correspondence hold *independently* of the precise field content of the theories involved. This is especially true in the limit described by (1.16). Therefore, it is generally believed that there exists at least a class of conformal field theories with many degrees of freedom that correspond to a theory involving gravity on an AdS background. Schematically,

$$\text{gravity on AdS}_{d+1}$$
$$\Updownarrow \tag{1.17}$$
$$d\text{-dimensional conformal field theory.}$$

While this may seem like a bold statement, there are several reasons why it should be given some credence. First, both theories have a large amount of symmetries, which can be identified in nontrivial ways. This is especially true if the gravity theory is three-dimensional. We discuss this in Section 1.4. Second, there are several explicit quantities one can compute to strengthen one's belief that the relation (1.17) has a fundamental truth to it. We will review three such computations in Section 1.5.

1.3 Electromagnetic duality

So far, we have mainly discussed the idea of holography and its realization through AdS/CFT. Chapter 4 will be concerned with a different kind of duality, which was discovered by Alday, Gaiotto and Tachikawa [26]. It relates four-dimensional gauge theories to CFTs on two-dimensional surfaces. In this section, we review some basic features of gauge theory to motivate this correspondence. Following up on the second possible failure of perturbation theory we discussed in Section 1.1.2, we first motivate the importance of nonperturbative effects. We give examples in electromagnetism and introduce electromagnetic duality at a classical level, which provides us with a first hint of the appearance of two-dimensional surfaces.

1.3.1 Tunneling and instantons

We start our discussion with the anharmonic oscillator, following the work of Bender and Wu [27]. This is a simple one-dimensional quantum-mechanical system where nonperturbative effects are nonetheless important. Consider the following potential:

$$V(x) = \frac{1}{2}mx^2 + \frac{1}{4!}\lambda x^4. \tag{1.18}$$

At $\lambda = 0$ this is the usual harmonic oscillator, whose ground state energy is $E_0 = 1/2$. We expect that we can express the effect of small but nonzero λ on physical observables such as E_0 in terms of a perturbation expansion:

$$\frac{E(\lambda) - E_0}{E_0} = \sum a_n \lambda^n. \tag{1.19}$$

Instead, Bender and Wu found that for large n, the coefficients a_n grow factorially in n. This means that no matter how small we choose $\lambda > 0$, the expansion (1.19) will diverge!

Therefore, if we steadfastly keep computing higher-order corrections to the ground state energy $E_0(\lambda)$, eventually our prediction will become *worse*. However, the argument by Dyson that we discussed in Section 1.1.2 also applies here: we should not expect the perturbation series to converge in an expansion around $\lambda = 0$, because the physics for $\lambda < 0$ is radically different from that for $\lambda < 0$. This is obvious if we plot the potential (1.18) as in Figure 1.6.

(a) $\lambda > 0$ (b) $\lambda < 0$
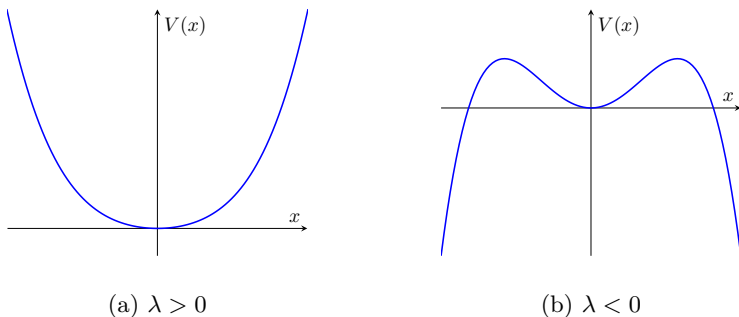
Figure 1.6: The potential $V(x) = \frac{1}{2}mx^2 + \frac{1}{4!}\lambda x^4$ for positive and negative λ.

For small positive λ, the potential merely results in a potential well that is slightly steeper than the unperturbed quadratic potential. In this case, it is reasonable to expect that the resulting ground state energy is not too different. However, for small but negative λ there are no longer even any bound states: a particle can tunnel from $x = 0$ to $x \to \pm\infty$!

This instability can be described using a finite-action solution of the corresponding Euclidean theory. Such configurations are known as *instantons*. The possible instantons can often be classified using topological methods. In this case, the particle can tunnel in two directions, which can be (somewhat pedantically) described using $\pi_0(S^0) \simeq \mathbb{Z}_2$. The topological perspective is especially useful in gauge theory, as we will see shortly.

The divergence of our perturbative expansion signals the presence of these *nonperturbative* phenomena. One can deal with this divergence by properly taking the corresponding instanton solutions of the Euclidean theory into account. See for example [28] for an introduction and a more detailed account of the anharmonic potential.

Instantons in gauge theory More intricate nonperturbative phenomena are possible if we consider gauge fields. At this point, the topological perspective we mentioned before starts to pay off. (For more detail, see for example [29] or [30].) As an example, let us look at the instantons of Euclidean $SU(2)$ Yang–Mills theory on $\mathbb{R}^4$, which is given by the following action:

$$S_{\mathrm{YM}} = - \int_{\mathbb{R}^4} \mathrm{Tr}\, F \wedge \star F. \tag{1.20}$$

Here, the field strength F is a $su(2)$-valued two-form, $\star$ denotes the Hodge dual and Tr denotes a matrix trace which results in a gauge-invariant expression. For the action to be finite, the field strength F should decay fast enough as it approaches the boundary of $\mathbb{R}^4$. That means we can add a point at infinity to compactify the base space to S^4. A sphere can be covered by two patches overlapping around the equator. Gauge bundles over the sphere are then classified by the transition functions between the patches. For S^4, these are maps from the S^3 at the equator to the gauge group. Since $SU(2) \simeq S^3$, this corresponds to

$$\pi_3(S^3) \simeq \mathbb{Z}. \tag{1.21}$$

The corresponding winding number $k \in \mathbb{Z}$ corresponds to the integral of a topological invariant of the gauge bundle, which is known as the *second Chern character*:

$$k = \frac{1}{8\pi^2} \int_{\mathbb{R}^4} \mathrm{Tr}\, F \wedge F. \tag{1.22}$$

For $k > 0$, we can use this to show that the Yang–Mills action has a lower bound:

$$S_{\mathrm{YM}} = -\frac{1}{2} \int_{\mathbb{R}^4} \mathrm{Tr}\left[(F + \star F) \wedge (F + \star F)\right] + \int_{\mathbb{R}^4} \mathrm{Tr}\, F \wedge F \geq 8\pi^2 k \tag{1.23}$$

This bound is attained by connections satisfying

$$\star F = -F. \tag{1.24}$$

By the Bianchi identity, such connections automatically satisfy the equation of motion. They are known as the *anti-self-dual instanton* solutions with instanton number k. (For $k < 0$, the minimal action comes from a solution of $\star F = F$, which is a *self-dual* instanton.)

1.3.2 Magnetic monopoles

There is one other class of nonperturbative objects that we want to introduce. For this, we return to electromagnetism. We can write the electric charge enclosed in a two-sphere as

$$\oint_{S^2} \star F = ne, \quad n \in \mathbb{Z}. \tag{1.25}$$

It is quantized in units of the electron charge e. Although standard electromagnetism does not include sources of magnetic flux, Dirac showed that it is nonetheless possible to write down a gauge potential which describes a *magnetic monopole*:

$$\oint_{S^2} \vec{B} \cdot d\vec{S} = \oint_{S^2} F = 2\pi m g_m, \quad m \in \mathbb{Z}. \tag{1.26}$$

Here, we have introduced a parameter g_m for magnetic charge. In modern language [31], this corresponds to a nontrivial $U(1)$ bundle over S^2. Such bundles are classified by their transition functions $\pi_1(U(1)) \simeq \mathbb{Z}$, which leads to the quantization above. The magnetic charge is also known as the *first Chern number* of the gauge bundle.

For nonabelian gauge theories, solving equations such as (1.24) is a nontrivial task. Luckily, there exists a systematic construction of general self-dual instanton configurations [32]. In Chapter 4, the monopole version of this construction by Nahm [33] for a $su(N)$ gauge theory will be essential. Briefly, Nahm's construction associates a monopole configuration to a $su(2)$ embedding in $su(N)$,

$$[T_i, T_j] = i\epsilon_{ijk}T_k, \qquad T_i \in su(N).$$

These T^i appear as boundary values of auxiliary fields X^i defined on an interval,

$$X^i(\sigma) \to \frac{T^i}{\sigma \pm 1} + \cdots, \quad \sigma \in [-1, 1]. \tag{1.27}$$

From the point of view of the gauge theory, the X^i do not have any obvious physical interpretation. However, it was found by Diaconescu [34] that this construction has an elegant embedding in string theory. The monopoles of four-dimensional $SU(N)$ super-Yang–Mills are given by stable configurations of D1 branes stretched between N D3 branes. Here, the X^i are the scalars of the D1 worldvolume theory, and the T^i prescribe their boundary value at the intersection with the D3 branes.

1.3.3 Electromagnetic duality

Now let us study a single electron of charge e and a magnetic monopole of charge g_m. By demanding that the wave function of an electron is single-valued in the background of a magnetic monopole, Dirac showed that the product of their charges must be an *integer* multiple of 2π. For simplicity, we assume that

$$\frac{e g_m}{2\pi} = 1. \tag{1.28}$$

Now as we can see from (1.25) and (1.26), sending $F \to F' = \star F$ in electromagnetism *exchanges* electric and magnetic charge. Moreover, we see that the electric charge e' after the transformation is given by

$$e' = \oint_{S^2} \star F' = \oint_{S^2} F = 2\pi g_m = \frac{4\pi^2}{e}. \tag{1.29}$$

Here, we have used (1.28) for the last equality. In addition to exchanging electric and magnetic fields, we see that this transformation *inverts* the coupling. Electrically charged particles that are weakly coupled in the original theory become strongly-coupled magnetic monopoles in the transformed theory and vice versa.

For gauge groups of higher rank, one can also add the instanton-counting term $F \wedge F$ from (1.22) to the action, which comes with an additional coupling constant θ. It is then useful to define the complex coupling

$$\tau = \frac{\theta}{2\pi} + \frac{4\pi i}{e^2}.$$ (1.30)

The transformation in (1.29) corresponds to $\tau \mapsto -1/\tau$ at $\theta = 0$. The path integral is also invariant under a shift $\tau \to \tau + 1$. Such transformations exchange electrically and magnetically charged matter and monopole configurations. If the spectrum of a theory happens to be *symmetric* under such an exchange, the theory could be invariant under these transformations. This idea was proposed by Montonen and Olive [35] and is known as *electromagnetic duality*.

Gauge theory labeled by a torus?   Note that these transformations generate $SL(2, \mathbb{Z})$, the group of modular transformations of a torus with complex parameter τ. They identify tori with an equivalent complex structure, just like electromagnetic duality identifies equivalent gauge theory configurations. Therefore, at least on a purely mathematical level, it is possible to say that a gauge theory with electromagnetic duality is *labeled by a torus*.

At this point, such a statement may seem a bit artificial. From the point of view of the four-dimensional theory, this torus would be an external object: perhaps mathematically useful, but with no intrinsic meaning. However, the same could be said of the external fields X^i in Nahm's construction, which turned out to have a physical interpretation in string theory after all.

Remarkably, a similar surprise is in store for this torus. We will return to this topic in Chapter 4, where we study a detailed correspondence involving four-dimensional gauge theories labeled by two-dimensional Riemann surfaces. For now, let us just mention the following. Long before AdS/CFT, Osborn [36] proposed that the $\mathcal{N} = 4$ super-Yang–Mills theory we encountered in Section 1.2 is the most natural candidate for a theory with electromagnetic duality. In terms of the D3 brane holographic correspondence in (1.11), this makes total sense: electromagnetic duality for the boundary theory corresponds to the $SL(2, \mathbb{Z})$ symmetry of IIB string theory! This was already pointed out by Maldacena immediately after stating the correspondence in [10].

1.4   Symmetries and asymptotics in AdS/CFT

Finally, let us write down the $(d + 1)$-dimensional anti-de Sitter (AdS) metric explicitly. In this section, we write the metric using Poincaré coordinates:

$$ds^2 = \frac{\ell^2}{z^2} \left(-dt^2 + d\vec{x}^2 + dz^2 \right).$$ (1.31)

Here, ℓ parametrizes the radius of curvature of AdS. At each fixed value of z, we have a d-dimensional timelike surface parametrized by a time coordinate t and $(d-1)$ spatial coordinates $\vec{x}$. Distances on this $\mathbb{R}^{1,d-1}$ submanifold grow asymptotically towards $z = 0$. In fact, even though it is at infinite distance, we can think of the $z = 0$ surface as a boundary of AdS_{d+1}. This can be seen by multiplying the metric (1.31) with the function $f(z)^2 = z^2/\ell^2$, which gives

$$ds'^2 = f(z)^2 ds^2 = -dt^2 + d\vec{x}^2 + dz^2. \tag{1.32}$$

This is just $\mathbb{R}^{1,d}$ with one coordinate z restricted to $z \geq 0$. Since multiplying the metric with $f(z)^2$ corresponds to a conformal transformation, the boundary at $z = 0$ is known as the *conformal boundary* of AdS_{d+1}.

1.4.1 Conformal symmetries in AdS

However, notice that we could have used *any* function $f(t, \vec{x}, z)$ to obtain the conformal compactification, as long as it grows like z^2 for $z \to 0$. In particular, we can take

$$f(t, \vec{x}, z) = \Omega(t, \vec{x}) \frac{z^2}{\ell^2}. \tag{1.33}$$

This acts on the boundary metric at $z = 0$ by

$$-dt^2 + d\vec{x}^2 \quad \mapsto \quad \Omega(t, \vec{x}) \left(-dt^2 + d\vec{x}^2 \right). \tag{1.34}$$

If there is any physics on the conformal boundary, it should be invariant under such transformations of the boundary metric, which are known as *Weyl transformations*. Any field theory that is covariantly coupled to a background metric is invariant under coordinate transformations. Generally, such transformations are gauge symmetries, leading to equivalent descriptions of the same physics, but without a conserved charge associated to them. For this reason, we say they are not *physical*: they are merely redundancies of the mathematical description.

However, if a theory is invariant under Weyl transformations, we can use them to absorb certain coordinate transformations, which *are* then physical. The coordinate transformations that can be absorbed using (1.34) are exactly the angle-preserving *conformal* transformations. For $\mathbb{R}^{1,d-1}$ the corresponding group is $SO(2,d)$. Furthermore, as we will show in Section 2.1, $SO(2,d)$ is also the isometry group of (1.31).

Any theory living on the boundary of AdS will therefore have to be a conformal field theory. It is therefore tempting to think of the CFT involved in the correspondence as living on the conformal boundary. For this reason, it is commonly referred to as the *boundary* theory, whereas the corresponding $(d+1)$-dimensional theory of gravity is referred to as the *bulk* theory. We will discuss several ways to make this correspondence more precise in Section 1.5.

1.4.2 The Virasoro algebra from AdS$_3$

Conformal symmetries are especially powerful in two dimensions. Using null coordinates $x^\pm = (x \pm t)/2$ on the boundary the AdS$_3$ metric is

$$ds^2 = \frac{\ell^2}{z^2} \left(4dx^+ dx^- + dz^2 \right). \tag{1.35}$$

The boundary Weyl transformations are now

$$4dx^+ dx^- \mapsto 4\Omega(x^+, x^-)dx^+ dx^-. \tag{1.36}$$

Now *any* chiral function of $x^\pm$ is a conformal transformation: under a coordinate transformation parametrized by $x^+ \mapsto f(x^+)$, the metric is mapped to

$$4dx^+ dx^- \mapsto 4f'(x^+)dx^+ dx^-, \tag{1.37}$$

and similarly for $x^- \mapsto g(x^-)$. All such transformations can be compensated using (1.36). This means that the two-dimensional algebra of conformal transformations is *infinite-dimensional*! It is generated by

$$\ell_m = -(x^+)^{m+1}\partial_+, \qquad \bar{\ell}_m = -(x^-)^{m+1}\partial_-, \tag{1.38}$$

which satisfy the following commutation relations:

$$[\ell_m, \ell_n] = (m-n)\ell_{m+n}, \qquad [\bar{\ell}_m, \bar{\ell}_n] = (m-n)\bar{\ell}_{m+n}. \tag{1.39}$$

As a result of this large set of symmetries, many properties of two-dimensional CFTs can be determined exactly, see for example [37] for a review. On a quantum level, this algebra can develop a *central extension*:

$$[L_m, L_n] = (m-n)L_{m+n} + \frac{c}{12}m(m^2-1)\delta_{m+n,0}. \tag{1.40}$$

The parameter c is also known as the *central charge* of the algebra. In this form, (1.40) is known as the Virasoro algebra. In field theory, the appearance of a central charge is a distinctly quantum phenomenon. Remarkably, Brown and Henneaux [38] found that the Virasoro algebra (1.40) also appears in a careful analysis of the *classical* symmetries of AdS$_3$! To be precise, they found

$$c_{\text{BH}} = \frac{3\ell}{2G}. \tag{1.41}$$

In a sense, this result was an early precursor of the AdS/CFT correspondence. It is entirely in the spirit of the general conjecture in (1.17).

The techniques required to derive this result will be reviewed in Chapter 2. A large part of this thesis is devoted to applying these techniques to find generalizations and applications of three-dimensional holography.

Finally, it is worth mentioning that the Brown–Henneaux central charge (1.41) can be used to explain the entropy of three-dimensional black holes. Under reasonable assumptions, Cardy [39] found that there exists a *universal* formula for

the entropy of a two-dimensional conformal field theory as a function of its central charge. Using the Brown–Henneaux result (1.41), one recovers the entropy of the three-dimensional black holes! This was first pointed out by Strominger [40]. It is remarkably simpler than the intricate analysis that went into the Strominger-Vafa entropy computation.

In this sense, three-dimensional gravity can be a useful probe of holography. Without invoking too much detail about the underlying string theory constructions, we can provide nontrivial tests for dualities on the level of symmetries. We will now discuss several other probes that also hold more generally, supporting the 'strong' AdS/CFT correspondence proposed in (1.17).

1.5 Probes of holography

Soon after the work of Maldacena first appeared, it was realized that many essential properties of CFTs can be reproduced without any reference to the intricate details of the classical planar D3 correspondence (1.16). This motivates the idea that the relation between AdS and CFT should hold more generally, at least as stated in (1.17). The translations of these properties have become an essential part of the dictionary of AdS/CFT, so we will review several of them here.

In Section 1.4, we saw that the boundary behavior of the AdS metric is subtle yet crucial for the holographic dictionary. As Gubser, Klebanov, Polyakov and Witten realized [41,42], the same is true for *all* fields on an AdS background. They proposed to interpret bulk fields as duals of operators in the boundary CFT. In Section 1.5.1 we will briefly review how this reproduces CFT two-point functions.

We then review how the confinement of matter coupled to gauge theories can be probed using Wilson lines. The latter have a simple bulk interpretation in AdS/CFT, which we discuss in Section 1.5.2.

Finally, Ryu and Takayanagi [43] understood how another essential quantum observable, *entanglement entropy*, could be mapped to minimal surfaces in the bulk. We review this identification in Section 1.5.3.

1.5.1 Correlators

Conformal symmetry greatly simplifies the analysis of a field theory. Its representations organize operators in towers of descendants built on top of *primary* operators. For simplicity, we restrict ourselves to scalar (non-spinning) operators. The conformal symmetry fixes the two-point function of such a scalar primary operator O with scaling weight Δ to be

$$\langle O(x)O(y)\rangle = \frac{1}{|x-y|^{2\Delta}}.$$

(1.42)

Since this result can be derived using only the conformal symmetries, it is true for *any* conformal field theory. We saw that these symmetries have their analogue in the bulk isometries, so it is natural to ask if a similarly general derivation allows us to reproduce (1.42) from Anti-de Sitter space.

In the dictionary proposed by Gubser, Klebanov, Polyakov and Witten [41,42], scalar primary CFT operators correspond to *scalar fields* in the bulk. The bulk field $\phi(\vec{x}, z)$ satisfies the AdS Klein-Gordon equation $\Box \phi = m^2 \phi$. Moreover, the weight Δ of the CFT primary is related to the mass m of the bulk field by

$$\Delta = \frac{d}{2} + \sqrt{\frac{d^2}{4} + m^2 \ell^2}. \tag{1.43}$$

To compute correlators, we also need to identify *sources* $J(x)$ for $O(x)$ in the bulk. Here, the proposal is to identify $J(x)$ with the value of $\phi(x, z)$ at the $z \to 0$ *boundary* of AdS. If the boundary behavior of ϕ is fixed, the Klein-Gordon equation determines it all across the bulk. We denote the corresponding solution to the equations of motion by ϕ_0. In the large N, large λ limit, this leads to the following proposal

$$Z_{\text{CFT}}[J(x)] = \exp\left(-S^{\text{grav}}[\phi_0]\big|_{\phi_0 \to J}\right). \tag{1.44}$$

Because ϕ_0 is on-shell, the gravity action reduces to a boundary integral:

$$S^{\text{grav}}[\phi_0] \sim \int d^d\vec{x}\, d^d\vec{x}'\, \frac{\phi_0(\vec{x}, 0)\phi_0(\vec{x}', 0)}{|\vec{x} - \vec{x}'|^{2\Delta}} \tag{1.45}$$

Since we identified $J(x) = \phi_0(\vec{x}, 0)$, taking two functional derivatives thus reproduces the CFT two-point function (1.42)!

1.5.2 Wilson lines

We mentioned in Section 1.1 that at very high energy scales, such as those accessed by the LHC, quarks can be thought of as weakly-interacting particles. However, the coupling becomes strong as we flow down to lower energy scales. At some point, the quarks are 'trapped' into quark-antiquark pairs (mesons) or quark triples (baryons). Understanding the precise mechanism behind this condensation, which is known as quark *confinement*, is one of the major open problems of theoretical physics. Since the AdS/CFT correspondence promises us the ability to do computations in strongly-coupled gauge theories, it is natural to ask if it can help us understand confinement.

For this, it is useful to use the following order parameter, which was introduced by Wilson [44] and also studied by 't Hooft [45]. We want to understand the force between two quarks, so we study a quark-antiquark pair that is separated by a spatial distance L and annihilated after a (Euclidean) time T. Furthermore, we assume that the quarks are approximately static after being moved apart. We can then view them as test charges for the strong force. This is sketched in Figure 1.7.

Such a trajectory corresponds to a closed current loop that couples to the color gauge potential. This results in what is known as a *Wilson loop*:

$$W(C) = \mathcal{P}\, e^{-\oint_C A}. \tag{1.46}$$
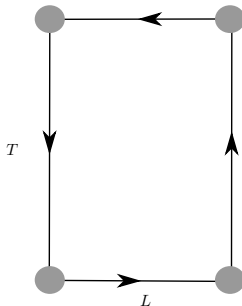
Figure 1.7: A square Wilson loop corresponding to a quark-antiquark pair.

Since it depends on the gauge potential along the entire contour C, a Wilson loop is a *nonlocal* observable in gauge theory. Assuming that the quarks are static and T is large, the expectation value of $W(C)$ is approximately determined by the potential $V(L)$ between the quarks:

$$\langle W(C) \rangle \approx e^{-V(L)T}. \tag{1.47}$$

This can be viewed as an order parameter for confinement. A normal Coulomb potential $V(L) \sim 1/L$ decays at large separation, so it does not confine. In contrast, one expects the potential to *grow* with the separation, $V(L) \sim L$, if the force is confining.

Such quantities are generally impossible to compute analytically and one has to resort to numerical methods. However, the AdS/CFT correspondence allows us to describe strongly-coupled gauge theories by doing bulk computations in classical gravity and it is tempting to look for a bulk interpretation of Wilson loops.

Maldacena [46] proposed the following dictionary entry. First, the $\mathcal{N} = 4$ theory coming from D3 branes does not contain matter fields in a fundamental representation. To remedy this, we can start with a stack of $N + 1$ D3 branes and move one away from the rest. This produces a massive W-boson, which we can think of as a quark coupled to the $SU(N)$ gauge theory on the remaining N D3 branes. It is modeled in the bulk by a string dangling into AdS from the position of the quark at the boundary.

In the limit (1.16), we can approximate (1.46) using the *action* of the corresponding bulk string worldsheet. For large T, the problem is invariant under time translations and we immediately recover the linear scaling in T of (1.47). We can then determine the quark-antiquark potential by studying the behavior of the string on equal-time slices in the bulk.

As we can see from the bulk sketch in Figure 1.8a, increasing the quark-antiquark separation L causes the string worldsheet to move further into the bulk. However, the redshift due to the curvature of AdS is *stronger* as one moves further into the bulk. This means that the string action actually falls off with $1/L$. Thus, in the boundary theory dual to empty AdS, such quarks feel a Coulomb-type force

and are not confined. However, this geometric perspective makes it very easy to modify the geometry so that it *does* confine. If we cap off the bulk AdS space with some 'hard wall' at $z = z_w$, at some point the string worldsheet can no longer reach further into the bulk. This is sketched in Figure 1.8b. Once the string hits the bulk wall, the redshift no longer increases. At that point, the bulk worldsheet area and the corresponding boundary potential scale proportional to the separation L, which means we can use this bulk geometry to describe confinement of the boundary theory.

(a) AdS vacuum
(b) AdS with hard wall
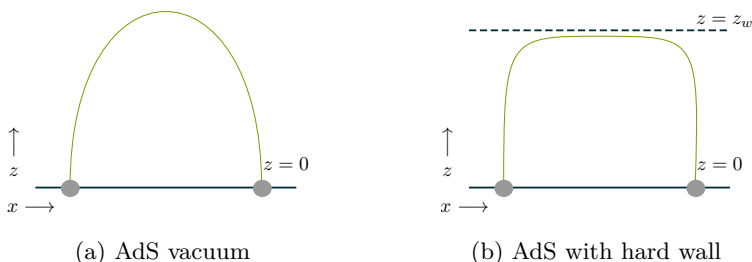
Figure 1.8: String worldsheet in the bulk (fixed time).

For more computational detail, see for example [22,23]. It is worth noting that this prescription maps a *nonlocal observable in strongly-coupled field theory* to a *simple geometric bulk quantity*. This kind of translation seems to be a general feature of the AdS/CFT dictionary. We will now discuss one more example.

1.5.3 Entanglement entropy

In Chapter 5, we will apply the AdS/CFT correspondence to study another nonlocal observable: the field theory's spatial *entanglement entropy*. Again, as we will now review, this observable turns out to be described in terms of a simple geometric bulk quantity if the boundary field theory is strongly coupled. We briefly review some basic aspects of this extensively-studied entry in the AdS/CFT dictionary, see for example [47] for a more complete introduction.

A defining feature of quantum mechanics is the fact that two degrees of freedom, such as spins, can be *entangled* with each other. Measuring one such spin collapses the state and affects consequent measurements on the other spin, even though the particles they describe may not be in causal contact. Perhaps the simplest example for this is the EPR pair,

$$\frac{1}{\sqrt{2}} \left(|00\rangle + |11\rangle \right). \tag{1.48}$$

This state describes a superposition of two particles, both of which have two states which are labeled by 0 and 1. If the first particle is measured to be in the 0 state, the second particle is necessarily also in the 0 state, hence they are entangled.

More generally, one can quantify the entanglement of a subsystem A by studying the *reduced* system that remains after tracing out its complement A^c. In particular, if we describe a general state $|\Psi\rangle$ in our Hilbert space using a density matrix $\rho = |\Psi\rangle\langle\Psi|$, the reduced density matrix associated to A is

$$\rho_A = \text{Tr}_{A^c} \rho. \tag{1.49}$$

Using the Von Neumann entropy, one can then assign a number to the entanglement between the region A and its complement,

$$S(A) = -\text{Tr}_A \rho_A \log \rho_A. \tag{1.50}$$

This is the *entanglement entropy* of a density matrix ρ associated to the subset A of the Hilbert space. It can also be defined in quantum field theory, as long as the Hilbert space factorizes into A and A^c. In the following, we will often be interested in *spatial* entanglement entropy, where A corresponds to the degrees of freedom associated to a subset of spacetime. By a slight abuse of notation, this subset itself is often also denoted by A.

Calculating the entanglement entropy directly from the definition (1.50) is often prohibitively hard, especially in field theory. To avoid computing the logarithm of ρ_A, one can use the Rényi entropies

$$S_n(A) = \frac{1}{1-n} \log \text{Tr} \left(\rho_A\right)^n \tag{1.51}$$

as an intermediate step. The nth Rényi entropy $S_n(A)$ can be understood as the path integral on an n-sheeted geometry, where n copies of spacetime are stitched together across the entangling region A. If the resulting expression can be analytically continued in n, the limit $n \to 1$ reproduces $S(A)$.

In two-dimensional CFTs, the sewing can be implemented using twist operators, which leads to a universal result for their entanglement entropy as follows. We take A to be an interval of length l on the one-dimensional spatial line of a CFT on a Euclidean plane. In the vacuum state $\rho = |0\rangle\langle0|$, the nth Rényi entropy can be understood as the two-point function of two n-fold twist operators. Their two-point functions are fixed by their weights, which depend only on n and on c, the central charge of the theory. Analytically continuing to $n \to 1$ then gives [48, 49]

$$S(A) = \frac{c}{6} \log \left(\frac{l}{a}\right). \tag{1.52}$$

This expression depends on a UV cutoff scale a, which regulates the local degrees of freedom at the boundary of A.

Holographic interpretation   This result depends on the specifics of the CFT_2 under consideration only through its central charge. One could therefore wonder if a similarly general holographic interpretation of entanglement entropy in terms of AdS_3 geometry exists.
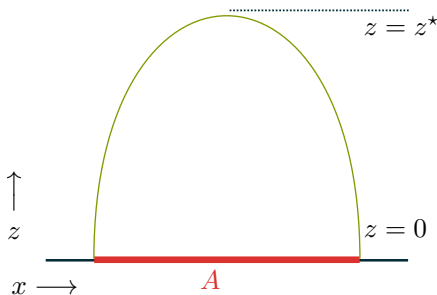
Figure 1.9: The bulk entangling surface.

Ryu and Takayanagi [43, 50, 51] found that this is indeed the case. They identified the *area* of a hypersurface in the bulk as a natural dual to boundary spatial entanglement entropy. Given a subregion A on the boundary, the corresponding bulk hypersurface $B(A)$ is given by the extremal surface that ends on ∂A on the boundary of AdS, without wrapping nontrivial cycles in the bulk. The spatial entanglement $S(A)$ is then computed holographically by[2]

$$S(A) = \frac{\text{Area}\,[B(A)]}{4G}. \tag{1.53}$$

Again, we see that a nonlocal observable in the boundary theory is related to a simple geometric object in the bulk.

As a brief example, let us reproduce the two-dimensional result (1.52) using this prescription [50]. We describe the bulk AdS$_3$ geometry using the Poincaré patch (1.31). In this background, the length of a constant $t = t_0$ curve is

$$L = \int ds = \int \sqrt{X(\mu)^2} d\mu = \ell \int \frac{dz}{z} \sqrt{1 + x'(z)^2}. \tag{1.54}$$

Here, we have parametrized the curve $X^\mu(\mu) = (t_0, x(\mu), z(\mu))$ using the bulk coordinate $\mu = z$. A minimal surface ending on two points $(t, x) = (0, \pm l/2)$ on the boundary will reach some maximal distance z^* into the bulk at $x = 0$. Furthermore, it is symmetric around that point, see Figure 1.9 for a sketch. Solving the Euler-Lagrange equations, we get

$$x(z) = z_* \sqrt{1 - \left(\frac{z}{z^*}\right)^2}, \quad z^* = \frac{l}{2}. \tag{1.55}$$

The length of this curve will be divergent since the boundary of AdS is at infinite

---

[2]Note that the string action that we identified with Wilson lines also measures the area of a bulk surface. However, this is a *timelike* surface, whereas the hypersurfaces associated to entanglement entropy are *spacelike*.

spacelike distance, so a UV cutoff is required. Integrating from $z = \epsilon$, we get

$$L = 2\ell \int_{\epsilon}^{z^*} \frac{dz}{z\sqrt{1 - (z/z^*)^2}} = 2\ell \log\left(\frac{z^*}{\epsilon}\left(\sqrt{1 - \left(\frac{\epsilon}{z^*}\right)^2} + 1\right)\right). \qquad (1.56)$$

Indeed, this expression diverges as $\epsilon \to 0$. Since the cutoff ϵ should be small compared to the interval size $z^* = l/2$, we can approximate this result by

$$L \approx 2\ell \log\frac{l}{\epsilon} \qquad (1.57)$$

Using the Brown–Henneaux central charge $c = 3\ell/2G$ associated to AdS$_3$ which we discussed in Section 1.4, the Ryu-Takayanagi prescription for the entanglement entropy of A gives

$$S(A) = \frac{L}{4G} = \frac{c}{3}\log\frac{\ell}{\epsilon}. \qquad (1.58)$$

Indeed, this precisely reproduces the CFT result in (1.52)! In Chapter 5 we use the Ryu-Takayanagi prescription to extract general lessons about the behavior of entanglement entropy in strongly-coupled field theories.

1.6 Outline

We started this chapter by motivating the study of non-perturbative phenomena and strong-coupling behavior. We introduced the holographic principle and its realization in the AdS/CFT correspondence. We also briefly mentioned electro-magnetic duality and the relation between four-dimensional gauge theories and two-dimensional Riemann surfaces it suggests. Finally, we introduced several concrete elements of the AdS/CFT dictionary.

The rest of this thesis is concerned with extensions and applications of these dualities. We will now give a brief outline of what is to come. (Further references will be given in the corresponding chapters.)

1.6.1 Asymptotic symmetries in three dimensions

As we mentioned in Section 1.4.2, the matching between AdS and CFT symmetries requires particular care if the bulk is three-dimensional. In Chapter 2 we give a detailed derivation of the asymptotic Virasoro symmetries of AdS$_3$ by identifying three-dimensional Einstein gravity with a Chern–Simons theory.

In fact, we derive an expression for the asymptotic charges of *any* Chern–Simons theory on a manifold with boundary. These charges form an affine algebra corresponding to the symmetries of a Wess–Zumino–Witten model on the boundary of the manifold. We then show how this affine algebra can be used to reproduce the Brown–Henneaux Virasoro algebra using a technique known as *Drinfeld–Sokolov reduction.*

The advantage of this approach is that it can be easily extended to other theories of gravity that are not (just) formulated in terms of a metric tensor. The Drinfeld–Sokolov approach allows us to derive the asymptotic symmetries of any three-dimensional theory of gravity that can be formulated as a Chern–Simons theory. We illustrate this by reproducing the (classical) $\mathcal{W}_3$-algebra from a Chern–Simons theory corresponding to higher spin gravity. We also review how general $\mathcal{W}$-algebras correspond to different embeddings of the Einstein subsector in higher spin theories.

1.6.2 Nonrelativistic holography

So far, we have mainly focused on the foundations of the AdS/CFT correspondence and its dictionary. Instead of studying 'top-down' dualities arising from a D-brane setup, one can also attempt to *model* a given strongly-coupled field theory using a suitable bulk gravity theory. This approach is known as 'bottom-up' holography. One of its major applications has been the study of quantum critical points, see for example [52] for a review and further references. These condensed-matter systems are typically not relativistic. In particular, there is no reason why the scaling symmetry at such critical points should treat space and time equally. For example, we may see a scaling symmetry such as

$$t \mapsto \lambda^\zeta t, \qquad \vec{x} \mapsto \lambda \vec{x}. \tag{1.59}$$

This is known as *Lifshitz* scaling. (The anisotropy between space and time is conventionally parametrized using z, but we use ζ here to avoid confusion with the bulk coordinate z.) In AdS/CFT, the boundary symmetries are realized as isometries of the bulk metric. Therefore, the latter should be adjusted accordingly, for example by including the parameter ζ in the AdS metric (1.31) as follows [53]

$$ds^2 = -\frac{dt^2}{z^{2\zeta}} + \frac{d\vec{x}^2 + dz^2}{z^2}. \tag{1.60}$$

This metric can still be obtained as a solution of a relativistic theory if appropriate background fields are turned on. However, the resulting boundary analysis is subtle, see [54] for a review. Consequently, one may be led to think that studying nonrelativistic phenomena using symmetry-breaking solutions of relativistic theories is perhaps not the correct approach. Instead, it could be more natural to look for a holographic description of such phenomena using theories that are inherently nonrelativistic.

Recall that we use pseudo-Riemannian geometry to describe theories with local Lorentz invariance. Similarly, there exist geometric constructions for nonrelativistic theories where space and time are treated differently. We will collectively refer to them here as *Newton–Cartan* geometry. Indeed, it has been found [55, 56] that in specific symmetry-breaking bulk Lifshitz models, the boundary theory naturally couples to a particular Newton–Cartan geometry. Furthermore, Newton–Cartan geometries can also be made dynamical, leading to nonrelativistic theories of gravity which can be used to describe bulk physics.

Intuitively, nonrelativistic holography should correspond to the low-energy limit of a relativistic setup. However, because the geometric formulation of relativistic and nonrelativistic systems is rather different, it is hard to make this intuition precise. As we mentioned, Einstein gravity can be described using Chern–Simons theory in three dimensions. It turns out that certain nonrelativistic theories of gravity can *also* be described as a Chern–Simons theory. In Chapter 3 we study the relation between the $\mathrm{AdS}_3/\mathrm{CFT}_2$ correspondence and a duality involving a nonrelativistic theory of gravity by relating the local symmetry algebras using a contraction. Furthermore, we can identify the bulk action, the phase space and even all boundary symmetries using this contraction.

1.6.3 Deriving AGT from six dimensions

We then turn to a different type of strong-coupling duality in Chapter 4. In Section 1.3.3, we briefly mentioned the idea that four-dimensional gauge theories may be related to two-dimensional Riemann surfaces. Over time, this idea has been made increasingly precise. Its most recent incarnation is known as the *Alday–Gaiotto–Tachikawa (AGT) correspondence*. It relates partition functions of four-dimensional supersymmetric gauge theories to correlators of two-dimensional conformal field theories on Riemann surfaces.

Remarkably, this relation was established by identifying quantities that can be computed *exactly* on each side of the correspondence. In contrast, the AdS/CFT correspondence is *motivated* by the D-brane construction we discussed in Section 1.2, but although it survived many highly nontrivial checks, it has not been established at the level of an equality between exactly computable quantities. In this sense, one could argue that the AGT correspondence is already better established than AdS/CFT.

However, the way in which AdS/CFT was discovered also has its advantages. By studying branes in different geometrical setups, it is relatively easy to find generalizations of AdS/CFT beyond the D3 brane system we discussed in Section 1.2. In contrast, the AGT correspondence establishes an equality which cannot be easily generalized without any underlying intuition. In that sense, the derivation of the AdS/CFT correspondence is more 'constructive': although it does not identify exact quantities, it provides a physical intuition for why the correspondence *should* be true, which can then be generalized to other settings.

One can therefore wonder if a similarly constructive derivation of the AGT correspondence exists. Since AGT relates two-dimensional and four-dimensional theories, it is natural to look for an overarching six-dimensional perspective. In Chapter 4, we investigate a proposed derivation of the AGT correspondence which involves the boundary dynamics of a higher-spin-type Chern–Simons theory. In particular, we focus on the origin of the relevant Drinfeld–Sokolov boundary conditions, which are related to the Nahm pole data we discussed in (1.27). In Chapter 4, we propose a different D-brane setup to explain the origin of the Nahm pole in this context. Furthermore, our setup allows us to include theories with general $\mathcal{W}$-symmetry corresponding to different embeddings of the Nahm pole data.

1.6.4 Holography out of equilibrium

As we mentioned briefly in Section 1.5.3, AdS/CFT maps complicated nonlocal boundary observables such as spatial entanglement entropy to simple geometric quantities in the bulk. In line with the 'bottom-up' approach to holography discussed in Section 1.6.2, we will use this mapping in Chapter 5 to study general properties of strongly-coupled field theories out of equilibrium.

Even though black holes radiate, they can be in thermal equilibrium in AdS due to its negative curvature. Such 'large' black holes correspond to thermal states in the boundary field theory. Small perturbations on top of this black hole geometry then correspond to near-equilibrium fluctuations in the boundary. This results in the *fluid-gravity* correspondence, which allows us to describe the hydrodynamic regime of strongly-coupled field theories using gravity. It has been used to model many physically relevant systems such as the quark-gluon plasma observed after heavy ion collisions, see for example [57] for a review.

However, this approach does not allow us to study the formation of thermal states in strongly-coupled theories. Naively, one expects a generic system with many degrees of freedom to settle into an approximately thermal state after a sufficient amount of energy is inserted. This process is known as *thermalization*.

As a nonlocal boundary observable with a simple bulk interpretation, entanglement entropy is a natural probe to study thermalization. For simplicity, we can assume that all injected energy is inserted at one instant of time and that it is spread out homogeneously across space. In field theory, this is also known as a global *quench*. For the purposes of entanglement entropy, it can be modeled holographically [58] using

$$ds^2 = \frac{1}{u^2}\left(-f(v,u)dv^2 - 2dvdu + d\vec{x}^2\right), \qquad f(v,u) = 1 - \left(\frac{u}{u_H}\right)^d. \qquad (1.61)$$

Here, u and v are outgoing and infalling Eddington-Finkelstein coordinates. This metric, which is known as the Vaidya geometry, corresponds to empty AdS for $v < 0$ and to an AdS-Schwarzschild black hole with horizon u_H for $v > 0$.

In Chapter 5, we use this holographic setup to study the evolution of spatial entanglement entropy after a global quench with arbitrary time dependence. We find analytic results for spatial boundary regions that are small compared to u_H, which parametrizes the temperature of the resulting thermal state. We then use these results to define a notion of distance to the adiabatic process that results in the same thermal state and we work out several examples corresponding to a representative set of quench profiles.

Chapter 2

Three-dimensional holography

As a testing ground for holography, three-dimensional gravity is particularly interesting. First, it is a relatively simple theory: since gravitational waves do not exist in three dimensions, we can focus on the boundary degrees of freedom. As we briefly mentioned in Section 1.4.2, a rich symmetry structure emerges at the boundary of three-dimensional Anti-de Sitter spacetimes.

Second, three-dimensional gravity can be interpreted as a Chern–Simons theory. This formulation uses the same mathematical tools that greatly simplified our analysis of nonperturbative effects in gauge theory in Section 1.3. Similarly, compared to the usual metric formulation, the Chern–Simons formulation allows a more systematic derivation of the boundary degrees of freedom of gravity.

Finally, by modifying the local symmetry algebra, Chern–Simons theory can also be used to describe different theories of gravity. These include nonrelativistic theories of gravity and theories involving higher spin fields, which we will encounter in Chapter 3 and 4, respectively. The unified Chern–Simons perspective allows us to study the boundary dynamics of all such theories using the same tools.

In this chapter, we will study the boundary dynamics of three-dimensional gravity in more detail. After a brief motivation, we introduce the Chern–Simons formulation of Einstein gravity with negative cosmological constant in Section 2.2. We derive the boundary charges of Chern–Simons theory in Section 2.3 and write out the boundary Wess–Zumino–Witten phase space in Section 2.4. Finally, we explain how Drinfeld–Sokolov reduction reproduces the Brown–Henneaux asymptotic symmetries of AdS_3 and work out a higher-spin example in Section 2.5.

Parts of this chapter have previously appeared in the appendices of [1] and in [2].

2.1 Motivation

We first introduce some basic notions of three-dimensional gravity using the metric formalism. With a cosmological constant Λ, the Einstein–Hilbert (EH) action is

$$S_{\text{EH}} = \frac{1}{16\pi G} \int d^3 x \sqrt{-g}\, (R - 2\Lambda) . \tag{2.1}$$

All solutions of three-dimensional Einstein gravity are homogeneous and isotropic, meaning that all points and all directions are equivalent. Locally, the only non-trivial information is contained in the (constant) scalar curvature. In other words, we can express the full Riemann tensor of all solutions to the equations of motion using only the Ricci scalar:

$$R_{\mu\nu\rho\sigma} = \frac{R}{6} \left(g_{\mu\rho} g_{\nu\sigma} - g_{\mu\sigma} g_{\nu\rho} \right) . \tag{2.2}$$

Once we specify Λ, the scalar curvature is set and the metric is fixed. In this section, we will study maximally symmetric solutions with negative curvature. These are the *Anti-de Sitter* (AdS) solutions we encountered in Section 1.2. They describe manifolds with a boundary, so we should worry about the *boundary conditions* associated to the equations of motion. Although all solutions are locally the same, we will see that they can be distinguished using *boundary charges*.

Global AdS₃ So far, we have only used the AdS₃ metric in *Poincaré* coordinates (1.31). These coordinates describe only part of the maximal solution, which is known as *global* AdS₃. It is described by

$$ds^2 = \ell^2 \left(-\cosh^2 \rho\, dt^2 + d\rho + \sinh^2 \rho\, d\varphi^2 \right) . \tag{2.3}$$

The curvature radius ℓ is related to the cosmological constant by $\Lambda = -1/\ell^2$. This space can be viewed as a hypersurface in $\mathbb{R}^{2,2}$ satisfying

$$- X_{-1}^2 - X_0^2 + X_2^2 + X_3^2 = -\ell^2. \tag{2.4}$$

The metric (2.3) is then induced by the flat metric on $\mathbb{R}^{2,2}$. From this embedding it is clear that the isometry group of global AdS₃ is $SO(2,2)$, just like the isometry group of a sphere in $\mathbb{R}^d$ is $SO(d)$. The isometry group acts transitively on the hypersurface and the stabilizer of a single point is $SO(1,2)$. This means that we can view (2.4) as the manifold associated to the corresponding quotient:

$$\text{global AdS}_3 \simeq SO(2,2)/SO(1,2). \tag{2.5}$$

Note that the time coordinate on the hypersurface described in (2.4) is periodic. We should remove this periodicity to avoid closed timelike curves, so we will actually work with the universal cover of (2.4) from now on. Finally, using the radial coordinate transformation $\cosh \rho = (\cos \chi)^{-1}$ with $\chi \in [0, \pi/2)$, we can write the metric as

$$ds^2 = \frac{\ell^2}{\cos^2 \chi} \left(-dt^2 + d\chi^2 + \sin^2 \chi\, d\varphi^2 \right) . \tag{2.6}$$

Thus we see that the conformal boundary of global AdS$_3$ is a cylinder at $\chi \to \pi/2$, corresponding to $\rho \to \infty$.

BTZ black holes We've determined that any and all solutions of Einstein's equations with negative cosmological constant are locally described by (2.3). One may therefore be tempted to conclude that no interesting solutions other than global AdS$_3$ exist. But this is false. As discovered [59] by Bañados, Teitelboim and Zanelli (BTZ), *black hole* solutions exist:

$$ds^2 = -\frac{\left(r^2 - r_+^2\right)\left(r^2 - r_-^2\right)}{\ell^2 r^2} dt^2 + \frac{\ell^2 r^2 dr^2}{\left(r^2 - r_+^2\right)\left(r^2 - r_-^2\right)}$$
$$+ r^2 \left(d\varphi - \frac{r_+ r_-}{\ell r^2} dt\right)^2 . \tag{2.7}$$

One can assign a mass M and angular momentum J to these BTZ black holes: in terms of the outer and inner horizons $r_\pm$,

$$M = \frac{r_+^2 + r_-^2}{8G\ell^2}, \qquad J = \frac{r_+ r_-}{4G\ell}. \tag{2.8}$$

In fact, BTZ black holes can be understood [60] as *quotients* of global AdS$_3$. For any value of M and J, the metric (2.7) can be constructed from global AdS$_3$ by identifying points using a discrete subgroup Γ of the isometry group $SO(2,2)$. What's more, all that these discrete symmetries are doing is a periodic identification of the coordinates, similar to the way we construct a circle from a line.

At first sight, this is rather confusing. Local observers cannot distinguish BTZ from global AdS$_3$. The BTZ metric has no curvature singularity, in contrast to for example the Schwarzschild metric (1.5) in $(3+1)$ dimensions. Then why would we assign a mass and angular momentum to the BTZ metric?

To resolve this confusion, it is important to realize that in general relativity, quantities such as mass and angular momentum are *global* properties of a metric. They correspond to *conserved charges* that are defined on the conformal *boundary* of spacetime. Constructing a BTZ black hole by performing a discrete coordinate identification on global AdS$_3$ also affects the conformal boundary. Indeed, it acts precisely by compactifying a particular linear combination of the boundary space and time coordinates to a circle! As a result, the boundary charges corresponding to mass and angular momentum are affected by the discrete identifications that lead to the BTZ metric.

In fact, as we briefly mentioned in Section 1.4.2, there actually exists an *infinite* set of such charges at the conformal boundary of AdS$_3$. Roughly speaking, they correspond to the Fourier modes of the circle. These are the asymptotic Virasoro charges discovered by Brown and Henneaux [38].

So far, our discussion has been rather informal. We will not give a precise derivation of the boundary charges in the metric formalism (but see for example [61–63] for reviews from various perspectives). The main reason for this is that such a

derivation would have no obvious generalization to the three-dimensional theories we will study in Chapter 3 and 4. Instead, we now switch to a different geometric formulation of Einstein gravity. It can be easily generalized to other theories of gravity and leads to a more systematic construction of AdS$_3$ boundary charges.

2.2 Einstein gravity and Chern–Simons theory

As we saw in Section 1.3, it is convenient to describe nonperturbative objects in Yang–Mills theory in terms of topological properties of bundles and connections. To study the boundary dynamics of AdS$_3$, it is useful to formulate three-dimensional gravity in similar terms.

However, even in three dimensions, gravity is clearly not the *same* as Yang–Mills theory. Instead, as discovered by Achúcarro, Townsend and Witten [64, 65], one can write three-dimensional Einstein gravity as a Chern–Simons theory. We will now review this identification in a language that will allow for easy generalization later on. Then, in Section 2.3, we will use the Chern–Simons formulation to work out the boundary charges of asymptotically AdS$_3$ spacetimes.

2.2.1 First-order Einstein gravity

In Einstein gravity, we usually think of spacetime as a pseudo-Riemannian manifold (M, g). It can equivalently be described in terms of local *frames*. This formulation is useful as an intermediate step in the identification of Einstein gravity with Chern–Simons theory.

Mathematically, a local frame is a choice of basis in the tangent bundle. At a point $p \in M$ described by coordinates x^μ, this leads to a set of vectors

$$e_a(p) = e_a^\mu(p) \frac{\partial}{\partial x^\mu}\bigg|_p. \tag{2.9}$$

If we choose $e_a^\mu(p) = \delta_a^\mu$, the resulting set of vectors is just the standard coordinate basis of the tangent space. More generally, the $e_a^\mu(p)$ can be arbitrary smooth functions, and our basis corresponds to a set of vector fields $e_a = e_a^\mu \partial_\mu$. The corresponding covectors $e^a = e_\mu^a\, dx^\mu$ form a basis of the cotangent space and are also known as *vielbeins*. It is often more convenient to use an *orthonormal* basis, which corresponds to a set of vector fields e_a satisfying

$$g(e_a, e_b) = \eta_{ab}. \tag{2.10}$$

Physically, such a choice of basis corresponds to a local Lorentz frame. The vectors e_a are the inertial frames of a set of freely falling observers who see only special relativity in their immediate surroundings.

However, when comparing vectors between their local inertial frames, such observers still need to take the curvature of spacetime into account. This can be done by introducing a notion of parallel transport on the frame bundle, which comes from a *spin* connection $\omega^a{}_b$. We can use it to define a derivative $D = d + \omega$

that is covariant under local Lorentz transformations. Like the usual Levi-Civita connection, ω is fully determined by requiring e^a to be parallel,

$$De^a = de^a + \omega^a{}_b \wedge e^b = 0. \tag{2.11}$$

This is known as the torsion-free condition. The curvature of this connection is

$$R^a{}_b = D\omega^a{}_b = d\omega^a{}_b + \omega^a{}_c \wedge \omega^c{}_b. \tag{2.12}$$

At each point, the Riemannian metric can be recovered by taking the inner product of the vielbeins in the local frame,

$$g_{\mu\nu}(p) = \eta_{ab} e^a_\mu(p) e^b_\nu(p). \tag{2.13}$$

This also shows that $e = \det(e^a_\mu) = \sqrt{-\det(g_{\mu\nu})} = \sqrt{-g}$. The frame metric η_{ab} is sometimes referred to as the tangent space metric. We can use these variables to rewrite the Einstein–Hilbert action (2.1). In three spacetime dimensions,

$$S_{\mathrm{EH}} = \frac{1}{16\pi G} \int_{M_3} \epsilon_{abc} \left(e^a \wedge R^{bc} - \frac{\Lambda}{3} e^a \wedge e^b \wedge e^c \right). \tag{2.14}$$

Similar actions are available for higher dimensions. We can introduce a dual spin connection and curvature tensor:

$$\Omega^a = \frac{1}{2} \epsilon^a{}_{bc} \omega^{bc}, \qquad R^a = \frac{1}{2} \epsilon^a{}_{bc} R^{bc}. \tag{2.15}$$

In terms of these variables, the action can be written as

$$\begin{aligned}
S_{\mathrm{EH}} = \frac{1}{16\pi G} \int_{M_3} \Big(& E^A \wedge \left(2d\Omega_A + \epsilon_{ABC} \Omega^A \wedge \Omega^B \right) \\
& - \frac{\Lambda}{3} \epsilon_{ABC} E^A \wedge E^B \wedge E^C \Big).
\end{aligned} \tag{2.16}$$

Here, we have capitalized the indices and vielbeins for later convenience. What is special about three dimensions is that all geometric objects are now *vectors* under the local $so(2,1)$ Lorentz symmetry. As we will see in Section 2.2.3, this fact allows us to write three-dimensional Einstein gravity as a Chern–Simons theory.

2.2.2 Chern–Simons action

First, let us mention some generalities about Chern–Simons forms. They arise from a general theory classifying principal fiber bundles using characteristic classes (see for example [29]). The Chern characters we encountered in Section 1.3 are a particular example of such characteristic classes. In equation (1.22), we saw how the second Chern character leads to the instanton number n of a Yang–Mills gauge theory on a four-manifold M_4,

$$\frac{1}{8\pi^2} \int_{M_4} \mathrm{Tr}\, F \wedge F = n \in \mathbb{Z}. \tag{2.17}$$

The instanton number measures a topological property of the gauge bundle, which quantifies to what degree $\operatorname{Tr} F \wedge F$ is not an exact form. However, it is closed, which means that it is at least *locally* exact. In a coordinate patch, we can therefore write

$$\operatorname{Tr} F \wedge F = d \left(\operatorname{Tr} \left[A \wedge dA + \frac{2}{3} A \wedge A \wedge A \right] \right). \tag{2.18}$$

The resulting three-form is know as a Chern–Simons form [66]. We can use it to define a *Chern–Simons theory* on a three-manifold M_3:

$$S_{\mathrm{CS}} = \frac{k}{4\pi} \int_{M_3} \operatorname{Tr} \left[A \wedge dA + \frac{2}{3} A \wedge A \wedge A \right]. \tag{2.19}$$

This action has seen many applications in physics and mathematics, ranging from massive gauge theories [67] to the Jones polynomial [68]. To have a well-defined path integral, the coupling constant of this theory should be quantized: we need $k \in \mathbb{Z}$ to ensure that the action produces a multiple of 2π independent of the M_4 we used to define the theory on M_3.

General Chern–Simons Lagrangian   To connect with gravity and to allow for generalizations later on, we will use a slight generalization of the Chern–Simons (CS) action. First, the gauge groups we use in Yang–Mills theories are generally compact: it turns out that this is not appropriate for gravity. Moreover, the trace in (2.19) corresponds to a particular choice of bilinear form on the Lie algebra. This choice is only unique (up to a prefactor) if the algebra is simple. Again, this will not be convenient both for Einstein gravity and in particular for our discussion in Chapter 3. Instead, we will work with the following action:

$$\mathcal{L}_{\mathrm{CS}} = \left\langle A, dA - \frac{2}{3} iA \wedge A \right\rangle. \tag{2.20}$$

Here, we have written (2.19) for a general Lie algebra $\mathfrak{g}$ using sharp brackets to denote an invariant bilinear form on this algebra. For $X, Y, Z \in \mathfrak{g}$ this means

$$\langle X, [Y, Z] \rangle = \langle [X, Y], Z \rangle. \tag{2.21}$$

For a given set of generators T_a of the Lie algebra, we denote its components by

$$\kappa_{ab} = \langle T_a, T_b \rangle. \tag{2.22}$$

We only consider nondegenerate bilinear forms and denote their inverse by κ^{ab}. Additionally, we choose to work with Hermitian generators, so that the (real) structure constants $f_{ab}{}^{c}$ are defined by

$$[T_a, T_b] = i f_{ab}{}^{c} T_c. \tag{2.23}$$

This factor of i is compensated by the factor $-i$ in the action (2.20).

Flatness   On a compact manifold, it is easy to see that the equations of motion of (2.20) imply that A is a flat connection. In our conventions, this means that

$$F = dA - iA \wedge A = 0. \tag{2.24}$$

On a manifold with boundary, this analysis is more subtle. We will deal with these subtleties in detail in Section 2.3.

Symmetries   Like the Yang–Mills action, the CS action is invariant under gauge transformations. Finite gauge transformations are parametrized by functions $U(x)$ valued in the Lie group associated to $\mathfrak{g}$,

$$A \rightarrow A' = iU^{-1}dU + U^{-1}AU. \tag{2.25}$$

If we write $U(x) = \exp(-i\lambda(x))$ using a Lie algebra-valued function $\lambda(x)$, the corresponding infinitesimal transformations are

$$A \rightarrow A' = d\lambda - i[A, \lambda]. \tag{2.26}$$

Finally, we note that the gauge transformations of a flat connection can be translated to diffeomorphisms on the base space. Recall that we can write the Lie derivative of the one-form A with respect to a vector field ξ as follows:

$$\mathcal{L}_\xi A = d\iota_\xi A + \iota_\xi dA. \tag{2.27}$$

Then, using $\lambda = A(\xi) = \iota_\xi A$,

$$\delta_{A(\xi)}A = d\iota_\xi A - i[A, \iota_\xi A] = \mathcal{L}_\xi A - \iota_\xi F. \tag{2.28}$$

Provided that the connection is flat, part of the gauge transformations therefore correspond to coordinate transformations. We have introduced the vielbein formulation of gravity because it exposes the rest of the gauge transformations: they correspond to local Lorentz transformations.

2.2.3   Action for Einstein gravity

We will now show that three-dimensional Einstein gravity with negative cosmological constant corresponds to $so(2, 2)$ Chern–Simons theory [64,65]. In this section, we reproduce the action. In Section 2.2.4, we solve the flatness condition to find the connection corresponding to the global AdS$_3$ metric.

We saw in Section 2.1 that $so(2, 2)$ is the isometry algebra of global AdS$_3$. It is generated by bulk translations T_A and rotations J_A. They satisfy the following commutation relations:

$$[T_A, T_B] = \frac{i}{\ell^2}\epsilon_{AB}{}^C J_C, \quad [J_A, J_B] = i\epsilon_{AB}{}^C J_C, \quad [J_A, T_B] = i\epsilon_{AB}{}^C T_C, \tag{2.29}$$

where $A = (0, 1, 2)$. The parameter ℓ is the radius of curvature. The bulk tangent space metric $\eta_{AB} = \text{diag}(-1, 1, 1)$ is used to raise and lower bulk indices and we

set $\epsilon_{012} = +1$. Since $so(2,2)$ is a semisimple Lie algebra, consisting of two simple $so(2,1)$ factors, it is useful to introduce

$$S_A = \frac{1}{2}(J_A + \ell T_A), \qquad \bar{S}_A = \frac{1}{2}(J_A - \ell T_A). \tag{2.30}$$

These generators satisfy the $so(2,1)$ commutation relations

$$[S_A, S_B] = i\epsilon_{AB}{}^C S_C, \qquad [\bar{S}_A, \bar{S}_B] = i\epsilon_{AB}{}^C \bar{S}_C. \tag{2.31}$$

We can then couple the vielbein E^A and the dual spin connection Ω^A to the translation and rotation generators T_A and J_A to construct a $so(2,2)$ connection $\mathbf{A}$. The latter can be split into two connections A and $\bar{A}$, one for each $so(2,1)$ factor:

$$\mathbf{A} = E^A T_A + \Omega^A J_A = A^A S_A + \bar{A}^A \bar{S}_A,$$
$$A^A = \Omega^A + \frac{1}{\ell} E^A, \quad \bar{A}^A = \Omega^A - \frac{1}{\ell} E^A. \tag{2.32}$$

Finally, to write out the action (2.20) explicitly, we need to choose an invariant bilinear form. For each $so(2,1)$ factor, we have one independent parameter, which we denote by γ_s and $\bar{\gamma}_s$:

$$\langle S_A, S_B \rangle = \frac{1}{2}\gamma_s \eta_{AB}, \quad \langle \bar{S}_A, \bar{S}_B \rangle = -\frac{1}{2}\bar{\gamma}_s \eta_{AB}, \quad \langle S_A, \bar{S}_B \rangle = 0. \tag{2.33}$$

Then the $so(2,2)$ Chern–Simons Lagrangian density splits into two $so(2,1)$ factors:

$$\mathcal{L}_{\mathrm{CS}}[\mathbf{A}] = \left\langle \mathbf{A}, d\mathbf{A} - \frac{2i}{3}\mathbf{A} \wedge \mathbf{A} \right\rangle = \mathcal{L}_{\mathrm{CS}}[A] + \mathcal{L}_{\mathrm{CS}}[\bar{A}],$$
$$\mathcal{L}_{\mathrm{CS}}[A] = \frac{1}{2}\gamma_s \left(\eta_{AB} A^A \wedge dA^B + \frac{1}{3}\epsilon_{ABC} A^A \wedge A^B \wedge A^C \right). \tag{2.34}$$

In terms of the vielbein and spin connection, this gives

$$\mathcal{L}_{\mathrm{CS}} = \frac{\gamma_s + \bar{\gamma}_s}{2\ell} \left(2E^A \wedge d\Omega^B \eta_{AB} + \epsilon_{ABC} E^A \wedge \Omega^B \wedge \Omega^C \right. \tag{2.35}$$
$$\left. + \frac{1}{3\ell^2}\epsilon_{ABC} E^A \wedge E^B \wedge E^C \right)$$
$$+ \frac{\gamma_s - \bar{\gamma}_s}{2} \left(\Omega^A \wedge d\Omega^B \eta_{AB} + \frac{1}{3}\epsilon_{ABC}\Omega^A \wedge \Omega^B \wedge \Omega^C + \frac{1}{\ell^2} E^A \wedge dE^B \eta_{AB} \right.$$
$$\left. + \frac{1}{\ell^2}\epsilon_{ABC} E^A \wedge E^B \wedge \Omega^C \right).$$

The term proportional to $\gamma_s + \bar{\gamma}_s$ reproduces the Einstein–Hilbert Lagrangian from (2.14) with negative cosmological constant $\Lambda = -1/\ell^2$. The term proportional to $\gamma_s - \bar{\gamma}_s$ is also known as the Lorentz–Chern–Simons term. It can be used to construct topologically massive gravity [67, 69]. In the following, we will only consider the Einstein term and set $\gamma_s = \bar{\gamma}_s$. In particular, if we choose

$$\gamma_s = \bar{\gamma}_s = \frac{k}{4\pi}, \qquad k = \frac{\ell}{4G}, \tag{2.36}$$

we reproduce the vielbein form of the Einstein–Hilbert action in (2.16).

2.2.4 Global AdS$_3$ solution

Now let us find the on-shell connection corresponding to the global AdS$_3$ metric. The J_A and T_A components of the equations of motion (2.24) reproduce the torsion-free condition (2.11) and the 3D Einstein equation,

$$0 = dE^A + \epsilon^A{}_{BC}\Omega^B \wedge E^C, \tag{2.37}$$

$$0 = d\Omega^A + \frac{1}{2}\epsilon^A{}_{BC}\left(\Omega^B \wedge \Omega^C + \frac{1}{\ell^2}E^B \wedge E^C\right). \tag{2.38}$$

For a given metric, we can solve the spin connection Ω^A in terms of the corresponding vielbein E^A using the torsion-free condition. The second equation is then a constraint on the curvature of this spin connection. For the global AdS$_3$ metric (2.3), we choose

$$E^0 = \ell\cosh\rho\, dt, \quad E^1 = -\ell\sinh\rho\, d\varphi, \quad E^2 = \ell d\rho. \tag{2.39}$$

Solving (2.37) then leads to

$$\Omega^0 = \cosh\rho\, d\varphi, \quad \Omega^1 = -\sinh\rho\, dt, \quad \Omega^2 = 0. \tag{2.40}$$

Following (2.32), the corresponding $so(2,1)$ connections are

$$A = 2\cosh\rho\, S_0 dx^+ - 2\sinh\rho\, S_1 dx^+ + S_2 d\rho, \tag{2.41}$$

$$\bar{A} = 2\cosh\rho\, \bar{S}_0 dx^- + 2\sinh\rho\, \bar{S}_1 dx^- - \bar{S}_2 d\rho. \tag{2.42}$$

Here we have introduced the null coordinates $x^\pm = \frac{1}{2}(\varphi \pm t)$. In Fefferman–Graham coordinates with $r = e^\rho$ the global AdS$_3$ metric reads

$$ds^2 = \frac{dr^2}{r^2} - \left(r^2 + 2 + r^{-2}\right)\frac{1}{4}dt^2 + \left(r^2 - 2 + r^{-2}\right)\frac{1}{4}d\varphi^2. \tag{2.43}$$

Finally, it will be useful to introduce yet another set of generators. In terms of the $so(2,1)$ generators S_A and $\bar{S}_A$ in (2.30), we define

$$L_{-1} = S_0 + S_1, \qquad L_0 = S_2, \qquad L_1 = S_0 - S_1, \tag{2.44a}$$

$$\bar{L}_{-1} = -(\bar{S}_0 - \bar{S}_1), \qquad \bar{L}_0 = -\bar{S}_2, \qquad \bar{L}_1 = -(\bar{S}_0 + \bar{S}_1). \tag{2.44b}$$

Both sets of generators satisfy the $sl(2,\mathbb{R})$ algebra

$$[L_m, L_n] = i(m-n)L_{m+n}. \tag{2.45}$$

In this basis, the global AdS$_3$ connection (2.41) becomes

$$A = L_0 d\rho + \left(e^\rho L_1 + e^{-\rho} L_{-1}\right) dx^+ = e^{i\rho L_0}\left(id + (L_1 + L_{-1})dx^+\right)e^{-i\rho L_0}, \tag{2.46}$$

$$\bar{A} = \bar{L}_0 d\rho - \left(e^\rho \bar{L}_1 + e^{-\rho} \bar{L}_{-1}\right) dx^- = e^{i\rho \bar{L}_0}\left(id - (\bar{L}_1 + \bar{L}_{-1})dx^-\right)e^{-i\rho \bar{L}_0}.$$

Since the two $sl(2,\mathbb{R})$ sectors commute, we can write this concisely as

$$\mathbf{A}_{AdS_3} = e^{i\rho(L_0 + \bar{L}_0)}\left(id + (L_1 + L_{-1})dx^+ - (\bar{L}_1 + \bar{L}_{-1})dx^-\right)e^{-i\rho(L_0 + \bar{L}_0)}. \tag{2.47}$$

This form of the $so(2,2)$ connection corresponding to the global AdS$_3$ metric will be particularly useful in the following.

2.3 Canonical analysis of Chern–Simons theory

So far, we have mentioned but ignored several important issues with Chern–Simons theory on a manifold with boundary. We will address them in this section.

First, the variational problem is not well defined. To solve this, we impose chiral boundary conditions on the connection.

Second, one needs to be careful with gauge transformations that affect the boundary. Using a Hamiltonian description, we show that a particular class of transformations actually has a *physical* effect: they contribute to charges defined on the boundary of the manifold. In this section, we follow the approach of Bañados [70], see also [71–73] for earlier work.

2.3.1 Variational problem

In Section 2.2.4, we found the flat connection $\mathbf{A}$ corresponding to global AdS$_3$ by solving $\mathbf{F} = 0$. However, we still need to do some work to show that this is actually the equation of motion of Chern–Simons theory on a manifold with boundary.

We can see from the conformal compactification in (2.6) that global AdS$_3$ is topologically a solid cylinder. The following discussion is not particular to $so(2,2)$, so we will revert to the conventions used in Section 2.2.2 and use A to denote a general connection with curvature F, both of which are valued in an arbitrary Lie algebra $\mathfrak{g}$. On the other hand, we keep the topology of AdS$_3$ and place our theory on a solid cylinder, which we denote by M. Varying the Chern–Simons action then gives

$$\delta S_{\mathrm{CS}} = 2 \int_M \langle \delta A, F \rangle + \int_{\partial M} \langle A, \delta A \rangle. \tag{2.48}$$

To conclude that $F = 0$ specifies a minimum of the action, the boundary term must vanish. Generically, there is no reason that it should. In fact, a similar issue arises in most field theories but we usually just require the fields to fall off quickly enough so that the boundary term vanishes. Since the Chern–Simons action is first order in derivatives, such a strategy would now require us to set A to zero at ∂M. This is a bad idea: as we can see from the connection in (2.41), it would rule out global AdS$_3$ as a solution!

Instead, we will impose *chiral* boundary conditions on A. We use coordinates $x^\pm = \frac{1}{2}(\varphi \pm t)$ on the boundary ∂M and parametrize the transverse direction by ρ. Then we can expand the connection A as follows,

$$A = A_\rho d\rho + A_- dx^- + A_+ dx^+. \tag{2.49}$$

Thus, we can also make sure that the boundary term in (2.48) vanishes by choosing

$$\boxed{A_-|_{\partial M} = 0} \tag{2.50}$$

$$\Downarrow$$

$$\langle A, \delta A \rangle|_{\partial M} = \left(\langle A_+, \delta A_- \rangle - \langle A_-, \delta A_+ \rangle \right) dx^+ \wedge dx^- \big|_{\partial M} = 0. \tag{2.51}$$

With this choice, the variational principle is well defined and $F = 0$ is indeed the equation of motion. More complicated boundary conditions would allow us to construct a boundary phase space with nontrivial chemical potentials [74, 75], but we will not consider those here.

Split algebra and chirality While (2.50) solves the variational problem, we typically do not want to set the dx^- component to zero for the entire connection. Let us illustrate this for the $so(2, 2)$ connection $\mathbf{A}$. As we can see from (2.32), setting $\mathbf{A}_- = 0$ would mean that the vielbein E^A cannot contain dx^- components. Then the resulting metric is degenerate in the x^- coordinate, which is clearly undesirable.

However, if the algebra in which the connection is valued splits into multiple factors, one can impose chiral boundary conditions and still have a nondegenerate metric. For Einstein gravity with negative cosmological constant,

$$so(2, 2) \simeq sl(2, \mathbb{R}) \oplus sl(2, \mathbb{R}). \tag{2.52}$$

Then we can demand that the dx^+ respectively the dx^- component of either factor vanishes. In other words, we can choose opposite chiralities in the $sl(2, \mathbb{R})$ factors,

$$L_a dx^+, \qquad \bar{L}_a dx^-. \tag{2.53}$$

This choice is compatible with the global AdS_3 background connection (2.47). With these boundary conditions, the connection in (2.47) is indeed a solution of a well-defined variational problem. We will be able to choose similar chiral boundary condition for all algebras considered in this thesis.

2.3.2 Improved generator of gauge transformations

Next, we will analyze the boundary behavior of gauge transformations. To do this, we will use the Hamiltonian formalism. The Regge-Teitelboim method [76] of constructing boundary charges was first applied to Chern–Simons theory by Bañados [70, 77]. For a nice introduction to constraints and boundary charges in Hamiltonian theories, see [78]. This discussion is somewhat technical, but the result will be worthwhile: we will obtain a general expression for boundary charges in Chern–Simons theory, which is valid for *any* gauge algebra.

Since M is a cylinder, we can foliate it using spatial disks Σ. Up to boundary terms, the Hamiltonian form of the action (2.20) is then given by

$$S_{\mathrm{CS}} = \int dt \int_\Sigma d^2 x \, \epsilon^{ij} \kappa_{ab} \left(\dot{A}_i^a A_j^b + A_t^a F_{ij}^b \right). \tag{2.54}$$

Here, we have written out the form components on Σ using the indices i, j, which run over the spatial coordinates ρ and φ. We use the convention $\epsilon^{\rho\varphi} = +1$.

The first term in the bulk action determines the Poisson brackets,[1]

$$\left\{A_i^a(x), A_j^b(y)\right\} = \kappa^{ab}\epsilon_{ij}\delta(x-y). \tag{2.55}$$

The phase space variables are the spatial components A_φ and A_ρ. They are each other's conjugate variables. The time component A_t has no conjugate variable. Instead, it should be interpreted as a Lagrange multiplier implementing the constraint $F_{\rho\varphi} = 0$, which demands that the connection is flat on Σ. To be precise, the equations of motion from varying A_t and A_i in (2.54) are

$$F_{\rho\varphi} = 0, \qquad \dot{A}_i = D_i A_t = \partial_i A_t - i[A_i, A_t]. \tag{2.56}$$

We now follow the presentation in [78]. In Hamiltonian mechanics, constraints generate gauge transformations. Given a Lie algebra-valued function Λ, the obvious choice for a generator of the gauge transformations associated to the constraint $F_{\rho\varphi} = 0$ would be

$$G_0[\Lambda] = \int_\Sigma \langle \Lambda, F \rangle. \tag{2.57}$$

Its action on the phase space variables can be determined by computing

$$\{G_0[\Lambda], A_i^a(x)\} = -\epsilon_{ij}\kappa^{ab}\frac{\delta G_0[\Lambda]}{\delta A_j^b(x)} \tag{2.58}$$

However, this functional derivative is not well defined! Varying $G_0[\Lambda]$ with respect to A_j^b gives a boundary term:

$$\delta G_0[\Lambda] = 2\int_\Sigma d^2x\,\epsilon^{ij}\kappa_{ab}\Lambda^a\left[\partial_i\delta A_j^b + f_{cd}{}^b A_i^c \delta A_j^d\right] \tag{2.59}$$

$$= -2\int_\Sigma d^2x\,\epsilon^{ij}\kappa_{ab}\left(\partial_i\Lambda^a - i[A_i,\Lambda]^a\right)\delta A_j^b \tag{2.60}$$

$$+ 2\int_\Sigma d^2x\,\epsilon^{ij}\partial_i\left(\kappa_{ab}\Lambda^a\delta A_j^b\right).$$

The first term is just the covariant derivative of the gauge parameter with respect to the Chern–Simons connection. This leads to the correct gauge transformation (2.26),

$$\delta_\Lambda A_i^a = D_i\Lambda^a = \partial_i\Lambda^a - i[A_i,\Lambda]^a. \tag{2.61}$$

However, the second term corresponds to a boundary term,

$$2\int_\Sigma d^2x\,\epsilon^{ij}\partial_i\left(\kappa_{ab}\Lambda^a\delta A_j^b\right) = 2\oint_{\partial\Sigma}\langle\Lambda,\delta A\rangle. \tag{2.62}$$

---

[1] A more careful derivation of this Poisson bracket proceeds as follows. One can introduce abstract conjugate momenta π_a^μ satisfying the usual Poisson bracket relations with A_μ^a and *constrain* them to be equal to the result of deriving the action with respect to $\dot{A}_\mu^a$. Following for example [79] or appendix A of [80], one sees that these constraints are second class. The Dirac bracket on the reduced phase space then reproduces the Poisson bracket in (2.55).

The presence of this boundary term in the variation of $G_0[\Lambda]$ means that the Poisson bracket in (2.55) is not well defined! We encountered a similar problem when varying the action in (2.48). In this case, however, we can solve it in a different way. Rather than restricting the set of connections further, we can now introduce a *compensating* boundary term: we replace the generator $G_0[\Lambda]$ by

$$G[\Lambda] = G_0[\Lambda] + Q[\Lambda]. \tag{2.63}$$

Here, $Q[\Lambda]$ is a boundary integral, which is required to satisfy

$$\delta Q[\Lambda] = -2 \oint_{\partial \Sigma} \langle \Lambda, \delta A \rangle. \tag{2.64}$$

With this requirement, the Poisson bracket of the improved generator $G[\Lambda]$ is well defined. It is the proper generator of gauge transformations in the Hamiltonian theory.

At this point, recall that the original generator $G_0[\Lambda]$ is proportional to the bulk flatness constraint, By construction, this means that it vanishes for on-shell connections. However, this is *not* necessarily true for the improved generator! For specific combinations of A and Λ, the boundary term $Q[\Lambda]$ may be nonzero even on shell. These are the *boundary charges* we were after. They will allow us to make a physical distinction between flat connections based on their boundary behavior.

Finally, note that it is not immediately obvious how we can use (2.64) to determine $Q[\Lambda]$. To integrate this expression, we need to specify what variations of A are allowed on $\partial \Sigma$. At the very least, we need to respect the boundary condition $A_-|_{\partial \Sigma} = 0$. In Section 2.4, we will see that this leads to an integrable expression. After that, we will see in Section 2.5 that it is also possible to impose *further* constraints on the boundary behavior of the connection and still obtain integrable charges.

2.4 Wess–Zumino–Witten phase space

The purpose of this section is to work out the boundary symmetries associated to Chern–Simons theory with chiral boundary conditions. First, we use part of the gauge symmetries generated by $G[\Lambda]$ to reach a convenient gauge fixing in the bulk. After imposing the constraint $F_{\rho\varphi} = 0$, we see that the remaining boundary symmetries are those of a chiral Wess–Zumino–Witten model [81, 82].

In fact, with chiral boundary conditions, the Chern–Simons action reduces to the chiral Wess–Zumino–Witten (WZW) action at the boundary. (We do not work this out here, but see for example [83] for a review.) For this reason, we will refer to the on-shell, gauge-fixed set of connections as the WZW phase space. To close this section, we work out the example of $so(2,2)$ Chern–Simons theory corresponding to Einstein gravity with a negative cosmological constant.

2.4.1 Gauge fixing and flatness

We can use the gauge transformations generated by $G[\Lambda]$ to set A_ρ to a constant on all of Σ. It will be convenient to choose the parametrization

$$A_\rho = ib(\rho)^{-1}\partial_\rho b(\rho). \tag{2.65}$$

In principle, this constant can be any vector in the Lie algebra. However, we will often have a reference connection in mind, such as the global AdS_3 connection in (2.47), which gives us a natural choice for A_ρ. We will work out the $so(2,2)$ example in Section 2.4.3. To show that the gauge choice in (2.65) is allowed, we follow the argument given in [84]: starting from an arbitrary connection A', its radial component transforms under a finite gauge transformation (2.25) as

$$A'_\rho \to A_\rho = iU^{-1}\partial_\rho U + U^{-1}A'_\rho U. \tag{2.66}$$

Then choose the parameter $U = Vb$, so that requiring $A_\rho = ib^{-1}\partial_\rho b$ means

$$i\partial_\rho V = -A'_\rho V. \tag{2.67}$$

We can solve this for V by exponentiating,

$$V = \mathcal{P}e^{i\int_{\rho_0}^{\rho} A'_\rho d\rho'} V_0. \tag{2.68}$$

Here, ρ_0 is an arbitrary initial point and $\mathcal{P}$ denotes path ordering. We can choose ρ_0 and V_0 such that U is the unit element at the boundary and the gauge transformation preserves our chiral boundary condition $A_-|_{\partial M} = 0$.

Next, we can impose the constraint $F_{\rho\varphi} = 0$ itself. Since A_ρ is now constant on Σ, $\partial_\varphi A_\rho$ vanishes. Then the constraint is

$$F_{\rho\varphi} = \partial_\rho A_\varphi - i[A_\rho, A_\varphi] = \partial_\rho A_\varphi - iA_\rho A_\varphi + iA_\varphi A_\rho = 0. \tag{2.69}$$

To solve this equation, plug in $A_\rho = ib^{-1}\partial_\rho b$ and multiply by $b(\cdot)b^{-1}$,

$$b\left(\partial_\rho A_\varphi\right)b^{-1} + \left(\partial_\rho b\right)A_\varphi b^{-1} - bA_\varphi b^{-1}\left(\partial_\rho b\right)b^{-1} = \partial_\rho\left(bA_\varphi b^{-1}\right) = 0. \tag{2.70}$$

This shows that all the ρ-dependence in A_φ is now determined by $b(\rho)$ as well! Thus we can describe A_φ using $b(\rho)$ and a ρ-*independent* connection $a_\varphi(t,\varphi)$,

$$A_\varphi = b(\rho)^{-1}a_\varphi(t,\varphi)b(\rho). \tag{2.71}$$

The equations of motion $\dot{A}_i = D_i A_t$ then imply that we can write any on-shell connection in terms of a *single* Lie algebra-valued function of x^+,

$$\boxed{A = b(\rho)^{-1}\left(id + a_+(x^+)dx^+\right)b(\rho).} \tag{2.72}$$

In the following, we will see that all remaining degrees of freedom parametrized by $a_+(x^+)$ are physical: they can be measured using the boundary charges $Q(\Lambda)$. We will sometimes refer to a as the *reduced* connection.

2.4.2 Residual transformations and symmetries

The gauge-fixed, on-shell connection (2.72) still has residual symmetries: it is preserved by gauge transformations of the form $\Lambda = b(\rho)\lambda(x^+)b^{-1}(\rho)$. Under such a gauge transformation, the reduced connection a transforms as

$$\delta_\lambda a = d\lambda - i[a, \lambda]. \tag{2.73}$$

The fact that the residual symmetries of (2.72) take such a clean form simplifies our analysis greatly. Once we have agreed on a choice of A_ρ, we only have to concern ourselves with the reduced connection $a_+(x^+)dx^+$ and its residual symmetries parametrized by $\lambda(x^+)$. Indeed, the radial dependence also drops out of the boundary charges in (2.74):

$$\delta Q[\Lambda] = \delta Q_\lambda = -2 \oint_{\partial\Sigma} \langle \lambda, \delta_\lambda a \rangle. \tag{2.74}$$

Since λ does not depend on a, these boundary charges are integrable. They satisfy

$$\{Q_\lambda, Q_\mu\} = \delta_\lambda Q_\mu = -2 \oint_{\partial\Sigma} \langle \mu, \delta_\lambda a \rangle = -iQ_{[\lambda,\mu]} + 2 \oint_{\partial\Sigma} \langle \lambda, d\mu \rangle. \tag{2.75}$$

Using our conventional basis T_a for the Lie algebra $\mathfrak{g}$, we can expand

$$\boxed{a_+(x^+) = F^a(x^+)T_a.} \tag{2.76}$$

The components of the invariant bilinear metric are given by $\kappa_{ab} = \langle T_a, T_b \rangle$ and the structure constants $f_{ab}{}^c$ satisfy $[T_a, T_b] = if_{ab}{}^c T_c$. With these conventions, the Poisson bracket of the currents $F^a(x^+)$ is given by

$$\boxed{\{F^a(x^+), F^b(y^+)\} = -\frac{1}{2}f^{ab}{}_c F^c(x^+)\delta(x^+ - y^+) + \frac{1}{2}\partial_{x^+}\delta(x^+ - y^+)\kappa^{ab}.} \tag{2.77}$$

This is the affine algebra $\hat{\mathfrak{g}}$ based on the Chern–Simons algebra $\mathfrak{g}$, with an extension determined by the invariant bilinear form. Indeed, as can be verified by substituting (2.72) in the Chern–Simons action, the components $F^a(x^+)$ in (2.76) are the currents of a chiral Wess–Zumino–Witten model. These currents parametrize the full classical phase space of Chern–Simons theory with chiral boundary conditions.

2.4.3 WZW phase space for Einstein gravity

Now let us work out the phase space of $so(2, 2)$ Chern–Simons theory as an example, using the $sl_2(\mathbb{R}) \oplus sl_2(\mathbb{R})$ basis introduced in (2.44). In equation (2.47) we saw that the connection corresponding to global AdS$_3$ is given by

$$\mathbf{A}_{AdS_3} = e^{i\rho(L_0+\bar{L}_0)}\left(id + (L_1 + L_{-1})dx^+ - (\bar{L}_1 + \bar{L}_{-1})dx^-\right)e^{-i\rho(L_0+\bar{L}_0)}.$$

This motivates the following choice for the radial component:

$$\mathbf{A}_\rho = L_0 + \bar{L}_0, \qquad b(\rho) = e^{-i\rho L_0}, \quad \bar{b}(\rho) = e^{-i\rho\bar{L}_0}. \tag{2.78}$$

Following (2.53), we choose chiral boundary conditions such that

$$L_a dx^+, \qquad \bar{L}_a dx^-.$$

Then we can write the full chiral gauge-fixed on-shell Chern–Simons connection (2.72) corresponding to Einstein gravity with negative cosmological constant as

$$\mathbf{A} = e^{i\rho(L_0+\bar{L}_0)} \left(id + F^a(x^+)L_a dx^+ + \bar{F}^a(x^-)\bar{L}_a \, dx^- \right) e^{-i\rho(L_0+\bar{L}_0)}. \qquad (2.79)$$

It is instructive to see what this corresponds to in terms of metric data. For that, let us expand (2.79) and write it in terms of the $so(2,1)$ generators S_A and $\bar{S}_A$ in (2.30),

$$\begin{aligned}
\mathbf{A} = & \left(L_0 + \bar{L}_0\right) d\rho + \left(e^\rho F^+ L_1 + F^0 L_0 + e^{-\rho} F^- L_{-1}\right) dx^+ \\
& + \left(e^\rho \bar{F}^+ \bar{L}_1 + \bar{F}^0 \bar{L}_0 + e^{-\rho} \bar{F}^- \bar{L}_{-1}\right) dx^- \\
= & \left(d\rho + F^0 dx^+\right) S_2 + \left(-d\rho - \bar{F}_0 dx^-\right) \bar{S}_2 \\
& + \left(e^\rho F^+ dx^+ + e^{-\rho} F^- dx^+\right) S_0 + \left(-e^\rho F^+ dx^+ + e^{-\rho} F^- dx^+\right) S_1 \\
& + \left(-e^\rho \bar{F}^+ dx^- - e^{-\rho} \bar{F}^- dx^-\right) \bar{S}_0 + \left(-e^\rho \bar{F}^+ dx^- + e^{-\rho} \bar{F}^- dx^-\right) \bar{S}_1.
\end{aligned} \qquad (2.80)$$

We can then use the relation to J_A and P_A in (2.30) to write down the vielbein and spin connection corresponding to (2.79):

$$E^0 = \frac{\ell}{2} \left(e^\rho \left(F^+ dx^+ + \bar{F}^+ dx^-\right) + e^{-\rho} \left(F^- dx^+ + \bar{F}^- dx^-\right) \right), \qquad (2.81a)$$

$$E^1 = \frac{\ell}{2} \left(-e^\rho \left(F^+ dx^+ - \bar{F}^+ dx^-\right) + e^{-\rho} \left(F^- dx^+ - \bar{F}^- dx^-\right) \right), \qquad (2.81b)$$

$$E^2 = \ell \left(d\rho + \frac{1}{2} F^0 dx^+ + \frac{1}{2} \bar{F}^0 dx^- \right), \qquad (2.81c)$$

$$\Omega^0 = \frac{1}{2} \left(e^\rho \left(F^+ dx^+ - \bar{F}^+ dx^-\right) + e^{-\rho} \left(F^- dx^+ - \bar{F}^- dx^-\right) \right), \qquad (2.81d)$$

$$\Omega^1 = \frac{1}{2} \left(-e^\rho \left(F^+ dx^+ + \bar{F}^+ dx^-\right) + e^{-\rho} \left(F^- dx^+ + \bar{F}^- dx^-\right) \right), \qquad (2.81e)$$

$$\Omega^2 = \frac{1}{2} \left(F^0 dx^+ - \bar{F}^0 dx^- \right). \qquad (2.81f)$$

All these vielbeins correspond to locally AdS$_3$ geometries. There are two affine $sl_2(\mathbb{R})$ algebras of boundary charges, whose Poisson bracket is given by (2.77).

To reproduce the Brown–Henneaux Virasoro algebra mentioned in Section 1.4.2, we have to make sure that the metric at the conformal boundary is *fixed*. In other words, up to Weyl rescaling, we impose *Dirichlet boundary conditions* on the metric. We can do this by setting the leading-order behavior of E^0 and E^1 to be equal to the AdS$_3$ vielbeins in (2.39). This corresponds to imposing the constraints

$$\boxed{F^+ \equiv 1, \quad \bar{F}^+ \equiv -1.} \qquad (2.82)$$

As we will now show, these constraints *reduce* the affine $sl_2(\mathbb{R})$ algebra to the Brown–Henneaux Virasoro symmetries, including the correct central charge.

2.5 Drinfeld–Sokolov reduction

So far, we have seen that Chern–Simons theory with chiral boundary conditions leads to affine WZW boundary charges. Requiring that the bulk connections correspond to asymptotically AdS$_3$ geometries with Dirichlet boundary conditions leads to the additional constraints (2.82). We will show that the reduced phase space has a *classical* Virasoro symmetry algebra corresponding to the Brown–Henneaux symmetries. Although we will not describe it here, this classical reduction can also be carried out [85] on the level of the action, which leads to Liouville theory. The general procedure which we will now describe is known as *Drinfeld–Sokolov reduction*, after its origins [86] in the study of integrable systems. We first work out the reduction of the affine $sl_2(\mathbb{R})$ algebra under the constraints in (2.82).

In the context of WZW models, Drinfeld–Sokolov reduction was first used [87] to study higher-spin generalizations of Virasoro symmetries known as $\mathcal{W}$-algebras. These arise if the reduction procedure is applied to $sl_N(\mathbb{R})$ with a specific $sl_2(\mathbb{R})$ embedding. Multiple embeddings exist, and we review how the resulting $\mathcal{W}$-symmetry depends on it. Following [84], we then work out explicitly the classical reduction of the affine $sl_3(\mathbb{R})$ algebra that leads to $\mathcal{W}_3$ symmetry.

For a general review on $\mathcal{W}$-algebras, see [88]. We will only study the Drinfeld–Sokolov reduction at a classical level, which is reviewed in [89, 90]. Quantum versions of the reduction of the symmetry algebra [91] and actions [72] also exist. Starting with [84, 92], the Chern–Simons approach to $\mathcal{W}$-symmetries has also found application in higher spin holography, see [93, 94] for a review.

2.5.1 Virasoro from $sl_2(\mathbb{R})$

In the following, we will focus on one particular $sl_2(\mathbb{R})$ factor of $so(2,2)$. For simplicity, we denote the relevant coordinate by φ. Imposing the asymptotically AdS$_3$ constraint (2.82), the reduced connection (2.76) is restricted to

$$a_\varphi = L_+ + F^0 L_0 + F^- L_-. \tag{2.83}$$

Now gauge transformations $\lambda = \lambda^a L_a$ can no longer be arbitrary: they have to leave $F^+ \equiv 1$ invariant. We can determine the allowed transformations by solving

$$0 = \delta_\lambda F^+ = \partial\lambda^+ - i[a_\varphi, \lambda]^+ = \partial\lambda^+ + \lambda^0 - F^0\lambda^+. \tag{2.84}$$

This is solved by

$$\lambda^0 = -\partial\lambda^+ + \lambda^+ F^0. \tag{2.85}$$

As we see, the gauge parameter λ now depends on the components of the connection. It is therefore not obvious that the infinitesimal charge δQ_λ defined in (2.74)

is integrable. So let's write it out explicitly:

$$\delta Q_\lambda = -2 \oint d\varphi \, \langle \lambda, \delta a_+ \rangle$$

$$= -2\gamma_s \oint d\varphi \left(-\lambda^+ \delta F^- + \frac{1}{2}\lambda^0 \delta F^0 \right) \tag{2.86}$$

$$= -2\gamma_s \oint d\varphi \left(-\lambda^+ \delta F^- + \frac{1}{2} \left(-\partial\lambda^+ + \lambda^+ F^0 \right) \delta F^0 \right) \tag{2.87}$$

In the second step, we plugged in λ^0 from (2.85). This charge is integrable! Using λ^+ as a parameter, we can write it as a total variation:

$$\delta Q_\lambda = \oint d\varphi \, \lambda^+ \delta T, \qquad T = 2\gamma_s \left(F^- - \frac{1}{4}(F^0)^2 - \frac{1}{2}\partial F^0 \right). \tag{2.88}$$

We denote the corresponding finite charges using

$$Q^{\mathrm{Vir}}[\lambda^+] = \oint d\varphi \, \lambda^+ T. \tag{2.89}$$

We see that the λ^- parameter drops out entirely. Since λ^0 is fixed, the only meaningful transformation parameter seems to be λ^+. Indeed, we will see that T transforms as a Virasoro current under the transformations generated by λ^+.

Invariant polynomial and gauge fixing For future purposes, it is useful to rederive the current T we just encountered in another way. The constraint $F^+ \equiv 1$ generates gauge transformations in the phase space (2.83) which is parametrized by the functions F^0 and F^-. Using the Poisson bracket in (2.77), we see that these functions transform as follows:

$$\delta_\Lambda F^0(\varphi) = \int d\psi \left\{ \Lambda(\psi)(F^+(\psi) - 1), F^0(\varphi) \right\}$$

$$= \frac{1}{\gamma_s}\Lambda(\varphi)F^+(\varphi) \equiv \frac{1}{\gamma_s}\Lambda(\varphi), \tag{2.90a}$$

$$\delta_\Lambda F^-(\varphi) = \int d\psi \left\{ \Lambda(\psi)(F^+(\psi) - 1), F^-(\varphi) \right\}$$

$$= \frac{1}{2\gamma_s} \left(\Lambda(\varphi)F^0(\varphi) + \partial_\varphi \Lambda(\varphi) \right). \tag{2.90b}$$

Here we have introduced a parameter $\Lambda(\varphi)$ for the gauge transformations generated by $F^+ \equiv 1$. First, notice that the combination we encountered in (2.88) is *invariant* under these transformations. For that reason, we are not *forced* to fix the gauge transformations coming from $F^+ \equiv 1$ and we can just work with the 'invariant current' T, which is a well-defined quantity on the reduced phase space.

Alternatively, we can use these transformations to *gauge fix* part of the remaining phase space variables. As we can see from (2.90a), we can set $F^0(\varphi)$ to zero by choosing $\Lambda(\varphi) = -\gamma_s F^0(\varphi)$.

Both approaches will be useful in the following. For larger algebras, such as the $sl_3(\mathbb{R})$ examples that we will study next, any gauge fixing we can do will greatly simplify the computations. On the other hand, we will consider *contractions* of the Chern–Simons algebra in Chapter 3. To make sure that none of the limits we take are singular, it will be useful to work with the invariant currents there.

Current transformations and Virasoro algebra Under the allowed transformation specified by (2.85), the connection components transform as

$$\delta F^0 = \lambda^+\partial F^0 + F^0\partial\lambda^+ - \partial^2\lambda^+ + 2\lambda^- - 2F^-\lambda^+,$$
$$\delta F^- = \partial\lambda^- + F^-\partial\lambda^+ - F^-F^0\lambda^+ + F^0\lambda^-. \tag{2.91}$$

The current defined in (2.88) then transforms as a Virasoro current,

$$\delta T = \lambda^+\partial T + 2T\partial\lambda^+ + \gamma_s\partial^3\lambda^+. \tag{2.92}$$

We can compute the Poisson bracket of the charges as follows,

$$\begin{aligned}
\{Q_\lambda, Q_\mu\} = \delta_\lambda Q_\mu &= -2\oint d\varphi\,\langle\mu,\delta_\lambda a_+\rangle = \oint d\varphi\,\mu^+\delta_\lambda T \\
&= \oint d\varphi\,\mu^+\left(\lambda^+\partial T + 2T\partial\lambda^+ + \gamma_s\partial^3\lambda^+\right) \\
&= Q^{\text{Vir}}\left[\mu^+\partial\lambda^+ - \lambda^+\partial\mu^+\right] + \gamma_s\oint d\varphi\,\mu^+\partial^3\lambda^+. \tag{2.93}
\end{aligned}$$

Indeed, this is the Virasoro charge algebra! To obtain the usual expression in terms of the Fourier modes of these charges, we can expand

$$T(\varphi) = -\frac{1}{2\pi}\sum_n L_n e^{-in\varphi}. \tag{2.94}$$

Note that we assume that the current is a 2π-periodic functions. The generators are obtained by choosing the corresponding Fourier modes as symmetry parameter,

$$L_n = -\oint d\varphi\,e^{in\varphi}\,T(\varphi) = -Q^{\text{Vir}}[e^{in\varphi}]. \tag{2.95}$$

Then the Poisson bracket in (2.93) leads to the following Poisson brackets and commutators for the Fourier modes,

$$\{L_m, L_n\} = -i(m-n)L_{m+n} - 2\pi i\gamma_s m^3\delta_{m+n,0}, \tag{2.96}$$
$$[L_m, L_n] = i\{L_m, L_n\} = (m-n)L_{m+n} + 2\pi\gamma_s m^3\delta_{m+n,0}, \tag{2.97}$$

As we found in (2.36), our definition of the bilinear form is related to the usual Chern–Simons level by $\gamma_s = k/4\pi$, and Einstein gravity corresponds to $k = \ell/4G$. Therefore, the above reproduces the Brown–Henneaux central charge:

$$c = 24\pi\gamma_s = 6k = \frac{3\ell}{2G}. \tag{2.98}$$

After shifting $L_m \to L_m + c\delta_{m,0}/24$, we get

$$[L_m, L_n] = (m-n)L_{m+n} + \frac{c}{12}m(m^2-1)\delta_{m+n,0}. \qquad (2.99)$$

This is the Virasoro algebra of AdS$_3$ asymptotic symmetries that we wrote down in Section 1.4.2. The other $sl_2(\mathbb{R})$ factor in $so(2,2)$ leads to another Virasoro algebra with the same central charge. Thus we have seen how the boundary charges of Einstein gravity with negative cosmological constant can be reproduced using a Drinfeld–Sokolov reduction of the asymptotic symmetries of $so(2,2)$ Chern–Simons.

2.5.2 General $\mathcal{W}$-algebras from $sl_N(\mathbb{R})$

So far, we have mainly been concerned with Einstein gravity, which corresponds to two chiral $sl_2(\mathbb{R})$ connections. However, other theories of gravity can also be described using a Chern–Simons formulation. We will now look at $sl_N(\mathbb{R})$ theories, which have been extensively studied in the context of current algebras and higher spin gravity, see for example [74, 84, 89–92, 95–98].

In addition to a spin two metric field, which corresponds to a $sl_2(\mathbb{R})$ subalgebra, the $sl_N(\mathbb{R})$ Chern–Simons theories describe additional fields with corresponding boundary charges. The coupling of these charges to the Virasoro charges associated to the metric sector depends heavily on the *embedding* of the $sl_2(\mathbb{R})$ algebra in the full $sl_N(\mathbb{R})$ algebra.

Given a set of $sl_2(\mathbb{R})$ generators $L_a \in sl_N(\mathbb{R})$, we can impose chiral boundary conditions and gauge fix the radial component as in (2.65),

$$A_-|_{\partial M} = 0, \qquad A_\rho = L_0 \in sl_N. \qquad (2.100)$$

Let us denote the $sl_N(\mathbb{R})$ generators by T_a. Again, for simplicity we denote the remaining boundary coordinate (in this case x^+) using φ. With this choice, the full gauge-fixed on-shell connection in (2.72) becomes

$$A = e^{i\rho L_0} \left(id + J^a(\varphi)T_a d\varphi \right) e^{-i\rho L_0}. \qquad (2.101)$$

To obtain an asymptotically AdS$_3$ metric, we should now impose boundary conditions similar to (2.82). For this, it is useful to organize the $sl_N(\mathbb{R})$ basis in multiplets of the $sl_2(\mathbb{R})$ subalgebra corresponding to L_a. The radial falloff of a current component J^a in the connection is then determined by the weight of the corresponding generator T^a under L_0. To be precise, if $[L_0, T_a] = iw_{(a)}T_a$, we see that the T_a component of A_φ is

$$A_z|_{T_a} T_a = J^a(\varphi) e^{i\rho L_0} T_a e^{-i\rho L_0} = e^{-w_{(a)}\rho} J^a(\varphi) T_a. \qquad (2.102)$$

Thus, if we fix the leading part of the connection in terms of the global AdS$_3$ connection (2.2.4), we constrain all the current components J^a of $w_{(a)} < 0$ generators,

$$\boxed{J^{L_+} \equiv 1 \quad \& \quad J^{T_a} \equiv 0 \quad \text{for all other negative weight generators } T_a.} \qquad (2.103)$$

These constraints generate additional gauge freedom, which can be used to fix all but the highest weight currents of each multiplet to zero. We will demonstrate this explicitly for one example in Section 2.5.3. This brings us to what is usually known as highest-weight or Drinfeld–Sokolov gauge, with a single current for each $sl_2(\mathbb{R})$ multiplet.

At this point, it is useful to introduce a more algebraic perspective on the embeddings and the corresponding multiplet structure (see for example [91, 96]). The possible decompositions of the $sl_N(\mathbb{R})$ fundamental representation are labeled by partitions λ of N,

$$\mathbf{N}_N = \bigoplus_{k=1}^{N} n_k \mathbf{k_2} \qquad \longleftrightarrow \qquad \lambda: \quad N = \sum n_k. \qquad (2.104)$$

Here, we use $\mathbf{k}_M$ to denote a k-dimensional fundamental representation of $sl_M(\mathbb{R})$. We are interested in the multiplet structure of $sl_N(\mathbb{R})$ under the adjoint action of its $sl_2(\mathbb{R})$ subalgebra. Through the corresponding decomposition $N = \sum n_k$ in (2.104), the choice of partition λ determines the number of $sl_2(\mathbb{R})$ multiplets in the adjoint representation of $sl_N(\mathbb{R})$. For example, if $N = 3$ we can choose $3 = 3$, $3 = 2 + 1$ or $3 = 1 + 1 + 1$, corresponding to

$$\mathbf{3}_3 = \mathbf{3}_2 \qquad \Longrightarrow \qquad \mathbf{3}_3 \otimes \bar{\mathbf{3}}_3 - \mathbf{1}_2 = \mathbf{5}_2 \oplus \mathbf{3}_2, \qquad (2.105)$$

$$\mathbf{3}_3 = \mathbf{2}_2 \oplus \mathbf{1}_2 \qquad \Longrightarrow \qquad \mathbf{3}_3 \otimes \bar{\mathbf{3}}_3 - \mathbf{1}_2 = \mathbf{3}_2 \oplus 2\,\mathbf{2}_2 \oplus \mathbf{1}_2, \qquad (2.106)$$

$$\mathbf{3}_3 = \mathbf{1}_2 \oplus \mathbf{1}_2 \oplus \mathbf{1}_2 \qquad \Longrightarrow \qquad \mathbf{3}_3 \otimes \bar{\mathbf{3}}_3 - \mathbf{1}_2 = 8\,\mathbf{1}_2. \qquad (2.107)$$

These partitions correspond to the principal, diagonal and trivial embedding of $sl_2(\mathbb{R})$ in $sl_3(\mathbb{R})$, respectively.

The residual symmetries of the affine $sl_N(\mathbb{R})$ WZW model constrained by (2.103) for the first two decompositions are the $\mathcal{W}_3$ algebra [87, 95] and $\mathcal{W}_3^{(2)}$ Polyakov-Bershadsky algebra [99], respectively. In addition to the Virasoro current, the former contains a spin three current, while the latter comes with two spin 3/2 and a spin one current. In the final decomposition, no positive radial weights appear so no constraints are imposed and we are still left with the full affine $sl_3(\mathbb{R})$ current algebra.

2.5.3 $\mathcal{W}_3$ from principal embedding in $sl_3(\mathbb{R})$

We now work out the Drinfeld–Sokolov reduction explicitly for $sl_3(\mathbb{R})$ with respect to the principal $sl_2(\mathbb{R})$ embedding following [84]. We take the generators L_a for the sl_2 subgroup and W_b for the remaining generators, where $a = -1, 0, 1$ and $b = -2, \ldots, 2$. They satisfy the following commutation relations,

$$[L_m, L_n] = i(m - n)L_{m+n}, \qquad (2.108a)$$

$$[L_m, W_n] = i(2m - n)W_{m+n}, \qquad (2.108b)$$

$$[W_m, W_n] = \frac{i\sigma}{3}(m - n)(2m^2 + 2n^2 - mn - 8)L_{m+n}. \qquad (2.108c)$$

Here, $\sigma < 0$ corresponds to the normalization of the W_b generators, which we can keep arbitrary. The bilinear form for the $sl_2(\mathbb{R})$ sector is

$$\langle L_0, L_0 \rangle = \frac{\gamma_s}{2}, \quad \langle L_+, L_- \rangle = -\gamma_s. \tag{2.109}$$

For the W_a sector, it is

$$\langle W_{+2}, W_{-2} \rangle = -4\sigma\gamma_s, \quad \langle W_{+1}, W_{-1} \rangle = \sigma\gamma_s, \quad \langle W_0, W_0 \rangle = -\frac{2\sigma\gamma_s}{3}. \tag{2.110}$$

Following (2.103), we see that there are now *three* asymptotically AdS$_3$ constraints:

$$F^{L_+} \equiv 1, \qquad F^{W_{+2}} \equiv 0, \qquad F^{W_{+1}} \equiv 0. \tag{2.111}$$

Due to the large amount of generators, it will be convenient to use the gauge transformations coming from these constraints to set some of the currents to zero. Let us denote the parameters corresponding to the three constraints by Λ, Ω_2 and Ω_1 respectively. We will only gauge fix currents if their variation is proportional to F^{L_+}, since we know that current does not vanish for any element of the phase space where the constraint $F^{L_+} = 1$ holds. Other currents, such as $F^{W_{-2}}$, may conceivably be zero for some states in the phase space, so we cannot rely on them to define a gauge fixing.

For each of the constraints above, we will look for the current component whose variation is proportional to F^{L_+} and gauge it to zero. For the gauge transformations parametrized by Λ, this component appears in the sl_2 sector:

$$\delta_\Lambda F^{L_0} = \frac{F^{L_+}\Lambda}{\gamma_s}, \tag{2.112}$$

$$\delta_\Lambda F^{L_-} = \frac{\partial\Lambda + F^{L_0}\Lambda}{2\gamma_s}. \tag{2.113}$$

Indeed, since the sl_2 is a closed subsector, this just gives the same transformations as in (2.90). Thus we see that we can still use the first constraint to set F^{L_0} to zero. Next, let us look at the second constraint. Here, the F^{L_+} current appears in the variation of the W_m sector:

$$\delta_{\Omega_2} F^{W_{-1}} = \frac{F^{L_+}\Omega_2}{2\gamma_s\sigma}, \tag{2.114}$$

$$\delta_{\Omega_2} F^{W_{-2}} = \frac{\partial\Omega_2 + 2F^{L_0}\Omega_2}{8\gamma_s\sigma}. \tag{2.115}$$

Thus we can use Ω_2 to set $F^{W_{-1}}$ to zero. Finally, the third constraint gives

$$\delta_{\Omega_1} F^{W_0} = -\frac{3F^{L_{+1}}\Omega_1}{2\gamma_s\sigma}, \tag{2.116}$$

$$\delta_{\Omega_1} F^{W_{-1}} = -\frac{\partial\Omega_1 + F^{L_0}\Omega_1}{2\gamma_s\sigma}, \tag{2.117}$$

$$\delta_{\Omega_1} F^{W_{-2}} = \frac{F^{L_{-1}}\Omega_1}{2\gamma_s\sigma}. \tag{2.118}$$

This allows us to set F^{W_0} to zero. The gauge fixed connection is then

$$a_\varphi = L_+ + F^{W_{-2}}(\varphi)W_{-2} + F^{L_-}(\varphi)L_-. \tag{2.119}$$

We can determine the currents by working out

$$\delta Q_\lambda = -2 \oint \langle \lambda, \delta a \rangle$$

$$= \oint \left(8\gamma_s \sigma \lambda^{W_+} \delta F^{W_{+2}} + 2\gamma_s \lambda^+ \delta F^{L_+} \right) d\varphi \tag{2.120}$$

$$= \oint \left(\epsilon \delta T + \chi \delta \mathcal{W} \right) d\varphi. \tag{2.121}$$

In the last line, we have defined the currents

$$T = 2\gamma_s F^{L_-}, \quad \mathcal{W} = 8\gamma_s \sigma F^{W_{-2}}. \tag{2.122}$$

The corresponding transformation parameters are $\chi = \lambda^{W_{+2}}$ and $\epsilon = \lambda^{L_+}$. The currents transform as:

$$\delta_\epsilon T = \epsilon \partial T + 2T \partial \epsilon + \gamma_s \partial^3 \epsilon, \tag{2.123a}$$

$$\delta_\epsilon \mathcal{W} = \epsilon \partial \mathcal{W} + 3\mathcal{W} \partial \epsilon, \tag{2.123b}$$

$$\delta_\chi T = 2\chi \partial \mathcal{W} + 3\mathcal{W} \partial \chi, \tag{2.123c}$$

$$\delta_\chi \mathcal{W} = \frac{16\sigma}{3\gamma_s} \left(T\chi \partial T + T^2 \partial \chi \right) + \frac{3\sigma}{2} \partial \chi \partial^2 T + 5\sigma \partial T \partial^2 \chi \tag{2.123d}$$

$$+ \frac{2\sigma}{3} \chi \partial^3 T + \frac{10\sigma}{3} T \partial^3 \chi + \frac{\gamma_s \sigma}{3} \partial^5 \chi.$$

Indeed, we see that $\mathcal{W}$ is a spin-2 current under the transformations generated by the Virasoro current T. With $\gamma_s = k/4\pi$, this is the classical $\mathcal{W}_3$-algebra [84].

Chapter 3

Zooming in on AdS$_3$/CFT$_2$

Having introduced the boundary analysis of three-dimensional gravity in the context of AdS$_3$, we now turn to its first new application. The holographic principle as we discussed it in Section 1.2.1 is believed to be more general than AdS/CFT. There has been a large effort to find a holographic description for theories that are not conformal, warped conformal or even *nonrelativistic*, both in the bulk and on the boundary.

In this chapter, we motivate a novel duality relating a nonconformal relativistic boundary theory to a nonrelativistic bulk theory. Using the tools developed in Chapter 2, we can arrive at these theories by taking a limit of a particular extension of the AdS$_3$/CFT$_2$ correspondence.

The work in this chapter has appeared previously in [1].

3.1 Introduction

The idea of holography has become the most powerful tool in understanding theories of quantum gravity. Its most celebrated realization is seen in the AdS/CFT correspondence [10, 42] which relates a general relativistic quantum gravity theory on an asymptotically anti-de Sitter (AdS) spacetime to a conformal field theory (CFT) living on the boundary of AdS.

While this duality has led to amazing progress in the last decades, with impact on a wide range of areas in theoretical physics, there are many fundamental questions that remain unanswered. One widely studied route towards gaining deeper insight is by taking consistent limits of the correspondence, therewith simplifying both sides while still retaining non-trivial features. Examples include the BMN limit [100], the limit considered by Kruczenski [101] as well as the closely related Spin Matrix Theory limit of Ref. [102]. Other actively pursued directions are to consider i). non-AdS vacua within Einstein gravity [54, 103, 104] or ii). bulk theories that are Chern–Simons, higher spin or non-Einsteinian gravity theories like Hořava–Lifshitz gravity[1].

In this chapter we will study a decoupling limit of the AdS$_3$/CFT$_2$ correspondence that can be formulated in the bulk as a Chern–Simons theory that is not equivalent to Einstein gravity. On the field theory side, the limit utilizes a $U(1)$ flavor symmetry, for example an R-symmetry of a superconformal field theory, and zooms in on the spectrum close to the lightest charged state of the theory on the cylinder. Thus we are zooming in on the sector of the theory near a BPS bound, much in the spirit of the Spin Matrix Theory proposal of [102] which considers limits to critical points of $\mathcal{N} = 4$ supersymmetric Yang–Mills theory, keeping only one-loop corrections to the BPS states. On the gravity side, the limit results in a Chern–Simons (CS) action that is defined on an algebra that can be viewed as a different real form of the complexified versions of the algebras used in the Chern–Simons (Newton–Cartan) gravity theories of [107–109]. In particular, our CS theory describes a novel version of non-Lorentzian geometry, which we call pseudo-Newton–Cartan (pseudo-NC) geometry. These theories have the feature that the holographic direction emerges in a much simpler way than in AdS because there is a special foliation structure associated with it.

While our primary focus will be on AdS$_3$/CFT$_2$, the limit we consider is quite general, as any $d+1$ dimensional CFT with a $U(1)$ flavor symmetry, a BPS bound and a free coupling constant admits a limit in which one zooms in on the spectrum

---

[1] For the discussion in this chapter it is relevant to note that Hořava–Lifshitz gravity [105] can be reformulated as a theory of dynamical Newton–Cartan geometry [106], and, moreover in three dimensions these theories and generalizations thereof can be formulated [107] (see also [108,109]) as Chern–Simons theories on non-Lorentzian kinematical algebras, such as the Bargmann or Newton–Hooke algebra. Chern–Simons theories also play a role in another avatar of non-AdS holography [110] involving warped CFTs (see for example [111–116]) as boundary field theories. Torsional Newton–Cartan geometry was first observed in the context of non-AdS holography in Refs. [55, 56, 117]. It is worth emphasizing that non-AdS holography is a vast subject, including for example also non-UV conformal models (see [118, 119] for recent reviews). However, for the purposes of this chapter, we focus on the subset of theories that have nonrelativistic symmetries.

close to the lightest charged state of the theory on $\mathbb{R} \times S^d$. In further detail, after using the state-operator map, the BPS operators have a conformal weight that is equal to the energy of the lightest charged state in units of the sphere radius. Using the BPS condition this energy in turn is equal to a $U(1)$ charge Q. We assume that the theory has a free marginal coupling constant g that can be used to compute the one-loop corrections to the conformal dimension away from the BPS bound. By turning on a 'chemical potential'[2] for the charge Q we can offset the dilatation operator D to $D - Q$ which still has a non-negative spectrum. This new dilatation operator has order g corrections when we turn on the interactions perturbatively. The limit zooms in on this 1-loop piece of the dilatation operator. The symmetry algebra in this limit is an Inönü–Wigner contraction of $so(2, d + 1) \oplus u(1)$ that leads to a relativistic algebra with scale but no conformal generators.

For the specific case of 2D CFTs the Lorentz generator is abelian and it turns out to be useful to add a second $u(1)$. One then considers an Inönü–Wigner contraction of $so(2, 2) \oplus u(1) \oplus u(1)$, i.e. two copies of $sl(2, \mathbb{R}) \oplus u(1)$. The resulting contracted algebra is then two copies of P_2^c, the two-dimensional centrally extended Poincaré algebra. This algebra admits an infinite-dimensional extension, namely a left- and right-moving warped Virasoro algebra, which turns out to appear as the asymptotic symmetry of our novel bulk gravity dual. We show that the CS action on two copies of P_2^c can be obtained by applying our contraction to the CS action on two copies of $sl(2, \mathbb{R}) \oplus u(1)$. We then demonstrate that the entire phase space of asymptotically AdS$_3$ solutions of the $so(2, 2) \oplus u(1) \oplus u(1)$ Chern–Simons theory can be mapped to the phase space of the limit theory. This procedure requires a fixed radial chemical potential for one of the two $u(1)$ connections which is related to the background 'chemical potential' needed to offset the dilatation operator close to a BPS bound.

We emphasize that since we can reach the full phase space of the P_2^c theory from the $sl(2, \mathbb{R}) \oplus u(1)$ theory, we can study many well-understood aspects of the AdS$_3$/CFT$_2$ correspondence in this limit. For example, this procedure allows us to find the vacuum of the theory. Following the coset procedure for homogeneous nonrelativistic spacetimes proposed in [120] we show that this three-dimensional vacuum geometry corresponds to the coset $(\mathbf{P}_2^c \times \mathbf{P}_2^c)/(\mathbf{P}_2^c \times U(1))$, where $\mathbf{P}_2^c$ stands for centrally extended 2D Poincaré group. We demonstrate that for this background 6 of the 8 generators of the $P_2^c \oplus P_2^c$ algebra are realized in terms of Killing vectors while the two central extensions are visible only once we study matter fields on these backgrounds.

Our limiting procedure of contracting $so(2, 2) \oplus u(1) \oplus u(1)$ by turning on a radial chemical potential to zoom in on the lightest charged state of the theory on the cylinder bears a strong resemblance to viewing nonrelativistic limits as contractions of Poincaré$\oplus u(1)$. There, one turns on a chemical potential to offset the Hamiltonian of the relativistic theory (splitting off the rest mass) before sending

---

[2] We write 'chemical potential' in quotation marks since this is not a usual chemical potential corresponding to a time component of a background $U(1)$ gauge field. Rather, it is the radial component of a background $U(1)$ potential in radial quantization.

the speed of light to infinity [121, 122]. In [109] a contraction was studied along these lines of a CS theory on the relativistic algebra $iso(2,1) \oplus u(1) \oplus u(1)$. In the large speed of light limit the two $u(1)$ gauge fields correspond to two quantum numbers of a nonrelativistic particle, the rest mass and rest spin [108]. This limit can be generalized in the presence of a cosmological constant leading to CS theory on what is known as the extended Newton–Hooke algebra. For a negative cosmological constant this algebra is isomorphic to $E_2^c \oplus E_2^c$, with E_2^c the two-dimensional centrally extended algebra of the Euclidean two-plane. The CS action on the extended Newton–Hooke algebra was considered in [107, 123]. The limit of $so(2,2) \oplus u(1) \oplus u(1)$ we take in this chapter leads to the algebra $P_2^c \oplus P_2^c$. This can be viewed as a different real form of a complexified version of the $E_2^c \oplus E_2^c$ algebra.

We know from the CS theory on $E_2^c \oplus E_2^c$ that the geometry is described by Newton–Cartan geometry in which time plays a special role. Essentially Newton–Cartan geometry is a covariant description of a special foliation structure where each leaf corresponds to a certain instant of time. In the case of the CS theory on $P_2^c \oplus P_2^c$, the bulk geometry is a version of Newton–Cartan (NC) geometry that we call pseudo-Newton–Cartan geometry. In this case the leaves are those corresponding to constant values of the emerging holographic coordinate and each such hypersurface has a two-dimensional Lorentzian signature. This suggests that pseudo-Newton–Cartan geometry in the bulk provides, in some sense, a much simpler realization of the holographic paradigm than the one that employs Riemannian geometry. Since the limit can be generalized to higher dimensions on the level of the algebra, we can speculate that the corresponding geometry (obtained by gauging the algebra) will appear more generally as a bulk dual in any dimension when zooming in on the spectrum close to the BPS bound. Just like NC geometry can be obtained by gauging the Bargmann algebra [107, 124, 125] in its usual real form, pseudo-NC geometry can be obtained by gauging a different real form of the complexified Bargmann algebra that we discuss here.

It is interesting to put the holographic correspondence that we obtain in this chapter in the larger context of non-AdS holography. So far, we have encountered roughly three classes of dualities. In its original form, the AdS/CFT correspondence relates a relativistic bulk gravity to a corresponding dual (conformal) relativistic field theory living on the boundary. For non-AdS holography, using for example asymptotically Schrödinger or Lifshitz spacetimes, there are setups with relativistic theories in the bulk, e.g. Einstein–Maxwell-dilaton or Einstein–Proca-dilaton theories, and nonrelativistic field theories living on the boundary. These boundary theories naturally couple to nonrelativistic geometries [126–128], such as (torsional) NC geometry, as first shown in the holographic context in [55, 56, 117, 129]. Additionally, it has been suggested that the latter field theories have perhaps a more natural holographic realization with nonrelativistic gravity theories in the bulk [53, 107, 110, 130]. What we see here, somewhat unexpectedly, is that there is a fourth situation in which one has a nonrelativistic bulk gravity theory but a scale invariant relativistic field theory on the boundary.

It is natural to wonder how these scale invariant two-dimensional field theories that appear in our novel holographic correspondence relate to standard 2D CFTs. Local unitary 2D scale invariant relativistic field theories for which the dilatation operator is diagonalizable and has a non-negative discrete spectrum admit currents for special conformal generators [131], i.e. the charge algebra of symmetries of the theory is $sl(2, \mathbb{R}) \oplus sl(2, \mathbb{R})$ which enhances to two commuting Virasoro algebras. This infinite-dimensional symmetry appears as the asymptotic symmetry algebra in AdS$_3$ gravity, as shown in the seminal paper [38]. In our case we will show that likewise the theory has a symmetry algebra that contains two copies of a warped Virasoro algebra and so has the symmetries of a CFT[3]. To understand the nature of the two-dimensional field theory better one would have to work out the unitary irreducible representations of the two copies of the warped Virasoro groups. We leave a more detailed analysis of this for the future and comment on related aspects in the discussion.

Outline and brief summary

This chapter is organized as follows. In Section 3.2 we present the various algebras that play a role in our holographic construction and also present the CS action that appears in our limit. In particular, in Section 3.2.1 we discuss the Inönü–Wigner contraction of $so(2,2) \oplus u(1) \oplus u(1)$ and show how this gives $P_2^c \oplus P_2^c$. We also present its alternative form in terms of the three-dimensional extended Newton–Hooke algebra with a non-standard real form. We then perform in Section 3.2.2 the same contraction at the level of the CS theory, resulting in a CS action for two copies of P_2^c, which inherits a chiral structure from its relativistic parent action. This action thus describes pseudo-Newton–Cartan gravity in three dimensions. To put our limit in a broader perspective, we also discuss in Section 3.2.3 the Inönü–Wigner contraction of $so(2, d+1) \oplus u(1)$. From the boundary point of view, this results in a novel algebra that contains relativistic and scale symmetries, but no conformal symmetries. From the bulk perspective we show that it corresponds to a different real form of the complexified $(d+2)$-dimensional Newton–Hooke algebra.

We then turn in Section 3.3 to studying the phase space of our limit theory by relating it to the phase space of the parent theory. To this end, we first show in Section 3.3.1 how we can obtain the most general P_2^c connection as a limit of the most general $sl(2, \mathbb{R}) \oplus u(1)$ connection. We then continue to show how the limit of the phase space of the $so(2,2) \oplus u(1) \oplus u(1)$ CS theory acts in terms of metric data. In Section 3.3.2 we examine what happens to the Poincaré and global AdS$_3$ geometries after the limit and study the symmetries of the resulting vacua. Finally, in Section 3.3.3 we consider a bulk scalar field model where all symmetries, including central extensions, are explicitly realized.

In Section 3.4, we then study the asymptotic symmetry algebra after the limit. The main result is presented in Section 3.4.1 where we show that in the limit

---

[3] See also [132] for recent related work. Note that these theories are different from the chiral warped CFTs studied in [111], since we have two copies of a warped Virasoro algebra.

theory one obtains a chiral and antichiral warped Virasoro algebra. To elucidate the appearance of this particular infinite-dimensional algebra, we repeat the same procedure in Section 3.4.2 at finite value of the contraction parameter and obtain a more general form of the algebra in that case. We then discuss in Section 3.4.3 how this more general result relates to the naively expected asymptotic symmetry algebra consisting of an uncoupled Virasoro and affine $u(1)$. We end with a discussion and outlook in Section 3.5.

3.2   Near-BPS limit of AdS Chern–Simons theory

In this chapter, we will be concerned with a Chern–Simons theory of gravity with a non-semisimple algebra. We refer the reader to Section 2.2.2 for our conventions for general Chern–Simons theory. Some earlier examples of Chern–Simons theory with non-semisimple algebras include [108,133], see [107,109] for more recent work.

3.2.1   Contraction of 2D conformal algebra with abelian charges

From the boundary perspective, our starting point is a two-dimensional conformal field theory with two $u(1)$ flavor symmetries. We are interested in an Inönü–Wigner contraction of the global symmetry algebra $so(2,2) \oplus u(1) \oplus u(1)$ that zooms in on the state with lowest charge under the flavor symmetries.[4] As we will see, the resulting algebra has a nondegenerate bilinear form, and can therefore be used to construct a Chern–Simons theory. After identifying the correct limit of the algebra in the following, we will proceed to studying the contraction of the corresponding bulk gravity.

Relativistic conformal algebra

In AdS$_3$/CFT$_2$, the $so(2,2)$ symmetry algebra has two interpretations. First of all, it is the global conformal algebra of the conformal field theory living on the boundary of AdS$_3$, as we discussed in Section 1.4.1. In this incarnation, we will exhibit it using the standard basis of translations, boosts, dilatation and special conformal transformations, which satisfy

$$
\begin{aligned}
[P_a, K_b] &= -2iD\eta_{ab} - 2iM\epsilon_{ab}, \quad [D, P_a] = iP_a, \quad [D, K_a] = -iK_a, \\
[M, P_a] &= i\epsilon_a{}^b P_b, \quad [M, K_a] = i\epsilon_a{}^b K_b.
\end{aligned}
\tag{3.1}
$$

Here and in the following, we will use a lowercase Latin index $a = (0,1)$ for boundary components, so η_{ab} and ϵ_{ab} are the 2-dimensional Minkowski metric and Levi–Civita symbol, respectively. Boundary indices are raised and lowered with η_{ab} and we set $\epsilon_{01} = +1$.

***

[4] Note that our initial algebra $so(2,2) \oplus u(1) \oplus u(1)$ is the bosonic part of the $\mathcal{N} = (2,2)$ superconformal algebra, where the abelian currents correspond to the R-charge current in each chiral sector.

From a bulk gravity perspective, $so(2,2)$ is also the isometry algebra of AdS$_3$. For this purpose, the natural generators are the bulk translations T_A and bulk rotations J_A given by

$$T_a = \frac{1}{2\ell}\epsilon_a{}^b(P_b + K_b)\,, \qquad T_2 = \frac{1}{\ell}D\,, \qquad J_a = \frac{1}{2}(P_a - K_a)\,, \qquad J_2 = M\,. \quad (3.2)$$

Here, ℓ is the bulk radius of curvature. The commutators of these generators can be found in equation (2.29). Finally, the $so(2,2)$ generators can be split into two chiral copies of $sl(2,\mathbb{R})$,

$$[L_n, L_m] = i(n - m)L_{n+m}\,, \qquad [\bar{L}_n, \bar{L}_m] = i(n - m)\bar{L}_{n+m}\,. \quad (3.3)$$

The left- and right-moving generators L_m and $\bar{L}_m$ are given by

$$L_{-1} = \frac{1}{2}\left(P_1 + P_0\right)\,, \quad L_0 = \frac{1}{2}\left(D + M\right)\,, \quad L_1 = \frac{1}{2}\left(K_1 - K_0\right)\,, \quad (3.4)$$

$$\bar{L}_{-1} = \frac{1}{2}\left(P_1 - P_0\right)\,, \quad \bar{L}_0 = \frac{1}{2}\left(D - M\right)\,, \quad \bar{L}_1 = \frac{1}{2}\left(K_1 + K_0\right)\,. \quad (3.5)$$

Upon Wick rotation ($t = it_E$) the left- and right-moving coordinates (x^+, x^-) become the complex coordinates $(z, \bar{z})$. Additionally, we assume that the 2D CFT has two flavor $u(1)$ symmetries generated by Q_1 and Q_2. For future convenience, we define the following combinations of $u(1)$ generators,

$$N_0 := \frac{1}{2}(\ell Q_1 + Q_2)\,, \quad \bar{N}_0 := \frac{1}{2}(\ell Q_1 - Q_2)\,. \quad (3.6)$$

We will see in the following that these combinations naturally appear in the chiral decomposition of the contracted algebra. Following (2.33), we parametrize the invariant bilinear form on the left- and right-moving $sl(2,\mathbb{R}) \oplus u(1)$ by

$$2\langle L_0, L_0 \rangle = -\langle L_{-1}, L_1 \rangle = \gamma_s\,, \qquad \langle N_0, N_0 \rangle = \frac{1}{2}\gamma_u\,, \quad (3.7)$$

$$2\langle \bar{L}_0, \bar{L}_0 \rangle = -\langle \bar{L}_{-1}, \bar{L}_1 \rangle = -\bar{\gamma}_s\,, \qquad \langle \bar{N}_0, \bar{N}_0 \rangle = -\frac{1}{2}\bar{\gamma}_u\,. \quad (3.8)$$

Let Φ be a field that transforms in a representation of the total symmetry group $so(2,2) \oplus u(1) \oplus u(1)$. At the level of the algebra, a representation is given by

$$\begin{aligned}
P_a\Phi &= -i\partial_a\Phi\,, \\
M\Phi &= -i\left(\epsilon_a{}^b x^a \partial_b + s\right)\Phi\,, \\
D\Phi &= -i\left(x^a\partial_a + \Delta\right)\Phi\,, \\
K_a\Phi &= -i\left(2\eta_{ac}x^c x^b\partial_b - x^2\partial_a + 2\eta_{ab}x^b\Delta - 2\epsilon_{ab}x^b s\right)\Phi\,, \\
Q_1\Phi &= q_1\Phi\,, \\
Q_2\Phi &= q_2\Phi\,.
\end{aligned} \quad (3.9)$$

The field Φ thus carries the labels Δ (conformal dimension), s (spin) and q_1, q_2 (charges).

Contracted algebra

There exists a general procedure for obtaining nonrelativistic algebras from a contraction of relativistic ones, which is loosely referred to as Inönü-Wigner contraction (see for example [122] for a review). In fact, this procedure does not exclusively yield nonrelativistic algebras, and has also been applied to studying the flat space limit of AdS holography [134–136].

The procedure is as follows. Define a basis for the initial algebra that depends on some parameter α. In this basis, the structure constants now depend on α but the algebra is still fundamentally unchanged. However, by taking $\alpha \to \infty$ one obtains a *contracted* algebra that is generically not isomorphic to the initial algebra.

Starting from $so(2,2) \oplus u(1) \oplus u(1)$, we want to consider the following contraction.[5] Define the generators $\mathcal{P}_a$, $\mathcal{K}_a$, $\mathcal{D}$, $\mathcal{M}$, $\mathcal{N}$ and $\mathcal{S}$ by setting

$$
\begin{aligned}
P_a &= \alpha \mathcal{P}_a, & K_a &= \alpha \mathcal{K}_a, \\
D &= \frac{1}{2}\mathcal{D} + \alpha^2 \mathcal{N}, & Q_1 &= -\frac{1}{2}\mathcal{D} + \alpha^2 \mathcal{N}, \\
M &= \frac{1}{2}\mathcal{M} + \alpha^2 \mathcal{S}, & Q_2 &= -\frac{1}{2}\mathcal{M} + \alpha^2 \mathcal{S}.
\end{aligned}
\tag{3.10}
$$

From (3.1) we find that they satisfy the following commutation relations,

$$
\begin{aligned}
[\mathcal{P}_a, \mathcal{K}_b] &= -2i\left(\frac{\mathcal{D}}{2\alpha^2} + \mathcal{N}\right)\eta_{ab} - 2i\left(\frac{\mathcal{M}}{2\alpha^2} + \mathcal{S}\right)\epsilon_{ab}, \\
[\mathcal{D}, \mathcal{P}_a] &= i\mathcal{P}_a, & [\mathcal{D}, \mathcal{K}_a] &= -i\mathcal{K}_a, \\
[\mathcal{M}, \mathcal{P}_a] &= i\epsilon_a{}^b\mathcal{P}_b, & [\mathcal{M}, \mathcal{K}_a] &= i\epsilon_a{}^b\mathcal{K}_b, \\
[\mathcal{N}, \mathcal{P}_a] &= \frac{i\mathcal{P}_a}{2\alpha^2}, & [\mathcal{N}, \mathcal{P}_a] &= -\frac{i\mathcal{K}_a}{2\alpha^2}, \\
[\mathcal{S}, \mathcal{P}_a] &= \frac{i\epsilon_a{}^b\mathcal{P}_b}{2\alpha^2}, & [\mathcal{S}, \mathcal{K}_a] &= \frac{i\epsilon_a{}^b\mathcal{K}_b}{2\alpha^2}.
\end{aligned}
\tag{3.11}
$$

At this point, we have only performed a basis transformation and the algebra is still unchanged. However, by sending $\alpha \to \infty$, we obtain an *inequivalent* algebra:

$$
\begin{aligned}
[\mathcal{P}_a, \mathcal{K}_b] &= -2i\mathcal{N}\eta_{ab} - 2i\mathcal{S}\epsilon_{ab}, \\
[\mathcal{D}, \mathcal{P}_a] &= i\mathcal{P}_a, & [\mathcal{D}, \mathcal{K}_a] &= -i\mathcal{K}_a, \\
[\mathcal{M}, \mathcal{P}_a] &= i\epsilon_a{}^b\mathcal{P}_b, & [\mathcal{M}, \mathcal{K}_a] &= i\epsilon_a{}^b\mathcal{K}_b.
\end{aligned}
\tag{3.12}
$$

All other commutators vanish and one observes that $\mathcal{N}$ and $\mathcal{S}$ are now central elements. This algebra, which we will call the *scaling nonconformal algebra*, will be the central object of study in this chapter. The generators $\mathcal{M}$ and $\mathcal{P}_a$ form a 2D Poincaré subalgebra and $\mathcal{D}$ is a dilatation generator. However, the $\mathcal{K}_a$ can no longer be thought of as conformal generators.

---

[5] This is not the only possible contraction. For other options, see [137].

A representation of this algebra on a field Φ is given by

$$
\begin{aligned}
\mathcal{P}_a \Phi &= -i\partial_a \Phi \,, \\
\mathcal{M} \Phi &= -i \left(\epsilon_a{}^b x^a \partial_b + \sigma \right) \Phi \,, \\
\mathcal{D} \Phi &= -i \left(x^a \partial_a + \delta \right) \Phi \,, \\
\mathcal{K}_a \Phi &= \left(2\eta_{ab} x^b N - 2\epsilon_{ab} x^b S \right) \Phi \,, \\
\mathcal{N} \Phi &= N \Phi \,, \\
\mathcal{S} \Phi &= S \Phi \,.
\end{aligned}
\tag{3.13}
$$

Like $so(2,2)$, the algebra (3.12) can be split in two factors. Here, the factors are given by a 2D Poincaré algebra with central extension, which we denote by P_2^c. To see this we define

$$
\mathcal{L}_{-1} = \frac{1}{2} \left(\mathcal{P}_1 + \mathcal{P}_0 \right) , \quad \mathcal{L}_0 = \frac{1}{2} \left(\mathcal{D} + \mathcal{M} \right) ,
\tag{3.14}
$$

$$
\mathcal{N}_0 = \mathcal{N} + \mathcal{S} , \quad \mathcal{N}_1 = \frac{1}{2} \left(\mathcal{K}_1 - \mathcal{K}_0 \right) ,
\tag{3.15}
$$

$$
\bar{\mathcal{L}}_{-1} = \frac{1}{2} \left(\mathcal{P}_1 - \mathcal{P}_0 \right) , \quad \bar{\mathcal{L}}_0 = \frac{1}{2} \left(\mathcal{D} - \mathcal{M} \right) ,
\tag{3.16}
$$

$$
\bar{\mathcal{N}}_0 = \mathcal{N} - \mathcal{S} , \quad \bar{\mathcal{N}}_1 = \frac{1}{2} \left(\mathcal{K}_1 + \mathcal{K}_0 \right) .
\tag{3.17}
$$

The nonzero commutators of these generators are

$$
[\mathcal{L}_{-1}, \mathcal{L}_0] = -i\mathcal{L}_{-1} , \qquad [\mathcal{L}_{-1}, \mathcal{N}_1] = -i\mathcal{N}_0 - \frac{i}{\alpha^2} \mathcal{L}_0 , \qquad [\mathcal{L}_0, \mathcal{N}_1] = -i\mathcal{N}_1 ,
$$

$$
[\mathcal{N}_0, \mathcal{L}_{-1}] = \frac{i}{\alpha^2} \mathcal{L}_- , \qquad [\mathcal{N}_0, \mathcal{N}_1] = -\frac{i}{\alpha^2} \mathcal{N}_1
\tag{3.18}
$$

and likewise for the barred generators. At finite α, this is just a redefinition of $sl(2, \mathbb{R}) \oplus u(1)$, but in the limit $\alpha \to \infty$ these are the commutation relations of P_2^c,

$$
[\mathcal{L}_{-1}, \mathcal{L}_0] = -i\mathcal{L}_{-1} , \qquad [\mathcal{L}_{-1}, \mathcal{N}_1] = -i\mathcal{N}_0 , \qquad [\mathcal{L}_0, \mathcal{N}_1] = -i\mathcal{N}_1 .
\tag{3.19}
$$

One can think of $\mathcal{L}_{-1}$ and $\mathcal{N}_1$ as translation generators in a two-dimensional Poincaré plane, with Lorentz boost $\mathcal{L}_0$. The central extension is given by $\mathcal{N}_0$. This algebra can be viewed as a different real form of the complexified centrally extended 2D Euclidean algebra E_2^c. The latter is sometimes referred to as the Nappi–Witten algebra [133]. We parametrize the most general invariant bilinear form on the two copies of P_2^c using

$$
\langle \mathcal{L}_0, \mathcal{L}_0 \rangle = \frac{1}{2} \gamma_1 , \qquad \langle \mathcal{L}_0, \mathcal{N}_0 \rangle = -\langle \mathcal{L}_{-1}, \mathcal{N}_1 \rangle = \gamma_2 ,
\tag{3.20}
$$

$$
\langle \bar{\mathcal{L}}_0, \bar{\mathcal{L}}_0 \rangle = -\frac{1}{2} \bar{\gamma}_1 , \qquad \langle \bar{\mathcal{L}}_0, \bar{\mathcal{N}}_0 \rangle = -\langle \bar{\mathcal{L}}_{-1}, \bar{\mathcal{N}}_1 \rangle = -\bar{\gamma}_2 .
\tag{3.21}
$$

We will see that (3.19) has an infinite-dimensional lift with generators $(\mathcal{L}_m, \bar{\mathcal{L}}_m)$.

In terms of $sl(2,\mathbb{R}) \oplus u(1)$ generators, the basis transformation above corresponds to

$$L_{-1} = \alpha \mathcal{L}_{-1}, \quad L_0 = \frac{1}{2}\mathcal{L}_0 + \frac{\alpha^2}{2}\mathcal{N}_0,$$
$$L_1 = \alpha \mathcal{N}_1, \quad N_0 = -\frac{1}{2}\mathcal{L}_0 + \frac{\alpha^2}{2}\mathcal{N}_0. \tag{3.22}$$

Then it follows that the coefficients of the P_2^c and $sl(2,\mathbb{R}) \oplus u(1)$ bilinear forms are related by

$$\gamma_s = \frac{1}{2}\gamma_1 + \alpha^2 \gamma_2, \qquad \gamma_u = \frac{1}{2}\gamma_1 - \alpha^2 \gamma_2, \tag{3.23}$$

and likewise for the barred sector. This means that at finite α, the bilinear form satisfies

$$\langle \mathcal{L}_{-1}, \mathcal{N}_1 \rangle = -\gamma_2 - \frac{\gamma_1}{2\alpha^2}, \quad \langle \mathcal{L}_0, \mathcal{N}_0 \rangle = \gamma_2,$$
$$\langle \mathcal{L}_0, \mathcal{L}_0 \rangle = \frac{\gamma_1}{2}, \quad \langle \mathcal{N}_0, \mathcal{N}_0 \rangle = \frac{\gamma_1}{2\alpha^4}. \tag{3.24}$$

In the above, we have discussed the limit of $so(2,2) \oplus u(1) \oplus u(1)$ as a conformal symmetry algebra. There is also a bulk perspective on this contraction. Define $\mathcal{T}_a$ and $\mathcal{R}_a$ by

$$\mathcal{T}_a = \frac{1}{2}\left(\mathcal{P}_a + \mathcal{K}_a\right), \qquad \mathcal{R}_a = \frac{1}{2}\left(\mathcal{P}_a - \mathcal{K}_a\right). \tag{3.25}$$

Rescaling $\mathcal{T}_a$, $\mathcal{D}$ and $\mathcal{N}$ by ℓ, the algebra (3.12) can be written as

$$[\mathcal{T}_a, \mathcal{R}_b] = i\mathcal{N}\eta_{ab}, \qquad [\mathcal{M}, \mathcal{T}_a] = i\epsilon_a{}^b \mathcal{T}_b, \qquad [\mathcal{M}, \mathcal{R}_a] = i\epsilon_a{}^b \mathcal{R}_b,$$
$$[\mathcal{D}, \mathcal{R}_a] = i\mathcal{T}_a, \qquad [\mathcal{D}, \mathcal{T}_a] = \frac{i}{\ell^2}\mathcal{R}_a, \tag{3.26}$$
$$[\mathcal{T}_a, \mathcal{T}_b] = -\frac{i}{\ell^2}\mathcal{S}\epsilon_{ab}, \qquad [\mathcal{R}_a, \mathcal{R}_b] = i\mathcal{S}\epsilon_{ab}.$$

Since the generator $\mathcal{S}$ corresponds to a central extension and η_{ab} has Minkowski signature, we will refer to this algebra as the extended pseudo-Newton–Hooke algebra. For $\ell \to \infty$, the first two lines of this algebra provide a different real form of the complexified Bargmann algebra[6]. The analogy with the Bargmann algebra becomes clear if we view $\mathcal{D}$ as the Hamiltonian, $\mathcal{M}$ as the generator of rotations, $\mathcal{T}_a$ as the momenta, $\mathcal{R}_a$ as the Galilei boosts and $\mathcal{N}$ as the mass generator. For finite l, the first two lines of (3.26) are a different real form of the Newton–Hooke algebra[7]. The addition of the central element $\mathcal{S}$ ensures that we can construct a non-degenerate invariant bilinear form on the algebra.

---

[6] The Bargmann algebra would be obtained by replacing the 2D Minkowski metric η_{ab} with the Euclidean metric δ_{ab}.

[7] The contraction we take is not one of the kinematical algebras classified by Bacry and Leblond (see also [138–140] for a recent classification). Instead, it is a different real form of the complexified extended Newton–Hooke algebra, which is isomorphic to two copies of E_2^c as opposed to P_2^c. The Chern–Simons theory for extended Newton–Hooke has been studied in [107, 123]

3.2.2 Chern–Simons action after contraction

As we saw in Section 2.2.3, the Chern–Simons Lagrangian with gauge algebra $so(2,2)$ reproduces the three-dimensional Einstein–Hilbert Lagrangian with cosmological constant [65]. We now add the $u(1)$ connections, whose components we parametrize by

$$\mathbf{A}_{u(1)} = Z^1 Q_1 + Z^2 Q_2 = U N_0 + \bar{U} \bar{N}_0 \,. \tag{3.27}$$

The relation between (Q_1, Q_2) and $(N_0, \bar{N}_0)$ is given in (3.6). Using the bilinear form in (3.7) their contribution to the CS Lagrangian is

$$
\begin{aligned}
\langle \mathbf{A}_{u(1)}, d\mathbf{A}_{u(1)} \rangle = {} & \frac{\gamma_u - \bar{\gamma}_u}{2} \left(\frac{1}{\ell^2} Z^1 \wedge dZ^1 + Z^2 \wedge dZ^2 \right) \\
& + \frac{\gamma_u + \bar{\gamma}_u}{\ell} Z^1 \wedge dZ^2 .
\end{aligned}
\tag{3.28}
$$

The total $so(2,2) \oplus u(1) \oplus u(1)$ connection then consists of the following components,

$$\mathbf{A} = E^A T_A + \Omega^A J_A + Z^1 Q_1 + Z^2 Q_2. \tag{3.29}$$

Recall that E^A is the vielbein, Ω^A is the (dual) spin connection and Z_1 and Z_2 are two bulk $u(1)$ gauge fields. In terms of these components, the total Chern–Simons Lagrangian is

$$
\begin{aligned}
\mathcal{L}_{\text{CS}} = {} & \frac{\gamma_s + \bar{\gamma}_s}{2\ell} \left(2 E^A \wedge d\Omega^B \eta_{AB} + \epsilon_{ABC} E^A \wedge \Omega^B \wedge \Omega^C \right. \\
& \left. + \frac{1}{3\ell^2} \epsilon_{ABC} E^A \wedge E^B \wedge E^C \right) \\
& + \frac{\gamma_s - \bar{\gamma}_s}{2} \left(\Omega^A \wedge d\Omega^B \eta_{AB} + \frac{1}{3} \epsilon_{ABC} \Omega^A \wedge \Omega^B \wedge \Omega^C \right. \\
& \left. + \frac{1}{\ell^2} E^A \wedge dE^B \eta_{AB} + \frac{1}{\ell^2} \epsilon_{ABC} E^A \wedge E^B \wedge \Omega^C \right) \\
& + \frac{\gamma_u - \bar{\gamma}_u}{2} \left(\frac{1}{\ell^2} Z^1 \wedge dZ^1 + Z^2 \wedge dZ^2 \right) + \frac{\gamma_u + \bar{\gamma}_u}{\ell} Z^1 \wedge dZ^2 .
\end{aligned}
\tag{3.30}
$$

Now let us determine the relation between the connection components in the standard algebra and the contracted algebra. We use the ℓ-rescaled bulk algebra in (3.26) and also scale the Q_1 generator correspondingly. The contracted connection can then be written as

$$\mathbf{A} = \tau \mathcal{D} + e^a \mathcal{T}_a + m\mathcal{N} + \omega\mathcal{M} + \omega^a \mathcal{R}_a + \zeta \mathcal{S}. \tag{3.31}$$

Here, τ and e^a are Newton–Cartan vielbeine and ω^a and ω play the role of boost/spin connections. The components m and ζ correspond to the central extensions of the algebra.

Taking into account that $\mathcal{T}_a$, $\mathcal{D}$ and $\mathcal{N}$ have been rescaled by a factor of ℓ, the basis transformation in (3.10) then leads to the following identifications,

$$
\begin{aligned}
E^2 &= \tau + \frac{m}{2\alpha^2}\,, \quad E^a = \frac{1}{\alpha}\epsilon_b{}^a e^b\,, \quad Z^1 = -\tau + \frac{m}{2\alpha^2}\,, \\
\Omega^2 &= \omega + \frac{\zeta}{2\alpha^2}\,, \quad \Omega^a = \frac{1}{\alpha}\omega^a\,, \quad Z^2 = -\omega + \frac{\zeta}{2\alpha^2}\,.
\end{aligned}
\tag{3.32}
$$

Using this in the action (3.30) and taking the limit $\alpha \to \infty$, the action on the contracted algebra $P_2^c \times P_2^c$ becomes

$$
\begin{aligned}
\mathcal{L} = \frac{1}{2\ell}(\gamma_2 + \bar{\gamma}_2)\bigg(& 2\tau \wedge d\zeta + 2\epsilon_{ab}e^a \wedge d\omega^b + 2m \wedge d\omega - \frac{1}{\ell^2}\tau \wedge \epsilon_{ab}e^a \wedge e^b \\
& + \tau \wedge \epsilon_{ab}\omega^a \wedge \omega^b + 2\eta_{ab}e^a \wedge \omega^b \wedge \omega\bigg) \\
+ \frac{1}{2}(\gamma_2 - \bar{\gamma}_2)\bigg(& \eta_{ab}\omega^a \wedge d\omega^b - \frac{1}{\ell^2}\eta_{ab}e^a \wedge de^b + \frac{2}{\ell^2}m \wedge d\tau + 2\omega \wedge d\zeta \\
& + \frac{2}{\ell^2}\eta_{ab}\tau \wedge e^a \wedge \omega^b - \frac{1}{\ell^2}\epsilon_{ab}e^a \wedge e^b \wedge \omega + \omega \wedge \epsilon_{ab}\omega^a \wedge \omega^b\bigg) \\
+ \frac{1}{\ell}(\gamma_1 + \bar{\gamma}_1)\tau & \wedge d\omega + \frac{1}{2}(\gamma_1 - \bar{\gamma}_1)\left(\frac{1}{\ell^2}\tau \wedge d\tau + \omega \wedge d\omega\right).
\end{aligned}
\tag{3.33}
$$

This is the CS action for two copies of P_2^c, using the connection (3.31) and the metric (3.20). This action was first derived in [107] for extended Newton–Hooke, which is a different real form of the complexification of our contracted algebra. Since the vielbein e^a now involves a Lorentzian structure, we will refer to the bulk geometry as pseudo-Newton–Cartan gravity.

In the next section we will see that, in order for the limit to be properly defined on the full phase space of AdS$_3$ gravity, the distinguished vielbein τ has to correspond to the *radial* direction. In contrast to the usual Fefferman–Graham procedure in AdS, which is simply a choice of coordinates, the vielbein τ therefore defines an (absolute) radial foliation which is *intrinsic* to the geometry. It would be very interesting to investigate the consequences of this phenomenon on the RG flow of the corresponding field theories.

3.2.3 Generalization to higher-dimensional algebra

The Inönü–Wigner contraction of the 2D conformal algebra shown above can in fact be achieved for any dimension. Consider the conformal algebra $so(d+1,2)$ in $d+1$ dimensions,

$$
\begin{aligned}
& [D, P_a] = iP_a, \quad [D, K_a] = -iK_a, \quad [P_a, K_b] = -2iD\eta_{ab} - 2iM_{ab}, \\
& [M_{ab}, K_c] = i\left(\eta_{ac}K_b - \eta_{bc}K_a\right), \quad [M_{ab}, P_c] = i\left(\eta_{ac}P_b - \eta_{bc}P_a\right), \quad (3.34) \\
& [M_{ab}, M_{cd}] = i\left(\eta_{ac}M_{bd} + \eta_{bd}M_{ac} - \eta_{ad}M_{bc} - \eta_{bc}M_{ad}\right),
\end{aligned}
$$

where $a, b = 0, ..., d$ and η_{ab} is the Minkowski metric. We add to this a $u(1)$ generator Q. We can also introduce another $so(d,1)$ algebra generated by Z_{ab}

whose commutation relations are

$$[Z_{ab}, Z_{cd}] = i \left(\eta_{ac} Z_{bd} + \eta_{bd} Z_{ac} - \eta_{ad} Z_{bc} - \eta_{bc} Z_{ad} \right) . \tag{3.35}$$

The total algebra is thus $so(d+1,2) \oplus u(1) \oplus so(d,1)$. In two spacetime dimensions we can write $Z_{ab} = Z \epsilon_{ab}$ and then Q and Z are the Q_1 and Q_2 generators of Section 3.2. Now let us make the following α-dependent basis transformation,

$$P_a = \alpha \mathcal{P}_a, \quad K_a = \alpha \mathcal{K}_a, \quad D = \frac{\mathcal{D}}{2} + \alpha^2 \mathcal{N}, \quad Q = \alpha^2 \mathcal{N} - \frac{\mathcal{D}}{2},$$
$$M_{ab} = \frac{\mathcal{M}_{ab}}{2} + \alpha^2 \mathcal{S}_{ab}, \quad Z_{ab} = \frac{\mathcal{M}_{ab}}{2} - \alpha^2 \mathcal{S}_{ab} . \tag{3.36}$$

We then see that for $\alpha \to \infty$ we obtain the algebra

$$[\mathcal{P}_a, \mathcal{K}_b] = -2i\mathcal{N}\eta_{ab} - 2i\mathcal{S}_{ab}, \quad [\mathcal{D}, \mathcal{P}_a] = i\mathcal{P}_a, \quad [\mathcal{D}, \mathcal{K}_a] = -i\mathcal{K}_a,$$
$$[\mathcal{M}_{ab}, \mathcal{K}_c] = i \left(\eta_{ac} \mathcal{K}_b - \eta_{bc} \mathcal{K}_a \right), \quad [\mathcal{M}_{ab}, \mathcal{P}_c] = i \left(\eta_{ac} \mathcal{P}_b - \eta_{bc} \mathcal{P}_a \right),$$
$$[\mathcal{M}_{ab}, \mathcal{M}_{cd}] = i \left(\eta_{ac} \mathcal{M}_{bd} + \eta_{bd} \mathcal{M}_{ac} - \eta_{ad} \mathcal{M}_{bc} - \eta_{bc} \mathcal{M}_{ad} \right), \tag{3.37}$$
$$[\mathcal{M}_{ab}, \mathcal{S}_{cd}] = i \left(\eta_{ac} \mathcal{S}_{bd} + \eta_{bd} \mathcal{S}_{ac} - \eta_{ad} \mathcal{S}_{bc} - \eta_{bc} \mathcal{S}_{ad} \right) .$$

If we had not included the Z_{ab} generators we would have found the algebra that is obtained by setting $\mathcal{S}_{ab} = 0$. The latter algebra is the scaling nonconformal algebra in general dimensions.

Importantly, the contraction of $so(d+1,2) \oplus u(1)$ leads to a $(d+1)$-dimensional relativistic algebra with dilatation generators but no conformal generators. Instead of the conformal generators we have the $\mathcal{K}_a$ generators and a central element $\mathcal{N}$. By defining

$$\mathcal{T}_a = \frac{1}{2} \left(\mathcal{P}_a + \mathcal{K}_a \right), \quad \mathcal{R}_a = \frac{1}{2} \left(\mathcal{P}_a - \mathcal{K}_a \right) \tag{3.38}$$

and by rescaling $\mathcal{T}_a$, $\mathcal{N}$ and $\mathcal{D}$ using a length scale ℓ, we obtain the algebra

$$[\mathcal{T}_a, \mathcal{R}_b] = i\mathcal{N}\eta_{ab}, \quad [\mathcal{D}, \mathcal{T}_a] = \frac{i}{\ell^2} \mathcal{R}_a, \quad [\mathcal{D}, \mathcal{R}_a] = i\mathcal{T}_a,$$
$$[\mathcal{M}_{ab}, \mathcal{T}_c] = i \left(\eta_{ac} \mathcal{T}_b - \eta_{bc} \mathcal{T}_a \right), \quad [\mathcal{M}_{ab}, \mathcal{R}_c] = i \left(\eta_{ac} \mathcal{R}_b - \eta_{bc} \mathcal{R}_a \right), \tag{3.39}$$
$$[\mathcal{M}_{ab}, \mathcal{M}_{cd}] = i \left(\eta_{ac} \mathcal{M}_{bd} + \eta_{bd} \mathcal{M}_{ac} - \eta_{ad} \mathcal{M}_{bc} - \eta_{bc} \mathcal{M}_{ad} \right),$$

For $\ell \to \infty$ this is a different real form of the complexified Bargmann algebra in d dimensions.

The algebra (3.39) is the d-dimensional generalization of (3.26) without the central element $\mathcal{S}$. Gauging this algebra leads to d-dimensional pseudo-Newton–Cartan geometry. It is tempting to speculate that (3.39) governs the bulk gravity theory for near-BPS limits of CFTs in any dimension.

3.3 Phase space of the limit theory

As we described in Chapter 2, the phase space of Chern–Simons theory with chiral boundary conditions can be described using the associated Wess–Zumino–Witten (WZW) model.

In this section, we study the limit of the phase space corresponding to the WZW model of $so(2,2) \oplus u(1) \oplus u(1)$ and show that it reproduces the full $P_2^c \oplus P_2^c$ WZW phase space. We then write down the metric components in terms of the original WZW currents. Next, we study the symmetries of the limit of the Poincaré and global AdS$_3$ vacua and show that these vacua can be written as a coset space. Finally, we show that the full contracted symmetry algebra, including the central extensions, can be realized on a scalar field coupled to a pseudo-Newton–Cartan background.

3.3.1 Mapping relativistic phase space to contracted phase space

In Section 2.4, we reviewed the standard parametrization of the classical phase space of $so(2,2)$ Chern–Simons theory on a manifold with a boundary in terms of the currents of a WZW model. This involves a choice of radial component $\mathbf{A}_\rho$ as well as a choice of chirality and results in the expression (2.79), which reads

$$\mathbf{A} = e^{i\rho(L_0 + \bar{L}_0)} \left(id + F^a(x^+) L_a dx^+ + \bar{F}^a(x^-) \bar{L}_a \, dx^- \right) e^{-i\rho(L_0 + \bar{L}_0)}. \qquad (3.40)$$

The WZW phase space is parametrized by the three current components $F^a(x^+)$. We now want to include two $u(1)$ factors. Following Section 2.3.1, we also have to choose a chirality for these generators. In terms of the generators (Q_1, Q_2) and $(N_0, \bar{N}_0)$ introduced in (3.27), we choose the following parametrization of the $u(1) \oplus u(1)$ connection,

$$U = F^N dx^+ + U_\rho d\rho \,, \qquad \bar{U} = \bar{F}^{\bar{N}} dx^- + \bar{U}_\rho d\rho, \qquad (3.41)$$

$$UN_0 + \bar{U}\bar{N}_0 = Z^1 Q_1 + Z^2 Q_2. \qquad (3.42)$$

Here, we have defined

$$Z_\rho^1 = \frac{\ell}{2} \left(U_\rho + \bar{U}_\rho \right) , \qquad Z_\rho^2 = \frac{1}{2} \left(U_\rho - \bar{U}_\rho \right) ,$$

$$Z^1 = \frac{\ell}{2} \left(F^N dx^+ + \bar{F}^{\bar{N}} dx^- \right) + Z_\rho^1 d\rho, \qquad (3.43)$$

$$Z^2 = \frac{1}{2} \left(F^N dx^+ - \bar{F}^{\bar{N}} dx^- \right) + Z_\rho^2 d\rho.$$

We allow for a contribution $U_\rho N_0 + \bar{U}_\rho \bar{N}_0$ coming from $u(1) \oplus u(1)$ in the radial component of the connection. We will see below that such a contribution is crucial in order to have a well-defined limit of the phase space.

We would like the full WZW phase space to be finite and nonzero in the $\alpha \to \infty$ limit. This can be achieved by scaling the currents $F^a(x^+)$ and $\bar{F}^a(x^+)$ appropriately. For clarity, we focus on the unbarred sector in the following,

$$\begin{aligned} A = e^{i\rho L_0} \left(id + \left(F^+ L_+ + F^0 L_0 + F^- L_- \right) dx^+ \right) e^{-i\rho L_0} \\ + F^N N_0 dx^+ + U_\rho N_0 d\rho. \end{aligned} \qquad (3.44)$$

Plugging in the algebra redefinition (3.22) for $sl(2, \mathbb{R}) \oplus u(1)$,

$$L_- = \alpha \mathcal{L}_-, \quad L_+ = \alpha \mathcal{N}_+, \quad L_0 = \frac{1}{2} \mathcal{L}_0 + \frac{\alpha^2}{2} \mathcal{N}_0, \quad N_0 = -\frac{1}{2} \mathcal{L}_0 + \frac{\alpha^2}{2} \mathcal{N}_0,$$

the resulting connection can be written as

$$A = \frac{1}{2} \left(1 - U_\rho\right) \mathcal{L}_0 d\rho + \frac{\alpha^2}{2} \left(1 + U_\rho\right) \mathcal{N}_0 d\rho \tag{3.45}$$
$$+ \left(e^\rho \alpha F^+ \mathcal{N}_+ + \frac{1}{2} \left(F^0 - F^N\right) \mathcal{L}_0 \right.$$
$$\left. + \frac{\alpha^2}{2} \left(F^0 + F^N\right) \mathcal{N}_0 + e^{-\rho} \alpha F^- \mathcal{L}_- \right) dx^+.$$

For A to be finite as $\alpha \to \infty$, we have to set $U_\rho = -1$. This means that the radial component of this $sl(2, \mathbb{R}) \oplus u(1)$ factor of the full connection has to be set to

$$A_\rho = \mathcal{L}_0 = L_0 - N_0. \tag{3.46}$$

Furthermore, the following combinations have to be finite in the $\alpha \to \infty$ limit,

$$\mathcal{F}^+ := \alpha F^+, \quad \mathcal{F}^0 := \frac{1}{2} \left(F^0 - F^N\right),$$
$$\mathcal{F}^- := \alpha F^-, \quad \mathcal{F}^N := \frac{\alpha^2}{2} \left(F^0 + F^N\right). \tag{3.47}$$

With those redefinitions, the connection is now

$$A = \mathcal{L}_0 d\rho + e^\rho \mathcal{F}^+ \mathcal{N}_+ dx^+ + \mathcal{F}^0 \mathcal{L}_0 dx^+ + \mathcal{F}^N \mathcal{N}_0 dx^+ + e^{-\rho} \mathcal{F}^- \mathcal{L}_- dx^+$$
$$= e^{i\rho \mathcal{L}_0} \left(id + \left(\mathcal{F}^+ \mathcal{N}_+ + \mathcal{F}^0 \mathcal{L}_0 + \mathcal{F}^N \mathcal{N}_0 + \mathcal{F}^- \mathcal{L}_- \right) dx^+ \right) e^{-i\rho \mathcal{L}_0}. \tag{3.48}$$

This is the most general P_2^c connection, which we obtain as a limit of the most general $sl(2, \mathbb{R}) \oplus u(1)$ connection! In other words, we can reach the full phase space of the P_2^c theory from a limit of the phase space of the $sl(2, \mathbb{R}) \oplus u(1)$ theory. The total radial component is

$$\mathbf{A}_\rho = \mathcal{L}_0 + \bar{\mathcal{L}}_0 = L_0 + \bar{L}_0 - N_0 - \bar{N}_0 = L_0 + \bar{L}_0 - \ell Q_1,$$
$$Z_\rho^1 = -\ell, \quad Z_\rho^2 = 0. \tag{3.49}$$

This background radial chemical potential offsets the dilatation generator $L_0 + \bar{L}_0$ and leads to the new dilatation generator $\mathcal{L}_0 + \bar{\mathcal{L}}_0$.

Let us now study what the limit of the $so(2,2) \oplus u(1) \oplus u(1)$ Chern–Simons phase space looks like in terms of the metric data. In Section 2.4.3 we worked out how metric data maps to $so(2,2)$ connections, which are flat if the metric is on-shell. The map from the most general $sl(2, \mathbb{R}) \oplus sl(2, \mathbb{R})$ current components F^a defined in (2.79) to the vielbein and spin connection data is laid out in (2.81).

We now want to show explicitly that the identification of the connection components in (3.32) implies that the components of the contracted connection are

nonzero and finite in the $\alpha \to \infty$ limit. The vielbeine e^a on the leaves of the foliation are given by

$$
\begin{aligned}
e^0 = \alpha E^1 &= \frac{\alpha \ell}{2} \left(-e^\rho \left(F^+ dx^+ - \overline{F}^+ dx^- \right) + e^{-\rho} \left(F^- dx^+ - \overline{F}^- dx^- \right) \right) \\
&= \frac{\ell}{2} \left(-e^\rho \left(\mathcal{F}^+ dx^+ - \overline{\mathcal{F}}^+ dx^- \right) + e^{-\rho} \left(\mathcal{F}^- dx^+ - \overline{\mathcal{F}}^- dx^- \right) \right),
\end{aligned}
\tag{3.50a}
$$

$$
\begin{aligned}
e^1 = \alpha E^0 &= \frac{\alpha \ell}{2} \left(e^\rho \left(F^+ dx^+ + \overline{F}^+ dx^- \right) + e^{-\rho} \left(F^- dx^+ + \overline{F}^- dx^- \right) \right) \\
&= \frac{\ell}{2} \left(e^\rho \left(\mathcal{F}^+ dx^+ + \overline{\mathcal{F}}^+ dx^- \right) + e^{-\rho} \left(\mathcal{F}^- dx^+ + \overline{\mathcal{F}}^- dx^- \right) \right).
\end{aligned}
\tag{3.50b}
$$

Next, τ and m can be expressed in terms of the currents as follows.

$$
\begin{aligned}
\tau &= \frac{1}{2} \left(E^2 - Z^1 \right) = \frac{1}{2} \left[\ell d\rho + \frac{\ell}{2} \left(F^0 dx^+ + \bar{F}^0 dx^- \right) - Z^1 \right] \\
&= \ell d\rho + \frac{\ell}{2} \mathcal{F}^0 dx^+ + \frac{\ell}{2} \overline{\mathcal{F}}^0 dx^-,
\end{aligned}
\tag{3.51a}
$$

$$
\begin{aligned}
m &= \alpha^2 \left(E^2 + Z^1 \right) = \alpha^2 \left[\ell d\rho + \frac{\ell}{2} \left(F^0 dx^+ + \bar{F}^0 dx^- \right) + Z^1 \right] \\
&= \ell \mathcal{F}^N dx^+ + \ell \bar{\mathcal{F}}^{\bar{N}} dx^-.
\end{aligned}
\tag{3.51b}
$$

Note that knowledge of the components we have listed so far specifies all functions $(F^a, \bar{F}^a)$. In particular, the remaining components can be integrated out. Explicitly, ω and ζ are

$$
\begin{aligned}
\omega &= \frac{1}{2} \left(\Omega^2 - Z^2 \right) = \frac{1}{2} \left[\frac{1}{2} \left(F^0 dx^+ - \bar{F}^0 dx^- \right) - Z^2 \right] \\
&= \frac{1}{2} \mathcal{F}^0 dx^+ - \frac{1}{2} \overline{\mathcal{F}}^0 dx^-,
\end{aligned}
\tag{3.52a}
$$

$$
\begin{aligned}
\zeta &= \alpha^2 \left(\Omega^2 + Z^2 \right) = \alpha^2 \left[\frac{1}{2} \left(F^0 dx^+ - \bar{F}^0 dx^- \right) + Z^2 \right] \\
&= \mathcal{F}^N dx^+ - \bar{\mathcal{F}}^{\bar{N}} dx^-.
\end{aligned}
\tag{3.52b}
$$

Finally, the ω^a can be expressed as

$$
\omega^0 = \alpha \Omega^0 = \frac{1}{2} \left(e^\rho \left(\mathcal{F}^+ dx^+ - \overline{\mathcal{F}}^+ dx^- \right) + e^{-\rho} \left(\mathcal{F}^- dx^+ - \overline{\mathcal{F}}^- dx^- \right) \right),
\tag{3.53a}
$$

$$
\omega^1 = \alpha \Omega^1 = \frac{1}{2} \left(-e^\rho \left(\mathcal{F}^+ dx^+ + \overline{\mathcal{F}}^+ dx^- \right) + e^{-\rho} \left(\mathcal{F}^- dx^+ + \overline{\mathcal{F}}^- dx^- \right) \right).
\tag{3.53b}
$$

We thus see that all the metric data is manifestly finite in the $\alpha \to \infty$ limit.

3.3.2 Solutions and Killing symmetries

We now want to study the limit of the Poincaré and global AdS$_3$ connections in more detail. In particular, we want to find the equivalent of the Killing symmetries for the pseudo-Newton–Cartan metric data.

Let us use M to denote a bulk spacetime world index. Consider a local gauge transformation with parameter $\Lambda = \xi^M A_M + \Sigma$. Since the translation generators couple to the vielbeine, A contains all translation generators. Without loss of generality, we can therefore choose ξ^M such that Σ contains *no* translation generators. For our contracted bulk algebra (3.26) this means that Σ can be parametrized by

$$\Sigma = \lambda^a \mathcal{R}_a + \lambda \mathcal{M} + \sigma \mathcal{N} + \beta \mathcal{S} \,. \tag{3.54}$$

On-shell, the connection A then transforms as follows under Λ,

$$\delta A_M = \mathcal{L}_\xi A_M + \partial_M \Sigma - i[A_M, \Sigma] \,. \tag{3.55}$$

We see that ξ^M corresponds to a diffeomorphism of the three-dimensional base manifold, while Σ generates internal transformations in the tangent bundle. Using the connection components defined in (3.31), we see that the Newton–Cartan metric data τ_M, m_M and $h_{MN} = -\eta_{ab} e^a_M e^b_N$ transforms as[8]

$$\delta \tau_M = \mathcal{L}_\xi \tau_M \,, \tag{3.56}$$
$$\delta h_{MN} = \mathcal{L}_\xi h_{MN} - \lambda_a \left(e^a_M \tau_N + e^a_N \tau_M \right) \,, \tag{3.57}$$
$$\delta m_M = \mathcal{L}_\xi m_M + \partial_M \sigma + \lambda_a e^a_M \,. \tag{3.58}$$

First, consider the connection corresponding to pure Poincaré AdS$_3$, which has vanishing Virasoro and affine $u(1)$ currents. The corresponding Newton–Cartan metric data is

$$\tau = \frac{dr}{r} \,, \quad m = 0 \,, \quad e^0 = \frac{dx}{r} \,, \quad e^1 = \frac{dt}{r} \,,$$
$$h_{MN} dx^M dx^N = \left(e^0_M e^0_N - e^1_M e^1_N \right) dx^M dx^N = \frac{1}{r^2} \left(-dt^2 + dx^2 \right) \,. \tag{3.59}$$

The Killing vectors of this solution can be found by solving (3.56)–(3.58),

$$\xi^t = ct + \mu x + a^t + \frac{1}{2} b^t r^2 \,, \quad \xi^x = cx + \mu t + a^x + \frac{1}{2} b^x r^2 \,, \quad \xi^r = cr \tag{3.60}$$
$$\lambda^0 = b^x r \,, \quad \lambda^1 = -b^t r \,, \quad \sigma = b^t t - b^x x \,. \tag{3.61}$$

Here, a^a and b^a are arbitrary (constant) two-vectors. Note that the internal transformations parametrized by λ drop out. They are internal Lorentz transformations of the frame defined by e^a which are always present but not necessary for our present considerations, so we will set $\lambda = 0$ in the following.

We can collect six Killing vectors in the following diffeomorphism generators,

$$\mathcal{P}_a = -i\partial_a \,, \quad \mathcal{K}_a = -ir^2 \partial_a \,, \quad \mathcal{D} = -i(r\partial_r + x^a \partial_a) \,, \quad \mathcal{M} = -i\epsilon_a{}^b x^a \partial_b \,. \tag{3.62}$$

---

[8] Note that we use a nonstandard sign in the definition of h_{MN} to compensate for the exchange of indices that occurs in (3.50). This exchange is ultimately due to the fact that we have defined $\mathcal{T}_a = (P_a + K_a)/2\ell$ without the $\epsilon_a{}^b$ factor in the uncontracted generator $T_a = \epsilon_a{}^b (P_b + K_b)/2\ell$.

They form a representation of the generators in (3.12) without central elements in terms of bulk diffeomorphisms. Here, r is a radial coordinate and $x^a = (t, x)$ parametrize the boundary. Using $x^\pm = x \pm t$ the Killing vectors split into two commuting sets,

$$\mathcal{L}_{-1} = -i\partial_+ , \quad \mathcal{L}_0 = -i\left(x^+\partial_+ + \frac{r}{2}\partial_r\right), \quad \mathcal{N}_1 = -ir^2\partial_- , \quad (3.63)$$

$$\bar{\mathcal{L}}_{-1} = -i\partial_- , \quad \bar{\mathcal{L}}_0 = -i\left(x^-\partial_- + \frac{r}{2}\partial_r\right), \quad \bar{\mathcal{N}}_1 = -ir^2\partial_+ , \quad (3.64)$$

These are three out of four generators of P_2^c. Note that the central elements are not visible at the level of Killing vectors. As we will show in the next section, they only act as internal symmetries on fields.

Second, the contraction of global AdS$_3$ with vanishing $u(1)$ currents leads to

$$\tau = d\rho , \quad h_{MN}dx^M dx^N = -\cosh^2\rho\, d\tau^2 + \sinh^2\rho\, d\varphi^2 , \quad m = 0 , \quad (3.65)$$

where φ is periodic with period 2π. As in Einstein gravity, this solution can be related to the Newton–Cartan metric data of the Poincaré solution we studied above. Consider (3.56)–(3.58) and leave out the diffeomorphisms. These transformations can be exponentiated to the following finite transformations,

$$\begin{aligned}
\tau'_M &= \tau_M , \\
m'_M &= m_M + \partial_M\sigma + \lambda_a e_M^a + \frac{1}{2}\lambda_a\lambda^a\tau_M , \\
h'_{MN} &= h_{MN} - \lambda_a e_M^a \tau_N - \lambda_a e_N^a \tau_M - \lambda_a\lambda^a\tau_M\tau_N .
\end{aligned} \quad (3.66)$$

We first perform the coordinate transformation

$$t = \frac{1}{2}(R^2 + 1)\tau , \qquad x = \frac{1}{2}(R^2 - 1)\varphi , \qquad r = R \quad (3.67)$$

where $R = e^\rho$ so that $h_{MN}dx^M dx^N$ in (3.59) matches $h_{MN}dx^M dx^N$ in (3.65) up to terms involving dR. Then we find a λ^a such that the transformed $h'_{MN}dx^M dx^N$ is exactly (3.65), which can be achieved by taking

$$\lambda^0 = -R\varphi , \qquad \lambda^1 = -R\tau . \quad (3.68)$$

Finally, to make sure that the transformed m connection remains equal to zero, we set σ to

$$\sigma = \frac{1}{4}(R^2 + 1)\tau^2 - \frac{1}{4}(R^2 - 1)\varphi^2 . \quad (3.69)$$

Now that we have related the pseudo-Newton–Cartan contractions of global and Poincaré AdS$_3$, we can also identify their Killing vectors. Two manifest Killing vectors in the global vacuum (3.65) are ∂_τ and ∂_φ. Using the coordinate transformation (3.67) we see that the global AdS$_3$ time and cylinder rotation generators correspond to

$$\begin{aligned}
\partial_\tau &= \frac{1}{2}(r^2 + 1)\partial_t = \frac{1}{2}(\mathcal{K}_0 + \mathcal{P}_0) = \mathcal{T}_0 , \\
\partial_\varphi &= \frac{1}{2}(r^2 - 1)\partial_x = \frac{1}{2}(\mathcal{K}_1 - \mathcal{P}_1) = -\mathcal{R}_1 .
\end{aligned} \quad (3.70)$$

We see that $\mathcal{T}_0$ and $\mathcal{R}_1$ are the contracted versions of the global AdS$_3$ generators T_1 and J_1 defined in (3.2), respectively. Note that the AdS algebra (3.2) has an inner automorphism, corresponding to a rotation in the 1–2 plane, which sends $(T_0, T_1, T_2) \mapsto (T_0, T_2, -T_1)$ and $(J_0, J_1, J_2) \mapsto (J_0, J_2, -J_1)$. In global AdS$_3$, T_1 is the generator of global AdS time. The inner automorphism means that in the AdS$_3$ geometry, a Killing vector for T_1 can equally be viewed as a generator for dilatations $T_2 = D/\ell$. Put differently, there are coordinate transformations, generated by the isometry corresponding to the inner automorphism, that map global AdS$_3$ back to global AdS$_3$ and map ∂_τ from T_1 to T_2. This automorphism, which is important for the state-operator map in AdS/CFT, is no longer present after we take the contraction.

Coset description

The vacuum solutions (3.59) and (3.65) are homogeneous spacetimes. As we mentioned in equation (2.5), we can think of AdS$_3$ as the coset $SO(2,2)/SO(2,1)$. Similarly, we could expect to be able to write these solutions as a coset space. Indeed, this can be done using the description of nonrelativistic geometries as coset spaces recently studied in [120].

For a general Lie group $\mathcal{G}$ with subgroup $\mathcal{H}$, we denote its coset by $\mathfrak{M} = \mathcal{G}/\mathcal{H}$. We split the Lie algebra $\mathfrak{g}$ in the subalgebra $\mathfrak{h}$ and its complement $\mathfrak{m}$. Note that $\mathfrak{m}$ is generically not a Lie algebra, and $\mathfrak{M}$ is generically not a Lie group. Choose a basis of $\mathfrak{g}$ that splits in elements of the subalgebra $\mathfrak{h}$, which we denote by T_I, and elements of the coset $\mathfrak{m}$, which we denote by T_a. We will use $I, J, K \ldots$ for indices of $\mathfrak{h}$ and $a, b, c, \ldots$ for indices of $\mathfrak{m}$.

The coset space $\mathfrak{M}$ is a manifold of dimension $|\mathfrak{m}|$, which we can parametrize using coordinates x^a. Now choose a coset representative

$$g = \prod_{a=0}^{|\mathfrak{m}|-1} \exp\left(x^a T_a\right) \in \mathcal{G}. \tag{3.71}$$

To construct an $\mathcal{H}$-invariant metric on $\mathfrak{M}$, we have to find a symmetric bilinear form Ω on $\mathfrak{g}/\mathfrak{h}$ that is invariant under the adjoint action of $\mathfrak{h}$. If we want to describe non-Riemannian geometries, the bilinear form Ω is degenerate and the corresponding construction has been worked out in [120]. Instead of a non-degenerate bilinear form, one has to use a *pair* of degenerate bilinear forms $(\kappa_{ab}, \kappa^{ab})$ that are $\mathfrak{h}$-invariant,

$$f_{aI}{}^c \kappa_{cb} + f_{bI}{}^c \kappa_{ca} = 0, \qquad \kappa^{ac} f_{cI}{}^b + \kappa^{bc} f_{cI}{}^a = 0. \tag{3.72}$$

It can be shown that for an appropriate choice of $\mathfrak{m}$ and $\mathfrak{h}$, the degenerate pair of bilinear forms $(\kappa_{ab}, \kappa^{ab})$ on the coset $\mathfrak{m}$ exactly induces the degenerate (pseudo)-Newton–Cartan metric on the coset $\mathfrak{M}$. The form κ_{ab}, which turns out to be of rank one, is used to define the one-form τ, while κ^{ab} turns out to be rank two for three-dimensional spacetime and defines the inverse spatial metric $h^{\mu\nu}$. For more details, we refer the reader to [120].

For the case we are interested in we start with the group $\mathcal{G} = \mathbf{P}_2^c \otimes \mathbf{P}_2^c$. To obtain a three-dimensional pseudo-Newton–Cartan manifold we have to quotient

out a subgroup with five generators. A natural candidate is $\mathbf{P}_2^c \otimes U(1)$ where $\mathbf{P}_2^c$ is the diagonal subgroup of $\mathbf{P}_2^c \otimes \mathbf{P}_2^c$.

Using the basis in (3.26), the diagonal subgroup plus the $U(1)$ of $\mathbf{P}_2^c \otimes \mathbf{P}_2^c$ is generated by $\mathfrak{h} = \{\mathcal{R}_1, \mathcal{R}_0, \mathcal{M}, \mathcal{S}, \mathcal{N}\}$ while the coset generators are $\mathfrak{m} = \{\mathcal{D}, \mathcal{T}_0, \mathcal{T}_1\}$[9]. The corresponding $\mathfrak{h}$-invariant bilinear forms are $\kappa_{ab} \propto \text{diag}\{1, 0, 0\}$ and $\kappa^{ab} \propto \text{diag}\{0, -1, 1\}$. By expanding the Maurer–Cartan 1-form $g^{-1}dg$ as follows

$$g^{-1}dg = iT_a e^a + iT_I m^I \tag{3.73}$$

we can read off the coset vielbeine e^a. The metrics are then $\tau_M \tau_N = \kappa_{ab} e_M^a e_N^b$ and $h^{MN} = \kappa^{ab} e_a^M e_b^N$. We can generalize this construction to higher dimensions using the contracted algebra in Section 3.2.3.

Now let us turn to the two solutions considered above. For the Poincaré AdS$_3$ limit, we choose the following coset representative

$$g = e^{i(\mathcal{T}_1 + \mathcal{R}_1)x} e^{i(\mathcal{T}_0 + \mathcal{R}_0)t} e^{i\mathcal{D}\rho} \,. \tag{3.74}$$

The Maurer-Cartan 1-form is

$$g^{-1}dg = e^\rho (\mathcal{T}_1 + \mathcal{R}_1)idx + e^\rho (\mathcal{T}_0 + \mathcal{R}_0)idt + i\mathcal{D}d\rho \,. \tag{3.75}$$

The corresponding vielbeine are

$$\tau = d\rho, \quad e^0 = e^\rho dt, \quad e^1 = e^\rho dx \,. \tag{3.76}$$

By defining $r = e^{-\rho}$, we reproduce the pseudo-Newton–Cartan geometry in the Poincaré coordinates (3.59). If we instead choose the coset representative to be

$$g = e^{i\mathcal{R}_1 \varphi} e^{i\mathcal{T}_0 \tau} e^{i\mathcal{D}\rho} \tag{3.77}$$

we reproduce the limit of the global AdS$_3$ solution

$$g^{-1}dg = i\mathcal{T}_0 \cosh\rho \, d\tau + i\mathcal{T}_1 \sinh\rho \, d\varphi + i\mathcal{D}d\rho + i\mathcal{R}_0 \sinh\rho \, d\tau + i\mathcal{R}_1 \cosh\rho \, d\varphi \,. \tag{3.78}$$

All these solutions locally have an algebra of Killing symmetries isomorphic to the centerless two-dimensional Poincaré algebra in (3.63). In order to see the central extensions, it is crucial to add matter fields which we now show using the simple example of a bulk scalar field.

3.3.3 Central extension on bulk scalar field

Consider the following bulk action of a complex scalar field coupled to pseudo-NC geometry,

$$S = \int d^3x e \left[iv^M \left(\psi D_M \psi^* - \psi^\star D_M \psi \right) - h^{MN} D_M \psi D_N \psi^\star \right] \,. \tag{3.79}$$

---

[9] Here, we have used the automorphism $\mathcal{T}_0 \leftrightarrow \mathcal{R}_1$, $\mathcal{D} \leftrightarrow \mathcal{M}$ and $\mathcal{N} \leftrightarrow \mathcal{S}$.

The covariant derivative is $D_M\psi = (\partial_M - im_M)\psi$ and e is the determinant of the matrix (τ_M, e_M^a). The inverse metric h^{MN} is defined as $h^{MN} = \eta^{ab}e_a^M e_b^N$ where the square matrix (v^M, e_a^M) is the inverse of (τ_M, e_M^a), so we have $v^M\tau_M = 1$, $v^M e_M^a = 0$, $e_a^M\tau_M = 0$ and $e_a^M e_M^b = \delta_a^b$. Using these inverse relations, (3.66) implies that v^M and h^{MN} transform as

$$h'^{MN} = h^{MN}, \qquad v'^M = v^M - \lambda^a e_a^M. \tag{3.80}$$

This transformation together with (3.66) leaves the action (3.79) invariant if ψ transforms as

$$\psi = e^{-i\sigma}\psi'. \tag{3.81}$$

Since the action (3.79) is invariant under the local pseudo-NC gauge symmetries it is guaranteed that it is invariant under the Killing symmetries of the background geometry. What is interesting is that some of these will act in a nontrivial manner on ψ giving rise to central extensions of the algebra of Killing symmetries. For example, if we evaluate (3.79) on the background (3.59), we obtain the action

$$S = \int d\rho dx^- dx^+ \left[i\left(\psi\partial_\rho\psi^* - \psi^\star\partial_\rho\psi\right) - 2e^{2\rho}\left(\partial_+\psi\partial_-\psi^\star + \partial_-\psi\partial_+\psi^\star\right)\right]. \tag{3.82}$$

This action is invariant under the following transformations

$$
\begin{aligned}
x'^\pm &= x^\pm + a^\pm, \\
\rho' &= \rho + \frac{1}{2}\log\lambda_+, \qquad x'^+ = \lambda_+ x^+, \\
\psi(\rho, x^-, x^+) &= \lambda_+^{1/2}\psi'(\rho', x'^-, x'^+), \\
\rho' &= \rho + \frac{1}{2}\log\lambda_-, \qquad x'^- = \lambda_- x^-, \\
\psi(\rho, x^-, x^+) &= \lambda_-^{1/2}\psi'(\rho', x'^-, x'^+), \\
x'^+ &= x^+ + e^{2\rho}v^+, \qquad \psi(\rho, x^-, x^+) = e^{iv^+ x'^-}\psi'(\rho', x'^-, x'^+), \\
x'^- &= x^- + e^{2\rho}v^-, \qquad \psi(\rho, x^-, x^+) = e^{iv^- x'^+}\psi'(\rho', x'^-, x'^+), \\
\psi(\rho, x^-, x^+) &= e^{iq}\psi'(\rho, x^-, x^+),
\end{aligned}
\tag{3.83}
$$

where $a^\pm$, $\lambda_\pm$, $v^\pm$ and q are constants. These transformations form the group $\mathbf{P}_2^c \otimes \mathbf{P}_2^c$ where the two extensions are identified. In other words we have under $\mathcal{N}$ and $\mathcal{S}$

$$\mathcal{N}\psi = \psi, \qquad \mathcal{S}\psi = 0. \tag{3.84}$$

The infinitesimal version of (3.83) is given by the Killing vectors (3.63) together with an additional internal transformation of the form

$$
\begin{aligned}
\mathcal{L}_{-1}\psi &= -i\partial_+\psi, \quad \mathcal{L}_0\psi = -i\left(x^+\partial_+ + \frac{1}{2}\partial_\rho + \frac{1}{2}\right)\psi, \\
\mathcal{N}_1\psi &= -i\left(e^{2\rho}\partial_- + ix^+\right)\psi, \\
\bar{\mathcal{L}}_{-1}\psi &= -i\partial_-\psi, \quad \bar{\mathcal{L}}_0\psi = -i\left(x^-\partial_- + \frac{1}{2}\partial_\rho + \frac{1}{2}\right)\psi, \\
\bar{\mathcal{N}}_1\psi &= -i\left(e^{2\rho}\partial_+ + ix^-\right)\psi.
\end{aligned}
\tag{3.85}
$$

It would be interesting to see if this scalar field couples to an operator on the boundary and to work out the representation of this operator under the global symmetry group.

3.4   Asymptotic symmetry algebras

As we reviewed in Section 2.5, the asymptotic Virasoro symmetries of AdS$_3$ can be understood in terms of a Drinfeld–Sokolov reduction of the $sl(2,\mathbb{R})$ WZW model coming from $so(2,2)$ Chern–Simons theory.

The reduction arises from a Dirichlet constraint on the leading radial components of the metric. In terms of the Newton–Hooke metric data, we can see from (3.50) that constraining the leading-order behavior of e^a corresponds to setting $\mathcal{F}^+ \equiv 1$. The P_2^c connection is then

$$a_+ = \mathcal{N}_+ + \mathcal{F}^0 \mathcal{L}_0 + \mathcal{F}^- \mathcal{L}_- + \mathcal{F}^N \mathcal{N}_0. \tag{3.86}$$

This restriction corresponds to adding a constraint χ to the initial Hamiltonian H_0,

$$\chi = \int dx\, \Lambda(x)\left(\mathcal{F}^+(x) - 1\right), \quad H_T = H_0 + \chi. \tag{3.87}$$

Here, Λ is an arbitrary function which acts as a Lagrange multiplier imposing the constraint $\mathcal{F}^+(x) \equiv 1$. It generates gauge transformations through the Poisson bracket (2.77) on the WZW phase space,

$$\{\mathcal{F}^a(x^+), \mathcal{F}^b(y^+)\} = -\frac{1}{2}f^{ab}{}_c \mathcal{F}^c(x^+)\delta(x^+ - y^+) + \frac{1}{2}\partial_{x^+}\delta(x^+ - y^+)\kappa^{ab}. \tag{3.88}$$

The structure constants are defined via $[T_a, T_b] = if_{ab}{}^c T_c$ and indices should be raised and lowered using the invariant bilinear form $\kappa_{ab} = \langle T_a, T_b \rangle$. Since we consider a nondegenerate form, its inverse exists and is denoted by κ^{ab}.

Using the bilinear form in (3.24) and the structure constants from (3.18), we find that the constraint χ generates the following gauge transformations on the currents in (3.86),

$$\delta_\Lambda \mathcal{F}^0(x) = \{\chi, \mathcal{F}^0(x)\} = \frac{\Lambda(x)\mathcal{F}^+(x)}{\gamma_1 + 2\alpha^2\gamma_2} \equiv \frac{\Lambda(x)}{\gamma_1 + 2\alpha^2\gamma_2}, \tag{3.89a}$$

$$\delta_\Lambda \mathcal{F}^-(x) = \{\chi, \mathcal{F}^-(x)\} = \frac{\partial\Lambda(x) + \Lambda(x)\mathcal{F}^0(x) + \Lambda(x)\mathcal{F}^N(x)/\alpha^2}{2\gamma_2 + \gamma_1/\alpha^2}, \tag{3.89b}$$

$$\delta_\Lambda \mathcal{F}^N(x) = \{\chi, \mathcal{F}^N(x)\} = \frac{\Lambda(x)\mathcal{F}^+}{2\gamma_2 + \gamma_1/\alpha^2} \equiv \frac{\Lambda(x)}{2\gamma_2 + \gamma_1/\alpha^2}. \tag{3.89c}$$

One could use these transformations to set part of the currents to zero. However, to make sure that no information is lost in the contraction, we will not do any gauge fixing. Instead, we will work with what we refer to as *physical* currents, which are combinations of the currents in (3.86) that are invariant under the gauge transformations generated by the constraint. This method is reviewed in Section 2.5.1 for the reduction of affine $sl_2(\mathbb{R})$ to Virasoro.

In this section, we will first compute the asymptotic symmetry algebra (ASA) at infinite contraction parameter α in Section 3.4.1. This gives a *warped* Virasoro-affine $u(1)$ algebra. We then work out explicitly the finite α ASA in Section 3.4.2, where we also show that its limit is well defined and reproduces the $\alpha \to \infty$ result.

However, at finite α the Chern–Simons algebra is equivalent to $sl(2,\mathbb{R}) \oplus u(1)$, as we discussed in the previous section. Its natural ASA is an *uncoupled* Virasoro-affine $u(1)$ algebra, as we demonstrate in Section 3.4.3. We then show explicitly how the coupled algebra at finite α can be obtained from a redefinition of the uncoupled algebra.

3.4.1 Warped Virasoro algebra in limit theory

Only certain combinations of the $\mathcal{F}^a$ in (3.86) correspond to a physical, conserved current with nontrivial boundary charges. Such 'physical' currents should be invariant under the gauge transformations in (3.89). In the limit $\alpha \to \infty$, the following combinations are invariant,

$$\mathcal{F}^- - \mathcal{F}^0 \mathcal{F}^N - \partial \mathcal{F}^N, \qquad \mathcal{F}^0 . \tag{3.90}$$

The physical currents should be made up out of such invariant building blocks. Recall that the infinitesimal boundary charges for Chern–Simons theory are given by (2.74),

$$\delta Q_\lambda = -2 \oint_{\partial \Sigma} \langle \lambda, \delta_\lambda a \rangle. \tag{3.91}$$

We contracted the Chern–Simons algebra, but the manifold on which the Chern–Simons connections are defined is unchanged. In other words, the fibers are different but the base manifold is still a cylinder, so we parametrize the boundary cycle $\partial \Sigma = S^1$ using a periodic coordinate φ. For a gauge parameter λ to preserve the constrained form of the connection in (3.86), we need

$$\lambda^0 = \mathcal{F}^0 \lambda^+ - \partial \lambda^+ . \tag{3.92}$$

Then the infinitesimal charge is given by

$$\delta Q_\lambda = -2 \oint d\varphi \langle \lambda, \delta a_+ \rangle \tag{3.93}$$

$$= \oint d\varphi \left(-\gamma_1 \lambda^0 \delta \mathcal{F}^0 + 2\gamma_2 \left(\lambda^+ \delta \mathcal{F}^- - \lambda^0 \delta \mathcal{F}^N - \lambda^N \delta \mathcal{F}^0 \right) \right) \tag{3.94}$$

$$= \oint d\varphi \left(\lambda^+ \left(-\gamma_1 \left[\mathcal{F}^0 \delta \mathcal{F}^0 + \partial \delta \mathcal{F}^0 \right] + 2\gamma_2 \left[\delta \mathcal{F}^- - \mathcal{F}^0 \delta \mathcal{F}^N - \delta \partial \mathcal{F}^N \right] \right) \tag{3.95}$$
$$- 2\gamma_2 \lambda^N \delta \mathcal{F}^0 \right) .$$

But now we have a problem: the $\mathcal{F}^0 \delta \mathcal{F}^N$-term is not a total variation, so the infinitesimal charge is not integrable as it stands. To fix this, we can define a new parameter $\bar{\lambda}^N$ via

$$\lambda^N = \bar{\lambda}^N + \mathcal{F}^N \lambda^+ . \tag{3.96}$$

Then the infinitesimal charge integrand is integrable and can be written as

$$-2\langle\lambda, \delta a_+\rangle = \lambda^+ \delta \left(-\gamma_1 \left[\frac{1}{2}(\mathcal{F}^0)^2 + \partial \mathcal{F}^0\right] + 2\gamma_2 \left[\mathcal{F}^- - \mathcal{F}^0 \mathcal{F}^N - \partial \mathcal{F}^N\right]\right)$$
$$- \bar{\lambda}^N \delta \left(2\gamma_2 \mathcal{F}^0\right) \tag{3.97}$$
$$= \lambda^+ \delta \mathcal{T} + \bar{\lambda}^N \delta \mathcal{J}. \tag{3.98}$$

Here, we have defined the two physical currents $\mathcal{T}$ and $\mathcal{J}$,

$$\mathcal{T} = -\gamma_1 \left[\frac{1}{2}(\mathcal{F}^0)^2 + \partial \mathcal{F}^0\right] + 2\gamma_2 \left[\mathcal{F}^- - \mathcal{F}^0 \mathcal{F}^N - \partial \mathcal{F}^N\right], \tag{3.99}$$
$$\mathcal{J} = -2\gamma_2 \mathcal{F}^0. \tag{3.100}$$

Indeed, these currents are composed out of the combinations in (3.90) and are therefore invariant under the constraint gauge transformations. Under the residual transformations satisfying (3.92), the physical currents transform as follows,

$$\delta \mathcal{T} = \lambda^+ \partial \mathcal{T} + 2\mathcal{T}\partial\lambda^+ + \gamma_1 \partial^3 \lambda^+ + \mathcal{J}\partial\bar{\lambda}^N - 2\gamma_2 \partial^2 \bar{\lambda}^N, \tag{3.101}$$
$$\delta \mathcal{J} = \lambda^+ \partial \mathcal{J} + \mathcal{J}\partial\lambda^+ + 2\gamma_2 \partial^2 \lambda^+. \tag{3.102}$$

The Poisson bracket of the boundary charges can be determined using the WZW Poisson bracket (3.88). First, it is useful to split Q_λ into a Virasoro and affine $u(1)$ charges,

$$Q_\lambda = \oint d\varphi \left(\lambda^+ \mathcal{T} + \bar{\lambda}^N \mathcal{J}\right) = Q^{\mathrm{Vir}}[\lambda^+] + Q^{u(1)}[\bar{\lambda}^N]. \tag{3.103}$$

They satisfy the following algebra,

$$\{Q^{\mathrm{Vir}}[\lambda^+], Q^{\mathrm{Vir}}[\mu^+]\} = Q^{\mathrm{Vir}}\left[\mu^+ \partial\lambda^+ - \lambda^+ \partial\mu^+\right] + \gamma_1 \oint d\varphi \mu^+ \partial^3 \lambda^+, \tag{3.104}$$

$$\{Q^{\mathrm{Vir}}[\lambda^+], Q^{u(1)}[\bar{\mu}^N]\} = -Q^{u(1)}\left[\lambda^+ \partial\bar{\mu}^N\right] + 2\gamma_2 \oint d\varphi \bar{\mu}^N \partial^2 \lambda^+. \tag{3.105}$$

Following (2.95), if we expand the Virasoro and affine $u(1)$ charges in terms of the modes

$$\mathcal{L}_m = -Q^{\mathrm{Vir}}[e^{im\varphi}], \qquad \mathcal{N}_m = -Q^{u(1)}[e^{im\varphi}], \tag{3.106}$$

we find that these modes satisfy the following commutation relations

$$\{\mathcal{L}_m, \mathcal{L}_n\} = -i(m-n)\mathcal{L}_{m+n} - 2\pi i\gamma_1 m^3 \delta_{m+n,0}, \tag{3.107}$$
$$\{\mathcal{L}_m, \mathcal{N}_n\} = in\mathcal{N}_{m+n} - 4\pi\gamma_2 m^2 \delta_{m+n,0}. \tag{3.108}$$

Replacing $i\{\cdot, \cdot\}$ by $[\cdot, \cdot]$, and shifting the zero modes of the algebra using the redefinition $\mathcal{L}_m \to \mathcal{L}_m + \pi\gamma_1 \delta_{m,0}$ and $\mathcal{N}_m \to \mathcal{N}_m + 4\pi\gamma_2 i\delta_{m,0}$, this yields

$$[\mathcal{L}_m, \mathcal{L}_n] = (m-n)\mathcal{L}_{m+n} + 2\pi\gamma_1 m(m^2 - 1)\delta_{m+n,0}, \tag{3.109a}$$
$$[\mathcal{L}_m, \mathcal{N}_n] = -n\mathcal{N}_{m+n} - 4\pi i\gamma_2 m(m+1)\delta_{m+n,0}. \tag{3.109b}$$

This is a warped Virasoro algebra with an extension in the Virasoro-affine $u(1)$ commutator and vanishing level of the affine $u(1)$. It appeared before in the context of Rindler holography [141] with vanishing Virasoro central charge. Here, we find it using a systematic Drinfeld–Sokolov reduction of a P_2^c WZW model.

3.4.2 Asymptotic symmetries from contraction

In fact we can do more. As we explained for the Chern–Simons algebra in Section 3.2, the Inönü-Wigner-type contraction is nothing but a basis transformation until we take $\alpha \to \infty$. We now want to demonstrate that this is also true on the level of the asymptotic symmetry algebra. To do that we first repeat the above computation at finite α. Again we start with

$$a_+ = \mathcal{N}_+ + \mathcal{F}^0 \mathcal{L}_0 + \mathcal{F}^- \mathcal{L}_- + \mathcal{F}^N \mathcal{N}_0. \tag{3.110}$$

We now use the finite α commutation relations from (3.18). The constrained connection is then preserved by

$$\lambda^0 = \left(\mathcal{F}^0 - \frac{\mathcal{F}^N}{\alpha^2} \right) \lambda^+ - \partial \lambda^+ - \frac{\lambda^N}{\alpha^2}. \tag{3.111}$$

Now let us write out the expression for infinitesimal charges. As before, we will see that a redefinition of λ^N will be necessary to obtain an integrable expression. Using the bilinear form at finite α in (3.24), we find

$$\delta Q_\lambda = -2 \oint d\varphi \, \langle \lambda, \delta a_+ \rangle \tag{3.112}$$

$$= -2 \oint d\varphi \left(-\lambda^+ \left(\gamma_2 + \frac{\gamma_1}{2\alpha^2} \right) \delta \mathcal{F}^- + \lambda^0 \left(\gamma_2 \delta \mathcal{F}^N + \frac{\gamma_1}{2} \delta \mathcal{F}^0 \right) \right. \tag{3.113}$$

$$\left. + \lambda^N \left(\frac{\gamma_1}{2\alpha^4} \delta \mathcal{F}^N + \gamma_2 \delta \mathcal{F}^0 \right) \right)$$

$$= -2 \oint d\varphi \, \lambda^+ \left[-\left(\gamma_2 + \frac{\gamma_1}{2\alpha^2} \right) \delta \mathcal{F}^- + \left(\mathcal{F}^0 + \frac{\mathcal{F}^N}{\alpha^2} \right) \left(\gamma_2 \delta \mathcal{F}^N + \frac{\gamma_1}{2} \delta \mathcal{F}^0 \right) \right.$$

$$\left. + \gamma_2 \delta \partial \mathcal{F}^N + \frac{\gamma_1}{2} \delta \partial \mathcal{F}^0 \right]$$

$$- 2 \oint d\varphi \, \lambda^N \left(\gamma_2 - \frac{\gamma_1}{2\alpha^2} \right) \left(\delta \mathcal{F}^0 - \frac{\delta \mathcal{F}^N}{\alpha^2} \right).$$

Again, we see that the infinitesimal charge is not integrable, which we fix by setting

$$\lambda^+ = \lambda^+, \quad \lambda^N = \bar{\lambda}^N + \mathcal{F}^N \lambda^+. \tag{3.114}$$

The boundary charges can then be written as $Q_\lambda = \oint d\varphi \left(\lambda^+ \mathcal{T} + \bar{\lambda}^N \mathcal{J} \right)$ with currents

$$\mathcal{T} = \gamma_1 \left(\frac{\mathcal{F}^-}{\alpha^2} - \frac{1}{2} (\mathcal{F}^0)^2 - \partial \mathcal{F}^0 - \frac{1}{2\alpha^4} \left(\mathcal{F}^N \right)^2 \right) \tag{3.115}$$

$$+ 2\gamma_2 \left(\mathcal{F}^- - \mathcal{F}^N \mathcal{F}^0 - \partial \mathcal{F}^N \right),$$

$$\mathcal{J} = \left(2\gamma_2 - \frac{\gamma_1}{\alpha^2} \right) \left(\mathcal{F}^0 - \frac{\mathcal{F}^N}{\alpha^2} \right). \tag{3.116}$$

Their variation is given by

$$\delta\mathcal{T} = \lambda^+\partial\mathcal{T} + 2\mathcal{T}\partial\lambda^+ + \gamma_1\partial^3\lambda^+ + \mathcal{J}\partial\bar{\lambda}^N - 2\left(\gamma_2 - \frac{\gamma_1}{2\alpha^2}\right)\partial^2\bar{\lambda}^N, \qquad (3.117)$$

$$\delta\mathcal{J} = \lambda^+\partial\mathcal{J} + \mathcal{J}\partial\lambda^+ + \left(2\gamma_2 - \frac{\gamma_1}{\alpha^2}\right)\left(\partial^2\lambda^+ + \frac{2\partial\bar{\lambda}^N}{\alpha^2}\right). \qquad (3.118)$$

As before we can write the charge algebra in terms of the Fourier modes

$$\mathcal{L}_n = -\oint d\varphi\, e^{in\varphi}\mathcal{T}(x^+), \qquad \mathcal{N}_n = -\oint d\varphi\, e^{in\varphi}\mathcal{J}(x^+). \qquad (3.119)$$

They satisfy the following commutation relations,

$$[\mathcal{L}_m, \mathcal{L}_n] = (m-n)\mathcal{L}_{m+n} + 2\pi\gamma_1 m^3\delta_{m+n,0}, \qquad (3.120a)$$

$$[\mathcal{L}_m, \mathcal{N}_n] = -n\mathcal{N}_{m+n} - 2\pi i\, m^2\left(2\gamma_2 - \frac{\gamma_1}{\alpha^2}\right)\delta_{m+n,0}, \qquad (3.120b)$$

$$[\mathcal{N}_m, \mathcal{N}_n] = -\frac{4\pi m}{\alpha^2}\left(2\gamma_2 - \frac{\gamma_1}{\alpha^2}\right)\delta_{m+n,0}. \qquad (3.120c)$$

This is a Virasoro algebra with *coupled* affine $u(1)$ algebra and nonzero affine $u(1)$ level. The contracted algebra can be obtained by sending $\alpha \to \infty$, and we indeed reproduce the asymptotic symmetry algebra at infinite α in (3.109).

3.4.3 Relation to uncoupled algebra

This result may seem confusing. One would expect that the asymptotic symmetry algebra of an $sl(2, \mathbb{R}) \oplus u(1)$ Chern–Simons theory would be an uncoupled Virasoro and affine $u(1)$ algebra. In fact, we can easily include a $u(1)$ generator N_0 in the computation of Section 2.5.1 and show that this is the case. The constrained connection, residual gauge transformations and boundary charges are then

$$a_+ = L_+ + F^0 L_0 + F^- L_- + F^N N_0, \qquad (3.121)$$

$$\lambda = \lambda^+ L_+ + (F^0\lambda^+ - \partial\lambda^+)L_0 + \lambda^- L_- + \lambda^N N_0, \qquad (3.122)$$

$$Q_\lambda = -2\oint\langle\lambda, \delta a_+\rangle = \oint d\varphi\,(\lambda^+ T + \lambda^N J)$$

$$= Q^{\text{Vir}}[\lambda^+] + Q^{u(1)}[\lambda^N]. \qquad (3.123)$$

Here, we have defined the physical currents

$$T = 2\gamma_s\left(F^- - \frac{1}{4}(F^0)^2 - \frac{1}{2}\partial F^0\right), \qquad J = -\gamma_u F^N. \qquad (3.124)$$

Indeed, they transform as Virasoro and affine $u(1)$ currents,

$$\delta T = \lambda^+\partial T + 2T\partial\lambda^+ + \gamma_s\partial^3\lambda^+, \qquad \delta J = -\gamma_u\partial\lambda^N. \qquad (3.125)$$

Again, we can decompose these currents in Fourier modes,

$$L_n = -\oint d\varphi \, e^{in\varphi} \, T(x^+), \qquad N_n = -\oint d\varphi \, e^{in\varphi} J(x^+). \qquad (3.126)$$

These charges satisfy an *uncoupled* Virasoro-affine $u(1)$ algebra with nonzero affine level,

$$[L_m, L_n] = (m - n)L_{m+n} + 2\pi\gamma_s m^3 \delta_{m+n,0}, \qquad (3.127\text{a})$$

$$[L_m, N_n] = 0, \qquad (3.127\text{b})$$

$$[N_m, N_n] = 2\pi\gamma_u \, m \, \delta_{m+n,0}. \qquad (3.127\text{c})$$

In fact, there is no contradiction here. The uncoupled symmetries can be transformed into the coupled algebra at finite α in (3.120). It is easiest to see this on the level of the current transformations. The first step is to match δJ with $\delta \mathcal{J}$. For this, define

$$-\gamma_u \lambda^N = \lambda^+ J - \frac{2\gamma_u}{\alpha^2}\left(\partial\lambda^+ + \frac{2\bar{\lambda}^N}{\alpha^2}\right). \qquad (3.128)$$

Then δJ reproduces (3.118). To obtain the correct Virasoro transformations, define

$$\mathcal{T} = T - \frac{\alpha^4}{8\gamma_u}J^2 - \frac{\alpha^2}{2}\partial J. \qquad (3.129)$$

This current satisfies the coupled transformation relation (3.117). The identification between the coupled and uncoupled modes $(\mathcal{L}_n, \mathcal{N}_n)$ and (L_n, N_n) then follows by expanding the above. As generators of symmetries on a classical phase space, the coupled and uncoupled algebras are therefore equivalent.

3.5 Conclusions and outlook

We conclude with a discussion and perspectives for further work.

The results of this chapter show that many of the features of the $\text{AdS}_3/\text{CFT}_2$ correspondence can be realized in a novel holographic correspondence, involving a pseudo-Newton–Cartan theory in the bulk and a particular near-BPS limit on the boundary. This provides a concrete model of beyond-AdS/CFT holography, opening up many avenues of further exploration in terms of generalizing other well-studied aspects of AdS/CFT.

As one possible direction, we note that the two copies of the Virasoro spacetime algebra in $\text{AdS}_3/\text{CFT}_2$ can be induced from a $sl(2, \mathbb{R}) \oplus sl(2, \mathbb{R})$ current algebra on the string worldsheet [142]. Here, the spacetime chirality is closely related to worldsheet chirality. For example, the left moving chiral algebra in spacetime is lifted from left movers on the string worldsheet and vice versa. Moreover, the string worldsheet analysis can give a microscopic interpretation of the central charge in terms of string winding modes. It is expected that similar string theory analyses should be valid even after we take the Inönü-Wigner limit. One would expect the corresponding world-sheet theory to be a WZW model on P_2^c, similar

to what is studied in [133, 143]. In connection to this, it is interesting to note that the target space of such a model can easily be inferred from the results of [133] by replacing E_2^c with P_2^c. This leads precisely to a pp-wave like geometry with signature $(-1, -1, 1, 1)$, i.e. two 'times', such that after a null reduction one obtains a pseudo-NC geometry in the same way that pp-waves connect to NC geometry after null reduction [56, 144–146].

Moreover, it would be interesting to study string theory on pseudo-Newton–Cartan gravity, using the AdS$_3$/CFT$_2$ results of Ref. [142], while one could also examine whether the Wakimoto representation of $sl(2, \mathbb{R}) \oplus u(1)$ on the world-sheet [147] can reproduce the representations of [143] by taking our contraction limit. Moreover, in a recent work [148] it was shown that NC geometry appears as the target space in nonrelativistic string theory, which may also be of use to understand strings on pseudo-NC geometry. In connection to this, it also seems relevant to note that the nonrelativistic limit of AdS/CFT considered in [149] shows that the resulting nonrelativistic string action has the supersymmetric Newton–Hooke group as a symmetry group.

Another worthwhile direction to pursue is to employ the concrete AdS/CFT model coming from the D1-D5 brane system in type IIB superstring theory, which provides a duality between $\mathcal{N} = (4, 4)$ superconformal field theory and string theory in AdS$_3$ [10, 142, 150]. Thus our gravity theory should have a supersymmetric extension, which is related to an appropriate limit of $\mathcal{N} = (2, 2)$ supergravity in three dimensions [151]. In fact, the bosonic sector of this supergravity theory exactly has two $u(1)$ gauge fields as R-charge currents so directly fits into the symmetry algebra we took as our starting point. Understanding this string theory and supergravity embedding after our limit should provide a rich structure as well.

At the level of solutions of pseudo-NC gravity, we have focused on the vacuum but an obvious next step is to examine the limit of the BTZ black hole [59] and its physics. Another class of solutions that could shed further light on the theory are the BPS supergravity solutions of [152–159] which are dual to CFT chiral primaries. More generally, one may wish to address bulk reconstruction in our setup. While for AdS$_3$/CFT$_2$ the entire relativistic bulk should be reconstructed from the boundary conformal field theory, pseudo-NC gravity represents in some sense a more minimal setup. In this case, we only need to reconstruct a foliation structure, namely two-dimensional pseudo-Riemannian geometry fibred over a dilatation one-form. Another, related direction would be to see if there is an analogue of holographic entanglement entropy [43] for our correspondence. For this, a minimal setup can be constructed using Chern–Simons theory [160, 161]. It would also be very interesting to investigate the implications of the radial fibration on the RG flow of the dual field theories.

More generally, it will be important to better understand the field theory that is dual to pseudo-NC gravity. In this connection it is worth remarking that our limit has a strong resemblance to the limit that gives rise to Spin Matrix Theory [102], which follows from the correspondence between AdS$_5$/CFT$_4$. To see this, define a coupling constant $g = \alpha^{-2}$ and identify the energy E and charge J as $E = \alpha^{-2} D = \mathcal{N} + \frac{g}{2} \mathcal{D}$ and $J = -\alpha^{-2} Q_1 = \mathcal{N} - \frac{g}{2} \mathcal{D}$ respectively. By the state-operator map the dilatation operator corresponds to the energy of states of the

theory on the cylinder. In Spin Matrix Theory, $\mathcal{N}$ is the length of the spin chain and $\mathcal{D}$ is the one-loop dilatation operator of the spin chain. The limit $\alpha \to \infty$ zooms in on states close to $E = J$ which is the lowest lying state in the spectrum, so by unitarity we have $E \geq J$. The Spin Matrix Theory limit [102] corresponds to sending $g \to 0$ while keeping $(E - J)/g$ fixed, which is precisely what happens in our limit for the operators D and Q_1 as we take $\alpha \to \infty$. This connection with Spin Matrix Theory seems to suggest that the symmetry of Spin Matrix Theory might be related to an another real form of the complexified Newton–Hooke algebra. On the other hand, applied to $\text{AdS}_3/\text{CFT}_2$, especially in relation to the $\mathcal{N} = (4, 4)$ superconformal field theory and its possible spin chain interpretation (see [162] for recent progress), this suggests that there might be some form of two-dimensional Spin Matrix Theory.

Regarding the field theory interpretation, it is important to emphasize that the finite α identifications we have made in Section 3.4.3 are entirely classical. We have found an infinite-dimensional algebra of conserved charges for classical Chern–Simons theory, which correspond to real-valued functions on the phase space. Upon quantization, these charges should lead to unitary operators on a Hilbert space of states. However, our classical computations do not tell us what the inner product or Hermitian conjugate on this Hilbert space should be. We have only obtained the algebra of symmetries that should be realized on it. Unitary representations of the coupled algebra do exist, and [141] has explained how to construct induced representations using its semidirect product structure. It would be very interesting to study their consequences from a field theory perspective. While the bulk may have allowed us to identify the relevant symmetries, we believe that field theory will be our guide towards their representations.

Finally, it could be interesting to find analogues of our holographic correspondence, such as higher spin and/or higher-dimensional generalizations. Following the higher spin AdS_3 work of e.g. [163], and its Chern–Simons theory construction [84, 92], it is possible to find connections between the non-AdS higher spin holography of [80, 164], TMG holography [165–170] and nonrelativistic higher spin works of [171] to the higher spin generalization of our work.

Chapter 4

Generalized Toda theory from six dimensions

As we mentioned in Section 1.3.3, the idea that four-dimensional gauge theories are related to two-dimensional Riemann surfaces has been around for a long time. Over time, it has been made increasingly precise. Its most recent incarnation is the discovery that partition functions of four-dimensional $\mathcal{N} = 2$ super-Yang–Mills theories can be mapped to correlators in two-dimensional Toda theories.

This relation is known as the Alday-Gaiotto-Tachikawa (AGT) correspondence. It has a natural interpretation in M-theory: four-dimensional $\mathcal{N} = 2$ theories can be constructed by compactifying M5 branes on Riemann surfaces. Consequently, it has been proposed that the AGT correspondence can be *derived* by obtaining Toda theory from a compactification of M5 branes along four dimensions. This compactification relies on a Drinfeld–Sokolov reduction of sl_N Chern–Simons theory along the lines of our discussion in Section 2.5.2.

In this chapter, we attempt to solidify this derivation of the AGT correspondence. We also propose an extension that includes more general Toda theories arising from different sl_2 embeddings.

The work in this chapter has appeared previously in [2].

4.1 Introduction

The Alday-Gaiotto-Tachikawa (AGT) correspondence is a remarkable relation between BPS sectors of four-dimensional supersymmetric gauge theories and two-dimensional non-supersymmetric conformal field theories [26,172]. The correspondence states that S^4 partition functions [173] of class $\mathcal{S}$ theories of type A_{N-1} [174] can be expressed as correlation functions in A_{N-1} Toda theory. In particular, the conformal blocks of the Toda theory were shown to be equivalent to the instanton partition functions, computed in the Ω background [175], whereas the three-point functions reproduce the one-loop determinants.

The correspondence can arguably be viewed as the culmination of a long effort towards the understanding of the non-perturbative structure of $\mathcal{N} = 2$ Yang–Mills theories [174–178]. In particular, the systematic construction of the class $\mathcal{S}$ theories provided great insight into the strong-coupling limits of these super-Yang–Mills theories [174]. In this construction, gauge couplings are identified with the complex structure parameters of a Riemann surface and strong-weak dualities are interpreted as a change of 'pairs of pants'-decomposition of the Riemann surface. The AGT correspondence then explicitly brings (non-perturbative) four-dimensional Yang–Mills into the realm of two-dimensional CFT. This connection is fruitful since the latter class of theories is in general much better understood. For example, S-duality invariance of the S^4 partition function of $\mathcal{N} = 2$ $SU(2)$ Yang–Mills with $N_f = 4$ corresponds to crossing symmetry of the Liouville four-point function, which was rigorously proven some time ago [179].

Increasing the rank, however, the AGT correspondence maps unsolved problems in the gauge theory to other unsolved problems in Toda theory. For example, the computation of partition functions of non-Lagrangian theories is mapped onto the determination of a general three-point function. However, the correspondence allows these problems to be phrased in very distinct settings, leading to new insights and progress [180, 181]. Moreover, a complete solution to either problem would kill two birds with one stone.

A physical interpretation of the AGT correspondence and its generalizations to higher rank and inclusion of defects seems to rely on a six-dimensional perspective.[1] Indeed, the construction of class $\mathcal{S}$ theories already hints at this since it assigns a class $\mathcal{S}$ theory of type A_{N-1} to a punctured Riemann surface Σ, by compactifying N M5 branes on Σ [174]. It is precisely this Riemann surface on which the Toda theory lives. The number of punctures denotes the number of primary insertions in the Toda correlation function.

To be precise, the six-dimensional interpretation of the AGT correspondence is that the supersymmetric partition function of the 6d $(2, 0)$ theory $\mathcal{T}$ of type A_{N-1} on $S^4 \times \Sigma$ has a four- and two-dimensional incarnation, which are equal. This is illustrated by the diagram in Figure 4.1. The arrows denote a supersymmetric zero-mode reduction to the gauge theory $\mathcal{S}$ and Toda theory respectively.

The equivalence of the lower two partition functions in Figure 4.1 is explained through a topological twist performed on Σ and the Weyl invariance of $\mathcal{T}$. These

---

[1] Relevant references will be given in the main body of the chapter.

$$Z_{\mathcal{T}}\left(S^4 \times \Sigma\right)$$

$$Z_{\mathcal{S}}\left(S^4\right) \qquad \Longleftrightarrow \qquad Z_{\text{Toda}}\left(\Sigma\right)$$

with arrows labeled $\Sigma \to 0$ and $S^4 \to 0$.

Figure 4.1: Equivalent reductions of the six-dimensional theory $\mathcal{T}$.

features enable us to send the size of either manifold to zero without affecting the value of the partition function, as long as we restrict to the supersymmetric sector. However, the lack of a Lagrangian description of $\mathcal{T}$ blocks a straightforward implementation of this strategy.

Over the past few years, many different approaches have been taken to overcome this difficulty. See for an incomplete list of references [182–190]. A constructive derivation of the correspondence is desirable as it could provide an idea of the scope of AGT-like correspondences between supersymmetric sectors of gauge theories and exactly solvable models. Moreover, due to its six-dimensional origin, such a derivation may also shed light on the worldvolume theory of multiple M5 branes.

In this chapter we will build on a recent derivation by Córdova and Jafferis [191]. Using the relation between the type A_{N-1} 6d $(2,0)$ theory on a circle and five-dimensional $\mathcal{N} = 2$ $SU(N)$ Yang–Mills theory [192–194], one performs a Kaluza-Klein reduction on S^4 to obtain A_{N-1} Toda theory on a Riemann surface Σ. The Toda fields are understood as boundary fluctuations of $SL(N, \mathbb{C})$ Chern–Simons theory on a manifold with asymptotically hyperbolic boundary. This is understood in the following way. Near the boundary, the Chern–Simons connection satisfies the boundary conditions

$$\mathcal{A} \to \frac{d\sigma}{\sigma}H + \frac{du}{\sigma}T_+ + \mathcal{O}\left(\sigma^0\right). \tag{4.1}$$

Here, H is an element of the Cartan of sl_N, which sits together with a raising operator T_+ in an $sl_2 \subset sl_N$ subalgebra. In a type IIA frame, these boundary conditions arise from a Nahm pole on the scalars of D4 branes ending on D6 branes [34, 195].

As we reviewed in Section 2.5, boundary conditions such as (4.1) are well known to provide a reduction of the $\widehat{sl_N}$ WZW theory induced by Chern–Simons on the boundary of asymptotically hyperbolic space, see for example [91, 96, 97]. For the principal sl_2 embedding found in [191], such constraints give Toda theory [95]. Consequently, one of the building blocks in establishing the AGT correspondence is obtained.

However, as we discussed in Section 2.5.2, the residual symmetries of the constrained WZW theory strongly depend on the embedding of sl_2 into sl_N. For example, for $N = 3$, the reduced boundary theory has $\mathcal{W}_3$ symmetry if the embedding is the principal one, but it has Polyakov-Bershadsky $\mathcal{W}_3^{(2)}$ symmetries for the diagonal embedding. More generally, sl_2 embeddings into sl_N are labeled by

the integer partitions λ of N. Each choice leads to a reduced boundary theory with different symmetries, which we will denote by $\mathcal{W}_\lambda$. These generalized Toda theories play a role in extensions of the AGT correspondence.

In [196] a relation was proposed between instanton partition functions of $\mathcal{N} = 2$ $SU(2)$ quiver gauge theories with an insertion of a surface operator, which arises from a codimension two defect in the 6d theory, and conformal blocks of $\widehat{sl_2}$ WZW theories. This was generalized in [197] to a relation between $SU(N)$ gauge theories and $\widehat{sl_N}$ WZW theories. These cases dealt with the so-called full surface operators.

It was conjectured in [198] that the $SU(N)$ instanton partition functions with more general surface operators, labeled by a partition λ of N, would be equivalent to the conformal blocks of theories with $\mathcal{W}_\lambda$ symmetry. The standard AGT and full surface operator setup are now special cases of this more general setup, corresponding to the partitions $N = N$ and $N = 1 + \ldots + 1$ respectively. The $\mathcal{W}_\lambda$ algebra, which is also labeled by a partition of N, is obtained by quantum Drinfeld–Sokolov reduction of $\widehat{sl_N}$. An explicit check was performed for the Polyakov-Bershadsky algebra $\mathcal{W}_3^{(2)}$, whose conformal blocks were shown to agree with instanton partition functions in the presence of a simple surface defect, with partition $3 = 2 + 1$. Further checks of the proposal have appeared in [199, 200].

Then, based on mathematical results in instanton moduli spaces, it was realized in [201] that the instanton partition function in the presence of a general surface operator on $\mathbb{C}^2$ could be conveniently computed as an ordinary instanton partition function on $\mathbb{C}/\mathbb{Z}_m \times \mathbb{C}$, where m corresponds to the maximum number of parts of the partition λ. This technique was further used in [202] to compute the S^4 partition functions of $\mathcal{N} = 2^*$ $SU(N)$ theories in the presence of a full surface operator, and was shown in the case of $SU(2)$ to reproduce the full $\widehat{sl_2}$ WZW correlation function. For $SU(N)$ results were obtained as well, but could not be compared due to lack of results on the WZW side.

In the following, we will denote the generalized Toda theory resulting from an sl_N reduction with partition λ by Toda$_\lambda$. The corresponding generalized AGT correspondence will be referred to as the AGT$_\lambda$ correspondence.

In the present chapter, we propose a setup to derive these AGT$_\lambda$ correspondences using the path laid out by Córdova and Jafferis. This approach is very natural for the problem at hand, since the general quantum Drinfeld–Sokolov reduction of $\widehat{sl_N}$ can be understood from a Chern–Simons perspective as well, by imposing the boundary conditions (4.1) for a general $sl_2 \subset sl_N$ embedding. Therefore, we wish to show that upon including the appropriate codimension two defects in the six-dimensional setup, one finds these more general boundary conditions. Along the way, we will also be able to clarify some aspects of the analysis in the original paper [191].

4.1.1 Overview and summary of results

Since the story is rather intricate and hinges on some important assumptions, we will briefly sketch the main logic and possible pitfalls of our arguments here.

The original derivation, which we review in Section 4.2.1, connects the 4d-2d correspondence to the 3d-3d correspondence through a Weyl rescaling. One of the main virtues of this connection is that a full supergravity background was already derived in [203] for the 3d-3d correspondence, which can then be put to use in the 4d-2d setting. The three-manifold M_3 on which the resulting Chern–Simons theory lives has nontrivial boundary. With specific boundary conditions, its boundary excitations lead to Toda theory.

These boundary conditions manifest themselves in a IIA frame in the form of a Nahm pole on the worldvolume scalars of a D4 brane ending on a D6 brane. The original derivation attributes the Nahm pole to the D6 branes that are also related to a non-zero Chern–Simons level. We point out that the Nahm pole should instead be attributed to a distinct set of branes, which we refer to as D6' branes. The original branes will always be referred to as D6 branes, and will still be related to the Chern–Simons coupling.

A crucial element in the original derivation is that the Nahm pole on the scalars transforms under Weyl rescaling to the relevant Drinfeld–Sokolov boundary condition on the Chern–Simons connection. It is argued that this boundary condition is a natural way to combine Nahm data into a flat connection, but the Drinfeld–Sokolov form is not the unique combination that achieves this. However, we have not been able to obtain a better understanding of this point and our construction still relies on this assumption. We expect that carefully examining the Weyl rescaling of the full supergravity background and the corresponding worldvolume supersymmetry equations should allow one to translate the Nahm pole arising in the 4d-2d frame to the Drinfeld–Sokolov boundary condition in the 3d-3d frame. However, a direct implementation of this procedure is ruled out by the lack of a Lagrangian description of multiple M5 branes.

The Weyl rescaling of the full supergravity background should also allow one to further explain the claim in [191] that the Killing spinors as obtained in [203] for the 3d-3d background become the usual 4d Killing spinors of [173, 204] after Weyl rescaling and an R-gauge transformation. This argument is not completely satisfactory, since the spinors in the 3d-3d frame are related to a squashed sphere geometry that preserves an $SU(2) \times U(1)$ isometry, whereas the Killing spinors in [204] are related to a squashed sphere with $U(1) \times U(1)$ isometry. We note that this slight discrepancy may in fact be immaterial at the level of partition functions, as was indeed originally found in [205] in the context of 3d partition functions and properly understood in [206].

The uplift to M-theory of the setup we propose leads to M5 branes on a holomorphic divisor in a generalized conifold, which we discuss in Section 4.3. Here, we crucially use the orbifold description of codimension two defects that was advocated in [200, 201].[2] This enables us to treat the defects purely geometrically, so that we do not have to worry about coupling the worldvolume theory to additional degrees of freedom on the defect.

---

[2] The gravity duals of class $\mathcal{S}$ theories also treat such codimension two defects geometrically [207].

We propose to use the conifold geometry as an approximation to the pole region of a full supergravity background that would be needed to account for a defect in a squashed S^4 background.[3] Although this approximation suffices for our purposes, it comes with a particular value of the squashing parameter that leads to a curvature singularity corresponding to the conifold point. In principle, such a singularity could couple to the M5 worldvolume theory. It would therefore be very interesting to obtain a class of supergravity backgrounds for arbitrary parameter values where this singularity can be avoided.

The radial slices of the divisor of the generalized conifold have a $U(1) \times U(1)$ isometry. Furthermore, it supports two supercharges, in agreement with the four-dimensional Ω background. In the special case where only a single D6' brane is present, corresponding to a trivial surface operator, the isometry enhances to $SU(2) \times U(1)$, but still only two supercharges are present. This may seem strange, since one expects a nontrivial surface operator to break part of the supersymmetries. However, placing a surface operator on a fully squashed S^4 does not break any additional isometries, hence the number of preserved supercharges on a fully squashed background is the same with or without a surface operator.

An important assumption in our derivation is that the connection to the 3d-3d correspondence still stands. Even though additional defects are present we claim that these only manifest themselves in the boundary conditions of the Chern–Simons theory. Since these defects are located at the asymptotic boundary of M_3, we believe that this claim is justified.

Finally, it is known that at $k = 1$ the Hilbert spaces of $SL(N, \mathbb{C})$ and $SL(N, \mathbb{R})$ Chern–Simons theories agree [210]. Therefore, at $k = 1$ the reduction to generalized real Toda theories proceeds as usual. For higher k, one obtains complex Toda$_\lambda$ theories. In the principal case, the original derivation puts forward a duality between complex Toda and real paraToda with a decoupled coset. It would be interesting to formulate a similar correspondence for complex Toda$_\lambda$ theories.

4.2 Review

In this section we review the derivation by Córdova and Jafferis of both the 3d-3d and AGT correspondence [191, 203]. Subsequently, we indicate how the Nahm pole boundary conditions lead to Toda$_\lambda$ theories.

4.2.1 Principal Toda theory from six dimensions

Consider the 6d $(2, 0)$ CFT of type A_{N-1} on two geometries which are related by a Weyl transformation [191]

$$S_\ell^4/\mathbb{Z}_k \times \Sigma \overset{\text{Weyl}}{\Longleftrightarrow} S_\ell^3/\mathbb{Z}_k \times M_3. \qquad (4.2)$$

We think of the $S_\ell^4/\mathbb{Z}_k$ as the Lens space $S_\ell^3/\mathbb{Z}_k$ fibred over an interval, shrinking to zero size at the endpoints. The three-dimensional manifold M_3 is a warped

---

[3]See also [208, 209] for a like-minded approach to the 3d-3d correspondence.

(a) $S_\ell^4/\mathbb{Z}_k \times \Sigma$

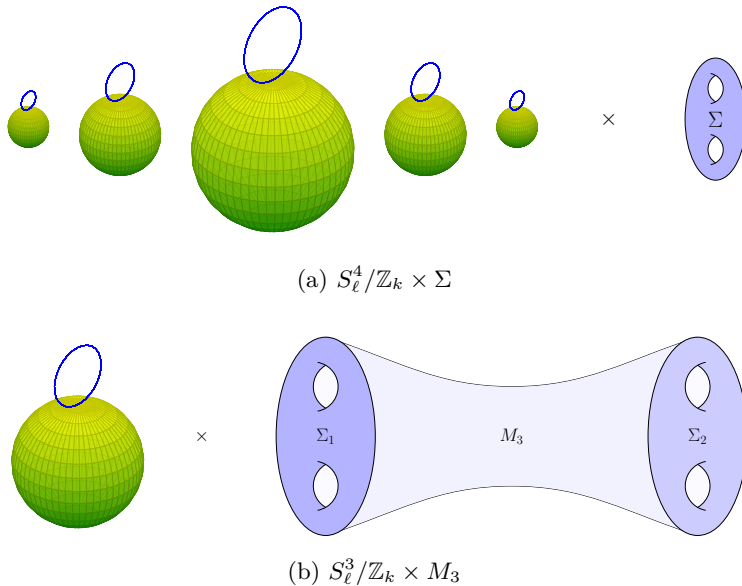(b) $S_\ell^3/\mathbb{Z}_k \times M_3$

Figure 4.2: The geometries associated to (a) the 4d-2d frame and (b) the 3d-3d frame. The Hopf fiber of the S^3 is indicated in blue.

product of a Riemann surface Σ and $\mathbb{R}$ and ℓ is a squashing parameter which controls the ratio between the Hopf fiber and base radius of the S^3. We will refer to these geometries as the 4d-2d and 3d-3d geometries respectively. See Figure 4.2 for an illustration.

In older work [211] it was shown how to couple 5d $\mathcal{N} = 2$ SYM to 5d $\mathcal{N} = 2$ off-shell supergravity. Using the equivalence between the A_{N-1} $(2,0)$ theory on a circle and 5d $\mathcal{N} = 2$ $SU(N)$ Yang–Mills theory [192–194], these general results allow one to preserve four supercharges from the $(2,0)$ theory on the geometry [203]

$$S_\ell^3/\mathbb{Z}_k \times M_3 \subset S_\ell^3/\mathbb{Z}_k \times T^*M_3 \times \mathbb{R}^2. \tag{4.3}$$

In the original derivation, the $(2,0)$ theory is reduced on the Hopf fiber. This translates in 5d to a flux for the graviphoton, which is compatible with the 5d supergravity background. For general squashing, it is required to turn on all bosonic fields in the off-shell supergravity multiplet. The resulting background allows for a supersymmetric zero mode reduction on the S^3 which gives rise to $SL(N, \mathbb{C})$ Chern–Simons on M_3 with coupling $q = k + i\sqrt{\ell^2 - 1}$.[4]

The complex Chern–Simons coupling consists of an integer k and a continuous parameter ℓ. The former arises from the graviphoton flux that couples to the D4 gauge fields through the 5d Chern–Simons coupling

$$\frac{1}{8\pi^2} \int_{S^2 \times M_3} \text{Tr}\,(C \wedge F \wedge F) \implies \frac{k}{4\pi} \int_{M_3} \text{Tr}\left(A \wedge dA + \frac{2}{3} A \wedge A \wedge A\right). \tag{4.4}$$

---

[4] This provides a derivation of the 3d-3d correspondence as formulated in [212–214].

The continuous parameter ℓ arises from the squashing parameter of the three-sphere. A salient detail of the reduction is that the fermions of the $(2,0)$ theory come to be interpreted as Faddeev-Popov ghosts for the gauge fixing of the non-compact part of the gauge algebra

$$sl(N, \mathbb{C}) \cong su(N) \oplus i\, su(N).$$

This provides a concrete explanation for the puzzle that the supersymmetric reduction of 5d *supersymmetric* Yang–Mills with *compact* gauge group $SU(N)$ becomes a *non-supersymmetric* Chern–Simons theory with *non-compact* gauge group. The ghost and gauge fixing terms in the effective action are subleading in R_{S^3}, so that in the far IR the gauge fixing is undone and the final result for the effective theory on M_3 is the full $SL(N, \mathbb{C})$ Chern–Simons theory. The complex connection

$$\mathcal{A} = A + iX$$

is built out of the original Yang–Mills connection together with three of the five worldvolume scalars X_i. The latter combine into a one-form on M_3 due to the topological twist. We denote the other two scalars by Y_a. They correspond to movement in the remaining $\mathbb{R}^2$ directions of (4.3).

We now return to the particular M_3 that arises from the Weyl rescaling of the 4d-2d background. Note that it has a nontrivial boundary consisting of two components $\Sigma \cup \Sigma$. So we need to specify boundary conditions, which ultimately lead to non-chiral complex Toda theory on Σ, as we recall in Section 4.2.2.

To understand what type of boundary conditions have to be imposed, let us first look at Table 4.1 that summarizes the 4d-2d setup.

	$S^4/\mathbb{Z}_k$			Σ		$\mathbb{R}^3$			$\mathbb{R}^2$	
	0	1	2	3	4	5	6	7	8	9	10
N M5	x	x	x	x	x	x					

Table 4.1: M-theory background relevant for the AGT correspondence.

The theory is topologically twisted along Σ. An $\mathbb{R}^2 \subset \mathbb{R}^3$ provides the fibers of its cotangent bundle $T^*\Sigma$. In the 3d-3d frame the entire $\mathbb{R}^3$ is used for the topological twist on M_3.

The setup is reduced on the Hopf fiber of the $S^3/\mathbb{Z}_k \subset S^4/\mathbb{Z}_k$. Equivalently, thinking of the S^4 as two k-centered Taub-NUTs glued along their asymptotic boundary, one reduces on the Taub-NUT circle fiber. It is well known that the M-theory reduction on the circle fiber of a multi-Taub-NUT yields D6 branes at the Taub-NUT centers. The IIA setup[5] is then given by Table 4.2.

---

[5] Note that the resulting three-sphere has curvature singularities at the poles even for $k = 1$.

	S^3			Σ		$\mathbb{R}^3$			$\mathbb{R}^2$	
	1	2	3	4	5	6	7	8	9	10
N D4	x	x	x	x	x					
k D6				x	x	x	x	x	x	x
k $\overline{\text{D6}}$				x	x	x	x	x	x	x

Table 4.2: Reduction of M-theory background to type IIA.

The D6 and $\overline{\text{D6}}$ branes sit at the north and south pole of the S^3 respectively and the D4 branes end on them. The boundary conditions on the D4 worldvolume fields are then claimed to be similar to those studied in [195] for D3 branes ending on D5 branes. That would imply that the D4 gauge field satisfies Dirichlet boundary conditions, while the triplet of scalars X_i satisfy the Nahm pole boundary conditions we mentioned in equation (1.27):

$$X_i \to \frac{T_i}{\sigma}. \tag{4.5}$$

Here, the T_i constitute an N dimensional representation of $su(2)$ and the coordinate σ parametrizes the interval over which the $S^3/\mathbb{Z}_k$ is fibred. This can be understood by thinking of the N D4 branes as comprising a charge N monopole on the D6 worldvolume. Indeed, the Nahm pole boundary conditions were originally discovered in a similar context [34].

We want to pause here for a moment to note that it is not quite clear why the present setup is related to the analyses of [34, 195]. The latter deal with (the T-dual of) a D4-D6 brane system with different codimensions, as described in Table 4.3.

	$\mathbb{R}$	$\mathbb{R}^2$		Σ		$\mathbb{R}^3$			$\mathbb{R}^2$	
	1	2	3	4	5	6	7	8	9	10
N D4	$\vdash$	x	x	x	x					
k D6		x	x	x	x	x	x	x		

Table 4.3: Type IIA setup in which Nahm poles arise as boundary conditions on the X_i triplet of D4 scalars.

Here, the $\vdash$ denotes the fact that the D4 branes end on the D6 branes. The D6 branes in Table 4.2 are instead similar to the ones studied in [215] (see also [216]). The corresponding orbifold singularities in the 4d-2d frame reduce to a graviphoton flux in the 3d-3d frame, which is responsible for the Chern–Simons coupling through (4.4). However, they cannot give rise to a Nahm pole. In Section 4.4, we propose an alternative perspective that simultaneously allows for a non-zero Chern–Simons coupling *and* correct codimensions between D4 and D6 branes for a Nahm pole to arise.

Leaving these comments aside for the moment, we must understand precisely what a Nahm pole in the topologically twisted scalars X_i would translate to in the 3d-3d picture. As remarked in Section 4.1.1, transforming the supersymmetry equations that lead to a Nahm pole under the Weyl transformation is a difficult problem. However, we know that the resulting connection $\mathcal{A} = A + iX$ will have to be flat. Furthermore, we expect that the leading behavior of $\mathcal{A}$ towards the boundary should still be fixed.

As we discussed in Section 2.3.1, the relation between Chern–Simons theory and Wess–Zumino–Witten models requires $\mathcal{A}$ to be chiral on the boundary.[6] If $(z, \bar{z})$ denote (anti)holomorphic coordinates on Σ, we should demand that $\mathcal{A}_{\bar{z}}$ vanishes. Thus, a natural equivalent of the boundary conditions (4.5) would be

$$\mathcal{A} = \mathcal{L}_0 \frac{d\sigma}{\sigma} + \mathcal{L}_+ \frac{dz}{\sigma} + \mathcal{O}\left(\sigma^0\right). \tag{4.6}$$

This is a flat connection. We have defined the sl_2 generators $\mathcal{L}_0 = iT_1$ and $\mathcal{L}_\pm = T_2 \mp iT_3$. They satisfy the standard commutation relations[7]

$$[\mathcal{L}_a, \mathcal{L}_b] = (a - b)\mathcal{L}_{a+b}. \tag{4.7}$$

These boundary conditions are precisely the ones that correspond to the reduction of the boundary $\widehat{sl_N}$ algebra to the $\mathcal{W}_N$ algebra. The antiholomorphic connection of the complex Chern–Simons theory behaves in the same way. Adding the contributions from the two components of ∂M_3 then gives rise to a full (non-chiral) *complex* Toda theory. It would be interesting to directly verify the transformation of the Nahm pole (4.5) to the connection boundary condition (4.6) under the Weyl transformation, as we already pointed out in Section 4.1.1.

4.2.2   Nahm pole and Drinfeld–Sokolov reduction

Using the radial coordinate $e^{-\rho} = 1/\sigma$, the leading order of the transformed Nahm pole boundary conditions (4.6) corresponds to the highest weight constraint (2.103). We denote the reduced quantum theory obtained from a general partition λ by Toda$_\lambda$. As we discussed in Section 2.5.2, the corresponding $\mathcal{W}_\lambda$ algebra contains a current for each sl_2 multiplet appearing in the decomposition of the adjoint of sl_N [89, 91, 96]. As we will see in the following section, Toda$_\lambda$ can be obtained from six dimensions using the generalized conifold.

However, in this chapter our starting point is a *complex $sl_N(\mathbb{C})$* Chern–Simons theory. Applying the Drinfeld–Sokolov procedure from Section 2.5 at the quantum level would give us a complex Toda theory. The AGT correspondence involves a real version of Toda theory. To mediate this, the following relation is suggested

---

[6] Nonchiral boundary conditions lead to reduced theories with nonzero chemical potentials [74, 97]. It would be interesting to see if they have a role to play in further generalizations of the AGT correspondence.

[7]We will use antihermitian generators in this chapter.

for the principal embedding [191]

$$\text{complex Toda}(N, k, s) \quad \Leftrightarrow \quad \text{real paraToda}(N, k, b) + \frac{\widehat{\mathfrak{su}}(k)_N}{\widehat{\mathfrak{u}}(1)^{k-1}}.$$

Here, $N-1$ gives the rank of the Toda theory. The parameters k and s are coupling constants in the complex Toda theory. On the right hand side, k describes the conformal dimension $\Delta = 1 - 1/k$ of the parafermions in paraToda. The real Toda coupling is

$$b = \sqrt{\frac{k - is}{k + is}}.$$

At $k = 1$ the right hand side reduces to real Toda theory [217]. Both real and complex generalized Toda theories can be obtained as Drinfeld–Sokolov reductions of $SL(N, \mathbb{R})$ or $SL(N, \mathbb{C})$ Chern–Simons theories. Geometric quantization of the latter two theories yields identical Hilbert spaces [210] for $k = 1$. After reduction, the complex and real Toda theory therefore agree at this particular level. Likewise, using a general $sl_2 \subset sl_N$ embedding, complex and real Toda_λ theory at $k = 1$ are identified.

4.3 Orbifold defects and the generalized conifold

In Section 4.3.1 we briefly summarize the setup pertaining to the AGT_λ correspondence. This leads us to consider generalized conifolds, denoted by $\mathcal{K}^{k,m}$, whose geometry we review in Section 4.3.2.

4.3.1 Codimension two defects and their geometric realization

We now consider the generalization of AGT that includes surface operators in the gauge theory partition function, which we refer to as AGT_λ. Under the correspondence, the ramified instanton partition functions are mapped to conformal blocks of Toda_λ theories [198–200]. Similarly, it is expected that one-loop determinants in the gauge theory map to three-point functions. This has been checked for the case of a full surface operator [202].

A six-dimensional perspective on this correspondence is provided by including codimension two defects in the 6d $(2,0)$ theory. These defects wrap Σ and lie along a two-dimensional surface in the gauge theory. Therefore, they represent a surface defect in the gauge theory, and change the theory on the Riemann surface.

There exists a natural class of codimension two defects that are labeled by partitions of N [174], as we will discuss in more detail below. Table 4.4 summarizes the M-theory background for the particular instance of AGT_λ that we are interested in.

	S^4			Σ		$\mathbb{R}^3$			$\mathbb{R}^2$	
	0	1	2	3	4	5	6	7	8	9	10
N M5	x	x	x	x	x	x					
Defect		x	x	x	x	x	x	x			

Table 4.4: Generalized AGT setup.

For the moment, we zoom in on the region near the north pole of the S^4, where the geometry locally looks like $\mathbb{C}^2$. In this region, we consider the realization of the defect as a $\mathbb{C}^2/\mathbb{Z}_m$ orbifold singularity that spans the 01910 directions of Table 4.4 [200, 201] (see also [218]). Note that these codimension two defects are usually described using an additional set of intersecting M5 branes together with an orbifold singularity. We want to emphasize here that we describe the defects using only the orbifold singularity. This interpretation is also supported by mathematical results on the equivalence between ramified instantons and instantons on orbifolds. See [201] and references therein.

This means that from the gauge theory perspective, i.e. the 0123 directions, that the geometry locally looks like $\mathbb{C}/\mathbb{Z}_m \times \mathbb{C}$. A partition λ is then naturally associated to the M5 branes

$$\lambda: \quad N = n_1 + \ldots + n_m.$$

It specifies the number of M5 branes with a particular charge under the orbifold group. Alternatively, when $\mathbb{C}^2/\mathbb{Z}_m$ is thought of as a limit of an m-centered Taub-NUT space, it specifies how the M5 branes are distributed among the m centers. The M5 branes wrap the 'cigars' in the second relative homology of TN_m. Upon reduction on the Taub-NUT circle fiber, the partition specifies how the N D4 branes are distributed among the m D6 branes.

Another generalization of the original AGT correspondence [196] that was already covered in the original derivation [191] concerns instanton partition functions on $\mathbb{C}^2/\mathbb{Z}_k$, an orbifold singularity that spans the 0123 directions of Table 4.4 [219, 220]. This generalization also naturally arises from a 3d-3d perspective since the $S^3/\mathbb{Z}_k$ in (4.2) is mapped to $S^4/\mathbb{Z}_k$ after the Weyl transformation. The geometry near the north pole of this quotiented four-sphere is precisely $\mathbb{C}^2/\mathbb{Z}_k$.

We now observe that there exists a simple (local) Calabi-Yau threefold that provides a particular realization of two ALE spaces $\mathbb{C}^2/\mathbb{Z}_k$ and $\mathbb{C}^2/\mathbb{Z}_m$, intersecting along a two-dimensional subspace. This is the (partially resolved) generalized singular conifold

$$\mathcal{K}^{k,m}: \quad xy = z^k w^m, \tag{4.8}$$

where we identify x or y with the 01 directions, z with the 23 and w with the 910 directions in the Table 4.4. For earlier occurrences of this space, see [221, 222]. More recently, it has also appeared in [223]. Note that $\mathcal{K}^{1,m}$ reflects the AGT$_\lambda$ setup described above. This will therefore be the geometry we focus on in the

following, although we will also make a brief comment on general k and m in Section 4.4.3.

We will use the generalized conifold as an approximation in the pole region of a squashed S^4 with defect included. This is a considerable simplification to the full supergravity background that would be needed to preserve supersymmetry on the S^4 with defect. One might worry that much information is lost by refraining from a similarly detailed and rigorous analysis as in [203]. However, we can still obtain a better understanding of the emergence of a general Nahm pole and the ensuing AGT$_\lambda$ correspondence. This will be the main result of this chapter.

4.3.2 Intersecting D6s from the generalized conifold

In this section, we provide more detail on the geometry of our proposal. First, we recall the relation between M-theory on a $\mathbb{Z}_k$ ALE space and k D6 branes in IIA. We then introduce the generalized conifold $\mathcal{K}^{k,m}$ and show how it effectively glues two such ALEs together into a single six-dimensional manifold, leading to two sets of k and m D6 branes upon reduction.

Consider the $\mathbb{Z}_k$ ALE space as a surface in $\mathbb{C}^3$ described by

$$xy = z^k. \tag{4.9}$$

Equivalently, we can think of this four-dimensional space as a $\mathbb{C}^2/\mathbb{Z}_k$ orbifold with

$$1 \in \mathbb{Z}_k: \quad (x, y) \in \mathbb{C}^2 \to (e^{2\pi i/k}x, e^{-2\pi i/k}y). \tag{4.10}$$

The latter makes it clear that the resulting space is singular. In particular, we see that there is a k-fold angular deficit at the origin in the circle

$$C := \left\{ (e^{i\alpha}x, e^{-i\alpha}y) \,|\, e^{i\alpha} \in U(1) \right\} \simeq S^1. \tag{4.11}$$

Reducing M-theory on the $\mathbb{Z}_k$ ALE along C gives rise in IIA to k D6 branes located at the origin and stretched along the transverse directions. The generalized conifold $\mathcal{K}^{k,m}$ in equation (4.8) describes a $\mathbb{Z}_k$ and $\mathbb{Z}_m$ ALE for fixed $w_0 \neq 0$ and $z_0 \neq 0$, respectively. We will make these considerations more precise in the following.

In its most common form, which we will denote by $\mathcal{K}^{1,1}$, the standard conifold is a hypersurface in $\mathbb{C}^4$ given by

$$xy = zw. \tag{4.12}$$

The space $\mathcal{K}^{1,1}$ is a cone. We denote its base by T, so that its metric is

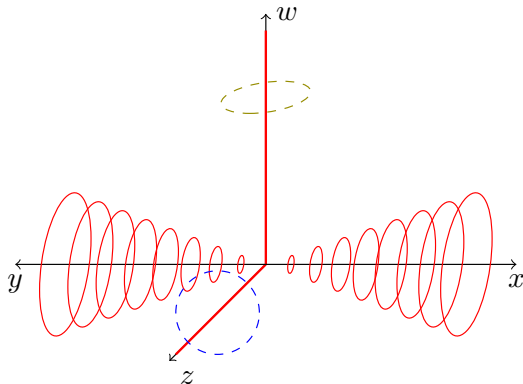$$ds^2_{\mathcal{K}^{1,1}} = d\rho^2 + \rho^2 ds^2_T. \tag{4.13}$$

Figure 4.3: Each axis represents the modulus of a complex number, the surrounding circles denote its phase. We will reduce on the red (solid) circles, corresponding to the phase of x and y, which shrink to a point at the z and w axes.

It can easily be seen from (4.12) that T is homeomorphic to $S^2 \times S^3$. For $\mathcal{K}^{1,1}$ to be Kähler, the base has to have the metric [224][8]

$$
\begin{aligned}
ds_T^2 = \frac{4}{9} &\left(d\psi + \cos^2(\theta_1/2)d\varphi_1 + \cos^2(\theta_2/2)d\varphi_2 \right)^2 \\
&+ \frac{1}{6}\left[\left(d\theta_1^2 + \sin^2\theta_1 d\varphi_1^2\right) + \left(d\theta_2^2 + \sin^2\theta_2 d\varphi_2^2\right) \right].
\end{aligned}
\tag{4.14}
$$

This describes two two-spheres, each with one unit of magnetic charge with respect to the shared Hopf fiber parametrized by ψ. In other words, T can be described by $SU(2) \times SU(2)/U(1)$. The quotient by $U(1)$ serves to identify the Hopf fibers of the $SU(2) \simeq S^3$ factors. More details can be found in Appendix 4.A.

Now we want to choose a circle which leads to intersecting D6 branes upon reduction to IIA. Following the circle (4.11) in the ALE case, we are led to consider the action

$$
(x, y, z, w) \mapsto (e^{i\alpha}x, e^{-i\alpha}y, z, w), \qquad \alpha \in [0, 2\pi).
\tag{4.15}
$$

As can be seen from Appendix 4.A, in terms of the Hopf coordinates in (4.14) describing the bulk of the base of the conifold, the circle is the orbit of

$$
(\theta_1, \theta_2, \varphi_1, \varphi_2, \psi) \mapsto (\theta_1, \theta_2, \varphi_1 + \alpha, \varphi_2 + \alpha, \psi - \alpha).
\tag{4.16}
$$

Thus the circle consists of equal θ_i orbits on the base two-spheres of T, together with a rotation in the Hopf fiber. At $\theta_i = 0$ or π these Hopf coordinates are no longer valid and the circle described by (4.16) can shrink to a point. In terms of the embedding $\mathbb{C}^4$ coordinates, these loci are hypersurfaces $z = 0$ and $w = 0$,

---

[8] Note that this reproduces the standard conifold metric upon redefining $\psi = (\psi' - \varphi_1 - \varphi_2)/2$.
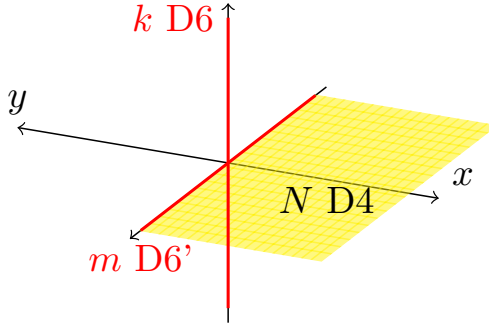
Figure 4.4: The resulting IIA brane content corresponding to N M5 branes on the $w = 0$ divisor $\mathfrak{D}_w$ of the generalized conifold $\mathcal{K}^{k,m}$ after reduction on the xy circle.

as we can see in (4.15). This is illustrated in Figure 4.3. Reduction of M-theory along the circle generated by (4.15) leads to two D6-branes stretched along the z and w directions, as illustrated in Figure 4.4:

$$\text{D6 from } x = y = z = 0 \text{ along } w, \quad \text{D6' from } x = y = w = 0 \text{ along } z.$$

Now let us look at the $w = 0$ divisor, which we denote by $\mathfrak{D}_w$. Setting $w = 0$ in the conifold equation (4.12) implies that $x = 0$ or $y = 0$. These are two branches meeting along the z axis. We will choose the latter one, so that the metric (4.13) restricts to

$$ds^2_{\mathfrak{D}_w} = d\rho^2 + \frac{\rho^2}{6}\left(d\theta_2^2 + \sin^2\theta_2 d\varphi_2^2\right) + \frac{4\rho^2}{9}\left(d\psi + \cos^2(\theta_2/2)d\varphi_2\right)^2. \quad (4.17)$$

This is a radially fibred S^3 with a particular squashing. Note that it preserves $SU(2) \times U(1)$ isometries. At $\rho = 1$ it is parametrized by (see Appendix 4.A)

$$\begin{aligned} x &= \cos\frac{\theta_2}{2}e^{i(\psi+\varphi_2)}, \\ z &= \sin\frac{\theta_2}{2}e^{i\psi}. \end{aligned} \quad (4.18)$$

In these coordinates, the action (4.15) whose orbit defines the M-theory circle is

$$(\theta_2, \varphi_2, \psi) \to (\theta_2, \varphi_2 + \alpha, \psi). \quad (4.19)$$

We see that the corresponding circles are just the equal θ_2 circles of the second $SU(2)$ factor of the conifold, sitting at the north pole $\theta_1 = 0$ of the first $SU(2)$ factor.

Where does this circle shrink? Again, we have to be careful about the range of our coordinates. At the north pole $\theta_2 = 0$, the action (4.15) shifts to the Hopf fiber,

$$\theta_2 = 0 : \quad (x, z) = (e^{i\beta}, 0), \quad \beta \to \beta + \alpha. \tag{4.20}$$

That is a circle of finite size unless $\rho = 0$. In contrast, the orbit of (4.15) shrinks to a point at the south pole $\theta_2 = \pi$ for all ρ,

$$\theta_2 = \pi : \quad (x, z) = (0, e^{i\delta}), \quad \delta \to \delta. \tag{4.21}$$

Therefore, from the perspective of the divisor, the D6' brane stretches along z at $x = y = 0$ and the D6 brane is pointlike at $x = y = z = 0$.

To obtain m D6 and D6' branes, the M-theory circle should shrink with an m-fold angular deficit. We can achieve this by quotienting the action (4.15) by $\mathbb{Z}_m \subset U(1)$. We denote the resulting generalized conifold by $\mathcal{K}^{m,m}$:[9]

$$xy = z^m w^m. \tag{4.22}$$

We are mainly interested in the $w = 0$ divisor $\mathfrak{D}_w$ of this space. From the point of view of the divisor $\mathfrak{D}_w$, an m-fold angular deficit stretches along the z axis. Reducing to IIA leads to m D6' branes that stretch along z and are located at $x = w = 0$.

A similar analysis for $z = 0$, $w \neq 0$ leads to a m-fold angular defect along w at $x = y = z = 0$. This defect is pointlike in $\mathfrak{D}_w$, intersecting only at $x = y = w = z = 0$. Upon reduction to IIA, it leads to m D6 branes. The conifold point at the origin corresponds to the location where the two orbifold singularities intersect.

The generalized conifold $\mathcal{K}^{k,m}$ is described by equation (4.8),

$$xy = z^k w^m.$$

It can be obtained by partially resolving the singularity along the w axis of (4.22). In a IIA frame, such a resolution corresponds to moving out $(m - k)$ D6 branes to infinity along the x or y axis. The resulting geometry is similar to that of $\mathcal{K}^{m,m}$, except that it has a k-fold angular deficit intersecting at the origin with an m-fold one. Consequently, reducing to IIA produces k D6 branes and m D6' branes.

By resolving all the way to $k = 1$, $\mathfrak{D}_w$ is equivalent to the $\mathbb{C}/\mathbb{Z}_m \times \mathbb{C}$ background studied in [201]. In terms of the coordinates (4.18), it is described by

$$x = \cos\frac{\theta_2}{2} e^{i(\psi + \varphi_2/m)}, \tag{4.23}$$

$$z = \sin\frac{\theta_2}{2} e^{i\psi}. \tag{4.24}$$

---

[9] Note that the labels on $\mathcal{K}^{m,n}$ are unrelated to the labels (p, q) that are sometimes used to describe possible base spaces of the conifold.

The metric (4.17) then becomes

$$ds^2_{\mathfrak{D}_w} = d\rho^2 + \frac{\rho^2}{6}\left(d\theta_2^2 + \frac{1}{m^2}\sin^2\theta_2 d\varphi_2^2\right)$$
$$+ \frac{4\rho^2}{9}\left(d\psi + \frac{1}{m}\cos^2(\theta_2/2)d\varphi_2^2\right)^2. \tag{4.25}$$

In this case, the sphere isometries are broken to $U(1) \times U(1)$. The M-theory circle shrinks with a $\mathbb{Z}_m$ angular deficit along the z axis. Note that the three-spheres at fixed radius are in fact also squashed. This leads to an additional 'squashing' singularity at the origin, corresponding to the conifold point.

Finally, we should comment on how the M5 branes are placed in this geometry. The $\mathfrak{D}_w$ divisor has two components ending on the $x = y = w = 0$ defect, and we can place the M5s together along either one. This setup preserves supersymmetry since the divisor is holomorphic. See for instance [225] for a similar setup in IIB.

Note that the M5 branes are in a sense fractional: a brane along the x axis needs to pair up with a brane along the y axis to be able to move off the defect. Upon reduction, these fractional M5 branes correspond to D4 branes that end on the D6' branes, as we illustrate in Figure 4.4.

As we will show in the next section, three of the scalars on the D4 branes will obtain a Nahm pole boundary condition dictated by how they are partitioned among the m D6' branes. On the other hand, the flux coming from the k D6 branes gives rise to the Chern–Simons coupling in the 3d-3d frame. Thus, both sets of D6 branes play distinct but crucial roles in our construction.

4.4 Toda$_\lambda$ theory from generalized conifolds

In this section, we outline a derivation of the AGT$_\lambda$ correspondence in the spirit of Córdova-Jafferis [191]. We will see that our proposal also sheds some light on the derivation of the original AGT correspondence. The reason for this is that the surface operator associated with the trivial partition $N = N$ is decoupled from the field theory. In our description, this is reflected by the fact that for $m = 1$ there is no orbifold singularity. Thus, we can view the original AGT correspondence as a special case of the AGT$_\lambda$ correspondence. This will be discussed first.

Moving on to the general AGT$_\lambda$ correspondence, a crucial role is played by the generalized conifolds $\mathcal{K}^{1,m}$. In the presence of our defect, the pole region of a squashed S^4 can be identified with an appropriate divisor in $\mathcal{K}^{1,m}$. In this limit, the chirality and amount of the S^4 Killing spinors agree with those of the divisor in $\mathcal{K}^{1,m}$, which we take as further evidence for our proposal.

It should be noted that we use the (generalized) conifold merely as a technical simplification. We expect a general set of supergravity backgrounds exists that allows for a squashed $S^4/\mathbb{Z}_k$ with defect included. However, since the supersymmetry analysis is particularly easy for the conifold, we specialize to the parameter values it dictates. Several subtleties that arise are expected to be resolved in the general set of supergravity backgrounds.

4.4.1   Compatibility of $\mathcal{K}^{1,1}$ with Córdova-Jafferis

As explained in the previous section, the standard conifold $\mathcal{K}^{1,1}$ produces a D6 and D6' brane if we reduce to type IIA. In our setup, the D4 branes end properly on the D6' brane. The latter is not present in the original derivation [191] where only the D6 brane is considered. The main reason for this discrepancy is that we choose a different circle fiber in (4.15). In contrast to the Hopf fiber of the three-sphere, which only shrinks at the poles of the S^4, our circle degenerates along the entire z-plane in the pole region.

To check that we can still build on the results of [203] we note that the D6 brane in [191] translates to a flux for the graviphoton field in the 3d-3d frame, which is ultimately responsible for a non-zero Chern–Simons level in three dimensions.[10] This feature is not lost in our construction, since reduction on the conifold still produces a similar D6 brane located at the north pole.

Our brane configuration is illustrated in Table 4.5.

	$\mathbb{R}$	$\mathbb{R}^2$		Σ		$\mathbb{R}^3$			$\mathbb{R}^2$	
	1	2	3	4	5	6	7	8	9	10
N D4 $\vdash$	x	x	x	x						
D6'		x	x	x	x	x	x	x		
D6				x	x	x	x	x	x	x

Table 4.5: Type IIA setup in the pole region after reduction on the circle of $\mathcal{K}^{1,1}$.

By the analysis of [34, 195], the D4-D6' system leads to a (principal) Nahm pole boundary condition on three of the D4 scalars, denoted by X_i in Section 4.2.1. This provides a reinterpretation of the results in [191], where it is claimed that the D6 brane is responsible for the Nahm pole.

We will now turn to consistency checks of our identification of the conifold as an approximation of the supergravity background relevant to the AGT correspondence. From the Nahm pole onwards, the original analysis of [191] then goes through. Namely, after Weyl rescaling to the 3d-3d frame, the Nahm pole translates into the reduction of the WZW model to Toda theory as reviewed in Section 4.2.

Geometry   Recall that the metric on the $w = 0$ divisor is given by (4.17),

$$ds^2_{\mathfrak{D}_w} = d\rho^2 + \frac{\rho^2}{6}\left(d\theta_2^2 + \sin^2\theta_2 d\varphi_2^2\right) + \frac{4\rho^2}{9}\left(d\psi + \cos^2\theta_2/2 d\varphi_2\right)^2.$$

This is the pole region of the metric of a squashed four-sphere,

$$ds^2 = d\sigma^2 + \left(\frac{f(\sigma)^2\ell^2}{4}\left(d\theta^2 + \sin^2(\theta)d\varphi^2\right) + f(\sigma)^2\left(d\psi + \cos^2(\theta/2)d\varphi\right)^2\right). \quad (4.26)$$

---

[10]See also [215, 216] for related discussions.

The original derivation [191] of the AGT correspondence considers the class of geometries (4.26) for general ℓ and any $f(\sigma)$ that vanishes linearly near $\sigma = 0, \pi$. The divisor of the conifold imposes the values $\ell = \frac{3}{\sqrt{6}}$ and $f(\sigma) = \frac{2}{3}\sigma + \mathcal{O}\left(\sigma^2\right)$.

Note that the conifold singularity translates to a squashing singularity of the metric (4.26) for these particular choices of $f(\sigma)$ and ℓ. We will not be too concerned about these curvature singularities. As argued in [191], the $(2,0)$ theory cannot couple to curvature scalars of dimension four or higher such as $R_{\mu\nu}R^{\mu\nu}$. In principle, it could couple to the Ricci scalar, but this can be resolved by an appropriate choice of the function $f(\sigma)$.

For the singular conifold, which dictates $f(\sigma)$ and ℓ as above, the Ricci scalar singularity is present. However, we expect the general set of supergravity backgrounds to contain solutions that exclude singularities in the Ricci scalar. The curvature singularity should be merely an artifact of the parameter values imposed by the conifold.

Supersymmetries   Here, we will show that the amount and chirality of supercharges preserved by the M5 brane on the conifold divisor match with what one expects for the 6d $(2,0)$ theory in the AGT setup. Subsequently, we will relate them to the supercharges in the 3d-3d frame.

It is well known that an M5 brane wrapped on a holomorphic divisor inside a Calabi-Yau three-fold has at most $(0,4)$ supersymmetry in the remaining two dimensions [226,227]. However, since the latter lie along the Riemann surface Σ, on which the theory is topologically twisted, only two Killing spinors survive.[11] Since the Killing spinors are chiral from both a six-dimensional and a two-dimensional perspective, they must be chiral in four dimensions as well,

$$\xi_{6d}^{\text{chiral}} = \xi_{2d}^{\text{chiral}} \otimes \xi_{4d}^{\text{chiral}}.$$

Now let us turn to the usual AGT setup. A 4d $\mathcal{N} = 2$ theory on a squashed S^4 with $U(1) \times U(1)$ isometries has an $SU(2)_R$ doublet of Killing spinors [204, 228],

$$
\begin{aligned}
\varepsilon^1 &= (\xi_1, \bar{\xi}_1) \\
&= e^{\frac{1}{2}i(\phi_1+\phi_2)} \left(e^{-i\frac{\theta}{2}}\sin(\tfrac{\sigma}{2}), -e^{i\frac{\theta}{2}}\sin(\tfrac{\sigma}{2}), ie^{-i\frac{\theta}{2}}\cos(\tfrac{\sigma}{2}), -ie^{i\frac{\theta}{2}}\cos(\tfrac{\sigma}{2})\right) \\
\varepsilon^2 &= (\xi_2, \bar{\xi}_2) \\
&= e^{-\frac{1}{2}i(\phi_1+\phi_2)} \left(e^{-i\frac{\theta}{2}}\sin(\tfrac{\sigma}{2}), e^{i\frac{\theta}{2}}\sin(\tfrac{\sigma}{2}), -ie^{-i\frac{\theta}{2}}\cos(\tfrac{\sigma}{2}), -ie^{i\frac{\theta}{2}}\cos(\tfrac{\sigma}{2})\right).
\end{aligned}
\tag{4.27}
$$

Near the north pole these reduce, up to a local Lorentz and $SU(2)_R$ gauge transformation, to the Ω background

$$\bar{\xi}_A^{\dot{\alpha}} = \delta_A^{\dot{\alpha}}, \qquad \xi_{\alpha A} = -\frac{1}{2}v_m(\sigma^m)_{\alpha\dot{\alpha}}\bar{\xi}_A^{\dot{\alpha}}. \tag{4.28}$$

Here, v_m is a Killing vector that generates a linear combination of the $U(1)^2$ isometry of the Ω background. It descends from the $U(1)^2$ isometry of the squashed

---

[11] This follows from the fact that the four supercharges form two doublets under the $SU(2)$ R-symmetry whose $U(1) \subset SU(2)$ subgroup is used to perform the twist.

sphere. Since v_m vanishes linearly with σ one sees that the Killing spinors are indeed chiral to zeroth order in σ. Hence, the amount and chirality of the super-charges preserved by the divisor of the conifold are consistent with the ordinary AGT setup.

As noted in [191], after Weyl rescaling to the 3d-3d frame, in a suitable R-symmetry gauge, the Killing spinors in (4.27) become independent of σ. This is required to make contact with the Killing spinors in the 3d-3d correspondence [203] which are independent of σ due to the topological twist on M_3.

A final subtlety is to be mentioned here. In the above, we have made contact with the Killing spinors corresponding to the $\mathcal{N} = 2$ theory on a squashed S^4 which preserves $U(1) \times U(1)$ isometries. However, the derivation of the 3d-3d correspondence in [203] makes use of a squashed sphere with $SU(2) \times U(1)$ isometries. As was first observed in [205] and then properly understood in [206], the three-dimensional supersymmetric partition function is in fact insensitive to these extra symmetries. This should provide a justification for the proposed relation between the partition functions evaluated in the 4d-2d and 3d-3d frame.

Twist   Another perspective on the equivalence of the preserved supersymmetries in the conifold case and the AGT setup lies in their relation to topological twists. The worldvolume theory on the M5 branes is automatically topologically twisted, since it wraps a Kähler cycle inside a Calabi-Yau threefold [229].[12] In terms of groups, the R-symmetry is broken by the setup to $U(2)$. The $U(1)$ R-symmetry given by the embedding

$$U(1) \subset U(2) \subset SO(4) \subset SO(5)$$

is used to twist the $U(1) \subset U(2)$ holonomy on the divisor (see e.g. Appendix A in [230]).

This feature is also reflected in the standard AGT setup. Indeed, at zeroth order in σ, the Killing spinors (4.28) precisely reflect the ordinary (Donaldson-Witten) topological twist: the $SU(2)_R$ index is identified with the dotted spinors index. The twist implemented by the conifold is a special version of this twist when the holonomy is reduced to $U(2)$.

4.4.2 $\mathcal{K}^{1,m}$ and $\mathbf{AGT}_\lambda$

We now want to explain the relevance of the generalized conifold for the AGT_λ correspondence. First, a partition is associated to the divisor that specifies the charges of the fractional M5 branes in the orbifold background

$$\lambda : \qquad N = n_1 + \ldots + n_m. \tag{4.29}$$

After reduction on the circle fiber, this partition encodes the number n_i of D4 branes ending on the ith D6' brane.

---

[12]The normal bundle to the divisor is its canonical bundle. Then, the two scalars correspond-ing to transverse movement inside $\mathcal{K}^{1,1}$ become holomorphic two-forms on the divisor [226, 227].

	$\mathbb{R}$	$\mathbb{R}^2$		Σ		$\mathbb{R}^3$			$\mathbb{R}^2$	
	1	2	3	4	5	6	7	8	9	10
N D4	$\vdash$	x	x	x	x					
m D6'		x	x	x	x	x	x	x		
D6				x	x	x	x	x	x	x

Table 4.6: Type IIA setup in the pole region after reduction on the circle of $\mathcal{K}^{1,m}$.

This imposes a Nahm pole on the three X^a D4 worldvolume scalars in terms of the $sl_2 \subset sl_N$ embedding associated to λ. In the 3d-3d frame, the D6 brane is solely reflected as a graviphoton flux which leads to a $k = 1$ Chern–Simons level [203].

In the M-theory frame, Weyl rescaling from 4d-2d to 3d-3d results in an asymptotically hyperbolic three-manifold M_3 corresponding to the directions 145 in Table 4.6. The half-line along the 1 direction is stretched to a line with an asymptotic boundary. Since the D6' branes are located at the edge of this half-line, the Nahm pole they induce becomes a constraint at the asymptotic boundary of M_3 in the Weyl rescaled frame.

The bulk of M_3 should therefore not be affected by the presence of the additional D6' branes introduced by the generalized conifold. The analysis of [203], which obtains complex Chern–Simons theory from reduction of the M5 worldvolume theory, should then still hold in the bulk of M_3. We thus claim that only the constraint on the boundary behavior of the Chern–Simons theory is different.

To be precise, the partition of the N D4 branes on m D6' branes translates in the 3d-3d frame to a block diagonal form of the connection at the boundary. For example,

$$\lambda: \quad 3 = 2 + 1 \qquad \longleftrightarrow \qquad \mathcal{A} = \begin{pmatrix} * & * & \\ * & * & \\ & & * \end{pmatrix}. \tag{4.30}$$

The Nahm pole then maps to a constraint in this block diagonal form,

$$\mathcal{A} = d\rho + e^\rho \mathcal{L}^+ dz + \cdots, \qquad \mathcal{L}^+ = \begin{pmatrix} 0 & 1 & \\ 0 & 0 & \\ & & 0 \end{pmatrix}. \tag{4.31}$$

As we recalled in Section 4.2.2, such a constraint precisely reduces a $SL(N)$ WZW model to the Toda theory associated to the partition λ. Recalling the equivalence between complex and real $SL(N)$ Chern–Simons at level $k = 1$ [210], this leads to a derivation of the AGT$_\lambda$ correspondence.

Geometry   The $w = 0$ divisor of $\mathcal{K}^{1,m}$ is equivalent to $\mathbb{C}/\mathbb{Z}_m \times \mathbb{C}$, as we showed in Section 4.3.2. The non-trivial Ω background that is manifested by the squashing of a radially fibred three-sphere, just as in the $k = m = 1$ case, is also visible there. The squashed three-sphere in this geometry preserves $U(1) \times U(1)$ isometries since

the base of the Hopf fibration is now orbifolded. This shows that the divisor in $\mathcal{K}^{1,m}$ reproduces the setup in which the AGT_λ correspondence was studied [201].[13]

Supersymmetries The generalized conifolds preserve the same amount of supersymmetry as the $m = 1$ conifold. This is particularly clear from the IIA perspective, where instead of a single D6 and D6' brane, we now have one D6 intersecting with m coincident D6' branes.

Likewise, the general AGT setup concerns a squashed S^4 with $U(1) \times U(1)$ isometries,

$$t^2 + \frac{|z|^2}{\ell^2} + \frac{|x|^2}{\tilde{\ell}^2} = 1$$

It is clear that including our defect at $x = 0$ does not break these isometries any further. Therefore, just as in our conifold construction, including such defects in the general AGT setup does not break any additional supersymmetry.

Furthermore, the divisor of the generalized conifold is still Kähler, so only chiral supersymmetries survive. This agrees with the chirality of the Killing spinors of an S^4 in the pole region.

4.4.3 General k and m

Finally, we comment on a conjecture arising from the general conifold $\mathcal{K}^{k,m}$. Here, we expect to obtain $SL(N, \mathbb{C})$ Chern–Simons theory at level k together with a boundary condition determined by the partition

$$\lambda : \ N = n_1 + \ldots + n_m.$$

According to this partition one should obtain a quantum Drinfeld–Sokolov reduction of complex Toda theory. To arrive at a duality with a real paraToda theory, in the spirit of [191], one could naively ask if

$$\text{Complex Toda}_\lambda(n, k, s) \ \overset{?}{\Leftrightarrow} \ \text{real paraToda}_\lambda(n, k, b) + \frac{\widehat{\mathfrak{su}}(k)_n}{\widehat{\mathfrak{u}}(1)^{k-1}}.$$

However, such a statement requires one to understand how parafermions couple to generalized Toda theories. We are not aware of the existence of any such constructions. An obvious first step would be to figure out how parafermions could couple to affine subsectors.

4.5 Conclusions and outlook

We have argued that the derivation of the AGT correspondence proposed in [191] can be understood by replacing the north pole region of the S^4, where the excitations of the four-dimensional gauge theory are localized, with a holomorphic

---

[13]The superconformal index of the 6d $(2, 0)$ theory in the presence of these orbifold singularities was computed in [218].

divisor inside the singular conifold $\mathcal{K}^{1,1}$. This interpretation has two main virtues. Firstly, it provides a clear perspective on the origin of the Nahm pole. Secondly, the generalized conifolds $\mathcal{K}^{1,m}$ allow us to outline a generalization of the derivation of the original AGT correspondence, which we denote by AGT_λ, involving the inclusion of surface operators on the gauge theory side and a generalization of Toda theory to Toda_λ on the two-dimensional side. We used an equivalent description of these surface operators as orbifold defects, as advocated in [200, 201].

Let us now turn to the possible pitfalls of our analysis and their potential resolutions. First of all, we make a number of assumptions and simplifications due to a lack of a full supergravity background and supersymmetry equations of the worldvolume theory in the presence our additional defects. Even in the original case, a full supergravity background and supersymmetry equations have only been written down for the 3d-3d frame [203]. For a precise understanding of the origin of the Nahm pole, one should furthermore obtain the supergravity background and supersymmetry equations of the 4d-2d frame. In the presence of our additional defects, such a background should include a geometry which resembles a conifold near its pole regions. Transforming the supersymmetry equations to the 3d-3d frame should then give rise to the Drinfeld–Sokolov boundary conditions on the Chern–Simons connection.

An obstruction to performing this transformation is that these equations can only be written down in a five-dimensional setting, since the Lagrangian formulation of the 6d A_{N-1} theory is unknown. In other words, one cannot directly transform the supersymmetry equations leading to a Nahm pole in 4d-2d to the 3d-3d equivalent which should give the correct Chern–Simons boundary conditions.

Furthermore, the derivation of the 3d-3d correspondence [203] is in a sense only concerned with the bulk of the Chern–Simons theory. Even there, ghosts appear, which gauge fix the noncompact part of the gauge group at finite $S^3_\ell/\mathbb{Z}_k$ size. On an M_3 with boundary, one should similarly impose boundary conditions on these ghosts, which are related to the boundary constraints of the Chern–Simons connection. It would be interesting to see if such ghost terms can be obtained in the 3d-3d frame, if they correspond to the proper Drinfeld–Sokolov constraints in the setting we propose, and how they translate to the 4d-2d Nahm pole setting.

At level $k = 1$, using the equality between the Hilbert spaces of complex and real $SL(N)$ Chern–Simons theory, the complex Toda_λ theory corresponds to a real Toda_λ theory. For higher k, it would be interesting to understand the equivalent of the parafermions that were necessary to make contact with real Toda in the original derivation [191].

In the main body of this chapter, we have not touched upon the relation between (a limit of) the superconformal index of the 6d $(2,0)$ theory of type A_{N-1} and vacuum characters of $\mathcal{W}_N$ algebras discovered in [190]. This relation was also derived in [191] following similar arguments to their derivation of the AGT correspondence. The geometry relevant to the superconformal index, $S^5 \times S^1$, can be Weyl rescaled to $S^3 \times EAdS_3$. One can understand this by thinking of the S^5 as an S^3 fibration

over a disc, where the S^3 shrinks at the boundary of the disc. The Weyl rescaling stretches the radial direction of the disk to infinite length and produces the $EAdS_3$ geometry.

The boundary conditions on the Chern–Simons connection are again argued to be of Drinfeld–Sokolov type. The D6 brane that arises from reduction on the Hopf fiber wraps the boundary circle of the disc and the S^1.

As in the derivation of the AGT correspondence, this D6 brane does not have the correct codimensions for a D4 brane to end on it, and for its scalars to acquire a Nahm pole. Again, we claim that the analogous identification of the divisor of a conifold in the S^5 reproduces the D6 brane and additionally produces the D6' on which the D4s can end. This construction generalizes to the inclusion of codimension two defects as orbifold singularities, as studied in [218]. This leads to a derivation of the conjecture, appearing before in [190], that the vacuum character of a general $\mathcal{W}_\lambda$ algebra is equal to the 6d superconformal index.

Further possibly interesting directions of research include the following. In the 3d-3d frame, the additional defects we introduced affect the boundary conditions of Chern–Simons theory. On the other hand, they also have two directions along the three-dimensional $\mathcal{N} = 2$ theory $T[M_3]$. It would be interesting to interpret the role these defects play on this side of the correspondence.

We can also include other types of defects. Codimension two defects that are pointlike on the Riemann surface translate to operator insertions in the Toda theory. They are similarly labeled by a partition of N, which we can associate to the choice of a (possibly semi-degenerate) Toda primary. In six dimensions, these defects wrap an S^4 that maps under Weyl rescaling to an S^3 times the radial direction of M_3. One can then couple such a codimension two defect to the five-dimensional Yang–Mills theory. Reducing to M_3 should produce a Wilson line in complex Chern–Simons theory.

Finally, the central charge of generalized Toda theories is known for any embedding, see for example [91]. It would be interesting to reproduce this central charge from six dimensions. This has been done for principal Toda in [182] by equivariantly integrating the anomaly eight-form over the $\mathbb{R}^4$ Ω background. Following the geometric description of the codimension two defects, one could integrate a suitable generalization of the anomaly polynomial on the orbifolded $\mathbb{C} \times \mathbb{C}/\mathbb{Z}_m$ Ω background. Reproducing the generalized Toda central charge from such a computation would provide a convincing check on the validity of a geometric description of the codimension two defects.

4.A   The conifold

Let us review some facts on the conifold. We mainly follow [224] but choose slightly different coordinates in places. The conifold $\mathcal{K}^{1,1}$ is a hypersurface in $\mathbb{C}^4$ defined by

$$zw = xy. \tag{4.32}$$

This equation defines a six-dimensional cone. By intersecting $\mathcal{K}^{1,1}$ with a seven-sphere of radius r, we can study its base, which we denote by T. The base T is topologically equivalent to $S^2 \times S^3$ and can be conveniently parametrized in the following way,

$$Z := \frac{1}{r} \begin{pmatrix} z & x \\ y & w \end{pmatrix} \qquad T: \quad \det Z = 0, \quad \operatorname{Tr} Z^\dagger Z = 1. \tag{4.33}$$

We can write down the most general solution to these equations by taking a particular solution Z_0 and conjugating it with a pair (L, R) of $SU(2)$ matrices,

$$Z = LZ_0 R^\dagger, \qquad Z_0 = \begin{pmatrix} 0 & 1 \\ 0 & 0 \end{pmatrix}, \quad L, R \in SU(2). \tag{4.34}$$

Each $SU(2)$ factor can be described using two complex coordinates,

$$\begin{aligned}
L &:= \begin{pmatrix} a & -\bar{b} \\ b & \bar{a} \end{pmatrix} \in SU(2), \quad (a, b) \in \mathbb{C}^2, \quad |a|^2 + |b|^2 = 1, \\
R &:= \begin{pmatrix} k & -\bar{l} \\ l & \bar{k} \end{pmatrix} \in SU(2), \quad (k, l) \in \mathbb{C}^2, \quad |k|^2 + |l|^2 = 1.
\end{aligned} \tag{4.35}$$

Now introduce Hopf coordinates on each $SU(2) \simeq S^3$,

$$\begin{aligned}
a &= \cos(\theta_1/2)e^{i(\psi_1 + \varphi_1)}, & k &= \cos(\theta_2/2)e^{i(\psi_2 + \varphi_2)}, \\
b &= \sin(\theta_1/2)e^{i\psi_1}, & l &= \sin(\theta_2/2)e^{i\psi_2},
\end{aligned} \tag{4.36}$$

Note that the parametrization of T in (4.34) is overcomplete. Two pairs of $SU(2)$ matrices (L, R) describe the same solution if and only if they are related by the $U(1)$ action

$$(L, R) \mapsto (L\Theta, R\Theta^\dagger), \qquad \Theta = \begin{pmatrix} e^{i\theta} & 0 \\ 0 & e^{-i\theta} \end{pmatrix} \in U(1) \subset SU(2). \tag{4.37}$$

This degeneracy should be quotiented out of the $SU(2) \times SU(2)$ parametrization. The $U(1)$ acts on the S^3 coordinates by

$$(a, b) \to (e^{i\theta}a, e^{i\theta}b), \quad (k, l) \to (e^{-i\theta}k, e^{-i\theta}l). \tag{4.38}$$

The resulting $SU(2) \times SU(2)/U(1)$ quotient is the conifold. Indeed, the invariant coordinates under this $U(1)$ action correspond to the ones used in (4.33). At $r = 1$,

$$x = ak, \quad y = -bl, \quad z = -al, \quad w = bk. \tag{4.39}$$

They are related by the defining equation (4.32) of the conifold. In terms of the Hopf coordinates (4.36), the $U(1)$ quotient (4.38) joins the two Hopf fiber coordinates in the invariant combination $\psi := \psi_1 + \psi_2$. T is then parametrized by

$$x = \cos\frac{\theta_1}{2}\cos\frac{\theta_2}{2}e^{i(\psi+\varphi_1+\varphi_2)}, \tag{4.40a}$$

$$y = -\sin\frac{\theta_1}{2}\sin\frac{\theta_2}{2}e^{i\psi}, \tag{4.40b}$$

$$z = -\cos\frac{\theta_1}{2}\sin\frac{\theta_2}{2}e^{i(\psi+\varphi_1)}, \tag{4.40c}$$

$$w = \sin\frac{\theta_1}{2}\cos\frac{\theta_2}{2}e^{i(\psi+\varphi_2)}. \tag{4.40d}$$

Demanding that $\mathcal{K}^{1,1}$ is Kähler implies that the metric on T is given by [224]

$$ds_T^2 = \frac{2}{3}\,\mathrm{Tr}\left(dZ^\dagger dZ\right) - \frac{2}{9}\left|\mathrm{Tr}\left(Z^\dagger dZ\right)\right|^2 \tag{4.41}$$

$$= \frac{4}{9}\left(d\psi + \cos^2(\theta_1/2)d\varphi_1 + \cos^2(\theta_2/2)d\varphi_2\right)^2 \tag{4.42}$$

$$+ \frac{1}{6}\left[\left(d\theta_1^2 + \sin^2\theta_1 d\varphi_1^2\right) + \left(d\theta_2^2 + \sin^2\theta_2 d\varphi_2^2\right)\right].$$

This is the metric we wrote down in (4.14). It describes two three-spheres with a shared Hopf fiber. If we think of this fibration as an electromagnetic $U(1)$ bundle, both spheres feel one unit of magnetic charge. Note that this metric is equivalent to the usual one under the coordinate redefinition $\psi = (\psi' - \varphi_1 - \varphi_2)/2$.

The divisor In the main text, we make extensive use of the $w = 0$ divisor of the conifold. Setting w to zero in (4.32) implies that either x or y vanishes. In terms of the coordinates in (4.40), these choices corresponds to setting either $\theta_1 = 0$ or $\theta_2 = \pi$. Thus we are at the north (or south) pole of one of the S^2 base factors of T. The remaining sphere, together with the fiber, now describes an ordinary S^3. Setting $\theta_1 = 0$, the parametrization in (4.40) reduces to Hopf coordinates

$$\begin{aligned} x &= \cos\frac{\theta_2}{2}e^{i(\psi+\varphi_2)}, \\ z &= \sin\frac{\theta_2}{2}e^{i\psi}. \end{aligned} \tag{4.43}$$

Chapter 5

Linear response of entanglement entropy from holography

In this chapter, we study the time evolution of entanglement entropy in strongly-coupled field theories using holography. We look at the response of the theory to violent shocks known as global quenches. Assuming the theory thermalizes, we can model this process in the bulk using a collapsing shell of matter.

As we reviewed in Section 1.5.3, entanglement entropy can be computed holographically in terms of the area of a minimal surface in the bulk. For small boundary intervals, we find an analytic expression for the time evolution of spatial entanglement entropy after a global quench with arbitrary time profile. We use this expression to quantify how far this process is from being adiabatic and we work out the corresponding expressions for a representative set of quench profiles.

The work in this chapter has appeared previously in [3].

5.1 Introduction

Understanding the evolution of many-body systems after generic time-dependent perturbations is a subject of great relevance, and currently one of the most difficult problems connecting many areas of physics, ranging from condensed matter to quantum information theory. If a system is prepared in a pure state, it will evolve unitarily and will remain in a pure state. However, finite subsystems are likely to thermalize. For example, if we consider a sufficiently small region, the number of degrees of freedom outside the region is much larger than in the inside, so a typical excited pure state would look thermal from the point of view of the subsystem [231].

A useful order parameter to consider is the entanglement entropy, which we introduced in Section 1.5.3. To compute this quantity one can imagine splitting the system in two regions, A and its complement A^c. Assuming that the Hilbert space factorizes as $\mathcal{H}_{\text{total}} = \mathcal{H}_A \otimes \mathcal{H}_{A^c}$, the entanglement entropy of a region A is then defined as the von Neumann entropy

$$S_A = -\operatorname{Tr}\left[\rho_A \log \rho_A\right] , \tag{5.1}$$

where $\rho_A = \operatorname{Tr}_{A^c}[\rho]$ is the reduced density matrix associated to A. Given its inherent nonlocal character, entanglement entropy could in principle capture quantum correlations not encoded in observables constructed from any set of local operators $\mathcal{O}_i$.

The reduced density matrix ρ_A is Hermitian and positive semi-definite, so it can formally be expressed as

$$\rho_A = \frac{e^{-H_A}}{\operatorname{Tr}[e^{-H_A}]} , \tag{5.2}$$

where the Hermitian operator H_A is known as the modular Hamiltonian. Now, consider any linear variation to the state of the system, $\rho = \rho^{(0)} + \lambda \delta\rho$, so that $\rho_A = \rho_A^{(0)} + \lambda \delta\rho_A$. The variations considered here are generic, so they include all sorts of time-dependent perturbations. For practical purposes we can consider a one-parameter family of states $\rho(\lambda)$ such that $\rho(0) = \rho^{(0)}$ corresponds to a density matrix of a reference state. To first order in the perturbation, the variation $\delta\mathcal{O}$ of any quantity $\mathcal{O}$ is then defined by $\delta\mathcal{O} = \partial_\lambda \mathcal{O}(\lambda)|_{\lambda=0}$. In particular, the variation of entanglement entropy (5.1) is given by $S_A = S_A^{(0)} + \lambda \delta S_A$, where

$$
\begin{aligned}
\delta S_A &= -\operatorname{Tr}\left[\delta\rho_A \log \rho_A\right] - \operatorname{Tr}\left[\rho_A \, \rho_A^{-1} \delta\rho_A\right] , \\
&= \operatorname{Tr}\left[\delta\rho_A H_A\right] - \operatorname{Tr}\left[\delta\rho_A\right] .
\end{aligned} \tag{5.3}
$$

The last term in (5.3) is identically zero, since the trace of the reduced density matrix equals one by definition. Hence, the leading order variation of the entanglement entropy is given by

$$\delta S_A = \delta\langle H_A \rangle , \tag{5.4}$$

which is known as the first law of entanglement entropy. The reference state is normally taken to be the vacuum, but the equation (5.4) holds equally for any other

reference state. The first law is useful in simple situations but its applicability is limited. For example, there are only very few cases for which H_A is known explicitly. The most famous example is the case where A is half-space, say $x_1 > 0$, and ρ corresponds to the vacuum state. In this case [232, 233]

$$H_A = 2\pi \int_A x_1 \, T_{00}(x) \, d^{d-1}x \,. \tag{5.5}$$

That is, H_A is given by the generator of Lorentz boosts. For a conformal field theory (CFT) this result may be conformally mapped to the case where A is a ball of radius R, in which case [234, 235]

$$H_A = 2\pi \int_A \frac{R^2 - r^2}{2R} T_{00}(x) \, d^{d-1}x \,. \tag{5.6}$$

More generally, the modular Hamiltonian is highly nonlocal and cannot be written in a closed form.[1] Another limitation is that not all states are perturbatively close to the reference state. For example, the density matrix of a thermal state is given by $\rho_{\mathrm{thermal}} = e^{-\beta H} / \mathrm{Tr}[e^{-\beta H}]$, which cannot be expanded around the vacuum. In these cases (5.4) does not hold.

In this chapter we will consider time-dependent perturbations induced by the so-called quantum quenches. Quantum quenches are unitary evolutions of pure states triggered by a shift of parameters such as mass gaps or coupling constants. To describe such processes, we can start with the Hamiltonian of the system H_0 (or the Lagrangian $\mathcal{L}_0$), and add a perturbation of the form

$$H_\lambda = H_0 + \lambda(t)\delta H_\Delta \qquad \rightarrow \qquad \mathcal{L}_\lambda = \mathcal{L}_0 + \lambda(t)\mathcal{O}_\Delta \,. \tag{5.7}$$

Here $\lambda(t)$ corresponds to an external parameter and H_Δ (or $\mathcal{O}_\Delta$) represents a deformation by an operator of conformal dimension Δ. We assume that the source is turned on at $t = 0$ and turned off at some $t = t_q$ and take as our reference state the vacuum of the original Hamiltonian H_0. We can distinguish between the following two kinds of quenches:

- *Global quenches.* Global quenches are unitary evolutions triggered by a homogeneous change of parameters in space. If the theory lives on a noncompact manifold such as flat space $\mathbb{R}^{(d-1,1)}$, this implies that the amount of energy injected to the system is infinite, which generally leads to thermalization. Then, the final state is indistinguishable from a thermal state, $\rho(t) \rightarrow \rho_{\mathrm{thermal}} + \mathcal{O}(e^{-S})$, so the density matrix cannot be written as a small perturbation over the reference state for all $t > 0$. This invalidates the first law (5.4). It is thus interesting to ask what are the general laws governing the time evolution of entanglement entropy in these cases.

---

[1] In (1+1)-dimensional CFTs there are a few other examples in which the modular Hamiltonian may be written as an integral over the stress-energy tensor times a local weight, see e.g. [236].

- *Local quenches.* Local quenches are unitary evolutions triggered by a change of parameters within a localized region or simply at a point. Since the excitations are localized, the amount of energy injected to the system is finite. Moreover, if the theory lives on a non-compact manifold, this energy is scattered out to spatial infinity and the system returns back to its original state at $t \to \infty$. Provided that the energy injected is infinitesimal, the state of the system for $t > 0$ can be regarded in some cases as a perturbation over the reference state so the first law (5.4) holds in these cases,[2] regardless of the time evolution and the inhomogeneity.

Let us focus on global quenches. To begin with, we can imagine that the perturbation is sharply peaked, i.e. $\lambda(t) \sim \delta(t)$, so that the quench is instantaneous. This is the simplest possible quench that we can study since we do not introduce the extra scale t_q. In this scenario, the evolution of the system can described by the injection of a uniform energy density at $t = 0$, evolved forward in time by the original Hamiltonian H_0. In the seminal paper [237], Calabrese and Cardy showed that for $(1 + 1)-$dimensional CFTs entanglement entropy of an interval of length $l = 2R$ grows linearly in time,

$$\delta S_A(t) = 2t s_{\mathrm{eq}}, \qquad t \leq t_{\mathrm{sat}}, \tag{5.8}$$

and then saturates discontinuously at $t = t_{\mathrm{sat}} = R$. Here s_{eq} denotes the entropy density of the final state, which is approximately thermal. Crucially, their result holds in the regime of large intervals, $R \gg \beta$, where $\beta = T^{-1}$ is the inverse temperature of the final state. As explained in [237], at least in this regime, the growth of entanglement has a natural explanation in terms of free streaming EPR pairs moving at the speed of light. Unfortunately, the techniques used in [237] rely on methods particular to $(1 + 1)-$dimensional CFTs so their results cannot be easily generalized to other theories and/or higher dimensions.

The emergence of holography [10,41,42] made it possible to tackle this problem for theories with a gravity dual. In this context, global quenches are commonly modeled by the formation of a black hole in the bulk —see [238–240] for some early works on this subject. The computation of entanglement entropy in holographic models is remarkably simple, reducing the problem to the study of certain extremal area surfaces in the corresponding dual geometry [43,58]. Interestingly, for holographic CFTs the entanglement growth for large subsystems after instantaneous global quenches was found to have a universal regime,

$$\delta S_A(t) = v_E s_{\mathrm{eq}} A_\Sigma t, \qquad t_{\mathrm{loc}} \ll t \ll t_{\mathrm{sat}}. \tag{5.9}$$

The constant v_E here is interpreted as an 'entanglement velocity', which generally depends on the number of spacetime dimensions d as well as on parameters of the final state, and A_Σ is the area of the entangling region's boundary $\Sigma = \partial A$.

---

[2]This statement is formally true up to some caveats. For instance, one can argue that since $H \neq H_0$ for $0 < t < t_q$, the modular Hamiltonian H_A has to be modified during this time interval. We can by pass this problem by focusing on the regime $t > t_q$, for which the evolution is governed by H_0.

Finally, t_{loc} is a local equilibration time which generally scales like the inverse final temperature $t_{\text{loc}} \sim \beta$, while t_{sat} is the saturation time and scales like the characteristic size of the region $t_{\text{sat}} \sim l$. This universal linear growth was first observed numerically in [241, 242] and analytically in [243–245], and was later generalized to various holographic setups in [246–271].[3] The universality here refers to the shape of the entangling region A, but it is worth emphasizing that v_E may depend on parameters of the final state. For instance, if the final state is thermal, one finds that

$$v_E = \sqrt{\frac{d}{d-2}} \left(\frac{d-2}{2(d-1)} \right)^{\frac{d-1}{d}}. \tag{5.10}$$

However, if the final state has an additional conserved $U(1)$ charge Q, the entanglement velocity will depend on the ratio of the chemical potential and the temperature [245]

$$v_E = \sqrt{\frac{d}{d-2}} \left[\left(\frac{d\varrho - \varrho - 1}{(\varrho+1)(d-1)} \right)^{\frac{2(d-1)}{d}} - \left(\frac{\varrho-1}{\varrho+1} \right) \right]^{\frac{1}{2}},$$
$$\varrho \equiv \sqrt{1 + \frac{d(d-2)^2\mu^2}{4\pi^2(d-1)T^2}}. \tag{5.11}$$

Given the simplicity of (5.8) and (5.9), Liu and Suh proposed a heuristic picture for the evolution of entanglement entropy which they dubbed as the 'entanglement tsunami' [244, 245]. According to this picture, the quench generates a wave of entanglement that spreads inward from the subsystem's boundary Σ, with the region covered by the wave becoming entangled with the outside. In some special cases, the tsunami picture might have a microscopic explanation in terms of quasi-particles, e.g. EPR pairs or GHZ blocks, with or without interactions [282, 283]. Indeed, if one sets $d = 2$ in the holographic result (5.10) one obtains $v_E = 1$ as in the free streaming model of [237], suggesting that $i)$ the spread of entanglement can be explained in terms of EPR pairs for all $(1+1)-$dimensional CFTs and $ii)$ the interactions between the pairs might not play a crucial role. Very recently, the free streaming model of [237] was generalized to higher dimensions [284], and it was found that

$$v_E^{\text{free}} = \frac{\Gamma[\frac{d-1}{2}]}{\sqrt{\pi}\Gamma[\frac{d}{2}]}, \tag{5.12}$$

which is smaller than the holographic result (5.10) for $d \geq 3$. This result implies that interactions must play a role, provided that the spread of entanglement for holographic theories actually admits a quasi-particle description. However, more recent studies have shown that this is not the case. For example in [285–287] it was argued that the quasi-particle picture fails to reproduce other holographic and CFT results, e.g. the entanglement entropy for multiple intervals.

---

[3]See also [272–281] for some interesting results on the spread of holographic entanglement entropy in other time-dependent scenarios such as local quenches and shock wave collisions.

It is worth recalling that the above results are valid only in the strict limit of large subsystems $l \gg \beta$ and assuming that the quench is instantaneous. Relaxing either of these conditions is challenging and the results might not be universal. For instance, if we stay in the limit of large subsystem but consider a different type of quench, the result for the spread of entanglement entropy will generally depend on the quench profile, as well as the operator that is being quenched. Perhaps the other limit that is under analytical control in this situation is the adiabatic limit, but it is somehow trivial. For sufficiently slow quenches, the system can be considered to be very close to equilibrium so the standard rules of thermodynamics apply. Thus, in this limit entanglement entropy for large subsystems reduces to thermal entropy, which is well defined for all t and evolves evolves adiabatically in a controlled way.

For small subsystems, the situation is much less understood, with a few exceptions [288, 289]. In [288] the authors focused on instantaneous quenches while in [289] the authors considered a t-linear source. From the analysis of [288] it was clear that in the limit of small subsystems both the quasi-particle picture and the tsunami picture break down. This is easy to understand: in the limit of small subsystems $l \ll \beta$ so $t_{\text{sat}} \ll t_{\text{loc}}$. This implies that the subsystem never enters the regime for which the linear growth formula (5.9) applies. Interestingly, their findings suggested that in this limit the evolution of the entanglement entropy exhibits a different kind of universality. Even though the results depend on the shape of the entangling region, they turn out to be independent of the parameters of the final state, at least for cases where the final state has a conserved $U(1)$ charge Q. In this chapter we will elaborate more on this universality, focusing in particular on the response of entanglement due to the expectation values of field theory operators.[4] More specifically, we will show that the result at leading order in the size of the region is only sensitive to the one-point function of the stress-energy tensor, provided that the operator being quenched has conformal dimension in the range $\Delta \in [d/2, d]$. Our result is valid for any rate and profile of injection of energy into the system, so we will be able to reproduce the results of [289] for the case of a t-linear source.

In order to understand our result for small intervals, one can imagine expanding the reduced density matrix in terms of some parameter λ_A that explicitly depends on region A, so that $\rho_A = \rho_A^{(0)} + \lambda_A \delta \rho_A$ without making any assumption on ρ. For example, in a thermal state one can have the dimensionless combination $\lambda_A \sim lT$, where l is a characteristic size of the entangling region and T is the temperature. At zeroth order in the size of the region, one finds that $\rho_A^{(0)} \simeq \text{Tr}_B[\rho_{\text{vac}}]$ where ρ_{vac} is the density matrix of the vacuum state (provided that the theory has a well defined UV fixed point). Therefore, in this limit, one can also arrive to a first

---

[4]A general quench can be modeled by introducing a time-dependent source in the field theory, which corresponds to switching on non-normalizable modes in bulk fields. This source has a direct effect on the entanglement entropy, which furthermore needs to be renormalized in a model-dependent way [290]. We will not consider these effects. Instead, we focus on the change in entanglement entropy due to the expectation values that are turned on by the presence of first source.

law like expression for the variation of the entanglement entropy in an arbitrary excited state ρ [291–293]. For states that are perturbatively close to the vacuum, we can directly use (5.6), assuming that the radius of the ball R is much smaller than any other length scale of the system. In this limit the expectation value of the energy density operator $\langle T_{00}(x)\rangle = \varepsilon$ is approximately constant in the region A and one can write

$$\delta S_A = 2\pi\varepsilon\,\Omega_{d-2}\int_0^R \frac{R^2-r^2}{2R}r^{d-2}dr = \frac{2\pi\varepsilon\,\Omega_{d-2}R^d}{d^2-1}\,. \tag{5.13}$$

Here, $\Omega_{d-2} = 2\pi^{\frac{d-1}{2}}/\Gamma[\frac{d-1}{2}]$ is the surface area of a $(d-2)$-dimensional unit sphere. Defining δE_A as the energy enclosed in region A,

$$\delta E_A = \varepsilon\,V_A\,, \qquad V_A \equiv \frac{\Omega_{d-2}}{d-1}R^{d-1}\,, \tag{5.14}$$

where V_A is the volume of region A, we arrive at

$$\delta S_A = \frac{\delta E_A}{T_A}\,, \qquad T_A \equiv \frac{d+1}{2\pi R}\,, \tag{5.15}$$

where T_A is known as the entanglement temperature [291–293]. For arbitrary static excited states, equation (5.15) still holds provided that $\varepsilon R^d \ll 1$. For instance, in a thermal state, $\varepsilon = \sigma T^d$ so (5.15) holds in the limit $RT \ll 1$. However, a comment on the entanglement temperature (5.15) is in order. As shown above, for ball-shaped regions the constant T_A follows directly from (5.6), which is valid for any CFT (whether or not it is holographic) so in this sense it is universal. For more generic regions, one can in principle arrive to a first law such as (5.15) but in that case T_A may depend not only on the shape of A, but also on the parameters of the theory. For example, for an infinite strip of width l it was found that in Einstein gravity [291]

$$T_A = \frac{2(d^2-1)\Gamma[\frac{d+1}{2(d-1)}]\Gamma[\frac{d}{2(d-1)}]^2}{\sqrt{\pi}\Gamma[\frac{1}{d-1}]\Gamma[\frac{1}{2(d-1)}]^2 l}\,. \tag{5.16}$$

However, in higher order theories of gravity such as Gauss-Bonnet, T_A depends in addition on the central charges of the theory [294].

For time-dependent excited states, the first law relation (5.15) is valid as long as the state is perturbatively close to the vacuum, but is not expected otherwise. For example, in the models of local quenches presented in [272] the first law was found to be valid for sufficiently small systems, regardless of the time evolution and the inhomogeneity. For global quenches it is not a priori expected to be valid, since the final state is not perturbatively close to the vacuum. In this case, in order to determine whether or not the first law relation holds true for small subsystems one must, in addition, compare l with all time scales characterizing the rate of change of $\varepsilon(t)$. For example, for instantaneous quenches $\varepsilon(t) \propto \theta(t)$, but entanglement entropy saturates at a finite time $t_{\text{sat}} \sim l$. This implies that (5.15) does not hold in this limit. On general grounds, we expect to recover

(5.15) whenever l is smaller than all characteristic time scales of the quench, i.e. $\dot{\varepsilon}(t)R^{d+1} \ll 1$, $\ddot{\varepsilon}(t)R^{d+2} \ll 1$, and so on. Indeed, we will see that our final formula for the evolution of entanglement entropy for small subsystems reduces to (5.15) for slowly varying global quenches.

The remainder of this chapter is organized as follows. In Section 5.2 we present the derivation of the holographic entanglement entropy after global quenches. This Section is divided in three parts. In Section 5.2.1 we explain the small subsystem limit and the necessary expansions in the bulk geometry. In Section 5.2.2 we obtain analytic expressions for the evolution of entanglement entropy $\delta S_A(t)$ under a general global quenches modeled by a Vaidya solution. We consider two geometries for the entangling region, a ball and a strip. In Section 5.2.3 we rewrite our result for $\delta S_A(t)$ as a linear response. The resulting expression can be written as a convolution between the energy density $\varepsilon(t)$, which plays the role of the source, and a specific kernel fixed by the geometry of the subsystem. We discuss the limiting case where we recover the first law relation (5.15) and introduce a quantity $\Upsilon_A(t)$ to quantify how far the system is from satisfying the first law. Then, in Section 5.3, we work out the evolution of $\delta S_A(t)$ and $\Upsilon_A(t)$ for various particular cases, including instantaneous quenches, power-law quenches, and periodically driving quenches. In Section 5.4 we give a brief summary of our main results and close with conclusions.

5.2 Holographic computation

5.2.1 Perturbative expansion for small subsystems

We will begin by giving a quick overview of the results of [288] on the spread of entanglement of small subsystems in holographic CFTs. However, we will relax one important condition. Namely, we will not assume that the quench is instantaneous, as long as it is homogeneous in space. For holographic CFTs, the entanglement entropy of a boundary region A can be calculated via [43, 58]

$$S_A = \frac{1}{4G_N^{(d+1)}} \text{ext} \left[\text{Area} \left(\Gamma_A \right) \right]. \tag{5.17}$$

Here, $G_N^{(d+1)}$ is the bulk Newton's constant and Γ_A is an extremal $(d-1)$-dimensional surface in the bulk such that $\partial \Gamma_A = \partial A = \Sigma$. We assume that the size of the region A is small in comparison to any other scale of the system. This will allow us to extract a universal contribution to the evolution of entanglement entropy following a global quench. Depending on the particular fields that are used to model the quench, the entanglement entropy would also contain non-universal terms which we do not consider.

In order to study the small subsystem limit we need to focus on the near-boundary region of the bulk geometry. In Fefferman-Graham coordinates, a gen-

eral asymptotically AdS metric can be written as

$$ds^2 = \frac{\ell^2}{z^2} \left(g_{\mu\nu}(z, x^\mu) dx^\mu dx^\nu + dz^2 \right). \tag{5.18}$$

According to the UV/IR connection [295, 296], the bulk radial coordinate z maps to a length scale in the boundary theory.[5] Now, for a given boundary region A, the corresponding extremal surface probes parts of the bulk geometry up to maximum depth z_*, which depends on the size of the region. For example, in pure AdS and for a ball-shaped region, z_* is directly equal to its radius R; for the infinite strip geometry z_* is proportional to its width l (up to a numerical coefficient) [298]. So, at least in pure AdS, z_* can probe all the way to $z_* \to \infty$ as $l \to \infty$. However, for excited states, there might be a maximum depth $z_* \to z_{IR}$ as $l \to \infty$. This includes cases with bulk horizons (either black hole or cosmological), hard walls (or end of the world branes) and entanglement shadows. For small subsystems, however, the corresponding extremal surface will only probe regions close to the boundary. Thus, without loss of generality one can assume that the characteristic size of the region will be given by $l \sim z_*$. The small subsystem limit is then governed by the near-boundary region, which is nothing but AdS plus small corrections.

Let us now discuss the general structure of the asymptotic expansion (5.18) for perturbations over empty AdS. From the Fefferman-Graham metric (5.18) we can obtain the CFT metric $d\tilde{s}^2 = \tilde{g}_{\mu\nu} dx^\mu dx^\nu$ by $\tilde{g}_{\mu\nu} = g_{\mu\nu}(0, x^\mu)$. We assume that the boundary theory lives on flat space, so we set $g_{\mu\nu}(0, x^\mu) = \eta_{\mu\nu}$. This will already impose some constrains on the near boundary expansion of the full metric, $g_{\mu\nu}(z, x^\mu) = \eta_{\mu\nu} + \delta g_{\mu\nu}(z, x^\mu)$. In particular, $\delta g_{\mu\nu}(z, x^\mu)$ will get corrections from several operators [299], which will crucially depend on the matter content of the bulk theory. The first correction that we will analyze is due to the metric itself and is therefore universal. The metric is dual to the stress-energy tensor, so the leading correction (normalizable mode) is proportional to its expectation value,

$$\delta g_{\mu\nu} = a \, z^d \, \langle T_{\mu\nu} \rangle + \cdots, \qquad a \equiv \frac{d\ell^{d-1}}{16\pi G_N^{(d+1)}} \tag{5.19}$$

Mapping the radial coordinate to a length scale $z \sim l$, we see that the leading correction is exactly of order $\delta g_{\mu\nu} \sim \mathcal{O}(l^d)$. There are also sub-leading corrections coming from higher point functions of the stress-energy tensor. For example, to quadratic order, the most general form allowed by Lorentz invariance is

$$\delta g_{\mu\nu} = a \, z^d \, \langle T_{\mu\nu} \rangle + z^{2d} \left(a_1 \, \langle T_{\mu\alpha} T^\alpha{}_\nu \rangle + a_2 \, \eta_{\mu\nu} \langle T_{\alpha\beta} T^{\alpha\beta} \rangle \right) + \cdots, \tag{5.20}$$

where a_1 and a_2 are some numerical constants. These extra corrections are sub-leading in l so we will not consider them here. We can also consider corrections due to operators dual to additional bulk fields. These additional bulk fields will introduce two kind of corrections in the asymptotic expansion: terms that are proportional to the source, and terms that are proportional to the expectation

---

[5]There are subtleties that arise in time-dependent configurations. See for example [297].

value of the dual operator.[6] Terms that are proportional to the source are non-normalizable so they will require model-dependent renormalization. Here, we will only focus on the normalizable contributions. For example, for a scalar operator $\mathcal{O}$ of conformal dimension $\Delta \leq d$, in the standard quantization

$$\delta g_{\mu\nu} = a\, z^d \, \langle T_{\mu\nu} \rangle + b\, z^{2\Delta} \langle \mathcal{O}^2 \rangle + \cdots . \qquad (5.21)$$

Note that this perturbation also involves a term of the form $\lambda(t)z^{2(d-\Delta)}$, where $\lambda(t)$ is the source of $\mathcal{O}$ (see for example [300]). We will subtract such terms and focus only on the effects of the expectation values that are turned on by the quench. More specifically, we will consider the difference

$$\delta S_A(t) = S_A(t) - S_A^{(0)} - S_A^{(\lambda)}. \qquad (5.22)$$

Here, $S_A^{(0)}$ is the entanglement entropy in the vacuum and $S_A^{(\lambda)}$ consists of model-dependent terms that describe the effect of the source $\lambda(t)$ itself on the entanglement entropy. We emphasize that such a splitting can only be achieved in the limit of small subsystems. More generally, we expect the appearance of cross terms that mix sources with expectation values at higher orders in the Fefferman-Graham expansion. Furthermore, note that the last term in (5.21) is the dominant term if the operator is sufficiently relevant, i.e. for $\frac{d}{2} - 1 < \Delta < \frac{d}{2}$.[7] We will not consider these cases here, but their effects could be addressed if one works with alternative quantization [301]. As a final example we can consider sourcing the quench with a bulk current J_μ. In this case the normalizable corrections take the form

$$\delta g_{\mu\nu} = a\, z^d \, \langle T_{\mu\nu} \rangle + z^{2d-2} \left(c_1 \, \langle J_\mu J_\nu \rangle + c_2 \, \eta_{\mu\nu} \langle J_\alpha J^\alpha \rangle \right) + \cdots , \qquad (5.23)$$

which are also subleading.

Before closing this section, let us comment on the perturbative expansion of entanglement entropy in terms of the characteristic size of the region A. In order to compute the leading order correction of entanglement entropy we proceed in the following way. Consider the functional $\mathcal{L}_A[\phi_A(\xi); \lambda_A]$ for the extremal surfaces, where $\mathcal{A} \equiv \mathrm{Area}\,(\Gamma_A) = \int d\xi \, \mathcal{L}[\phi_A(\xi); \lambda_A]$, $\phi_A(\xi)$ denotes collectively all the embedding functions, and λ_A is a generic dimensionless parameter in which the perturbation is carried out, i.e. $\lambda_A \ll 1$. We can expand both $\mathcal{L}_A$ and $\phi_A(\xi)$ as follows.

$$\begin{aligned} \mathcal{L}_A[\phi_A(\xi); \lambda_A] &= \mathcal{L}_A^{(0)}[\phi_A(\xi)] + \lambda_A \mathcal{L}_A^{(1)}[\phi_A(\xi)] + \mathcal{O}(\lambda_A^2), \\ \phi_A(\xi) &= \phi_A^{(0)}(\xi) + \lambda_A \phi_A^{(1)}(\xi) + \mathcal{O}(\lambda_A^2). \end{aligned} \qquad (5.24)$$

In principle, it should be possible to obtain the functions $\phi_A^{(n)}(\xi)$ by solving the equations of motion order by order in λ_A. These equations are generally highly non-linear and difficult to solve. However, the key point here is that at the leading

---

[6]Cross terms can show up at higher order in the Fefferman-Graham expansion.

[7]The unitarity bound implies that $\Delta > \frac{d}{2} - 1$.

order in λ_A we have

$$
\begin{aligned}
\mathcal{A}_{\text{on-shell}}[\phi_A(\xi)] = \int d\xi \, \mathcal{L}_A^{(0)}[\phi_A^{(0)}(\xi)] + \lambda_A \int d\xi \, \mathcal{L}_A^{(1)}[\phi_A^{(0)}(\xi)] \\
+ \lambda_A \int d\xi \, \phi_A^{(1)}(\xi) \left[\frac{d}{d\xi} \frac{\partial \mathcal{L}_A^{(0)}}{\partial \phi_A'(\xi)} - \frac{\partial \mathcal{L}_A^{(0)}}{\partial \phi_A(\xi)} \right]_{\phi_A^{(0)}} + \cdots
\end{aligned}
\tag{5.25}
$$

Therefore, we only need $\phi_A^{(0)}(\xi)$ to obtain the leading order correction to the area. In our case, the expansion parameter as seen from the Fefferman-Graham expansion is given by $\lambda_A \sim \delta\langle T_{00}(x)\rangle l^d \ll 1$, where l is the characteristic length of the entangling region. Notice that the small λ_A-expansion probes short distances, i.e. the most UV part of the theory, so the strict limit $\lambda_A \to 0$ we expect to recover the embedding in pure AdS, which is known analytically. The leading correction to the functional will then already contain information about the time-dependence and thermalization.

5.2.2 Entanglement entropy after global quenches

Let us focus on specific holographic duals of global quenches. We will consider generic AdS-Vaidya metrics, which in Eddington-Finkelstein coordinates are given by[8]

$$
ds^2 = \frac{1}{u^2} \left(-f(v,u)dv^2 - 2dvdu + d\vec{x}^2 \right), \qquad f(v,u) = 1 - g(v)\left(\frac{u}{u_H}\right)^d, \tag{5.26}
$$

where $g(v)$ is an arbitrary function of the infalling null coordinate v.[9] A specific example of a quench that leads to the metric above is given in Appendix 5.A. We emphasize that this is not the most general bulk solution for a global quench, and that the details may depend on the specific source that is turned on. However, there is strong numerical and analytic evidence to support the idea that even simple models such as AdS-Vaidya already capture the relevant universal features of the time-evolution and subsequent thermalization after a global quench [260, 302–306]. For example, in the recent paper [306] it was found that the gross features of the correlations following the quench are controlled by just a few parameters: the pump duration and the initial and final temperatures, which are all tunable in (5.26).

We will distinguish between two cases:

- *Quenches of finite duration.* Here $g(v)$ interpolates smoothly between two values over a fixed time interval $\delta t = t_q$. Normally $g(v \to 0) = 0$ so that the initial state is pure AdS, and $g(v \to t_q) = 1$ so the final state is an

---

[8]We have set the AdS radius to unity $\ell = 1$ but it can be restored via dimensional analysis if necessary.

[9]Perhaps the only condition on $g(v)$ is that $g'(v) > 0 \; \forall \, v$. This is required in order to satisfy the Null Energy Condition (NEC) in the bulk, and strong subadditivity inequality in the dual CFT [250, 251].

AdS black hole with horizon at $u = u_H$. Holographically, this describes a thermalizing, out-of-equilibrium system evolving from zero temperature to a final temperature,

$$T = \frac{2(d-1)}{4\pi u_H} \, . \tag{5.27}$$

Since $\delta\langle T_{00}(t)\rangle \to \sigma T^d$ at late times, the expansion parameter in this case is given by $\lambda_A \sim (u_*/u_H)^d \sim (Tl)^d$. We will mainly focus on this kind of quenches in this chapter.

- *Quenches of infinite duration.* In these quenches, one is constantly pumping energy to the system so both $g(v)$ and $\delta\langle T_{00}(t)\rangle$ grow indefinitely. We can formally expand in terms of $\lambda_A \sim (u_*/u_H)^d$, where u_H is a reference scale. However, since $\delta\langle T_{00}(t)\rangle \propto g(t)$ (see Appendix 5.B for details) we must keep in mind that for a fixed l, the expansion will eventually become bad at sufficiently late times.

As reviewed in the previous section, it is possible to obtain analytic expressions in the limit where the interval size is much smaller than the energy density at a given time. We will be interested in obtaining the first order correction to

$$S_A = \frac{1}{4G_N^{(d+1)}} \text{ext}\left[\mathcal{A}(t)\right], \qquad \mathcal{A}(t) = \int_0^{u_*} du\, \mathcal{L}_A \,, \tag{5.28}$$

where u_* is the maximal depth of the entangling surface. The specific form of $\mathcal{L}_A$ will depend on the shape of A. We will consider the following two geometries:

- A $(d-1)$-dimensional ball of radius R. Here, we parametrize by functions $\{r(u), v(u)\}$, with boundary conditions $r(0) = R$, $v(0) = t$. We obtain the following Lagrangian.

$$\mathcal{L}_{\text{ball}} = \frac{A_\Sigma r^{d-2}}{R^{d-2} u^{d-1}} \sqrt{r'^2 - f(v,u)v'^2 - 2v'}, \tag{5.29}$$

where $A_\Sigma = 2\pi^{\frac{d-1}{2}} R^{d-2}/\Gamma[\frac{d-1}{2}]$ is the area of its $(d-2)$-dimensional boundary.

- A $(d-1)$-dimensional strip of width l. Here, we parametrize by functions $\{x(u), v(u)\}$, with boundary conditions $x(0) = \pm l/2$, $v(0) = t$. The Lagrangian is given by

$$\mathcal{L}_{\text{strip}} = \frac{A_\Sigma}{u^{d-1}} \sqrt{x'^2 - f(v,u)v'^2 - 2v'}, \tag{5.30}$$

where $A_\Sigma = 2l_\perp^{d-2}$ is the area of the two disjoint boundaries of the strip.

Now let us return to the small interval expansion. The first order correction to the vacuum entanglement is obtained by evaluating the first order correction of

the area Lagrangian $\mathcal{L}$ on the vacuum embeddings. For the two geometries, the latter is given by

$$\mathcal{L}_{\text{ball}}^{(1)} = \frac{A_\Sigma}{2R^{d-2}u_H^d} \frac{ur^{d-2}v'^2 g(v)}{\sqrt{r'^2 - v'^2 - 2v'}} \,, \tag{5.31}$$

$$\mathcal{L}_{\text{strip}}^{(1)} = \frac{A_\Sigma}{2u_H^d} \frac{uv'^2 g(v)}{\sqrt{x'^2 - v'^2 - 2v'}} \,. \tag{5.32}$$

The vacuum embeddings corresponding to the ball and the strip are

$$r(u) = \sqrt{u_*^2 - u^2} \,, \qquad u_* = R \,, \tag{5.33}$$

and

$$x(u) = \frac{l}{2} - \frac{u^d}{du_*^{d-1}} {}_2F_1\left[\frac{1}{2}, \frac{d}{2(d-1)}, \frac{3d-2}{2(d-1)}, \frac{u^{2(d-1)}}{u_*^{2(d-1)}}\right] \,, \tag{5.34}$$

$$u_* = \frac{\Gamma[\frac{1}{2(d-1)}]l}{2\sqrt{\pi}\Gamma[\frac{d}{2(d-1)}]} \,, \tag{5.35}$$

respectively, while the embedding for v is given in both the cases by

$$v(u) = t - u \,. \tag{5.36}$$

Plugging these vacuum solutions into the corresponding Lagrangians we find that, at the leading order, the change in entanglement entropy is given by

$$\delta S_{\text{ball}}(t) = \frac{A_\Sigma}{8G_N^{(d+1)}u_H^d} \int_0^{u_*} du \, g(t-u)u\left[1 - (u/u_*)^2\right]^{\frac{d-1}{2}} \,, \tag{5.37}$$

$$\delta S_{\text{strip}}(t) = \frac{A_\Sigma}{8G_N^{(d+1)}u_H^d} \int_0^{u_*} du \, g(t-u)u\sqrt{1 - (u/u_*)^{2(d-1)}} \,. \tag{5.38}$$

In the next section we will argue that these expressions have a natural interpretation in terms of a linear response, and we will explore some of their general properties. Finally, we will use these expressions to study specific quench examples that are interesting in their own right.

5.2.3 Linear response of entanglement entropy

An important observation on the expressions (5.37)-(5.38) is that they can be written as convolution integrals! In particular, if we interpret the radial direction as a time variable $u = t'$, we can arrive at generic expressions that look like

$$\delta S_A(t) = \mathfrak{f}(t) * \mathfrak{g}(t) \equiv \int_{-\infty}^{\infty} dt' \, \mathfrak{f}(t-t')\mathfrak{g}(t') \,, \tag{5.39}$$

for some appropriate $\mathfrak{f}(t)$ and $\mathfrak{g}(t)$. In the context of linear time-invariant theory one of these functions, say $\mathfrak{f}(t)$, represents the input or source function while $\mathfrak{g}(t)$

is interpreted as the impulse response of the system. However, the role of $\mathfrak{f}(t)$ and $\mathfrak{g}(t)$ are actually interchangeable since, by properties of the convolution integral, we have that $\mathfrak{f}(t) * \mathfrak{g}(t) = \mathfrak{g}(t) * \mathfrak{f}(t)$.

Let us now recall that in time-independent cases the first law relation (5.15) holds, so δS_A is proportional to the change in the energy δE_A contained in the region. This is natural since, as argued in Section 5.2.1, the first correction to the metric near the boundary comes from the contribution of the stress-energy tensor. Now, for the Vaidya-type quenches under consideration we find that (see Appendix 5.B)

$$\langle T_{00}(t) \rangle \equiv \varepsilon(t) = \frac{(d-1)g(t)}{16\pi G_N^{(d+1)} u_H^d} \, , \tag{5.40}$$

$$\langle T_{ii}(t) \rangle \equiv P(t) = \frac{g(t)}{16\pi G_N^{(d+1)} u_H^d} \, . \tag{5.41}$$

Without loss of generality, we thus identify the energy density (5.40) as our source function, so that

$$\mathfrak{f}(t) = \varepsilon(t) \, . \tag{5.42}$$

This is a natural choice because it only depends on the quench state and not on the parameters of the subsystem A. On the other hand, the response function will naturally depend on the region A,

$$\mathfrak{g}_{\mathrm{ball}}(t) = \frac{2\pi A_\Sigma \, t}{(d-1)} \left[1 - (t/t_*)^2\right]^{\frac{d-1}{2}} \left[\theta(t) - \theta(t - t_*)\right] \, , \tag{5.43}$$

$$\mathfrak{g}_{\mathrm{strip}}(t) = \frac{2\pi A_\Sigma \, t}{(d-1)} \sqrt{1 - (t/t_*)^{2(d-1)}} \left[\theta(t) - \theta(t - t_*)\right] \, , \tag{5.44}$$

where $t_* = u_*$. A few comments are in order here. First notice that we have absorbed the limits of the integral into the response function so that the integral for δS_A is written as in (5.39). Second, the time scale t_* controls both i) the time interval over which the response function has support and ii) its rate of change within such interval. And third, the response function vanishes for $t < 0$ so the system is causal. Notice also that if the quench has compact support, i.e. $\varepsilon(t)$ increases only over a finite time $\delta t = t_q$, then the entanglement entropy will saturate at a time

$$t_{\mathrm{sat}} = t_q + t_* . \tag{5.45}$$

It is also worth pointing out that δS_A inherits all the properties of convolution integrals. For our purposes, the relevant ones are

- *Linearity.* If the source is a linear function $\mathfrak{f}(t) = A_1 \cdot \mathfrak{f}_1(t) + A_2 \cdot \mathfrak{f}_2(t)$,

$$\delta S_A(t) = A_1 \cdot \mathfrak{f}_1(t) * \mathfrak{g}(t) + A_2 \cdot \mathfrak{f}_2(t) * \mathfrak{g}(t) \, . \tag{5.46}$$

- *Time-translation invariance.* If $\delta S_A(t) = \mathfrak{f}(t) * \mathfrak{g}(t)$, then

$$\delta S_A(t - t_0) = \mathfrak{f}(t - t_0) * \mathfrak{g}(t) \, . \tag{5.47}$$

- *Differentiation.* If $\delta S_A(t) = \mathfrak{f}(t) * \mathfrak{g}(t)$, then

$$\frac{d\delta S_A(t)}{dt} = \frac{d\mathfrak{f}(t)}{dt} * \mathfrak{g}(t) = \mathfrak{f}(t) * \frac{d\mathfrak{g}(t)}{dt} \,. \tag{5.48}$$

- *Integration.* If $\delta S_A(t) = \mathfrak{f}(t) * \mathfrak{g}(t)$, then

$$\int dt \, \delta S_A(t) = \left(\int dt \, \mathfrak{f}(t) \right) \cdot \left(\int dt \, \mathfrak{g}(t) \right) \,. \tag{5.49}$$

These properties can be helpful to analyze complicated sources, for example by decomposing them in terms of elementary functions, or to prove general properties for the growth of entanglement entropy. We will see explicit examples of both in the next few sections.

Adiabatic limit and the first law of entanglement entropy

Let us consider for a moment the case where $\mathfrak{f}(t) = \varepsilon$ is a constant. In this case, the variation of entanglement entropy reduces to the integral of the response function. It is easy to see that in this limit we recover the first law relation:

$$\delta S_A = \varepsilon \int_0^{t_*} dt' \, \mathfrak{g}_A(t') = \frac{\delta E_A}{T_A} \,, \tag{5.50}$$

where $E_A = \varepsilon V_A$ and T_A is given in (5.15)-(5.16) for the ball and the strip, respectively.

We can generalize the above result to include adiabatic or slowly-varying quenches. For this, we need to consider a time-dependent source that is approximately constant over all time intervals of order $\delta t = t_*$. Given such a source, it is clear that one can still write

$$\delta S_A(t) = \varepsilon(t) \int_0^{t_*} dt' \, \mathfrak{g}_A(t') = \frac{\delta E_A(t)}{T_A} \,. \tag{5.51}$$

To see this more rigorously, we can integrate δS_A by parts to obtain:

$$\delta S_A(t) = \varepsilon(t-t')\mathfrak{G}_A(t') \Big|_{t'=0}^{t'=t_*} - \int_0^{t_*} dt' \, \frac{d\varepsilon(t-t')}{dt'} \mathfrak{G}_A(t') \,, \tag{5.52}$$

where

$$\frac{d\mathfrak{G}_A(t)}{dt} = \mathfrak{g}_A(t) \qquad \text{for} \qquad 0 \leq t \leq t_* \,. \tag{5.53}$$

The constant of integration for $\mathfrak{G}_A(t)$ is chosen such that $\mathfrak{G}_A(0) = -V_A/T_A$, which in turn implies $\mathfrak{G}_A(t_*) = 0$. For example, for a ball one finds

$$\mathfrak{G}_{\text{ball}}(t) = -\frac{2\pi A_\Sigma t_*^2}{d^2 - 1} \left[1 - (t/t_*)^2 \right]^{\frac{d+1}{2}} + C_{\text{ball}} \,, \tag{5.54}$$

with $C_{\text{ball}} = 0$, while for a strip

$$\mathfrak{G}_{\text{strip}}(t) = \frac{2\pi A_\Sigma t^2}{d^2 - 1} \left[\sqrt{1 - (t/t_*)^{2(d-1)}} + \frac{d-1}{2} {}_2F_1 \left(\frac{1}{2}, \frac{1}{d-1}, \frac{d}{d-1}, (t/t_*)^{2(d-1)} \right) \right]$$
$$+ C_{\text{strip}}, \tag{5.55}$$

with $C_{\text{strip}} = -V_{\text{strip}}/T_{\text{strip}}$. With these functions at hand, one arrives at

$$\delta S_A(t) = -\varepsilon(t)\mathfrak{G}_A(0) - \int_0^{t_*} dt' \, \frac{d\varepsilon(t - t')}{dt'} \mathfrak{G}_A(t'),$$
$$= \frac{\delta E_A(t)}{T_A} - \int_0^{t_*} dt' \, \frac{d\varepsilon(t - t')}{dt'} \mathfrak{G}_A(t'). \tag{5.56}$$

Notice also that, with this choice of integration constants, the function $\mathfrak{G}_A(t)$ is negative definite but its norm is bounded by $|\mathfrak{G}_A| \leq V_A/T_A$. Assuming that it takes its maximum value, we can see that the integral can be neglected as long as

$$\frac{d\varepsilon(t)}{dt} \ll \frac{\varepsilon(t)}{t_*}. \tag{5.57}$$

That is, the variation of the energy density in a time interval from t to $t + \delta t$ must be much smaller than the energy density at any given time in this interval divided by the width of the support of the response function. This defines our adiabatic regime. Finally, combining with the λ_A-expansion, and since $t_* \sim l$, this implies that the regime for which the first law (5.51) is valid is given by

$$\frac{d\varepsilon(t)}{dt} l^{d+1} \ll \varepsilon(t) l^d \ll 1. \tag{5.58}$$

An analogue of relative entropy for time-dependent excited states

It is interesting to note that the second term in (5.56) can be interpreted as a kind of relative entropy [299]. Let us define

$$\Upsilon_A(t) \equiv \frac{\delta E_A(t)}{T_A} - \delta S_A(t). \tag{5.59}$$

We can see that i) this quantity vanishes whenever the first law is satisfied i.e. for equilibrium states (and is negligible for slowly varying quenches). For a quench of compact support, this implies that $\Upsilon_A(t) = 0$ both for $t < 0$ and $t > t_{\text{sat}}$. ii) It is positive definite, so it must increase and then decrease in the interval $0 < t < t_{\text{sat}}$. And iii) for a general quench (slowly or quickly varying), it serves as a measure of how different the out-of-equilibrium state at time t is in comparison to an equilibrium state with the same energy density $\varepsilon(t)$. This follows directly from its definition combined with the fact that $\Upsilon_A(t) \geq 0$.

In order to check the positivity of $\Upsilon_A(t)$ it is convenient to express (5.59) as a convolution integral. Changing the variable of differentiation in (5.56), i.e. $d\varepsilon(t - t')/dt' \to -d\varepsilon(t - t')/dt$, and defining

$$\tilde{\mathfrak{G}}_A(t) \equiv \mathfrak{G}_A(t) \left[\theta(t) - \theta(t - t_*) \right], \tag{5.60}$$

we obtain

$$\Upsilon_A(t) = -\frac{d\varepsilon(t)}{dt} * \tilde{\mathfrak{G}}_A(t) \geq 0\,. \tag{5.61}$$

The proof of the inequality is trivial since $\tilde{\mathfrak{G}}_A(t) \leq 0$ and $d\varepsilon(t)/dt \geq 0 \ \forall\, t$, which is required by the Null Energy Condition (NEC) in the bulk. It is worth noticing that the NEC is intimately connected to the strong subadditivity (SSA) inequality of entanglement entropy in the boundary theory [250,251] (see [307] for a rigorous proof). Combining this result with the above, we can conclude that, in these time-dependent excited states, SSA implies $\Upsilon_A(t) \geq 0$, in complete analogy with the standard relative entropy $S_A(\rho_1|\rho_0)$ for time-independent states [299].

As mentioned above, $\Upsilon_A(t)$ is expected to increase and decrease in the interval $0 < t < t_{\text{sat}}$. Let us study its time derivative in more detail. Either from the differentiation property of the convolution integral or from the definition of $\Upsilon_A(t)$ we obtain

$$\begin{aligned}
\frac{d\Upsilon_A(t)}{dt} &= -\frac{d\varepsilon(t)}{dt} * \frac{d\tilde{\mathfrak{G}}_A(t)}{dt} \\
&= \frac{d\varepsilon(t)}{dt}\frac{V_A}{T_A} - \frac{d\varepsilon(t)}{dt} * \mathfrak{g}_A(t)\,.
\end{aligned} \tag{5.62}$$

The first term in (5.62) is just a boundary term: it comes from the derivative of the $\theta(t)$ term in (5.60). Provided that the quench has compact support, we can divide the time evolution in two regimes:

- *Driven regime* ($0 < t < t_q$): in this stage of the evolution $d\varepsilon(t)/dt > 0$, so both terms in (5.62) contribute. The first term is always positive but the second term is negative since $\mathfrak{g}_A(t) \geq 0$. The behavior of $d\varepsilon(t')/dt$ in the interval $t - t_* < t' < t$ determines which of these two terms dominates.

- *Transient regime* ($t_q < t < t_{\text{sat}}$): in this stage of the evolution the source is already turned off so $d\varepsilon(t)/dt = 0$ and the first term in (5.62) vanishes. The second term is still negative and finite since $\mathfrak{g}_A(t) \geq 0$ and $d\varepsilon(t')/dt$ still has support in the interval $t - t_* < t' < t$. Therefore,

$$\frac{d\Upsilon_A(t)}{dt} \leq 0 \qquad t_q < t < t_{\text{sat}}\,. \tag{5.63}$$

Before closing this section let us point out that $\Upsilon_A(t)$ can be rewritten directly in terms of the quench parameters by means of the appropriate Ward identity. For example, for a quench by a scalar operator we find

$$\partial^\mu \langle T_{\mu\nu}\rangle = -\langle \mathcal{O}_\phi\rangle \partial_\nu \mathcal{J}_\phi \qquad \Longrightarrow \qquad \frac{d\varepsilon(t)}{dt} = \langle \mathcal{O}_\phi(t)\rangle\frac{d\mathcal{J}_\phi(t)}{dt}\,, \tag{5.64}$$

where $\mathcal{O}_\phi$ is the operator dual to the bulk field ϕ and $\mathcal{J}_\phi$ is the corresponding source. For a quench by an external electric field $\vec{E}$ (see Appendix 5.A) we find that

$$\partial^\mu \langle T_{\mu\nu}\rangle = -\langle J_\mu\rangle F^{\mu\nu} \qquad \Longrightarrow \qquad \frac{d\varepsilon(t)}{dt} = \langle \vec{J}(t)\rangle \cdot \vec{E}(t)\,, \tag{5.65}$$

125

where $\vec{J}$ is the current that couples to $\vec{E}$. It would be interesting to obtain similar expressions for the growth of entanglement from the field theory perspective and compare them with the ones obtained above in the holographic context. In particular, it would be very interesting to ask how the functions $\mathfrak{g}_A(t)$ and $\mathfrak{G}_A(t)$ arise from field theory computations and to explore their properties.

5.3   Particular cases

In this section we will study the time evolution of entanglement entropy in some particular cases of interest. First, we will review the results of [288] for instantaneous quenches (where $t_q \to 0$) and analyze the quantity $\Upsilon_A(t)$ defined above in more detail. Then we will consider a representative set of quenches of finite t_q and study the driven and transient regimes. Finally, we consider quenches of infinite duration, where $t_q \to \infty$. In this scenario, the transient regime disappears and entanglement entropy never reaches saturation. We pay particular attention to the case of a linearly driven quench, where we recover the results of [289], and the periodically driven quench, where we make contact with the results of [308, 309].

5.3.1   Instantaneous quench

Let us first consider an instantaneous quench, where the source is given by

$$\mathfrak{f}(t) = \varepsilon(t) = \varepsilon_0 \, \theta(t) \, . \tag{5.66}$$

Then, the entanglement entropy (5.39) reduces to the convolution of (5.66) with the appropriate response function, (5.43) for the ball or (5.44) for the strip. The two integrals were carried out explicitly in [288], leading to

$$\delta S_A(t) = \begin{cases} 0 & t < 0 \, , \\ \delta S_A^{\text{eq}} \mathcal{F}_A(t/t_{\text{sat}}) & 0 < t < t_{\text{sat}} \, , \\ \delta S_A^{\text{eq}} & t > t_{\text{sat}} \, , \end{cases} \tag{5.67}$$

where $\delta S_A^{\text{eq}} = \delta E_A / T_A$ is the equilibrium value of entanglement entropy after saturation,

$$\delta S_{\text{ball}}^{\text{eq}} = \frac{4\pi^{\frac{d-1}{2}} R^d \varepsilon_0}{(d^2-1)\Gamma[\frac{d-1}{2}]} \, , \tag{5.68}$$

$$\delta S_{\text{strip}}^{\text{eq}} = \frac{\sqrt{\pi}\Gamma[\frac{1}{d-1}]\Gamma[\frac{1}{2(d-1)}]^2 l_\perp^{d-2} l^2 \varepsilon_0}{2(d^2-1)\Gamma[\frac{d+1}{2(d-1)}]\Gamma[\frac{d}{2(d-1)}]^2} \, , \tag{5.69}$$

and $\mathcal{F}_A(x)$ is a function that characterizes its growth and thermalization,

$$\mathcal{F}_{\text{ball}}(x) = 1 - \left(1 - x^2\right)^{\frac{d+1}{2}} \, , \tag{5.70}$$

$$\mathcal{F}_{\text{strip}}(x) = \frac{2\Gamma[\frac{d+1}{2(d-1)}]x^2}{\sqrt{\pi}\Gamma[\frac{1}{d-1}]} \left[\sqrt{1 - x^{2(d-1)}} + \frac{d-1}{2} {}_2F_1\left(\frac{1}{2}, \frac{1}{d-1}, \frac{d}{d-1}, x^{2(d-1)}\right) \right] \, .$$
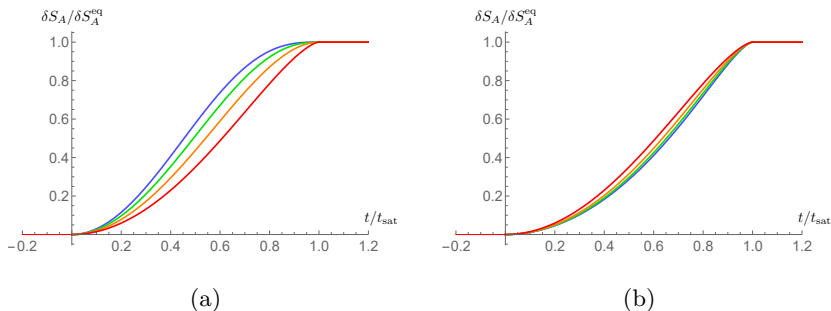
Figure 5.1: Evolution of $\delta S_A(t)$ for the ball (a) and the strip (b) in $d = \{2, 3, 4, 5\}$ dimensions, depicted in red, orange, green and blue, respectively.

An important observation here is that, contrary to the large subsystem limit, S_A^{eq} does not scale like the volume, so it is not extensive.[10] We will see the implications of this below. The saturation time in each case is given by the width of the response function, i.e.

$$
t_{\text{sat}} = t_* = \begin{cases} R \,, & \text{(ball)} \\ \dfrac{\Gamma[\frac{1}{2(d-1)}]l}{2\sqrt{\pi}\Gamma[\frac{d}{2(d-1)}]} \,. & \text{(strip)} \end{cases} \tag{5.71}
$$

Figure 5.1 shows the evolution of entanglement entropy for the ball and the strip in various number of dimensions. Let us now review the basic properties of the entanglement growth pointed out in [288]:

- *Early-time growth.* For $t \ll t_{\text{sat}}$ there is a universal regime, where

$$
\delta S_A(t) = \frac{\pi}{d-1}\varepsilon_0 A_\Sigma t^2 + \cdots \tag{5.72}
$$

  This result is independent of the shape of the region and holds both for small and large subsystems. The proof presented in [288] made it clear that this behavior is fixed by the symmetries of the dual theory, in this case conformal symmetry.

- *Quasi-linear growth.* For intermediate times $t \sim t_{\text{max}}$, there is a regime for some $0 < t_{\text{max}} < t_{\text{sat}}$ where

$$
\delta S_A(t) - \delta S_A(t_{\text{max}}) = v_A^{\text{max}} s_A^{\text{eq}} A_\Sigma (t - t_{\text{max}}) + \cdots \tag{5.73}
$$

  where $s_A^{\text{eq}} = \delta S_A^{\text{eq}}/V_A$. Contrary to the large subsystem limit, s_A^{eq} here depends on the shape of the region and so does v_A^{max}. Therefore, (5.73) is not universal in the same sense as (5.9). However, it turns out that v_A^{max} does *not* depend on the parameters of the state (e.g. chemical potentials

---

[10]For large subsystems, the equilibrium value of entanglement entropy is proportional to the thermal entropy density: $\delta S_A^{\text{eq}} = s^{\text{th}} V_A$.

and conserved charges), while the tsunami velocity v_E generally does. This new universal behavior for small subsystems follows directly from the fact that the leading correction near the boundary is given by the stress-energy tensor, while the contributions from other operators are subleading (see the discussion at the end of Section 5.2.1). The maximum rate of growth is found to be

$$v_{\text{ball}}^{\text{max}} = \frac{(1+d)(d-1)^{\frac{d-3}{2}}}{d^{d/2}} = \begin{cases} \frac{3}{2}\,, & d=2\,, \\ 0.7698\,, & d=3\,, \\ 0.5413\,, & d=4\,, \\ 0\,, & d\to\infty\,, \end{cases} \tag{5.74}$$

for the case of the ball, and

$$v_{\text{strip}}^{\text{max}} = \frac{4(d-1)^{3/2}\Gamma[\frac{3d-1}{2(d-1)}]\Gamma[\frac{d}{2(d-1)}]}{d^{\frac{d}{2(d-1)}}\Gamma[\frac{1}{2(d-1)}]\Gamma[\frac{1}{d-1}]} = \begin{cases} \frac{3}{2}\,, & d=2\,, \\ 0.9464\,, & d=3\,, \\ 0.7046\,, & d=4\,, \\ 0\,, & d\to\infty\,. \end{cases} \tag{5.75}$$

for the strip. We emphasize that v_A^{max} is not necessarily a physical velocity. However, the fact that $v_A^{\text{max}} > 1$ in $d = 2$ implies that the quasi-particle picture [237] and the tsunami picture [244] break down in the limit of small regions.[11] On the other hand, if we define an instantaneous rate of growth,

$$\mathfrak{R}_A(t) = \frac{1}{s_A^{\text{eq}}A_\Sigma}\frac{d\,\delta S_A(t)}{dt}\,, \tag{5.76}$$

it can be shown that for *any* subsystem $\langle \mathfrak{R}_A(t)\rangle \equiv v_A^{\text{avg}} \leq 1$. The proof of this inequality follows from bulk causality [288]. In particular, for the two geometries that we are considering, we find that

$$v_{\text{ball}}^{\text{avg}} = \frac{1}{d-1} = \begin{cases} 1\,, & d=2\,, \\ \frac{1}{2}\,, & d=3\,, \\ \frac{1}{3}\,, & d=4\,, \\ 0\,, & d\to\infty\,, \end{cases} \tag{5.77}$$

and

$$v_{\text{strip}}^{\text{avg}} = \frac{\sqrt{\pi}\Gamma[\frac{d}{2(d-1)}]}{\Gamma[\frac{1}{2(d-1)}]} = \begin{cases} 1\,, & d=2\,, \\ 0.5991\,, & d=3\,, \\ 0.4312\,, & d=4\,, \\ 0\,, & d\to\infty\,. \end{cases} \tag{5.78}$$

---

[11]In nonlocal higher-dimensional theories, v_E can also exceed the speed of light [310].
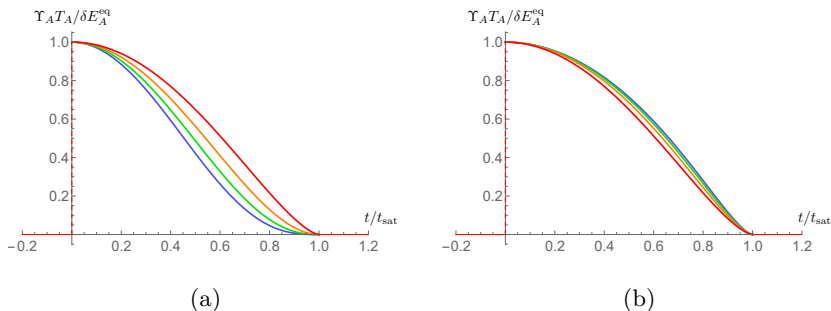
Figure 5.2: Evolution of $\Upsilon_A(t)$, defined in (5.59), for the case of the ball (a) and the strip (b) in $d = \{2, 3, 4, 5\}$ dimensions, depicted in red, orange, green and blue, respectively.

- *Approach to saturation.* In the limit $t \to t_{\text{sat}}$, entanglement entropy is also universal (with respect to the state) and resembles a continuous, second-order phase transition

$$\delta S_A(t) - \delta S_A^{\text{eq}} \propto (t_{\text{sat}} - t)^{\gamma_A} , \tag{5.79}$$

where

$$\gamma_{\text{ball}} = \frac{d+1}{2} , \qquad \gamma_{\text{strip}} = \frac{3}{2} . \tag{5.80}$$

This is in contrast with the result for large subsystems, where the saturation can be continuous or discontinuous, depending both on the shape of the region and the parameters of the state.

Before proceeding with more examples, let us study and comment on the quantity $\Upsilon_A(t)$ defined in (5.59). From the definition, it follows that for instantaneous quenches

$$\Upsilon_A(t) = \varepsilon_0 V_A/T_A - \delta S_A^{\text{eq}} \mathcal{F}_A(t/t_{\text{sat}}) , \qquad 0 < t < t_{\text{sat}} , \tag{5.81}$$

and $\Upsilon_A(t) = 0$ otherwise. Figure 5.2 shows different examples of the evolution of $\Upsilon_A(t)$ for instantaneous quenches, both for the ball and the strip in various dimensions. These figures illustrate the expected behavior from our discussion in Section 5.2.3: i) it vanishes in equilibrium (both for $t < 0$ and $t > t_{\text{sat}}$), ii) it is positive definite, and iii) it decreases monotonically in the transient regime, which in this case is given by $0 < t < t_{\text{sat}}$. Notice that since the quench is instantaneous, the "driven regime" is thus limited to the single point $t = 0$, where $\Upsilon_A(t)$ increases discontinuously. Finally, it is worth pointing out that the behavior of $\Upsilon_A(t)$ throughout its evolution exemplifies its role as a measure of "distance" between the out-of-equilibrium state and an equilibrium state at the same energy density: it is maximal right after the quench and relaxes back to zero as $t \to t_{\text{sat}}$.

	Case I: $t_q < t_*$	Case II: $t_* < t_q$
Pre-quench	$t < 0$	$t < 0$
Initial	$0 < t < t_q$	$0 < t < t_*$
Intermediate	$t_q < t < t_*$	$t_* < t < t_q$
Final	$t_* < t < t_{\text{sat}}$	$t_q < t < t_{\text{sat}}$
Post-saturation	$t > t_{\text{sat}}$	$t > t_{\text{sat}}.$

Table 5.1: The different regimes for power-law quenches.

5.3.2 Power-law quench

Let us now study some representative quenches of finite duration t_q. The family of quenches that we will consider are power-law quenches, with energy density of the form

$$\mathfrak{f}(t) = \varepsilon(t) = \sigma\, t^p[\theta(t) - \theta(t - t_q)] + \varepsilon_0\, \theta(t - t_q)\,. \tag{5.82}$$

Here, $\varepsilon_0 = \sigma\, t_q^p$ is the final energy density. Notice that, given the linearity of the convolution integral, considering the family of power-law quenches given above for $p \in \mathbb{Z}$ is already general enough to represent *any* quench that is analytic on the interval $t \in (0, t_q)$. Therefore, we will restrict our attention to power-law quenches with integer p.

Again, the entanglement entropy (5.39) reduces to the convolution of (5.82) with the appropriate response function: (5.43) for the ball or (5.44) for the strip. Interestingly, for both geometries the integral can be performed analytically. There are two distinct cases to consider: I. $t_q < t_*$ and II. $t_* < t_q$. In both cases the saturation time is given by $t_{\text{sat}} = t_q + t_*$ and the evolution can be split and analyzed in various intervals, as illustrated in Table 5.1.

The pre-quench and post-saturation regimes are in equilibrium so Υ_A vanishes. This yields $\delta S_A = 0$ for $t < 0$ and $\delta S_A = \varepsilon_0 V_A / T_A$ for $t > t_{\text{sat}}$, as expected. The initial, intermediate and final regimes are generally time dependent. The final expressions are lengthy, so for ease of notation we will define some indefinite integrals,

$$\mathcal{I}_A^{(p)}(t, t') = \int dt'\, (t - t')^p \mathfrak{g}_A(t')\,. \tag{5.83}$$

These integrals can be performed analytically for any value of p and both geometries of interest. To proceed, we expand the binomial $(t - t')^p$ and perform the individual integrals. The final result can be written as

$$\mathcal{I}_A^{(p)}(t, t') = \frac{2\pi A_\Sigma}{d - 1} \sum_{k=0}^{p} \binom{p}{k} \frac{t^{p-k}(-t')^{k+2}}{k + 2} \mathcal{T}_A^{(p,k)}(t')\,, \tag{5.84}$$

where

$$\mathcal{T}_{\text{ball}}^{(p,k)}(t') = {}_2F_1\left[\tfrac{1-d}{2}, \tfrac{k+2}{2}, \tfrac{k+4}{2}, \tfrac{t'^2}{t_*^2}\right]\,, \tag{5.85}$$

$$\mathcal{T}_{\text{strip}}^{(p,k)}(t') = {}_2F_1\left[-\tfrac{1}{2}, \tfrac{k+2}{2(d-1)}, \tfrac{k+2d}{2(d-1)}, \tfrac{t'^{2(d-1)}}{t_*^{2(d-1)}}\right]\,. \tag{5.86}$$

In terms of these integrals, $\delta S_A(t)$ can be expressed as follows,

$$
\delta S_A^{(\mathrm{I})}(t) = \begin{cases} 0\,, & t < 0\,, \\ \sigma \mathcal{I}_A^{(p)}(t,t')|_0^t\,, & 0 < t < t_q\,, \\ \varepsilon_0 \mathcal{I}_A^{(0)}(t,t')|_0^{t-t_q} + \sigma \mathcal{I}_A^{(p)}(t,t')|_{t-t_q}^t\,, & t_q < t < t_*\,, \\ \varepsilon_0 \mathcal{I}_A^{(0)}(t,t')|_0^{t-t_q} + \sigma \mathcal{I}_A^{(p)}(t,t')|_{t-t_q}^{t_*}\,, & t_* < t < t_{\mathrm{sat}}\,, \\ \varepsilon_0 \mathcal{I}_A^{(0)}(t,t')|_0^{t_*}\,, & t > t_{\mathrm{sat}}\,, \end{cases}
\tag{5.87}
$$

and

$$
\delta S_A^{(\mathrm{II})}(t) = \begin{cases} 0\,, & t < 0\,, \\ \sigma \mathcal{I}_A^{(p)}(t,t')|_0^t\,, & 0 < t < t_*\,, \\ \sigma \mathcal{I}_A^{(p)}(t,t')|_0^{t_*}\,, & t_* < t < t_q\,, \\ \varepsilon_0 \mathcal{I}_A^{(0)}(t,t')|_0^{t-t_q} + \sigma \mathcal{I}_A^{(p)}(t,t')|_{t-t_q}^{t_*}\,, & t_q < t < t_{\mathrm{sat}}\,, \\ \varepsilon_0 \mathcal{I}_A^{(0)}(t,t')|_0^{t_*}\,, & t > t_{\mathrm{sat}}\,, \end{cases}
\tag{5.88}
$$

respectively, where all the evaluations are for the integration variable t'. These expressions can be easily understood graphically—see Figure 5.3 for an example.

The special case of a linear quench ($p = 1$) was considered in [289] so it is interesting to study it in some detail. Specifically, the authors of [289] looked at a steady state system where $t_q \to \infty$ and focused on the fully driven regime, where $t > t_*$. Under these assumptions, they found that entanglement entropy satisfies a "First Law Of Entanglement Rates" (FLOER), given by

$$
\frac{d\delta S_A(t)}{dt} = \frac{d\varepsilon(t)}{dt}\frac{V_A}{T_A}\,.
\tag{5.89}
$$

The origin of this law is very easy to understand from the definition of the "time-dependent relative entropy" $\Upsilon_A(t)$ in equation (5.61). Since $d\varepsilon(t)/dt$ is constant in this regime, it follows that $\Upsilon_A(t)$ is also a constant. Then from (5.59) we can immediately derive equation (5.89). It is worth pointing out the fact that Υ_A is constant in non-equilibrium steady states is in agreement with the interpretation of Υ_A as a measure of the distance between a given state with respect to an equilibrium state at the same energy density.

It is also interesting to study the other regimes of the linear quench. In Figure 5.4 we plot $\delta S_A(t)$, $\mathfrak{R}_A(t)$ and $\Upsilon_A(t)$ for some representative cases of the ratio $t_q/t_* = \{0.1, 1, 10\}$. The behavior of these quantities is very similar for the two geometries that we considered, so for brevity we have only included plots of the case of the ball. For $t_q/t_* \ll 1$ the quench is almost instantaneous, so all the physical observables resemble those of Section 5.3.1. In the opposite regime $t_q/t_* \gg 1$, most part of the evolution is fully driven, so apart from the initial and final transients, the evolution is governed by the FLOER (5.89). Finally, in the intermediate regime $t_q \sim t_*$ we see a smooth crossover between the latter two cases. In the exact limit $t_q \to t_*$, the fully driven (or intermediate) regime disappears and the evolution is fully captured by the two transients (the initial and final regimes).
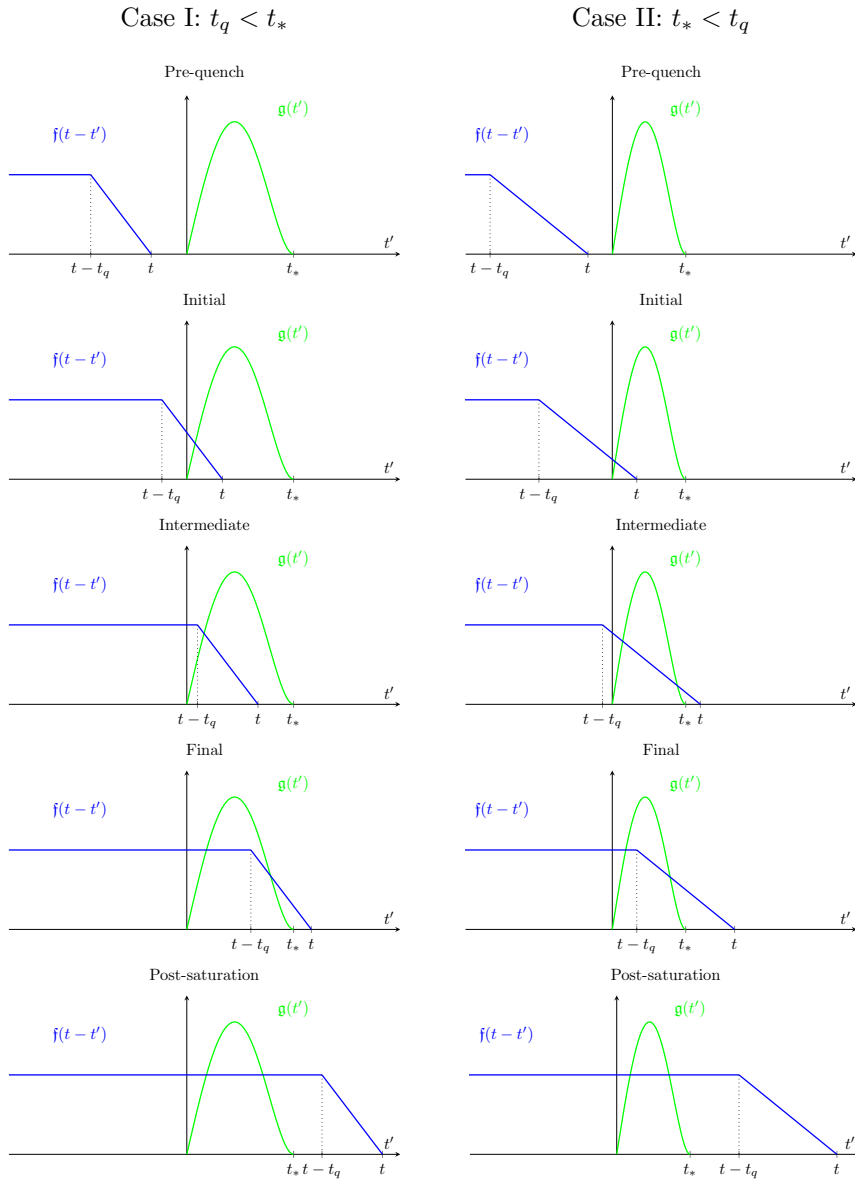
Figure 5.3: Schematic representation of the convolution integral for a power-law quench with $p = 1$. The right and left columns show the two possible cases I: $t_q < t_*$ and II: $t_* < t_q$, respectively. In the pre-quench and post-saturation regimes the integral is a constant. In the initial, intermediate and final growth regimes the integral is time dependent and can be performed by splitting it in various intervals, as shown in equations (5.87) and (5.88).
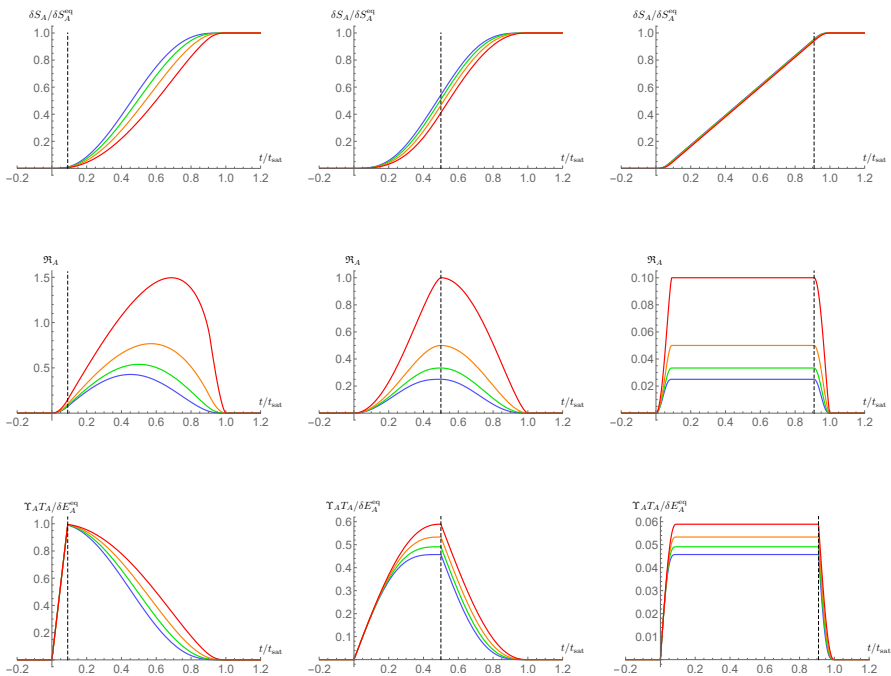
Figure 5.4: Plots of entanglement entropy $\delta S_A(t)$, instantaneous rate of growth $\mathfrak{R}_A(t)$ and time-dependent relative entropy $\Upsilon_A(t)$ for the ball, after a linearly driven quench with $p = 1$. Different values of $d = \{2, 3, 4, 5\}$ are depicted in red, yellow, green and blue, respectively, and we have chosen values $t_q/t_* = \{0.1, 1, 10\}$ from left to the right. In all plots, the dashed vertical line signals the end of the driven phase $t = t_q$.

Finally, in Figure 5.5 we plot $\delta S_A(t)$, $\mathfrak{R}_A(t)$ and $\Upsilon_A(t)$ for other values of the power p. For concreteness, we have only included plots for the case of the ball and we have fixed the number of dimensions to $d = 2$. Other values of d behave similarly. For the plots we have chosen the same representative cases for the duration of the quench: $t_q/t_* = \{0.1, 1, 10\}$. Here we list some general observations valid for arbitrary p:

- The early-time growth generally depends on the power p. From the final formulas it follows that, for both geometries,

$$\delta S_A(t) = \frac{2\pi\sigma A_\Sigma t^{p+2}}{(d-1)(2 + 3p + p^2)} + \cdots .\qquad(5.90)$$

This generalizes the result (5.72) for instantaneous quenches ($p = 0$) to arbitrary p. The proof presented in [288] for the universality of the early-time growth was entirely based on symmetries and can be easily generalized
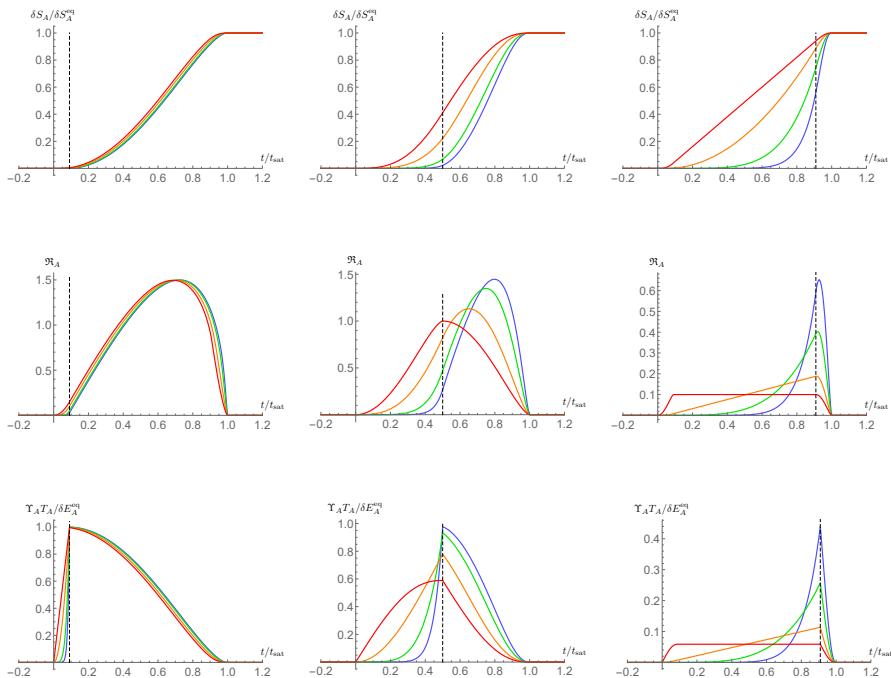
Figure 5.5: Plots of entanglement entropy $\delta S_A(t)$, instantaneous rate of growth $\mathfrak{R}_A(t)$ and time-dependent relative entropy $\Upsilon_A(t)$ for the ball, after a power-law quench with $p = \{1, 2, 5, 10\}$, depicted in red, yellow, green and blue, respectively. For the plots we have fixed the number of dimensions to $d = 2$ and we have chosen values $t_q/t_* = \{0.1, 1, 10\}$ from left to the right. In all plots, the dashed vertical line signals the end of the driven phase $t = t_q$.

to quenches of finite duration. Following the same reasoning, it is possible to conclude that (5.90) should hold independently of the shape and size of the entangling region.

- The maximum rate of growth decreases monotonically as we increase t_q, so it peaks in the limit of instantaneous quenches $t_q \to 0$. Since this limit is universal (independent of p), we conclude that (5.74) and (5.75) are the true maxima for the rate of growth of entanglement for any t_q. On the other hand, the maximum rate of growth at fixed t_q grows with p, reaching a maximum of $v_A^{\max}(t_q, p \to \infty) = v_A^{\max}(t_q \to 0, p)$, which correspond to the same value as that of the instantaneous quench. This follows from the fact that a power-law quench with $p \to \infty$ varies very rapidly near $t \to t_q$ so it behaves similarly to an instantaneous quench at $t = t_q$.

- The proof that $\langle \mathfrak{R}_A(t) \rangle \equiv v_A^{\mathrm{avg}} \leq 1$ presented in [288] holds for a quench of finite duration. In order to see this, one can think of the finite t_q background

as a collection of thin shells spread over the range $v \in [0, t_q]$ so the derivation follows in a similar manner. It is easy to see that the average velocities (5.77) and (5.78) generalize to

$$v_A^{\mathrm{avg}}(t_q, p) = \frac{v_A^{\mathrm{avg}}(t_q \to 0)}{1 + t_q/t_*} , \qquad (5.91)$$

independent of p, so finite t_q decreases the average speed of entanglement propagation.

- Near saturation $t \to t_{\mathrm{sat}}$, entanglement entropy is always continuous and resembles a second order phase transition,

$$\delta S_A(t) - \delta S_A^{\mathrm{eq}} \propto (t_{\mathrm{sat}} - t)^{\gamma_A} , \qquad (5.92)$$

where

$$\gamma_{\mathrm{ball}} = \frac{d+3}{2} , \qquad \gamma_{\mathrm{strip}} = \frac{5}{2} , \qquad (5.93)$$

for *any* $p > 0$. It is interesting that the above result does not extrapolate to the instantaneous quench ($p = 0$), which seems to be an isolated case. These exponents can be derived directly from the two integrals of the stage prior to saturation in (5.87) and (5.88), respectively. The leading term of each integral goes like $(t_{\mathrm{sat}} - t)^{\frac{d+1}{2}}$ for the ball and $(t_{\mathrm{sat}} - t)^{\frac{3}{2}}$ for the strip. However, the contribution of the two integrals cancel exactly. The exponents in (5.93) then come from the first subleading terms of the integrals. The reason why the $p = 0$ case is special is because the second integral in (5.87) and (5.88) is absent, so the values of γ come from the leading behavior of the first integral. This implies that the behavior of entanglement entropy near saturation can single out instantaneous quenches over quenches of finite duration!

- $\Upsilon_A(t)$ is bounded from above: $\Upsilon_A(t) \leq \delta E_A^{\mathrm{eq}}/T_A$. This maximum value is attained *i*) right after an instantaneous quench and *ii*) at $t = t_q$ in the limit $p \to \infty$. As mentioned above, a power-law quench with $p \to \infty$ resembles an instantaneous quench at $t = t_q$ so *i*) and *ii*) actually correspond to a similar physical situation. The existence of such a bound is interesting and reasonable from the point of view of the interpretation of $\Upsilon_A(t)$ as a measure of out-of-equilibrium dynamics: it tells us that the furthest that a time-dependent state can be from equilibrium is right after an instantaneous quench (which is the most violent dynamical perturbation). We also observe that the derivative of $\Upsilon_A(t)$ is discontinuous at $t = t_q$ so it efficiently captures the transition from the driven to the transient regime. This is in contrast with the other two observables, $\delta S_A(t)$ and $\mathfrak{R}_A(t)$, for which the derivatives are continuous.

5.3.3 Periodically driven quench

As a last example, we will consider a periodically driven system. The idea here is to phenomenologically model the setup of [308, 309] and obtain analytic results

for the evolution of entanglement entropy in the regime where the linear response is valid. For concreteness, we will assume that the energy density is given by[12]

$$\mathfrak{f}(t) = \varepsilon(t) = \varepsilon_0 \sin(\omega t)\theta(t) \,, \tag{5.94}$$

where ω is the driving frequency and ϵ_0 is an arbitrary constant. Given the linearity of the convolution integral, a source with a single frequency as in (5.94) is general enough to reproduce *any* other periodic source that admits a Fourier decomposition.

Once more, the entanglement entropy (5.39) reduces to the convolution of (5.94) with the appropriate response function: (5.43) for the ball or (5.44) for the strip. We start driving the system at $t = 0$ and assume that the quench duration is infinite, $t_q \to \infty$. Under these circumstances, the evolution of entanglement entropy can be divided into three intervals: pre-quench $(t < 0)$, initial $(0 < t < t_*)$ and fully driven regime $(t > t_*)$, where

$$\delta S_A(t) = \begin{cases} 0\,, & t < 0\,, \\ \varepsilon_0 \int_0^t dt' \sin(\omega(t-t'))\mathfrak{g}_A(t')\,, & 0 < t < t_*\,, \\ \varepsilon_0 \int_0^{t_*} dt' \sin(\omega(t-t'))\mathfrak{g}_A(t')\,, & t > t_*\,. \end{cases} \tag{5.95}$$

The initial stage is a quick transient. We will be mostly interested in the fully driven phase so in the rest of this section we will assume that $t > t_*$. It is easy to see that in this regime, entanglement entropy satisfies the equation of a simple harmonic oscillator. Differentiating (5.95) twice with respect to t we obtain

$$\frac{d^2 \delta S_A}{dt^2} + \omega^2 \delta S_A = 0\,, \tag{5.96}$$

whose solutions we denote by:

$$\delta S_A(t) = \mathfrak{A}_A(\omega) \sin(\omega t + \phi_A(\omega))\,. \tag{5.97}$$

Surprisingly, it is possible to obtain analytic results for $\mathfrak{A}_A(\omega)$ and $\phi_A(\omega)$ for the two geometries of interest. For ease of notation, we will rewrite (5.97) as

$$\delta S_A(t) = \psi_A(\omega) \cos(\omega t) + \chi_A(\omega) \sin(\omega t)\,, \tag{5.98}$$

and then express the amplitude and phase through

$$\mathfrak{A}_A(\omega) = \sqrt{\psi_A^2(\omega) + \chi_A^2(\omega)}\,, \qquad \phi_A(\omega) = \arctan\left(\frac{\psi_A(\omega)}{\chi_A(\omega)}\right)\,. \tag{5.99}$$

---

[12]Notice that a periodic energy density is unphysical since it violates the null energy condition [250, 251]. We can easily make (5.94) non-decreasing by adding a monotonically increasing term to compensate (which we will do below). However, in light of the linearity property of the convolution integral, these two terms can be treated independently.

For the case of the ball we can obtain closed expressions for arbitrary d in terms of hypergeometric functions:

$$\psi_{\text{ball}} = -\frac{\varepsilon_0 \omega \pi^{\frac{d+2}{2}} t_*^{d+1} {}_0 F_1\left[\frac{d+4}{2}, -\frac{(\omega t_*)^2}{4}\right]}{2\Gamma[\frac{d+4}{2}]}, \tag{5.100}$$

$$\chi_{\text{ball}} = \frac{\varepsilon_0 \pi^{\frac{d+1}{2}} t_*^d {}_1 F_2\left[1, \frac{1}{2}, \frac{d+3}{2}, -\frac{(\omega t_*)^2}{4}\right]}{\Gamma[\frac{d+3}{2}]}. \tag{5.101}$$

For a strip, one can obtain expressions for a fixed number of dimensions. For example, in $d = 3$ one obtains:

$$\psi_{\text{strip}}^{(d=3)} = \frac{\varepsilon_0 \omega \pi^{\frac{3}{2}} l_\perp t_*^3}{24 \Gamma[\frac{9}{4}] \Gamma[\frac{11}{4}]} \left(\Gamma[\frac{5}{4}] \Gamma[\frac{9}{4}] \omega^2 t_*^2 {}_0 F_3 \left[\frac{3}{2}, \frac{7}{4}, \frac{11}{4}, \left(\frac{\omega t_*}{4}\right)^4\right] \right. \tag{5.102}$$

$$\left. - 6\Gamma[\frac{3}{4}] \Gamma[\frac{11}{4}] {}_0 F_3 \left[\frac{1}{2}, \frac{5}{4}, \frac{9}{4}, \left(\frac{\omega t_*}{4}\right)^4\right] \right),$$

$$\chi_{\text{strip}}^{(d=3)} = \frac{\varepsilon_0 \pi l_\perp t_*^2}{12} \left(3\pi {}_0 F_3 \left[\frac{1}{4}, \frac{3}{4}, 2, \left(\frac{\omega t_*}{4}\right)^4\right] \right. \tag{5.103}$$

$$\left. - 2\omega^2 t_*^2 {}_1 F_4 \left[1, \frac{3}{4}, \frac{5}{4}, \frac{3}{2}, \frac{5}{2}, \left(\frac{\omega t_*}{4}\right)^4\right] \right).$$

Expressions for higher dimensions are straightforward to obtain but become increasingly cumbersome, so we will not transcribe them here.

It is interesting to study the behavior of $\mathfrak{A}_A$ and ϕ_A as a function of ω for the various cases of interest. In Figure 5.6 we plot the amplitudes and relative phases for both the ball and the strip in different number of dimensions $d = \{2, 3, 4, 5, 6\}$. In all cases, the amplitudes peak at $\omega \to 0$ and slowly decay as $\omega \to \infty$, displaying mild oscillations at intermediate frequencies. The behavior of the relative phases is markedly different in various cases. For the case of the ball in $d = \{2, 3\}$ and the strip in any number of dimensions the phase varies monotonically in the whole range $\phi_A \in (0, 2\pi)$. For the case of the ball in $d \geq 4$ we see an interesting phenomenon: the relative phase is constrained in a finite interval around $\phi_{\text{ball}} = \pi$. This interval becomes narrower as ω is increased, indicating that the entanglement entropy tends to be out of phase with respect to the source. Indeed, in the strict limit $\omega \to \infty$ the relative phase approaches π, which implies that the entanglement entropy is exactly out of phase with the source in this limit.

We remind the reader that a periodic source as in (5.94) is unphysical since it violates the NEC [250, 251]. In keeping with the laws of black hole thermodynamics, the black hole mass should be non-decreasing. It is easy to make (5.94) non-decreasing by simply adding an monotonically increasing source. The easiest example is to add a linear pump:

$$\mathfrak{f}(t) = \varepsilon(t) = \varepsilon_0 \left(\sin\left(\omega t\right) + \zeta t\right) \theta(t), \qquad \zeta \geq \omega. \tag{5.104}$$
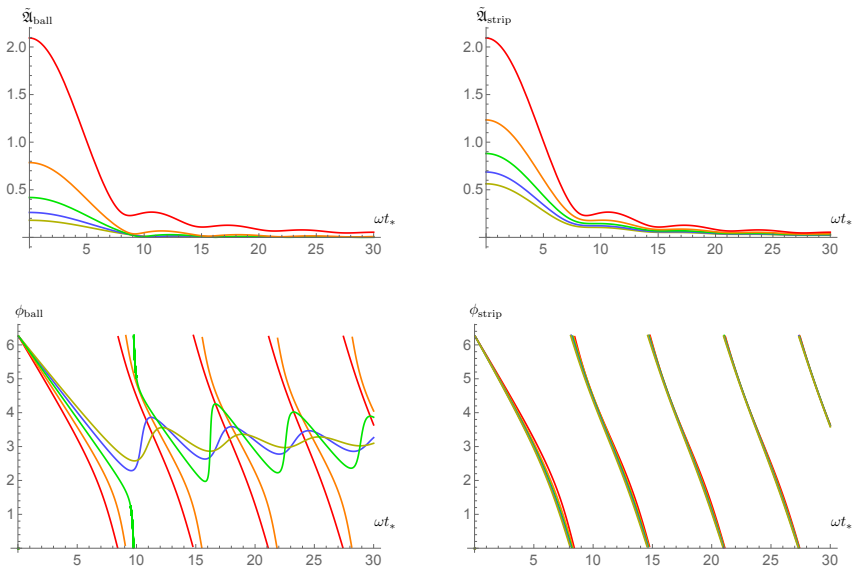
Figure 5.6: Normalized amplitude $\tilde{\mathfrak{A}}_A = \mathfrak{A}_A/A_\Sigma \varepsilon_0$ and relative phase ϕ_A as a function of ωt_* for the two geometries of interest: the ball and the strip. The various lines correspond to $d = \{2, 3, 4, 5, 6\}$ depicted in red, orange, green, blue and yellow, respectively.

Since we are considering linear response, we can simply add the expressions for the periodic and linear quenches, the later corresponding to the case $p = 1$ and $t_q \to \infty$ in the notation of the previous subsection.

The full entanglement evolution, with and without the linear driving, is plotted for sample parameters in Figure 5.7. It is worth noticing that the evolution of entanglement entropy is monotonically increasing for the cases where the energy density respects the NEC. This follows directly from property of differentiation of the convolution integral. Since $\mathfrak{g}_A(t) \geq 0$ and, assuming that $d\varepsilon(t)/dt \geq 0$, it follows that in the linear response regime

$$\frac{d\delta S_A(t)}{dt} = \frac{d\varepsilon(t)}{dt} * \mathfrak{g}_A(t) \geq 0 \,, \tag{5.105}$$

so the system is dissipative. In contrast, the authors of [308, 309] obtained a more intricate phase space, where the system transitions from a dissipation dominated phase (linear response) to a resonant amplification phase where entanglement entropy is not necessarily monotonic. These non-monotonicities arise because the extremal surfaces in such a regime probe deeper into the bulk and bend backwards in time, thus receiving contributions from different time slices. It would be interesting to compute higher order contributions to the entanglement entropy for small subsystems to study this transition analytically. Finally, the time-dependent relative entropy behaves as expected with and without the linear pump. For the
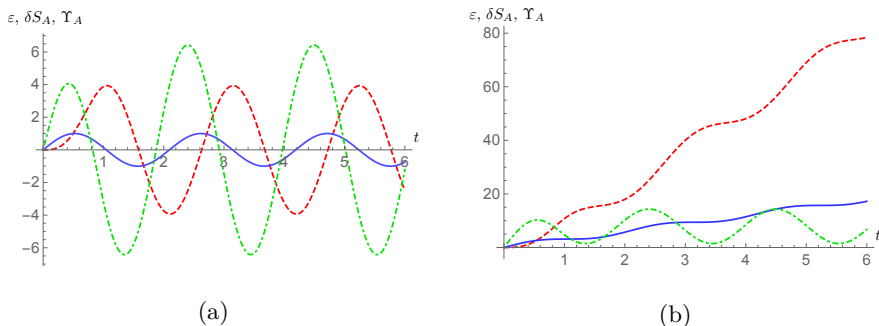
Figure 5.7: Sample plots for the source $\varepsilon(t)$ (solid blue) entanglement entropy $\delta S_A(t)$ (dashed red) and relative entropy $\Upsilon_A(t)$ (dot-dashed green) for a ball-shaped region in $d = 3$ dimensions. For the plots we have chosen the following parameters: $\varepsilon_0 = 1$, $t_* = 1$ and $\omega = 3$, for (a) a purely periodic source and (b) a source respecting the bulk NEC with $\zeta = 3$.

purely oscillatory source, $\Upsilon_A(t)$ quickly reaches a periodic evolution after the initial transient. From the definition (5.59) it follows that in the fully driven regime

$$\Upsilon_A(t) = \psi_A(\omega)\cos(\omega t) + \left(\chi_A(\omega) + \frac{\varepsilon_0 V_A}{T_A}\right)\sin(\omega t).\qquad(5.106)$$

Therefore, $\Upsilon_A(t)$ has an amplitude and phase that can be determined from analogous expressions to (5.99), with $\chi_A \to \chi_A + \varepsilon_0 V_A/T_A$. For the oscillatory source with a linear pump term, $\Upsilon_A(t)$ oscillates around a constant value $\Upsilon_A^{(p=1)}$ which is bigger than the amplitude of the oscillation. This is indeed expected since $\Upsilon_A(t) \geq 0$ for any source that respects the bulk NEC.

5.4 Conclusions and outlook

In this chapter, we have studied analytic expressions for the evolution of entanglement entropy after a variety of time-dependent perturbations. We obtained these results from holography, using a Vaidya geometry as a model of a quench. Analytic results can be obtained to leading order in the small subsystem limit, comparing to the energy injected in the quench. In this limit, the change in entanglement entropy $\delta S_A(t)$ follows a linear response, where the energy density takes the role of the source—see Figure 5.8 for a schematic diagram showing how this linear response fits in the different regimes of entanglement propagation. Being a linear response, the resulting expression for $\delta S_A(t)$ can be conveniently written as a convolution integral (5.39) of the source against a kernel which depends only on the geometry of the subsystem under consideration. We determined this kernel (also known as response function) for ball and strip subsystems in (5.43) and (5.44), respectively.
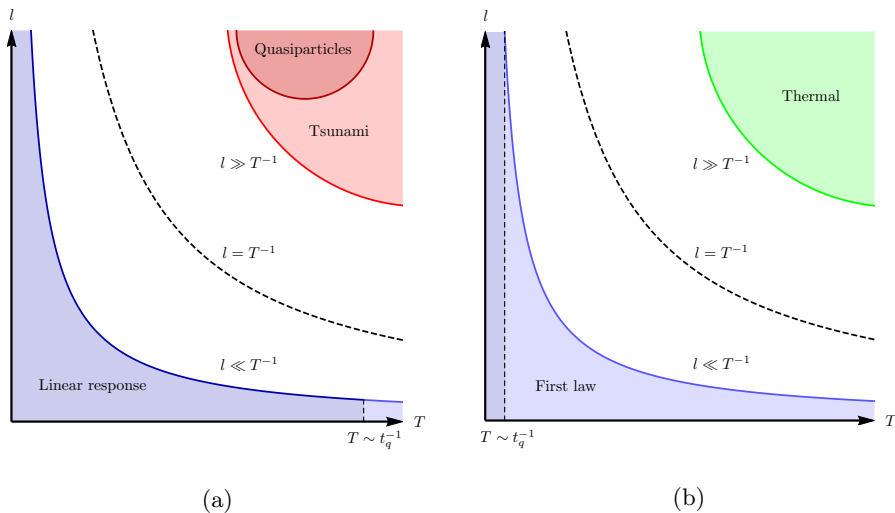
(a)

(b)

Figure 5.8: Schematic diagram of the different regimes of interest of entanglement propagation for (a) fast quenches $t_q \to 0$ and (b) slow quenches $t_q \to \infty$. The blue region corresponds to the small subsystem limit. The dashed vertical line in this region is a separatrix that signals the point at which the first law of entanglement starts to be valid. The dashed regions in the upper right corners correspond to the large subsystem limit. For fast quenches the spread of entanglement this region is well described by the heuristic entanglement tsunami picture, however in some special cases it admits an microscopic interpretation in terms of quasi-particles. For sufficiently slow quenches the system can be considered very close to equilibrium so the standard rules of thermodynamics apply. In this limit entanglement entropy reduces to thermal entropy, which evolves adiabatically.

For small time-independent perturbations around the vacuum, entanglement entropy satisfies a relation similar to the first law of thermodynamics. Our linear response relation reduces to this first law if the quench profile varies sufficiently slowly. In order to quantify this statement, we introduced a quantity $\Upsilon_A(t)$ in (5.59) as a measure for how far the system is from satisfying the first law of entanglement entropy. This $\Upsilon_A(t)$ can be thought of as comparing the reduced density matrix of our system at a time t to a thermal density matrix at the same energy density. It also resembles relative entropy in several ways. First, it is positive for quench profiles that satisfy the NEC in the bulk. Second, it vanishes at equilibrium, so for quenches of finite duration it returns to zero once the system has thermalized. Furthermore, in contrast to $\delta S_A(t)$ or the rate of growth $\mathfrak{R}_A(t)$, the quantity $\Upsilon_A(t)$ undergoes a discontinuous first-order transition at the end of the driven phase of a quench, which clearly signals the approach to thermality that follows.

After incorporating the instantaneous quenches studied in [288] in our frame-

work, we turned to quenches of finite duration t_q with a power-law time dependence $\varepsilon(t) \propto t^p$. Since our convolution expression is linear in the source, these are in principle general enough to determine $\delta S_A(t)$ for any quench that is analytic in the interval $t \in (0, t_q)$. Quenches of finite duration exhibit some distinct features. Most notably, the rate of growth of entanglement decreases with increasing t_q for a fixed p. Furthermore, inspection of $\Upsilon_A(t)$ confirms that the system is maximally out-of-equilibrium after an instantaneous quench. This sets an upper bound, $\Upsilon_A(t) \leq \delta E_A^{\text{eq}}/T_A$, which can be attained right after an instantaneous quench, or at $t = t_q$ in the limit $p \to \infty$. We also commented on the results of [289] for linearly increasing sources and showed that they can be easily understood in terms of the linear response formalism.

Finally, we studied the evolution of entanglement entropy after quenches involving a periodic source. We focused on sources with a single frequency $\varepsilon(t) \propto \sin(\omega t)$. However, given the linearity of the convolution integral, our results can be easily generalized to any periodic source that admits a Fourier decomposition. Following an initial transient regime, $\delta S_A(t)$ and $\Upsilon_A(t)$ are both periodic but out of phase with respect to the energy density. We found analytic expressions for the amplitudes and relative phases for the ball and strip geometries in any number of dimensions. We found an interesting transition for ball-shaped regions in $d \geq 4$, where the entanglement entropy tends to be completely out of phase with respect to the source for large enough frequencies. We also commented on the numerical results of [308, 309], finding qualitative agreement with our results in the regime where the linear response is valid.

There are a number of open questions related to our work that are worth exploring. For example, our results for the entanglement growth are valid in the strict limit of infinite coupling, as is evident from the use of Einstein gravity in the bulk. It would be worthwhile to explore the universality of our results in holographic theories with higher derivative corrections. For instance, in time-independent cases, adding a Gauss-Bonnet term changes the entanglement temperature T_A for strip regions but not for ball regions [294]. It would be interesting to see the effect of various higher-curvature corrections to our entanglement kernels.

It should also be possible to derive a linear response of entanglement entropy from a purely field theoretic computation. One way to see this is as follows. Using the replica trick, entanglement entropy can be computed from two-point functions of twist operators. For small subsystems, these two-point functions can be expanded using their OPEs. Furthermore, if we study this two-point function using, say, the Schwinger-Keldysh formalism, it is expected to have a linear response relation in the appropriate limit.[13]

It would also be interesting to find a field theory derivation of our linear response expressions for large c CFTs, perhaps along the lines of [312]. In the large c limit, the leading contribution is given by the stress-energy tensor, which is dual to the leading metric contribution to $\delta S_A(t)$ discussed here. A natural question to ask is what the response function $\mathfrak{g}_A(t)$ corresponds to in field theory language.

---

[13]See also [311] for related results.

Another natural generalization would be to compute subleading corrections from other operators running in the OPE. A similar question was considered recently in [313] for time-independent scenarios. Based on their findings, we expect that the linear response that we found here should include extra contributions from one-point functions of operators dual to other light bulk fields, each with a different kernel.

5.A Example: Electric field quench in AdS$_4$/CFT$_3$

As a concrete example, we will consider an electric field quench in the context of AdS$_4$/CFT$_3$. The starting point is the Einstein–Hilbert action with a negative cosmological constant coupled to a Maxwell field,[14]

$$S = \frac{1}{2\kappa^2} \int d^4x \sqrt{-g} \left(R + 6 - F^2 \right) , \qquad (5.107)$$

where $\kappa^2 = 8\pi G$. The gauge field A_μ is dual to a conserved current in the boundary theory $J^\mu = \{\rho, \vec{J}\}$. The quench is introduced here by an external, time-dependent electric field $\vec{E} = E(t)\hat{x}$. In the boundary theory, $\vec{E}$ sources $\vec{J}$, so the system is described by the following partition function,

$$Z[\vec{E}] = \int \mathcal{D}\vec{J} e^{i \int d^dx (\mathcal{L} + \vec{E} \cdot \vec{J})} . \qquad (5.108)$$

Interestingly, the above system admits an analytic, fully backreacted solution for an arbitrary electric field $E(t)$ [305]. The bulk solution can be written in the following form,

$$ds^2 = \frac{1}{u^2} \left(-f(v,u)dv^2 - 2dvdu + dx^2 + dy^2 \right) , \qquad (5.109)$$

$$F = -E(v)dv \wedge dx , \qquad (5.110)$$

where

$$f(v,u) = 1 - u^3 m(v) , \quad m(v) = \frac{1}{2} \int_{-\infty}^{v} E(v')^2 dv' . \qquad (5.111)$$

The metric (5.109) is written in terms of Eddington-Finkelstein coordinates, so v labels ingoing null trajectories. This variable is related to the standard time coordinate t through

$$dv = dt - \frac{du}{f(v,u)} . \qquad (5.112)$$

In particular, near the boundary $u \to 0$ we have that $f(v,u) \to 1$ so

$$v \simeq t - u . \qquad (5.113)$$

---

[14]Alternatively, we could start with Einstein gravity coupled to a DBI action and turn on an electric field on the brane, see for example [314–317].

Re-expressing the above solution in terms of the standard AdS coordinates, we find that

$$F_{xt} = E(v), \quad F_{xu} = -E(v)/f(v,u).$$ (5.114)

The electric field $E(t) = \lim_{u \to 0} F_{xt}$ induces a current in the boundary theory

$$J(t) = -(4\pi G)^{-1} \lim_{u \to 0} F_{xu},$$

so the conductivity turns out to be a constant even nonlinearly,

$$\sigma(\omega) = \sigma_{DC} = \frac{J(\omega)}{E(\omega)} = \frac{1}{4\pi G}.$$ (5.115)

A trivial consequence is that the energy (ADM mass) $M = (8\pi G)^{-1}m$ increases at the rate predicted by Joule heating, $dM/dt = \vec{E} \cdot \vec{J}$, which from the boundary perspective, this follows from the fact that the stress tensor satisfies

$$\partial_\mu T^{\mu\nu} = F^{\mu\nu} J_\mu.$$ (5.116)

This equation can be derived on general grounds from the appropriate Ward identity.

5.B Holographic stress-energy tensor

In order to compute the stress-energy tensor for a general Vaidya quench we have to write the metric (5.26) in Fefferman-Graham coordinates

$$ds^2 = \frac{1}{z^2} \left(g_{\mu\nu}(z,x)dx^\mu dx^\nu + dz^2 \right).$$ (5.117)

For an asymptotically AdS$_{d+1}$ geometry, the function $g_{\mu\nu}(z,x)$ has the following expansion near the boundary (located at $z \to 0$),

$$\begin{aligned} g_{\mu\nu}(z,x) &= g_{\mu\nu}^{(0)}(x) + z^2 g_{\mu\nu}^{(2)}(x) + \cdots \\ &\quad + z^d g_{\mu\nu}^{(d)}(x) + z^d \log(z^2) h_{\mu\nu}^{(d)}(x) + \cdots. \end{aligned}$$ (5.118)

From this expansion we can extract the CFT metric, $d\tilde{s}^2 = g_{\mu\nu}^{(0)}(x)dx^\mu dx^\nu$, and the expectation value of the stress-energy tensor [62, 318]

$$\langle T_{\mu\nu}(x) \rangle = \frac{d}{16\pi G_N^{(d+1)}} \left(g_{\mu\nu}^{(d)}(x) + X_{\mu\nu}^{(d)}(x) \right).$$ (5.119)

The last term in (5.119) is related to the gravitational conformal anomaly, and vanishes in odd dimensions. In even dimensions we have, for example,

$$\begin{aligned} X_{\mu\nu}^{(2)} &= -g_{\mu\nu} g_\alpha^{(2)\alpha}, \quad (5.120) \\ X_{\mu\nu}^{(4)} &= -\frac{1}{8} g_{\mu\nu} \left[\left(g_\alpha^{(2)\alpha} \right)^2 - g_\alpha^{(2)\beta} g_\beta^{(2)\alpha} \right] - \frac{1}{2} g_\mu^{(2)\alpha} g_{\alpha\nu}^{(2)} + \frac{1}{4} g_{\mu\nu}^{(2)} g_\alpha^{(2)\alpha}. \end{aligned}$$

In higher dimensions $X^{(d)}_{\mu\nu}$ is given by similar but more long-winded expressions that we will not transcribe here.

Consider the case $f(v, u) = 1$, i.e. pure AdS in Eddington-Finkelstein coordinates. The transformation in this case is the following,

$$v = t - z\,, \qquad u = z\,, \tag{5.121}$$

and leads to

$$ds^2 = \frac{1}{z^2}\left(\eta_{\mu\nu}dx^\mu dx^\nu + dz^2\right)\,. \tag{5.122}$$

As expected, this is empty AdS written in Poincaré coordinates, where we have $\langle T_{\mu\nu}(x)\rangle = 0$. For $f(v, u) \neq 1$ we can proceed perturbatively. Specifically, after the coordinate transformation

$$v = t - z\left[1 + \frac{(d-1)g(t)z^d}{2d(d+1)u_H^d} + \cdots\right]\,, \tag{5.123}$$

$$u = z\left[1 - \frac{g(t)z^d}{2d\,u_H^d} + \cdots\right]\,, \tag{5.124}$$

we arrive at

$$ds^2 = \frac{1}{z^2}\left[(\eta_{\mu\nu} + \tau_{\mu\nu}z^d + \cdots)dx^\mu dx^\nu + dz^2\right]\,, \tag{5.125}$$

where

$$\tau_{00} = \frac{(d-1)g(t)}{d\,u_H^d}\,, \qquad \tau_{ii} = \frac{g(t)}{d\,u_H^d}\,. \tag{5.126}$$

From here it follows that

$$\langle T_{00}(t)\rangle \equiv \varepsilon(t) = \frac{(d-1)g(t)}{16\pi G_N^{(d+1)}u_H^d}\,, \tag{5.127}$$

$$\langle T_{ii}(t)\rangle \equiv P(t) = \frac{g(t)}{16\pi G_N^{(d+1)}u_H^d}\,. \tag{5.128}$$

Notice that the stress-energy tensor is traceless, as expected for a CFT.

Summary and outlook

We conclude this thesis with a brief summary and outlook, highlighting some elements of the individual chapters. A non-technical Dutch summary can be found on page 171.

Background The perturbative approach to quantum field theory has been immensely successful. It has led to some of the most precise experimentally-verified predictions in physics. However, it also has several shortcomings, two of which are discussed in Chapter 1. First, a perturbative approach is only useful if small coupling constants are available. In many physically relevant theories, such as the gauge theory describing the strong nuclear force, this is not the case. Second, various nonperturbative effects such as magnetic monopoles and instantons in gauge theory lead to an inherent limitation on the applicability of perturbative methods. Both of these shortcomings motivate dual descriptions of quantum field theory through a string-theoretic construction.

The Alday–Gaiotto–Tachikawa (AGT) correspondence relates supersymmetric four-dimensional gauge theories to two-dimensional conformal field theories. It can be understood as the most recent incarnation of the idea that four-dimensional gauge theories can be described in terms of two-dimensional Riemann surfaces. This idea can be traced back to the symmetry in Maxwell's equations exchanging electric and magnetic charge.

The AdS/CFT correspondence allows us to describe a d-dimensional strongly-coupled conformal field theory (CFT) in terms of a $(d+1)$-dimensional gravitational theory on an anti-de Sitter (AdS) spacetime. The latter is a maximally symmetric spacetime with negative scalar curvature. Its isometries are equal to the d-dimensional conformal group. Moreover, AdS is a solid cylinder where distances increase asymptotically towards the boundary of the cylinder. The metric on this conformal boundary is only defined up to Weyl transformations, and we often think of the dual CFT as living on the boundary of AdS. For this reason, the field theory is commonly known as the boundary theory, while the gravitational theory is referred to as the bulk theory.

In this thesis, we have investigated several applications and extensions of the AdS/CFT and AGT correspondence. Although the AdS/CFT correspondence has its origins in detailed string theory constructions, many aspects of the associated dictionary seem to rely only on basic features of its geometry and symmetry.

Consequently, one can *apply* the AdS/CFT correspondence to model strongly-coupled field theories in terms of a suitable bulk theory. However, many interesting strongly-coupled theories one may wish to study are not relativistic, and it is not obvious how AdS/CFT should be generalized to accommodate them. Likewise, while the AGT correspondence provides a detailed identification between two specific sets of theories, it cannot be easily generalized without a constructive understanding of its string theory origins.

Asymptotic symmetries in three dimensions The AdS/CFT correspondence comes with a dictionary relating various elements of the two theories it identifies. Symmetries are a basic entry in this dictionary. If the bulk gravity theory is three-dimensional, its asymptotic symmetry algebra is generally infinite-dimensional. This is discussed in detail in Chapter 2.

For AdS$_3$ Einstein gravity, the asymptotic symmetries should reproduce the Virasoro symmetries of two-dimensional CFTs. To understand this result, it is useful to formulate three-dimensional gravity as a Chern–Simons theory. The asymptotic symmetries of a Chern–Simons theory form an affine algebra. Imposing Dirichlet boundary conditions on the metric corresponds to a Drinfeld–Sokolov reduction of the affine algebra. For the $sl_2(\mathbb{R})$ corresponding to AdS$_3$ Einstein gravity, this reproduces the asymptotic Virasoro algebra including the correct central charge. However, this procedure is general. It can also be applied to different algebras corresponding to other theories of gravity that do not (just) contain a metric field.

Nonrelativistic holography from AdS$_3$ Nonrelativistic theories can be coupled to a background spacetime using Newton–Cartan geometry. It is reasonable to expect that such Newton–Cartan theories, including gravitational theories where the metric data is allowed to fluctuate, can be obtained as a suitable limit of relativistic theories. However, the geometric description of relativistic and non-relativistic theories is rather different. This is mainly due to the fact that local Lorentz symmetry is broken in Newton–Cartan theories by designating one special direction, which is usually the time direction.

On the other hand, certain three-dimensional Newton–Cartan theories of gravity can also be formulated as a Chern–Simons theory. As we show in Chapter 3, this enables a precise identification between such theories and a limit of a relativistic theory. The corresponding asymptotic symmetry algebra consists of a left- and right-moving warped Virasoro algebra with vanishing affine $u(1)$ level. It contains scaling symmetry but no special conformal transformations. It would be very interesting to gain a better understanding of the associated two-dimensional field theories, perhaps even as a string worldsheet theory. Moreover, it turns out that the designated direction of the nonrelativistic bulk geometry is in this case the *radial* direction, which will have important consequences for the bulk/boundary mapping in such theories.

Generalized AGT from conifolds   It has been suggested that the relation between four-dimensional supersymmetric gauge theories and two-dimensional Toda CFTs proposed by the AGT correspondence can be understood using two different but equivalent compactifications of the A_{N-1} six-dimensional $(2,0)$ theory. The compactification to two dimensions is argued to lead to Toda theory as the boundary modes of a three-dimensional sl_N Chern–Simons theory. In Chapter 4, we argue that the Drinfeld–Sokolov boundary conditions of the latter arise from a different D-brane system than what was originally proposed. The geometry of the M-theory uplift of the improved D-brane system can be approximated using a generalized conifold.

Furthermore, this new construction can be extended to generalized Toda theories, which arise as the boundary modes of sl_N Chern–Simons theory after a non-principal $sl_2 \subset sl_N$ Drinfeld–Sokolov reduction. However, the result of this reduction is a *complex* Toda theory, while the AGT correspondence involves a *real* Toda theory. They agree for unit Chern–Simons level. It would be very interesting to work out the relation between real and complex generalized Toda theories at higher level. Additionally, the generalized conifolds lead to a purely geometric interpretation of the defects associated to generalized Toda theories in AGT. Reproducing the central charge of such theories using an equivariant reduction of the six-dimensional anomaly polynomial would be a good check of this interpretation.

Holographic entanglement entropy after quenches   Entanglement entropy in holographic strongly-coupled field theories can be translated to the area of minimal surfaces in the bulk. This prescription allows one to write down analytic expressions corresponding to highly nontrivial boundary behavior, such as the evolution of entanglement entropy after a global quantum quench. The latter can be modeled in the bulk using an infalling shell of matter (a Vaidya metric), which collapses to form a black hole. We can use this approach to study general features of the dynamics of a particular class of strongly-coupled systems.

In Chapter 5, we consider boundary intervals that are small compared to the resulting black hole, obtain analytic results for arbitrary quench profiles and work out explicit expressions for a representative set of quenches. The extent to which such quenches deviate from adiabatic behavior can be made precise by comparing the resulting evolution of entanglement entropy to the first law of entanglement entropy. It would be interesting to reproduce the kernels in the resulting linear response expressions directly from field theory, for example in the large c expansion in two-dimensional CFTs.

Outlook

Over the last 20 years, the AdS/CFT correspondence has proven to be a magnificent and many-faceted gift. Perhaps its only flaw is the fact that its original form is in a sense *too* symmetric. To learn which aspects of the concrete dualities that have been derived from string theory are fundamental and which are accidental, we can follow several different paths.

First, we can search for predictions that rely only on some high-level details of the correspondence. The holographic identification of spatial entanglement entropy in terms of minimal surfaces in the bulk is perhaps the most fruitful of such predictions discovered so far. It would be very interesting if other identifications, for example involving an appropriate notion of complexity, could be made at a similar level of precision. Second, we can try to find generalizations of the original correspondence, for example by studying controlled limits of 'top-down' string theory models, or by building 'bottom-up' models motivated by other areas of physics. Nonrelativistic holography has proven to be a particularly interesting branch of such generalizations.

It seems fair to say that we are still only scratching the surface of a full understanding of nonrelativistic Newton–Cartan-type theories of gravity. For one, little is known about the actions corresponding to such theories. Learning more about the intrinsic geometry of Newton–Cartan structures and their natural curvature invariants could be of great help here, just as a proper understanding of Riemannian geometry makes it relatively easy to construct the Einstein–Hilbert action. Conserved charges associated to such geometric data must also be defined, and our three-dimensional Chern–Simons perspective may give hints for how this should be done.

Next, nonrelativistic field theories should be able to describe at least some approximation of thermal behavior. If they are to be related holographically to nonrelativistic theories of gravity, the latter should also contain solutions that model this approximately thermal behavior. Making any aspect of these bulk solutions more precise will certainly teach us important lessons about Newton–Cartan gravity and its holographic description. One possible approach to this problem would be via a limit of relativistic black hole thermodynamics, and we hope that our three-dimensional results will likewise be of some use here.

As for the AGT correspondence, we have advocated a constructive approach towards its derivation. If we do not have a fundamental understanding of the mechanism through which the equality proposed by the AGT correspondence arises, we have not yet fully understood the duality it signifies. Although certainly technically involved, working out all aspects of the derivation of the AGT correspondence from six dimensions presents a rare opportunity to reach a new level of detail in our understanding of strong-coupling dualities.

Bibliography

[1] J. Hartong, Y. Lei, N. A. Obers and G. Oling, *Zooming in on AdS_3/CFT_2 near a BPS bound*, *JHEP* **05** (2018) 016, [`1712.05794`].

[2] S. van Leuven and G. Oling, *Generalized Toda theory from six dimensions and the conifold*, *JHEP* **12** (2017) 050, [`1708.07840`].

[3] S. F. Lokhande, G. W. J. Oling and J. F. Pedraza, *Linear response of entanglement entropy from holography*, *JHEP* **10** (2017) 104, [`1705.10324`].

[4] J. S. Schwinger, *On Quantum electrodynamics and the magnetic moment of the electron*, *Phys. Rev.* **73** (1948) 416–417.

[5] J. S. Schwinger, *On gauge invariance and vacuum polarization*, *Phys. Rev.* **82** (1951) 664–679.

[6] T. Aoyama, M. Hayakawa, T. Kinoshita and M. Nio, *Tenth-Order QED Contribution to the Electron g-2 and an Improved Value of the Fine Structure Constant*, *Phys. Rev. Lett.* **109** (2012) 111807, [`1205.5368`].

[7] D. Hanneke, S. Fogwell and G. Gabrielse, *New Measurement of the Electron Magnetic Moment and the Fine Structure Constant*, *Phys. Rev. Lett.* **100** (2008) 120801, [`0801.1134`].

[8] D. J. Gross and F. Wilczek, *Ultraviolet Behavior of Nonabelian Gauge Theories*, *Phys. Rev. Lett.* **30** (1973) 1343–1346.

[9] H. D. Politzer, *Reliable Perturbative Results for Strong Interactions?*, *Phys. Rev. Lett.* **30** (1973) 1346–1349.

[10] J. M. Maldacena, *The Large N limit of superconformal field theories and supergravity*, *Int. J. Theor. Phys.* **38** (1999) 1113–1133, [`hep-th/9711200`].

[11] F. J. Dyson, *Divergence of perturbation theory in quantum electrodynamics*, *Phys. Rev.* **85** (1952) 631–632.

[12] S. W. Hawking, *Black holes in general relativity*, *Commun. Math. Phys.* **25** (1972) 152–166.

[13] J. M. Bardeen, B. Carter and S. W. Hawking, *The Four laws of black hole mechanics*, *Commun. Math. Phys.* **31** (1973) 161–170.

[14] J. D. Bekenstein, *Black holes and entropy*, *Phys. Rev.* **D7** (1973) 2333–2346.

[15] S. W. Hawking and G. F. R. Ellis, *The Large Scale Structure of Space-Time*. Cambridge Monographs on Mathematical Physics. Cambridge University Press, 2011, 10.1017/CBO9780511524646.

[16] A. Strominger and C. Vafa, *Microscopic origin of the Bekenstein-Hawking entropy*, *Phys. Lett.* **B379** (1996) 99–104, [`hep-th/9601029`].

[17] R. Bousso, *The Holographic principle*, *Rev. Mod. Phys.* **74** (2002) 825–874, [`hep-th/0203101`].

[18] L. Susskind, *The World as a hologram*, *J. Math. Phys.* **36** (1995) 6377–6396, [`hep-th/9409089`].

[19] G. 't Hooft, *Dimensional reduction in quantum gravity*, *Conf. Proc.* **C930308** (1993) 284–296, [`gr-qc/9310026`].

[20] O. Aharony, S. S. Gubser, J. M. Maldacena, H. Ooguri and Y. Oz, *Large N field theories, string theory and gravity*, *Phys. Rept.* **323** (2000) 183–386, [`hep-th/9905111`].

[21] H. Nastase, *Introduction to AdS-CFT*, 0712.0689.

[22] M. Ammon and J. Erdmenger, *Gauge/gravity duality*. Cambridge University Press, Cambridge, 2015.

[23] M. Natsuume, *AdS/CFT Duality User Guide*, *Lect. Notes Phys.* **903** (2015) pp.1–294, [`1409.3575`].

[24] G. 't Hooft, *A Planar Diagram Theory for Strong Interactions*, *Nucl. Phys.* **B72** (1974) 461.

[25] N. Beisert et al., *Review of AdS/CFT Integrability: An Overview*, *Lett. Math. Phys.* **99** (2012) 3–32, [`1012.3982`].

[26] L. F. Alday, D. Gaiotto and Y. Tachikawa, *Liouville Correlation Functions from Four-dimensional Gauge Theories*, *Lett. Math. Phys.* **91** (2010) 167–197, [`0906.3219`].

[27] C. M. Bender and T. T. Wu, *Anharmonic oscillator. 2: A Study of perturbation theory in large order*, *Phys. Rev.* **D7** (1973) 1620–1636.

[28] M. Mariño, *Instantons and Large N*. Cambridge University Press, 2015.

[29] M. Nakahara, *Geometry, topology and physics*. Taylor & Francis, 2003.

[30] M. Dunajski, *Solitons, instantons, and twistors*. Oxford Univ. Press, 2010.

[31] T. T. Wu and C. N. Yang, *Concept of Nonintegrable Phase Factors and Global Formulation of Gauge Fields*, *Phys. Rev.* **D12** (1975) 3845–3857.

[32] M. F. Atiyah, N. J. Hitchin, V. G. Drinfeld and Yu. I. Manin, *Construction of Instantons*, *Phys. Lett.* **A65** (1978) 185–187.

[33] W. Nahm, *A Simple Formalism for the BPS Monopole*, *Phys. Lett.* **90B** (1980) 413–414.

[34] D.-E. Diaconescu, *D-branes, monopoles and Nahm equations*, *Nucl. Phys.* **B503** (1997) 220–238, [`hep-th/9608163`].

[35] C. Montonen and D. I. Olive, *Magnetic Monopoles as Gauge Particles?*, *Phys. Lett.* **72B** (1977) 117–120.

[36] H. Osborn, *Topological Charges for N=4 Supersymmetric Gauge Theories and Monopoles of Spin 1*, *Phys. Lett.* **83B** (1979) 321–326.

[37] P. H. Ginsparg, *APPLIED CONFORMAL FIELD THEORY*, in *Les Houches Summer School in Theoretical Physics: Fields, Strings, Critical Phenomena Les Houches, France, June 28-August 5, 1988*, pp. 1–168, 1988. `hep-th/9108028`.

[38] J. D. Brown and M. Henneaux, *Central Charges in the Canonical Realization of Asymptotic Symmetries: An Example from Three-Dimensional Gravity*, *Commun. Math. Phys.* **104** (1986) 207–226.

[39] J. L. Cardy, *Operator Content of Two-Dimensional Conformally Invariant Theories*, *Nucl. Phys.* **B270** (1986) 186–204.

[40] A. Strominger, *Black hole entropy from near horizon microstates*, *JHEP* **02** (1998) 009, [`hep-th/9712251`].

[41] S. S. Gubser, I. R. Klebanov and A. M. Polyakov, *Gauge theory correlators from noncritical string theory*, *Phys. Lett.* **B428** (1998) 105–114, [`hep-th/9802109`].

[42] E. Witten, *Anti-de Sitter space and holography*, *Adv. Theor. Math. Phys.* **2** (1998) 253–291, [`hep-th/9802150`].

[43] S. Ryu and T. Takayanagi, *Holographic derivation of entanglement entropy from AdS/CFT*, *Phys. Rev. Lett.* **96** (2006) 181602, [`hep-th/0603001`].

[44] K. G. Wilson, *Confinement of Quarks*, *Phys. Rev.* **D10** (1974) 2445–2459.

[45] G. 't Hooft, *On the Phase Transition Towards Permanent Quark Confinement*, *Nucl. Phys.* **B138** (1978) 1–25.

[46] J. M. Maldacena, *Wilson loops in large N field theories*, *Phys. Rev. Lett.* **80** (1998) 4859–4862, [`hep-th/9803002`].

[47] M. Rangamani and T. Takayanagi, *Holographic Entanglement Entropy*, *Lect. Notes Phys.* **931** (2017) pp.1–246, [`1609.01287`].

[48] C. Holzhey, F. Larsen and F. Wilczek, *Geometric and renormalized entropy in conformal field theory*, *Nucl. Phys.* **B424** (1994) 443–467, [`hep-th/9403108`].

[49] P. Calabrese and J. L. Cardy, *Entanglement entropy and quantum field theory*, *J. Stat. Mech.* **0406** (2004) P06002, [`hep-th/0405152`].

[50] S. Ryu and T. Takayanagi, *Aspects of Holographic Entanglement Entropy*, *JHEP* **08** (2006) 045, [`hep-th/0605073`].

[51] T. Nishioka, S. Ryu and T. Takayanagi, *Holographic Entanglement Entropy: An Overview*, *J. Phys.* **A42** (2009) 504008, [`0905.0932`].

[52] S. A. Hartnoll, *Lectures on holographic methods for condensed matter physics*, *Class. Quant. Grav.* **26** (2009) 224002, [`0903.3246`].

[53] S. Kachru, X. Liu and M. Mulligan, *Gravity duals of Lifshitz-like fixed points*, *Phys. Rev.* **D78** (2008) 106005, [`0808.1725`].

[54] M. Taylor, *Lifshitz holography*, *Class. Quant. Grav.* **33** (2016) 033001, [`1512.03554`].

[55] M. H. Christensen, J. Hartong, N. A. Obers and B. Rollier, *Torsional Newton-Cartan Geometry and Lifshitz Holography*, *Phys. Rev.* **D89** (2014) 061901, [`1311.4794`].

[56] M. H. Christensen, J. Hartong, N. A. Obers and B. Rollier, *Boundary Stress-Energy Tensor and Newton-Cartan Geometry in Lifshitz Holography*, *JHEP* **01** (2014) 057, [`1311.6471`].

[57] M. Rangamani, *Gravity and Hydrodynamics: Lectures on the fluid-gravity correspondence*, *Class. Quant. Grav.* **26** (2009) 224003, [`0905.4352`].

[58] V. E. Hubeny, M. Rangamani and T. Takayanagi, *A Covariant holographic entanglement entropy proposal*, *JHEP* **07** (2007) 062, [`0705.0016`].

[59] M. Banados, C. Teitelboim and J. Zanelli, *The Black hole in three-dimensional space-time*, *Phys. Rev. Lett.* **69** (1992) 1849–1851, [`hep-th/9204099`].

[60] M. Banados, M. Henneaux, C. Teitelboim and J. Zanelli, *Geometry of the (2+1) black hole*, *Phys. Rev.* **D48** (1993) 1506–1525, [`gr-qc/9302012`].

[61] P. Kraus, *Lectures on black holes and the AdS(3) / CFT(2) correspondence*, *Lect. Notes Phys.* **755** (2008) 193–247, [`hep-th/0609074`].

[62] K. Skenderis, *Lecture notes on holographic renormalization*, *Class. Quant. Grav.* **19** (2002) 5849–5876, [`hep-th/0209067`].

[63] A. Fiorucci and G. Compère, *Advanced Lectures in General Relativity*. PhD thesis, Brussels U., PTM, 2018. `1801.07064`.

[64] A. Achucarro and P. K. Townsend, *A Chern-Simons Action for Three-Dimensional anti-De Sitter Supergravity Theories*, Phys. Lett. **B180** (1986) 89.

[65] E. Witten, *(2+1)-Dimensional Gravity as an Exactly Soluble System*, Nucl. Phys. **B311** (1988) 46.

[66] S.-S. Chern and J. Simons, *Characteristic forms and geometric invariants*, Annals Math. **99** (1974) 48–69.

[67] S. Deser, R. Jackiw and S. Templeton, *Topologically Massive Gauge Theories*, Annals Phys. **140** (1982) 372–411.

[68] E. Witten, *Quantum Field Theory and the Jones Polynomial*, Commun. Math. Phys. **121** (1989) 351–399.

[69] S. Deser, R. Jackiw and S. Templeton, *Three-Dimensional Massive Gauge Theories*, Phys. Rev. Lett. **48** (1982) 975–978.

[70] M. Banados, *Global charges in Chern-Simons field theory and the (2+1) black hole*, Phys. Rev. **D52** (1996) 5816–5825, [`hep-th/9405171`].

[71] S. Elitzur, G. W. Moore, A. Schwimmer and N. Seiberg, *Remarks on the Canonical Quantization of the Chern-Simons-Witten Theory*, Nucl. Phys. **B326** (1989) 108–134.

[72] H. L. Verlinde, *Conformal Field Theory, 2-D Quantum Gravity and Quantization of Teichmuller Space*, Nucl. Phys. **B337** (1990) 652–680.

[73] H. L. Verlinde and E. P. Verlinde, *CONFORMAL FIELD THEORY AND GEOMETRIC QUANTIZATION*, in *Trieste School and Workshop on Superstrings Trieste, Italy, April 3-14, 1989*, pp. 422–449, 1989.

[74] J. de Boer and J. I. Jottar, *Boundary conditions and partition functions in higher spin AdS_3/CFT_2*, JHEP **04** (2016) 107, [`1407.3844`].

[75] M. Banados and R. Caro, *Holographic ward identities: Examples from 2+1 gravity*, JHEP **12** (2004) 036, [`hep-th/0411060`].

[76] T. Regge and C. Teitelboim, *Role of Surface Integrals in the Hamiltonian Formulation of General Relativity*, Annals Phys. **88** (1974) 286.

[77] M. Banados, *Three-dimensional quantum geometry and black holes*, AIP Conf. Proc. **484** (1999) 147–169, [`hep-th/9901148`].

[78] M. Bañados and I. A. Reyes, *A short review on Noether's theorems, gauge symmetries and boundary terms*, Int. J. Mod. Phys. **D25** (2016) 1630021, [`1601.03616`].

[79] M. Blagojevic, *Gravitation and gauge symmetries*. IOP Publishing, Bristol, 2002.

[80] H. Afshar, M. Gary, D. Grumiller, R. Rashkov and M. Riegler, *Non-AdS holography in 3-dimensional higher spin gravity - General recipe and example*, *JHEP* **11** (2012) 099, [`1209.2860`].

[81] E. Witten, *Nonabelian Bosonization in Two-Dimensions*, *Commun. Math. Phys.* **92** (1984) 455–472.

[82] S. P. Novikov, *The Hamiltonian formalism and a many valued analog of Morse theory*, *Usp. Mat. Nauk* **37N5** (1982) 3–49.

[83] L. Donnay, *Asymptotic dynamics of three-dimensional gravity*, *PoS* **Modave2015** (2016) 001, [`1602.09021`].

[84] A. Campoleoni, S. Fredenhagen, S. Pfenninger and S. Theisen, *Asymptotic symmetries of three-dimensional gravity coupled to higher-spin fields*, *JHEP* **11** (2010) 007, [`1008.4744`].

[85] O. Coussaert, M. Henneaux and P. van Driel, *The Asymptotic dynamics of three-dimensional Einstein gravity with a negative cosmological constant*, *Class. Quant. Grav.* **12** (1995) 2961–2966, [`gr-qc/9506019`].

[86] V. G. Drinfeld and V. V. Sokolov, *Lie algebras and equations of Korteweg-de Vries type*, *J. Sov. Math.* **30** (1984) 1975–2036.

[87] M. Bershadsky and H. Ooguri, *Hidden SL(n) Symmetry in Conformal Field Theories*, *Commun. Math. Phys.* **126** (1989) 49.

[88] P. Bouwknegt and K. Schoutens, *W symmetry in conformal field theory*, *Phys. Rept.* **223** (1993) 183–276, [`hep-th/9210010`].

[89] L. Feher, L. O'Raifeartaigh, P. Ruelle, I. Tsutsui and A. Wipf, *On the general structure of Hamiltonian reductions of the WZNW theory*, `hep-th/9112068`.

[90] A. Campoleoni, S. Fredenhagen and S. Pfenninger, *Asymptotic W-symmetries in three-dimensional higher-spin gauge theories*, *JHEP* **09** (2011) 113, [`1107.0290`].

[91] J. de Boer and T. Tjin, *The Relation between quantum W algebras and Lie algebras*, *Commun. Math. Phys.* **160** (1994) 317–332, [`hep-th/9302006`].

[92] M. Henneaux and S.-J. Rey, *Nonlinear $W_{infinity}$ as Asymptotic Symmetry of Three-Dimensional Higher Spin Anti-de Sitter Gravity*, *JHEP* **12** (2010) 007, [`1008.4579`].

[93] A. Perez, D. Tempo and R. Troncoso, *Higher Spin Black Holes*, *Lect. Notes Phys.* **892** (2015) 265–288, [`1402.1465`].

[94] M. Ammon, M. Gutperle, P. Kraus and E. Perlmutter, *Black holes in three dimensional higher spin gravity: A review*, *J. Phys.* **A46** (2013) 214001, [`1208.5182`].

[95] P. Forgacs, A. Wipf, J. Balog, L. Feher and L. O'Raifeartaigh, *Liouville and Toda Theories as Conformally Reduced WZNW Theories*, *Phys. Lett.* **B227** (1989) 214–220.

[96] F. A. Bais, T. Tjin and P. van Driel, *Covariantly coupled chiral algebras*, *Nucl. Phys.* **B357** (1991) 632–654.

[97] J. de Boer and J. I. Jottar, *Thermodynamics of higher spin black holes in AdS_3*, *JHEP* **01** (2014) 023, [`1302.0816`].

[98] A. Castro and E. Llabrés, *Unravelling Holographic Entanglement Entropy in Higher Spin Theories*, *JHEP* **03** (2015) 124, [`1410.2870`].

[99] M. Bershadsky, *Conformal field theories via Hamiltonian reduction*, *Commun. Math. Phys.* **139** (1991) 71–82.

[100] D. E. Berenstein, J. M. Maldacena and H. S. Nastase, *Strings in flat space and pp waves from N=4 superYang-Mills*, *JHEP* **04** (2002) 013, [`hep-th/0202021`].

[101] M. Kruczenski, *Spin chains and string theory*, *Phys. Rev. Lett.* **93** (2004) 161602, [`hep-th/0311203`].

[102] T. Harmark and M. Orselli, *Spin Matrix Theory: A quantum mechanical model of the AdS/CFT correspondence*, *JHEP* **11** (2014) 134, [`1409.4417`].

[103] K. Balasubramanian and J. McGreevy, *Gravity duals for non-relativistic CFTs*, *Phys. Rev. Lett.* **101** (2008) 061601, [`0804.4053`].

[104] D. T. Son, *Toward an AdS/cold atoms correspondence: A Geometric realization of the Schrodinger symmetry*, *Phys. Rev.* **D78** (2008) 046003, [`0804.3972`].

[105] P. Horava, *Quantum Gravity at a Lifshitz Point*, *Phys. Rev.* **D79** (2009) 084008, [`0901.3775`].

[106] J. Hartong and N. A. Obers, *Hořava-Lifshitz gravity from dynamical Newton-Cartan geometry*, *JHEP* **07** (2015) 155, [`1504.07461`].

[107] J. Hartong, Y. Lei and N. A. Obers, *Nonrelativistic Chern-Simons theories and three-dimensional Hořava-Lifshitz gravity*, *Phys. Rev.* **D94** (2016) 065027, [`1604.08054`].

[108] G. Papageorgiou and B. J. Schroers, *A Chern-Simons approach to Galilean quantum gravity in 2+1 dimensions*, *JHEP* **11** (2009) 009, [`0907.2880`].

[109] E. A. Bergshoeff and J. Rosseel, *Three-Dimensional Extended Bargmann Supergravity*, *Phys. Rev. Lett.* **116** (2016) 251601, [`1604.08042`].

[110] D. M. Hofman and B. Rollier, *Warped Conformal Field Theory as Lower Spin Gravity*, *Nucl. Phys.* **B897** (2015) 1–38, [`1411.0672`].

[111] D. M. Hofman and A. Strominger, *Chiral Scale and Conformal Invariance in 2D Quantum Field Theory*, Phys. Rev. Lett. **107** (2011) 161601, [1107.2917].

[112] S. Detournay, T. Hartman and D. M. Hofman, *Warped Conformal Field Theory*, Phys. Rev. **D86** (2012) 124018, [1210.0539].

[113] S. El-Showk and M. Guica, *Kerr/CFT, dipole theories and nonrelativistic CFTs*, JHEP **12** (2012) 009, [1108.6091].

[114] W. Song and A. Strominger, *Warped AdS3/Dipole-CFT Duality*, JHEP **05** (2012) 120, [1109.0544].

[115] W. Song and J. Xu, *Correlation Functions of Warped CFT*, JHEP **04** (2018) 067, [1706.07621].

[116] K. Jensen, *Locality and anomalies in warped conformal field theory*, JHEP **12** (2017) 111, [1710.11626].

[117] J. Hartong, E. Kiritsis and N. A. Obers, *Field Theory on Newton-Cartan Backgrounds and Symmetries of the Lifshitz Vacuum*, JHEP **08** (2015) 006, [1502.00228].

[118] J. McGreevy, *Holographic duality with a view toward many-body physics*, Adv. High Energy Phys. **2010** (2010) 723105, [0909.0518].

[119] U. Gursoy, *Improved Holographic QCD and the Quark-gluon Plasma*, Acta Phys. Polon. **B47** (2016) 2509, [1612.00899].

[120] K. T. Grosvenor, J. Hartong, C. Keeler and N. A. Obers, *Homogeneous Nonrelativistic Geometries as Coset Spaces*, 1712.03980.

[121] K. Jensen and A. Karch, *Revisiting non-relativistic limits*, JHEP **04** (2015) 155, [1412.2738].

[122] E. Bergshoeff, J. Rosseel and T. Zojer, *Newton–Cartan (super)gravity as a non-relativistic limit*, Class. Quant. Grav. **32** (2015) 205003, [1505.02095].

[123] G. Papageorgiou and B. J. Schroers, *Galilean quantum gravity with cosmological constant and the extended q-Heisenberg algebra*, JHEP **11** (2010) 020, [1008.0279].

[124] R. Andringa, E. Bergshoeff, S. Panda and M. de Roo, *Newtonian Gravity and the Bargmann Algebra*, Class. Quant. Grav. **28** (2011) 105011, [1011.1145].

[125] E. A. Bergshoeff, J. Hartong and J. Rosseel, *Torsional Newton–Cartan geometry and the Schrödinger algebra*, Class. Quant. Grav. **32** (2015) 135017, [1409.5555].

[126] D. T. Son, *Newton-Cartan Geometry and the Quantum Hall Effect*, `1306.0638`.

[127] K. Jensen, *On the coupling of Galilean-invariant field theories to curved spacetime*, `1408.6855`.

[128] J. Hartong, E. Kiritsis and N. A. Obers, *Schrödinger Invariance from Lifshitz Isometries in Holography and Field Theory*, *Phys. Rev.* **D92** (2015) 066003, [`1409.1522`].

[129] J. Hartong, E. Kiritsis and N. A. Obers, *Lifshitz space–times for Schrödinger holography*, *Phys. Lett.* **B746** (2015) 318–324, [`1409.1519`].

[130] T. Griffin, P. Hořava and C. M. Melby-Thompson, *Lifshitz Gravity for Lifshitz Holography*, *Phys. Rev. Lett.* **110** (2013) 081602, [`1211.4872`].

[131] J. Polchinski, *Scale and Conformal Invariance in Quantum Field Theory*, *Nucl. Phys.* **B303** (1988) 226–236.

[132] M. Guica, *An integrable Lorentz-breaking deformation of two-dimensional CFTs*, `1710.08415`.

[133] C. R. Nappi and E. Witten, *A WZW model based on a nonsemisimple group*, *Phys. Rev. Lett.* **71** (1993) 3751–3753, [`hep-th/9310112`].

[134] A. Bagchi and R. Gopakumar, *Galilean Conformal Algebras and AdS/CFT*, *JHEP* **07** (2009) 037, [`0902.1385`].

[135] A. Bagchi, *Correspondence between Asymptotically Flat Spacetimes and Nonrelativisitc Conformal Field Theories*, *Phys. Rev. Lett.* **105** (2010) 171601, [`1006.3354`].

[136] M. Gary, D. Grumiller, M. Riegler and J. Rosseel, *Flat space (higher spin) gravity with chemical potentials*, *JHEP* **01** (2015) 152, [`1411.3728`].

[137] R. Basu, S. Detournay and M. Riegler, *Spectral Flow in 3D Flat Spacetimes*, *JHEP* **12** (2017) 134, [`1706.07438`].

[138] J. Figueroa-O'Farrill, *Classification of kinematical Lie algebras*, `1711.05676`.

[139] J. M. Figueroa-O'Farrill, *Kinematical Lie algebras via deformation theory*, `1711.06111`.

[140] J. M. Figueroa-O'Farrill, *Higher-dimensional kinematical Lie algebras via deformation theory*, `1711.07363`.

[141] H. Afshar, S. Detournay, D. Grumiller and B. Oblak, *Near-Horizon Geometry and Warped Conformal Symmetry*, *JHEP* **03** (2016) 187, [`1512.08233`].

[142] A. Giveon, D. Kutasov and N. Seiberg, *Comments on string theory on AdS(3)*, *Adv. Theor. Math. Phys.* **2** (1998) 733–782, [`hep-th/9806194`].

[143] E. Kiritsis and C. Kounnas, *String propagation in gravitational wave backgrounds*, *Phys. Lett.* **B320** (1994) 264–272, [`hep-th/9310202`].

[144] C. Duval, G. Burdet, H. P. Kunzle and M. Perrin, *Bargmann Structures and Newton-cartan Theory*, *Phys. Rev.* **D31** (1985) 1841–1853.

[145] C. Duval, G. W. Gibbons and P. Horvathy, *Celestial mechanics, conformal structures and gravitational waves*, *Phys. Rev.* **D43** (1991) 3907–3922, [`hep-th/0512188`].

[146] B. Julia and H. Nicolai, *Null Killing vector dimensional reduction and Galilean geometrodynamics*, *Nucl. Phys.* **B439** (1995) 291–326, [`hep-th/9412002`].

[147] A. Giveon and M. Rocek, *Supersymmetric string vacua on AdS(3) x N*, *JHEP* **04** (1999) 019, [`hep-th/9904024`].

[148] T. Harmark, J. Hartong and N. A. Obers, *Nonrelativistic strings and limits of the AdS/CFT correspondence*, *Phys. Rev.* **D96** (2017) 086019, [`1705.03535`].

[149] J. Gomis, J. Gomis and K. Kamimura, *Non-relativistic superstrings: A New soluble sector of AdS(5) x S**5*, *JHEP* **12** (2005) 024, [`hep-th/0507036`].

[150] J. R. David, *Anti-de Sitter gravity associated with the supergroup SU(1,1|2) x SU(1,1|2)*, *Mod. Phys. Lett.* **A14** (1999) 1143–1148, [`hep-th/9904068`].

[151] J. M. Izquierdo and P. K. Townsend, *Supersymmetric space-times in (2+1) adS supergravity models*, *Class. Quant. Grav.* **12** (1995) 895–924, [`gr-qc/9501018`].

[152] J. M. Maldacena and L. Maoz, *Desingularization by rotation*, *JHEP* **12** (2002) 055, [`hep-th/0012025`].

[153] V. Balasubramanian, J. de Boer, E. Keski-Vakkuri and S. F. Ross, *Supersymmetric conical defects: Towards a string theoretic description of black hole formation*, *Phys. Rev.* **D64** (2001) 064011, [`hep-th/0011217`].

[154] O. Lunin, J. M. Maldacena and L. Maoz, *Gravity solutions for the D1-D5 system with angular momentum*, `hep-th/0212210`.

[155] O. Lunin and S. D. Mathur, *AdS / CFT duality and the black hole information paradox*, *Nucl. Phys.* **B623** (2002) 342–394, [`hep-th/0109154`].

[156] O. Lunin, S. D. Mathur and A. Saxena, *What is the gravity dual of a chiral primary?*, *Nucl. Phys.* **B655** (2003) 185–217, [`hep-th/0211292`].

[157] I. Kanitscheider, K. Skenderis and M. Taylor, *Holographic anatomy of fuzzballs*, *JHEP* **04** (2007) 023, [hep-th/0611171].

[158] K. Skenderis and M. Taylor, *Fuzzball solutions and D1-D5 microstates*, *Phys. Rev. Lett.* **98** (2007) 071601, [hep-th/0609154].

[159] I. Kanitscheider, K. Skenderis and M. Taylor, *Fuzzballs with internal excitations*, *JHEP* **06** (2007) 056, [0704.0690].

[160] M. Ammon, A. Castro and N. Iqbal, *Wilson Lines and Entanglement Entropy in Higher Spin Gravity*, *JHEP* **10** (2013) 110, [1306.4338].

[161] J. de Boer and J. I. Jottar, *Entanglement Entropy and Higher Spin Holography in AdS$_3$*, *JHEP* **04** (2014) 089, [1306.4347].

[162] M. Baggio, O. Ohlsson Sax, A. Sfondrini, B. Stefański and A. Torrielli, *Protected string spectrum in AdS$_3$/CFT$_2$ from worldsheet integrability*, *JHEP* **04** (2017) 091, [1701.03501].

[163] M. R. Gaberdiel and R. Gopakumar, *An AdS$_3$ Dual for Minimal Model CFTs*, *Phys. Rev.* **D83** (2011) 066007, [1011.2986].

[164] M. Gary, D. Grumiller and R. Rashkov, *Towards non-AdS holography in 3-dimensional higher spin gravity*, *JHEP* **03** (2012) 022, [1201.0013].

[165] D. Anninos, W. Li, M. Padi, W. Song and A. Strominger, *Warped AdS(3) Black Holes*, *JHEP* **03** (2009) 130, [0807.3040].

[166] D. Grumiller and N. Johansson, *Consistent boundary conditions for cosmological topologically massive gravity at the chiral point*, *Int. J. Mod. Phys.* **D17** (2009) 2367–2372, [0808.2575].

[167] D. Grumiller, R. Jackiw and N. Johansson, *Canonical analysis of cosmological topologically massive gravity at the chiral point*, 0806.4185.

[168] W. Li, W. Song and A. Strominger, *Chiral Gravity in Three Dimensions*, *JHEP* **04** (2008) 082, [0801.4566].

[169] B. Chen and J. Long, *High Spin Topologically Massive Gravity*, *JHEP* **12** (2011) 114, [1110.5113].

[170] B. Chen, J. Long and J.-B. Wu, *Spin-3 topologically massive gravity*, *Phys. Lett.* **B705** (2011) 513–520, [1106.5141].

[171] E. Bergshoeff, D. Grumiller, S. Prohazka and J. Rosseel, *Three-dimensional Spin-3 Theories Based on General Kinematical Algebras*, *JHEP* **01** (2017) 114, [1612.02277].

[172] N. Wyllard, *A(N-1) conformal Toda field theory correlation functions from conformal N = 2 SU(N) quiver gauge theories*, *JHEP* **11** (2009) 002, [0907.2189].

[173] V. Pestun, *Localization of gauge theory on a four-sphere and supersymmetric Wilson loops*, *Commun. Math. Phys.* **313** (2012) 71–129, [0712.2824].

[174] D. Gaiotto, *N=2 dualities*, *JHEP* **08** (2012) 034, [0904.2715].

[175] N. A. Nekrasov, *Seiberg-Witten prepotential from instanton counting*, *Adv. Theor. Math. Phys.* **7** (2003) 831–864, [hep-th/0206161].

[176] N. Seiberg and E. Witten, *Electric - magnetic duality, monopole condensation, and confinement in N=2 supersymmetric Yang-Mills theory*, *Nucl. Phys.* **B426** (1994) 19–52, [hep-th/9407087].

[177] N. Seiberg and E. Witten, *Monopoles, duality and chiral symmetry breaking in N=2 supersymmetric QCD*, *Nucl. Phys.* **B431** (1994) 484–550, [hep-th/9408099].

[178] E. Witten, *Solutions of four-dimensional field theories via M theory*, *Nucl. Phys.* **B500** (1997) 3–42, [hep-th/9703166].

[179] J. Teschner, *On the Liouville three point function*, *Phys. Lett.* **B363** (1995) 65–70, [hep-th/9507109].

[180] V. Mitev and E. Pomoni, *Toda 3-Point Functions From Topological Strings*, *JHEP* **06** (2015) 049, [1409.6313].

[181] M. Isachenkov, V. Mitev and E. Pomoni, *Toda 3-Point Functions From Topological Strings II*, *JHEP* **08** (2016) 066, [1412.3395].

[182] L. F. Alday, F. Benini and Y. Tachikawa, *Liouville/Toda central charges from M5-branes*, *Phys. Rev. Lett.* **105** (2010) 141601, [0909.4776].

[183] N. Nekrasov and E. Witten, *The Omega Deformation, Branes, Integrability, and Liouville Theory*, *JHEP* **09** (2010) 092, [1002.0888].

[184] A. Mironov, A. Morozov and S. Shakirov, *A direct proof of AGT conjecture at beta = 1*, *JHEP* **02** (2011) 067, [1012.3137].

[185] R. Dijkgraaf and C. Vafa, *Toda Theories, Matrix Models, Topological Strings, and N=2 Gauge Systems*, 0909.2453.

[186] M. Aganagic, N. Haouzi and S. Shakirov, A_n-*Triality*, 1403.3657.

[187] J. Yagi, *Compactification on the Ω-background and the AGT correspondence*, *JHEP* **09** (2012) 101, [1205.6820].

[188] M.-C. Tan, *M-Theoretic Derivations of 4d-2d Dualities: From a Geometric Langlands Duality for Surfaces, to the AGT Correspondence, to Integrable Systems*, *JHEP* **07** (2013) 171, [1301.1977].

[189] J. Teschner and G. S. Vartanov, *Supersymmetric gauge theories, quantization of $\mathcal{M}_{\mathrm{flat}}$, and conformal field theory*, Adv. Theor. Math. Phys. **19** (2015) 1–135, [`1302.3778`].

[190] C. Beem, L. Rastelli and B. C. van Rees, *$\mathcal{W}$ symmetry in six dimensions*, JHEP **05** (2015) 017, [`1404.1079`].

[191] C. Cordova and D. L. Jafferis, *Toda Theory From Six Dimensions*, JHEP **12** (2017) 106, [`1605.03997`].

[192] N. Seiberg, *Five-dimensional SUSY field theories, nontrivial fixed points and string dynamics*, Phys. Lett. **B388** (1996) 753–760, [`hep-th/9608111`].

[193] N. Seiberg, *Notes on theories with 16 supercharges*, Nucl. Phys. Proc. Suppl. **67** (1998) 158–171, [`hep-th/9705117`].

[194] M. R. Douglas, *On D=5 super Yang-Mills theory and (2,0) theory*, JHEP **02** (2011) 011, [`1012.2880`].

[195] D. Gaiotto and E. Witten, *Supersymmetric Boundary Conditions in N=4 Super Yang-Mills Theory*, J. Statist. Phys. **135** (2009) 789–855, [`0804.2902`].

[196] L. F. Alday and Y. Tachikawa, *Affine SL(2) conformal blocks from 4d gauge theories*, Lett. Math. Phys. **94** (2010) 87–114, [`1005.4469`].

[197] C. Kozcaz, S. Pasquetti, F. Passerini and N. Wyllard, *Affine sl(N) conformal blocks from N=2 SU(N) gauge theories*, JHEP **01** (2011) 045, [`1008.1412`].

[198] N. Wyllard, *W-algebras and surface operators in N=2 gauge theories*, J. Phys. **A44** (2011) 155401, [`1011.0289`].

[199] N. Wyllard, *Instanton partition functions in N=2 SU(N) gauge theories with a general surface operator, and their W-algebra duals*, JHEP **02** (2011) 114, [`1012.1355`].

[200] Y. Tachikawa, *On W-algebras and the symmetries of defects of 6d N=(2,0) theory*, JHEP **03** (2011) 043, [`1102.0076`].

[201] H. Kanno and Y. Tachikawa, *Instanton counting with a surface operator and the chain-saw quiver*, JHEP **06** (2011) 119, [`1105.0357`].

[202] S. Nawata, *Givental J-functions, Quantum integrable systems, AGT relation with surface operator*, Adv. Theor. Math. Phys. **19** (2015) 1277–1338, [`1408.4132`].

[203] C. Cordova and D. L. Jafferis, *Complex Chern-Simons from M5-branes on the Squashed Three-Sphere*, JHEP **11** (2017) 119, [`1305.2891`].

[204] N. Hama and K. Hosomichi, *Seiberg-Witten Theories on Ellipsoids*, *JHEP* **09** (2012) 033, [1206.6359].

[205] Y. Imamura and D. Yokoyama, *N=2 supersymmetric theories on squashed three-sphere*, *Phys. Rev.* **D85** (2012) 025015, [1109.4734].

[206] C. Closset, T. T. Dumitrescu, G. Festuccia and Z. Komargodski, *The Geometry of Supersymmetric Partition Functions*, *JHEP* **01** (2014) 124, [1309.5876].

[207] D. Gaiotto and J. Maldacena, *The Gravity duals of N=2 superconformal field theories*, *JHEP* **10** (2012) 189, [0904.4466].

[208] S. Gukov and D. Pei, *Equivariant Verlinde formula from fivebranes and vortices*, *Commun. Math. Phys.* **355** (2017) 1–50, [1501.01310].

[209] S. Gukov, D. Pei, W. Yan and K. Ye, *Equivariant Verlinde Algebra from Superconformal Index and Argyres–Seiberg Duality*, *Commun. Math. Phys.* **357** (2018) 1215–1251, [1605.06528].

[210] T. Dimofte, *Complex Chern–Simons Theory at Level k via the 3d–3d Correspondence*, *Commun. Math. Phys.* **339** (2015) 619–662, [1409.0857].

[211] C. Cordova and D. L. Jafferis, *Five-Dimensional Maximally Supersymmetric Yang-Mills in Supergravity Backgrounds*, *JHEP* **10** (2017) 003, [1305.2886].

[212] T. Dimofte, S. Gukov and L. Hollands, *Vortex Counting and Lagrangian 3-manifolds*, *Lett. Math. Phys.* **98** (2011) 225–287, [1006.0977].

[213] T. Dimofte, D. Gaiotto and S. Gukov, *Gauge Theories Labelled by Three-Manifolds*, *Commun. Math. Phys.* **325** (2014) 367–419, [1108.4389].

[214] T. Dimofte, D. Gaiotto and S. Gukov, *3-Manifolds and 3d Indices*, *Adv. Theor. Math. Phys.* **17** (2013) 975–1076, [1112.5179].

[215] R. Dijkgraaf, L. Hollands, P. Sulkowski and C. Vafa, *Supersymmetric gauge theories, intersecting branes and free fermions*, *JHEP* **02** (2008) 106, [0709.4446].

[216] N. Itzhaki, D. Kutasov and N. Seiberg, *I-brane dynamics*, *JHEP* **01** (2006) 119, [hep-th/0508025].

[217] A. LeClair, D. Nemeschansky and N. P. Warner, *S matrices for perturbed N=2 superconformal field theory from quantum groups*, *Nucl. Phys.* **B390** (1993) 653–680, [hep-th/9206041].

[218] M. Bullimore and H.-C. Kim, *The Superconformal Index of the (2,0) Theory with Defects*, *JHEP* **05** (2015) 048, [1412.3872].

[219] T. Nishioka and Y. Tachikawa, *Central charges of para-Liouville and Toda theories from M-5-branes*, *Phys. Rev.* **D84** (2011) 046009, [`1106.1172`].

[220] N. Wyllard, *Coset conformal blocks and N=2 gauge theories*, `1109.4264`.

[221] A. M. Uranga, *Brane configurations for branes at conifolds*, *JHEP* **01** (1999) 022, [`hep-th/9811004`].

[222] K. Dasgupta and S. Mukhi, *Brane constructions, conifolds and M theory*, *Nucl. Phys.* **B551** (1999) 204–228, [`hep-th/9811139`].

[223] J. McOrist and A. B. Royston, *Relating Conifold Geometries to NS5-branes*, *Nucl. Phys.* **B849** (2011) 573–609, [`1101.3552`].

[224] P. Candelas and X. C. de la Ossa, *Comments on Conifolds*, *Nucl. Phys.* **B342** (1990) 246–268.

[225] P. Ouyang, *Holomorphic D7 branes and flavored N=1 gauge theories*, *Nucl. Phys.* **B699** (2004) 207–225, [`hep-th/0311084`].

[226] J. M. Maldacena, A. Strominger and E. Witten, *Black hole entropy in M theory*, *JHEP* **12** (1997) 002, [`hep-th/9711053`].

[227] R. Minasian, G. W. Moore and D. Tsimpis, *Calabi-Yau black holes and (0,4) sigma models*, *Commun. Math. Phys.* **209** (2000) 325–352, [`hep-th/9904217`].

[228] V. Pestun, *Localization for $\mathcal{N} = 2$ Supersymmetric Gauge Theories in Four Dimensions*, in *New Dualities of Supersymmetric Gauge Theories* (J. Teschner, ed.), pp. 159–194. Springer, 2016. `1412.7134`. DOI.

[229] M. Bershadsky, C. Vafa and V. Sadov, *D-branes and topological field theories*, *Nucl. Phys.* **B463** (1996) 420–434, [`hep-th/9511222`].

[230] A. Gadde, S. Gukov and P. Putrov, *Fivebranes and 4-manifolds*, `1306.4320`.

[231] D. N. Page, *Average entropy of a subsystem*, *Phys. Rev. Lett.* **71** (1993) 1291–1294, [`gr-qc/9305007`].

[232] J. J. Bisognano and E. H. Wichmann, *On the Duality Condition for a Hermitian Scalar Field*, *J. Math. Phys.* **16** (1975) 985–1007.

[233] W. G. Unruh, *Notes on black hole evaporation*, *Phys. Rev.* **D14** (1976) 870.

[234] P. D. Hislop and R. Longo, *Modular Structure of the Local Algebras Associated With the Free Massless Scalar Field Theory*, *Commun. Math. Phys.* **84** (1982) 71.

[235] H. Casini, M. Huerta and R. C. Myers, *Towards a derivation of holographic entanglement entropy*, *JHEP* **05** (2011) 036, [`1102.0440`].

[236] J. Cardy and E. Tonni, *Entanglement hamiltonians in two-dimensional conformal field theory*, *J. Stat. Mech.* **1612** (2016) 123103, [`1608.01283`].

[237] P. Calabrese and J. L. Cardy, *Evolution of entanglement entropy in one-dimensional systems*, *J. Stat. Mech.* **0504** (2005) P04010, [`cond-mat/0503393`].

[238] U. H. Danielsson, E. Keski-Vakkuri and M. Kruczenski, *Spherically collapsing matter in AdS, holography, and shellons*, *Nucl. Phys.* **B563** (1999) 279–292, [`hep-th/9905227`].

[239] U. H. Danielsson, E. Keski-Vakkuri and M. Kruczenski, *Black hole formation in AdS and thermalization on the boundary*, *JHEP* **02** (2000) 039, [`hep-th/9912209`].

[240] S. B. Giddings and A. Nudelman, *Gravitational collapse and its boundary description in AdS*, *JHEP* **02** (2002) 003, [`hep-th/0112099`].

[241] J. Abajo-Arrastia, J. Aparicio and E. Lopez, *Holographic Evolution of Entanglement Entropy*, *JHEP* **11** (2010) 149, [`1006.4090`].

[242] T. Albash and C. V. Johnson, *Evolution of Holographic Entanglement Entropy after Thermal and Electromagnetic Quenches*, *New J. Phys.* **13** (2011) 045017, [`1008.3027`].

[243] T. Hartman and J. Maldacena, *Time Evolution of Entanglement Entropy from Black Hole Interiors*, *JHEP* **05** (2013) 014, [`1303.1080`].

[244] H. Liu and S. J. Suh, *Entanglement Tsunami: Universal Scaling in Holographic Thermalization*, *Phys. Rev. Lett.* **112** (2014) 011601, [`1305.7244`].

[245] H. Liu and S. J. Suh, *Entanglement growth during thermalization in holographic systems*, *Phys. Rev.* **D89** (2014) 066012, [`1311.1200`].

[246] V. Balasubramanian, A. Bernamonti, J. de Boer, N. Copland, B. Craps, E. Keski-Vakkuri et al., *Thermalization of Strongly Coupled Field Theories*, *Phys. Rev. Lett.* **106** (2011) 191601, [`1012.4753`].

[247] V. Balasubramanian, A. Bernamonti, J. de Boer, N. Copland, B. Craps, E. Keski-Vakkuri et al., *Holographic Thermalization*, *Phys. Rev.* **D84** (2011) 026010, [`1103.2683`].

[248] V. Keranen, E. Keski-Vakkuri and L. Thorlacius, *Thermalization and entanglement following a non-relativistic holographic quench*, *Phys. Rev.* **D85** (2012) 026005, [`1110.5035`].

[249] E. Caceres and A. Kundu, *Holographic Thermalization with Chemical Potential*, *JHEP* **09** (2012) 055, [`1205.2354`].

[250] R. Callan, J.-Y. He and M. Headrick, *Strong subadditivity and the covariant holographic entanglement entropy formula*, *JHEP* **06** (2012) 081, [1204.2309].

[251] E. Caceres, A. Kundu, J. F. Pedraza and W. Tangarife, *Strong Subadditivity, Null Energy Condition and Charged Black Holes*, *JHEP* **01** (2014) 084, [1304.3398].

[252] Y.-Z. Li, S.-F. Wu, Y.-Q. Wang and G.-H. Yang, *Linear growth of entanglement entropy in holographic thermalization captured by horizon interiors and mutual information*, *JHEP* **09** (2013) 057, [1306.0210].

[253] Y.-Z. Li, S.-F. Wu and G.-H. Yang, *Gauss-Bonnet correction to Holographic thermalization: two-point functions, circular Wilson loops and entanglement entropy*, *Phys. Rev.* **D88** (2013) 086006, [1309.3764].

[254] W. Fischler, S. Kundu and J. F. Pedraza, *Entanglement and out-of-equilibrium dynamics in holographic models of de Sitter QFTs*, *JHEP* **07** (2014) 021, [1311.5519].

[255] V. E. Hubeny and H. Maxfield, *Holographic probes of collapsing black holes*, *JHEP* **03** (2014) 097, [1312.6887].

[256] M. Alishahiha, A. Faraji Astaneh and M. R. Mohammadi Mozaffar, *Thermalization in backgrounds with hyperscaling violating factor*, *Phys. Rev.* **D90** (2014) 046004, [1401.2807].

[257] P. Fonda, L. Franti, V. Keränen, E. Keski-Vakkuri, L. Thorlacius and E. Tonni, *Holographic thermalization with Lifshitz scaling and hyperscaling violation*, *JHEP* **08** (2014) 051, [1401.6088].

[258] V. Keranen, H. Nishimura, S. Stricker, O. Taanila and A. Vuorinen, *Dynamics of gravitational collapse and holographic entropy production*, *Phys. Rev.* **D90** (2014) 064033, [1405.7015].

[259] A. Buchel, R. C. Myers and A. van Niekerk, *Nonlocal probes of thermalization in holographic quenches with spectral methods*, *JHEP* **02** (2015) 017, [1410.6201].

[260] E. Caceres, A. Kundu, J. F. Pedraza and D.-L. Yang, *Weak Field Collapse in AdS: Introducing a Charge Density*, *JHEP* **06** (2015) 111, [1411.1744].

[261] S.-J. Zhang, B. Wang, E. Abdalla and E. Papantonopoulos, *Holographic thermalization in Gauss-Bonnet gravity with de Sitter boundary*, *Phys. Rev.* **D91** (2015) 106010, [1412.7073].

[262] V. Keranen, H. Nishimura, S. Stricker, O. Taanila and A. Vuorinen, *Gravitational collapse of thin shells: Time evolution of the holographic entanglement entropy*, *JHEP* **06** (2015) 126, [1502.01277].

[263] S.-J. Zhang and E. Abdalla, *Holographic Thermalization in Charged Dilaton Anti-de Sitter Spacetime*, *Nucl. Phys.* **B896** (2015) 569–586, [1503.07700].

[264] E. Caceres, M. Sanchez and J. Virrueta, *Holographic Entanglement Entropy in Time Dependent Gauss-Bonnet Gravity*, *JHEP* **09** (2017) 127, [1512.05666].

[265] G. Camilo, B. Cuadros-Melgar and E. Abdalla, *Holographic quenches towards a Lifshitz point*, *JHEP* **02** (2016) 014, [1511.08843].

[266] D. Roychowdhury, *Holographic thermalization from nonrelativistic branes*, *Phys. Rev.* **D93** (2016) 106008, [1601.00136].

[267] I. Ya. Aref'eva, A. A. Golubtsova and E. Gourgoulhon, *Analytic black branes in Lifshitz-like backgrounds and thermalization*, *JHEP* **09** (2016) 142, [1601.06046].

[268] M. Mezei and D. Stanford, *On entanglement spreading in chaotic systems*, *JHEP* **05** (2017) 065, [1608.05101].

[269] M. Mezei, *On entanglement spreading from holography*, *JHEP* **05** (2017) 064, [1612.00082].

[270] D. S. Ageev and I. Ya. Aref'eva, *Holographic Non-equilibrium Heating*, *JHEP* **03** (2018) 103, [1704.07747].

[271] H. Xu, *Entanglement growth during Van der Waals like phase transition*, *Phys. Lett.* **B772** (2017) 517–522, [1705.02604].

[272] M. Nozaki, T. Numasawa and T. Takayanagi, *Holographic Local Quenches and Entanglement Density*, *JHEP* **05** (2013) 080, [1302.5703].

[273] T. Ugajin, *Two dimensional quantum quenches and holography*, 1311.2562.

[274] J. F. Pedraza, *Evolution of nonlocal observables in an expanding boost-invariant plasma*, *Phys. Rev.* **D90** (2014) 046010, [1405.1724].

[275] A. F. Astaneh and A. E. Mosaffa, *Quantum Local Quench, AdS/BCFT and Yo-Yo String*, *JHEP* **05** (2015) 107, [1405.5469].

[276] M. Rangamani, M. Rozali and A. Vincart-Emard, *Dynamics of Holographic Entanglement Entropy Following a Local Quench*, *JHEP* **04** (2016) 069, [1512.03478].

[277] J. R. David, S. Khetrapal and S. P. Kumar, *Universal corrections to entanglement entropy of local quantum quenches*, *JHEP* **08** (2016) 127, [1605.05987].

[278] C. Ecker, D. Grumiller, P. Stanzer, S. A. Stricker and W. van der Schee, *Exploring nonlocal observables in shock wave collisions*, *JHEP* **11** (2016) 054, [1609.03676].

[279] M. Rozali and A. Vincart-Emard, *Comments on Entanglement Propagation*, *JHEP* **06** (2017) 044, [1702.05869].

[280] J. Erdmenger, D. Fernandez, M. Flory, E. Megias, A.-K. Straub and P. Witkowski, *Time evolution of entanglement for holographic steady state formation*, *JHEP* **10** (2017) 034, [1705.04696].

[281] A. Jahn and T. Takayanagi, *Holographic entanglement entropy of local quenches in AdS4/CFT3: a finite-element approach*, *J. Phys.* **A51** (2018) 015401, [1705.04705].

[282] M. Fagotti and P. Calabrese, *Evolution of entanglement entropy following a quantum quench: Analytic results for the XY chain in a transverse magnetic field*, *Phys. Rev.* **A78** (2008) , [0804.3559].

[283] V. Alba and P. Calabrese, *Entanglement and thermodynamics after a quantum quench in integrable systems*, 1608.00614.

[284] H. Casini, H. Liu and M. Mezei, *Spread of entanglement and causality*, *JHEP* **07** (2016) 077, [1509.05044].

[285] C. T. Asplund and A. Bernamonti, *Mutual information after a local quench in conformal field theory*, *Phys. Rev.* **D89** (2014) 066015, [1311.4173].

[286] S. Leichenauer and M. Moosa, *Entanglement Tsunami in (1+1)-Dimensions*, *Phys. Rev.* **D92** (2015) 126004, [1505.04225].

[287] C. T. Asplund, A. Bernamonti, F. Galli and T. Hartman, *Entanglement Scrambling in 2d Conformal Field Theory*, *JHEP* **09** (2015) 110, [1506.03772].

[288] S. Kundu and J. F. Pedraza, *Spread of entanglement for small subsystems in holographic CFTs*, *Phys. Rev.* **D95** (2017) 086008, [1602.05934].

[289] A. O'Bannon, J. Probst, R. Rodgers and C. F. Uhlemann, *First law of entanglement rates from holography*, *Phys. Rev.* **D96** (2017) 066028, [1612.07769].

[290] M. Taylor and W. Woodhead, *Renormalized entanglement entropy*, *JHEP* **08** (2016) 165, [1604.06808].

[291] J. Bhattacharya, M. Nozaki, T. Takayanagi and T. Ugajin, *Thermodynamical Property of Entanglement Entropy for Excited States*, *Phys. Rev. Lett.* **110** (2013) 091602, [1212.1164].

[292] D. Allahbakhshi, M. Alishahiha and A. Naseh, *Entanglement Thermodynamics*, *JHEP* **08** (2013) 102, [1305.2728].

[293] G. Wong, I. Klich, L. A. Pando Zayas and D. Vaman, *Entanglement Temperature and Entanglement Entropy of Excited States*, *JHEP* **12** (2013) 020, [1305.3291].

[294] W.-z. Guo, S. He and J. Tao, *Note on Entanglement Temperature for Low Thermal Excited States in Higher Derivative Gravity*, *JHEP* **08** (2013) 050, [1305.2682].

[295] L. Susskind and E. Witten, *The Holographic bound in anti-de Sitter space*, hep-th/9805114.

[296] A. W. Peet and J. Polchinski, *UV / IR relations in AdS dynamics*, *Phys. Rev.* **D59** (1999) 065011, [hep-th/9809022].

[297] C. A. Agón, A. Guijosa and J. F. Pedraza, *Radiation and a dynamical UV/IR connection in AdS/CFT*, *JHEP* **06** (2014) 043, [1402.5961].

[298] V. E. Hubeny, *Extremal surfaces as bulk probes in AdS/CFT*, *JHEP* **07** (2012) 093, [1203.1044].

[299] D. D. Blanco, H. Casini, L.-Y. Hung and R. C. Myers, *Relative Entropy and Holography*, *JHEP* **08** (2013) 060, [1305.3182].

[300] T. Nishioka, *Relevant Perturbation of Entanglement Entropy and Stationarity*, *Phys. Rev.* **D90** (2014) 045006, [1405.3650].

[301] I. R. Klebanov and E. Witten, *AdS / CFT correspondence and symmetry breaking*, *Nucl. Phys.* **B556** (1999) 89–114, [hep-th/9905104].

[302] D. Garfinkle, L. A. Pando Zayas and D. Reichmann, *On Field Theory Thermalization from Gravitational Collapse*, *JHEP* **02** (2012) 119, [1110.5823].

[303] D. Garfinkle and L. A. Pando Zayas, *Rapid Thermalization in Field Theory from Gravitational Collapse*, *Phys. Rev.* **D84** (2011) 066006, [1106.2339].

[304] S. Bhattacharyya and S. Minwalla, *Weak Field Black Hole Formation in Asymptotically AdS Spacetimes*, *JHEP* **09** (2009) 034, [0904.0464].

[305] G. T. Horowitz, N. Iqbal and J. E. Santos, *Simple holographic model of nonlinear conductivity*, *Phys. Rev.* **D88** (2013) 126002, [1309.5088].

[306] L. K. Joshi, A. Mukhopadhyay, F. Preis and P. Ramadevi, *Exact time dependence of causal correlations and nonequilibrium density matrices in holographic systems*, *Phys. Rev.* **D96** (2017) 106006, [1704.02936].

[307] A. C. Wall, *Maximin Surfaces, and the Strong Subadditivity of the Covariant Holographic Entanglement Entropy*, *Class. Quant. Grav.* **31** (2014) 225007, [1211.3494].

[308] R. Auzzi, S. Elitzur, S. B. Gudnason and E. Rabinovici, *On periodically driven AdS/CFT*, *JHEP* **11** (2013) 016, [1308.2132].

[309] M. Rangamani, M. Rozali and A. Wong, *Driven Holographic CFTs*, *JHEP* **04** (2015) 093, [1502.05726].

[310] P. Sabella-Garnier, *Time dependence of entanglement entropy on the fuzzy sphere*, *JHEP* **08** (2017) 121, [`1705.01969`].

[311] S. Leichenauer, M. Moosa and M. Smolkin, *Dynamics of the Area Law of Entanglement Entropy*, *JHEP* **09** (2016) 035, [`1604.00388`].

[312] T. Anous, T. Hartman, A. Rovai and J. Sonner, *Black Hole Collapse in the 1/c Expansion*, *JHEP* **07** (2016) 123, [`1603.04856`].

[313] M. J. S. Beach, J. Lee, C. Rabideau and M. Van Raamsdonk, *Entanglement entropy from one-point functions in holographic states*, *JHEP* **06** (2016) 085, [`1604.05308`].

[314] K. Hashimoto, S. Kinoshita, K. Murata and T. Oka, *Electric Field Quench in AdS/CFT*, *JHEP* **09** (2014) 126, [`1407.0798`].

[315] S. Amiri-Sharifi, H. R. Sepangi and M. Ali-Akbari, *Electric Field Quench, Equilibration and Universal Behavior*, *Phys. Rev.* **D91** (2015) 126007, [`1504.03559`].

[316] S. Amiri-Sharifi, M. Ali-Akbari, A. Kishani-Farahani and N. Shafie, *Double Relaxation via AdS/CFT*, *Nucl. Phys.* **B909** (2016) 778–795, [`1601.04281`].

[317] M. Ali-Akbari and F. Charmchi, *Holographic Equilibration under External Dynamical Electric Field*, *Phys. Lett.* **B773** (2017) 271–276, [`1612.09098`].

[318] S. de Haro, S. N. Solodukhin and K. Skenderis, *Holographic reconstruction of space-time and renormalization in the AdS / CFT correspondence*, *Commun. Math. Phys.* **217** (2001) 595–622, [`hep-th/0002230`].

Toegankelijke samenvatting

In de afgelopen eeuw hebben we veel voortgang geboekt met ons begrip van de bouwstenen van de natuur. Alles wat we om ons heen zien, inclusief wijzelf, bestaat uit moleculen, die weer bestaan uit atomen. Op hun beurt bestaan atomen uit nog kleinere bouwstenen, die protonen, neutronen en elektronen genoemd worden.

Sommige van zulke bouwstenen, zoals de protonen en elektronen, zijn elektrisch geladen. Door deze lading werkt er een elektrische kracht tussen zulke deeltjes. We begrijpen heel goed hoe deze elektrische kracht werkt, en het is redelijk makkelijk om voorspellingen te doen aan de hand van deze kracht. Met deze kennis kan je bijvoorbeeld heel goed uitrekenen wat het energieverbruik van een bepaald elektrisch apparaat zal zijn.

Eén van de redenen waarom we de elektrische kracht goed begrijpen is dat deze kracht over het algemeen vrij zwak is. Positief en negatief geladen deeltjes trekken elkaar aan, maar over het algemeen kunnen we goed onderscheid maken tussen de individuele deeltjes. Sommige krachten zijn vele male sterker dan de elektrische kracht. Deeltjes die gevoelig zijn voor zulke krachten worden zo sterk tot elkaar aangetrokken dat ze over het algemeen samengeklonterd zijn tot één geheel.

Hierdoor had men lange tijd niet door dat protonen en neutronen zelf óók bestaan uit nog kleinere bouwstenen, die bekend staan als quarks. De kracht tussen deze quarks is onder normale omstandigheden enorm groot, waardoor het heel moeilijk is om ze te onderscheiden in de protonen en neutronen in de materie om ons heen. Zulke deeltjes worden ook wel *sterk gekoppeld* genoemd: eenmaal samen is het haast onmogelijk om ze uit elkaar te krijgen.

Er bestaat een heel goede theoretische beschrijving (in de natuurkunde ook vaak simpelweg een *theorie* genoemd) van de materie die we om ons heen zien. Deze theorie staat ook welk bekend als het Standaardmodel. De gebruikelijke methodes van de theoretische natuurkunde zijn echter vooral geschikt voor theorieën die *zwak* gekoppelde deeltjes beschrijven, zoals elektrisch geladen deeltjes. Hierdoor is het heel moeilijk om voorspellingen te doen over bijvoorbeeld het ontstaan en het gedrag van atoomkernen, die bestaan uit sterk gekoppelde quarks.

Door protonen met enorme snelheden tegen elkaar te laten botsen kunnen we de quarks waaruit ze bestaan tijdelijk uit elkaar krijgen. Dit gebeurt bijvoorbeeld in de Large Hadron Collider (LHC) in Genève. Hierdoor is het kortstondig mogelijk om de beschrijving van quarks in het Standaardmodel te testen met onze gebruikelijke methodes, en de theorie heeft al deze experimentele testen tot nu toe glansrijk doorstaan. We zijn echter nog niet klaar: als we ook buiten de

LHC willen begrijpen hoe atomen in elkaar steken, moeten we de wereld van sterk gekoppelde deeltjes beter begrijpen.

Het holografisch woordenboek

Ook in de natuurkunde komen nieuwe inzichten soms uit onverwachte hoek. Zo'n twintig jaar geleden was er een enorme ontwikkeling in de snaartheorie, een tak van de natuurkunde die ons in staat stelt om theorieën zoals het Standaardmodel in contact te brengen met zwaartekracht. Hier ontdekte de Argentijnse natuurkundige Juan Maldacena dat bepaalde theorieën van sterk gekoppelde deeltjes in zekere zin *equivalent* zijn aan bepaalde zwaartekrachtstheorieën.

Eén van de wonderlijke aspecten van deze ontdekking is dat de zwaartekracht in een hogere dimensie blijkt te leven dan de sterk gekoppelde deeltjes die hij beschrijft. Om die reden staat de ontdekking van Maldacena ook wel bekend als *holografie*. Hiermee wordt verwezen naar hologrammen zoals die op je bankpas: ze lijken er driedimensionaal uit te zien als je er op de juiste manier naar kijkt, terwijl de bankpas zelf plat is. Op dezelfde manier geeft de holografie van Maldacena ons een methode om sterk gekoppelde deeltjes te interpreteren in termen van zwaartekracht in een hogere dimensie.

Je kunt over deze ontdekking nadenken als een *woordenboek* tussen twee verschillende talen. Als een ware Steen van Rosetta heeft het holografisch woordenboek ons in staat gesteld om verbanden te leggen tussen onze ogenschijnlijk totaal verschillende theorieën over zwaartekracht en sterk gekoppelde deeltjes. Sinds deze ontdekking is een groot deel van de natuurkundige gemeenschap bezig geweest met het uitbreiden en preciezer maken van de vertalingen van dit woordenboek. Vragen die in één taal van het woordenboek zo goed als onoplosbaar leken, zijn in de andere taal soms haast kinderlijk eenvoudig te beantwoorden.

In hoofdstuk 5 van dit proefschrift wordt gebruik gemaakt van zo'n vertaling uit het holografisch woordenboek. Daarin onderzoeken we hoe zwaartekracht gebruikt kan worden om de reactie van sterk gekoppelde systemen op bijvoorbeeld een harde klap te beschrijven. Het is haast onmogelijk om zulke gewelddadige verstoringen van het evenwicht van een sterk gekoppeld systeem met de gebruikelijke methodes te beschrijven. Het blijkt echter dat met behulp van de taal van zwaartekracht heel eenvoudige en algemene antwoorden op zulke vragen gegeven kunnen worden.

Trillende trommelvellen en driedimensionale zwaartekracht

Een groot deel van dit proefschrift gaat over een bepaald onderdeel van het holografisch woordenboek. Het blijkt dat zwaartekracht in sommige gevallen simpeler werkt dan in de wereld zoals wij die zien. In het alledaagse leven merken we drie ruimtedimensies: voor en achter, links en rechts, omhoog en omlaag. Einstein leerde ons dat we over de tijd moeten nadenken als de vierde dimensie, dus in totaal leven we in een vierdimensionale *ruimtetijd*.

In de theorie van Einstein is de zwaartekracht een gevolg van de kromming van deze ruimtetijd, die in ons geval vierdimensionaal is. Wiskundig gezien is het echter geen enkel probleem om zwaartekracht te bestuderen in een willekeurig

aantal dimensies. Sterker nog, de zwaartekrachtstheorie van Einstein blijkt veel makkelijker te worden als het gaat om een *driedimensionale* ruimtetijd.

Een driedimensionale ruimtetijd beschrijft twee ruimtedimensies. Je kan hierover nadenken als het vel van een trommel: daar kan bijvoorbeeld een kleine mier naar links en rechts en naar voor en achter over lopen. In die zin heeft het trommelvel twee ruimtedimensies. Als je de trommel met rust laat, beweegt het vel niet: het staat gespannen in een bepaalde positie doordat het aan de rand van de trommel bevestigd is.

Het vel kan echter ook trillen als je er een klap op geeft. Dit brengt een geluid voort zoals je dat kent van bijvoorbeeld een trommel in een drumstel. Elke trommel klinkt echter een beetje anders. Dat komt doordat de mogelijke trillingen van een trommelvel worden bepaald door de vorm van de trommel. Om precies te zijn: elk trommelvel kan op meerdere manieren trillen. Elk van deze trillingen leidt tot een andere toon, en de vorm van de trommel bepaalt welke van deze tonen het meest tot uiting komen. Je kan experimenteel vaststellen hoe een trommel klinkt door er gewoon eens op te slaan, maar als je de vorm van een trommel kent kan je zijn klank ook voorspellen!

Het blijkt dat de zwaartekrachtstheorie van Einstein zich voor een driedimensionale ruimtetijd net zo gedraagt. In dat geval kan de ruimte net als het vel van een trommel weinig kanten op: zodra je de vorm van de *rand* van de ruimte vastlegt wordt de rest van de ruimte daartussen opgespannen.

Net als een trommelvel kan je de driedimensionale ruimtetijd ook laten trillen. Natuurlijk kan je hier niet zo makkelijk een experiment mee uitvoeren als met een echte trommel, maar de wiskundige berekeningen lijken verrassend veel op elkaar. Hoofdstuk 2 van dit proefschrift gaat over methodes en technieken om de verschillende tonen in de klank van zulke driedimensionale ruimtetijden te bepalen.

Zulke tonen uit de driedimensionale zwaartekracht blijken ook een bijzondere rol te spelen in de andere taal van het holografisch woordenboek. Deze zwaartekrachtstonen vertellen ons met welke klasse van sterk gekoppelde theorieën we te maken hebben. Kennis van de mogelijke tonen en hun onderlinge samenspel stelt ons zo in staat om in één klap vrij veel te weten te komen over de sterk gekoppelde kant van het holografisch woordenboek.

Andere edities van het holografisch woordenboek

Om die reden is het bestuderen van zulke trillingen in driedimensionale ruimtetijd een goede manier om mogelijke uitbreidingen van het holografisch woordenboek te vinden. Het oorspronkelijke woordenboek geeft ons een heel precieze vertaling, maar wel tussen een vrij beperkte klasse aan theorieën. Hierdoor is het soms moeilijk te bepalen of het succes van het oorspronkelijke woordenboek een éénmalige meevaller is.

Om die reden is het interessant om te kijken of er variaties op het oorspronkelijke woordenboek mogelijk zijn. Kunnen we nog steeds vertalingen vinden als we één van de talen vervangen door een ander dialect, of zelfs door een geheel andere taal? Door zo aan de boutjes en moeren van het holografisch woordenboek

te sleutelen hopen we erachter te komen welke fundamentele principes aan het bestaan van zulke woordenboeken ten grondslag liggen.

In hoofdstuk 3 van dit proefschrift worden de trillingen van een ander soort ruimtetijd onderzocht. In zekere zin zijn deze ruimtetijden een beetje ouderwets: ze lijken meer op hoe ons begrip van zwaartekracht vóór Einstein eruit zag. Alhoewel sommige van onze moderne methodes dus niet direct van toepassing zijn, is het dus goed mogelijk dat het bestuderen van zo'n ouderwetse vorm van zwaartekracht ons iets leert over het hoe en waarom van het holografisch woordenboek.

De Alday–Gaiotto–Tachikawa-correspondentie

Hoofdstuk 4 van dit proefschrift gaat niet over holografie, maar over een andere wonderbaarlijke relatie tussen twee ogenschijnlijk verschillende delen van de natuurkunde. Deze relatie is ontdekt door de Argentijnse, Italiaanse en Japanse natuurkundigen Luis Fernando Alday, Davide Gaiotto en Yuji Tachikawa en staat daarom bekend als de *AGT-correspondentie*.

Waar het holografisch woordenboek ons in staat stelt om sterk gekoppelde systemen te beschrijven in termen van zwaartekracht met één extra dimensie, relateert de AGT-correspondentie theorieën met twéé dimensies verschil. Deze theorieën bevatten bovendien geen van beiden zwaartekracht.

Zoals eerder beschreven zien we vier dimensies in de wereld om ons heen: drie ruimtedimensies en één tijdsdimensie. Het Standaardmodel is daarom ook een vierdimensionale theorie, waarin bepaalde deeltjes sterk gekoppeld en dus moeilijk te beschrijven zijn. Het is mogelijk om wiskundige 'trucs' uit te halen om deze theorieën overzichtelijker te maken. De bekendste daarvan gaat uit van het bestaan van een extra symmetrie, die ook wel *supersymmetrie* genoemd wordt. (Er zijn ook verschillende natuurkundige argumenten die voor de aanwezigheid van zulke supersymmetrie pleiten. De nieuwe deeltjes die zulke symmetrieën voorspellen zijn echter tot op heden nog niet waargenomen.)

Vierdimensionale theorieën over supersymmetrische materie bestaan al enige tijd, maar de laatste twintig jaar is men zulke theorieën steeds beter en systematischer gaan begrijpen. Zo is het bijvoorbeeld duidelijk geworden dat veel van zulke theorieën op een gestructureerde manier in elkaar zitten. Net als de atomen en moleculen die ze beschrijven kan je zulke theorieën zélf beschouwen als een collectie van enkele fundamentele bouwstenen. De instructies voor het in elkaar zetten van deze bouwstenen worden gegeven in termen van een tweedimensionaal object, wat er bijvoorbeeld uit kan zien als een donut.

Alday, Gaiotto en Tachikawa beseften dat zo'n donut niet alleen als bouwtekening dient voor het in elkaar zetten van een vierdimensionale theorie. Zij merkten op dat veel voorspellingen van een bepaalde klasse vierdimensionale supersymmetrische theorieën tevens te interpreteren zijn als voorspellingen van een zeker soort tweedimensionale theorie. Net als het holografisch woordenboek werd hierdoor een woordenboek samengesteld, maar nu tussen vier dimensies en twee dimensies!

Alhoewel er nog veel te ontdekken valt, zijn er goede argumenten te geven voor het bestaan voor het holografisch woordenboek. Het *4d-2d woordenboek* van de AGT-correspondentie kwam echter in zekere zin uit de lucht vallen: destijds was er geen achterliggend principe bekend wat deze wonderbaarlijke relatie mogelijk maakte. Er waren weinig twijfels over de juistheid van het woordenboek, maar de achterliggende principes waren minder goed te verklaren.

Enkele jaren geleden stelden Clay Córdova en Daniel Jafferis, twee Amerikaanse natuurkundigen, een programma op waarmee deze mysterieuze relatie te verklaren zou zijn. Ze opperden het idee om de vierdimensionale en tweedimensionale werelden samen te voegen tot een zesdimensionaal geheel. Vanuit dit overkoepelend perspectief konden vervolgens de twee elementen van het 4d-2d woordenboek worden bereikt door de resterende dimensies samen te drukken.

Een deel van dit programma heeft een verrassende overlap met de methodes en technieken om driedimensionale ruimtetijden te bestuderen die in hoofdstuk 2 besproken worden. Hierdoor kwamen we op het idee om te kijken of we de afleiding van de AGT-correspondentie door Córdova en Jafferis konden uitbreiden naar andere theorieën. Tevens bleek dat het bestuderen van zulke uitbreidingen ons hielp om de oorspronkelijke afleiding beter te begrijpen.

Hoe nu verder?

Alle resultaten die beschreven zijn in dit proefschrift zijn in zekere zin kleine stapjes op weg naar een groter doel. Het hebben van zulke woordenboeken, die ook wel bekend staan als *dualiteiten*, helpt ons om sterk gekoppelde theorieën beter te begrijpen. Het zou fantastisch zijn als deze inzichten gebruikt kunnen worden om betere voorspellingen over het gedrag van de atomen om ons heen te maken. Waar de scheikunde grotendeels is gebouwd op ons begrip van de elektrische kracht, zou een beter begrip van de sterke krachten in atoomkernen de wereld op een dag hopelijk ook ten goede kunnen veranderen.

Anderzijds hopen we ook meer te leren over de fundamentele eigenschappen van zwaartekracht. In december 2015 zijn voor het eerst zwaartekrachtsgolven op aarde waargenomen. Deze rimpelingen van de ruimtetijd stellen ons in staat om met een geheel nieuwe blik naar het heelal te kijken. Hierdoor zou het goed kunnen dat oplossingen van enkele van de vele raadsels over zwaartekracht in de komende jaren binnen het bereik van de wetenschap gaan komen.

Acknowledgments

First of all, my deepest gratitude goes to Diego. You've taught me so much about physics, about life, and about what it means to be a scientist. Thank you for all the opportunities and support you gave me. Erik, thank you for your help in finishing this thesis and for those small peeks at far-reaching views over the long roads of string theory we have yet to walk.

Next, I want to thank my family. Marijke, Joan and Michiel, over so many years you have all contributed so much to making this possible. Thank you for your unwavering support.

An almost equally enormous debt is owned to those who have been there from the very beginning. Sjoerd, Bart, Jelle B., from the mean streets of Beverwijk you've helped me along this road in more ways than I could have ever imagined. Jaap, thank you for your boundless enthusiasm about mathematics and music. Jorian, Eliane, Lotte K., Sam V., Nick F., Jorrit, Nick M. and Pieter P., thank you for the good times at the Dapperplein and KNSM-Laan.

Manus, Vincent de B., Jasper R. and Sjoerd, the original quatrumviraat plus, you were there when all this started off for me. Thanks for all those mornings, days, and long evenings at the Roeterseiland. (And thanks to Vincent for the coffee machine, we put it to good use.) Thanks also to Niek, Felix, Abel and Marcus, Bart L. and Jaco.

Sjoerd and Manus, I'm honored to have you by my side at the defence.

My time in Berlin on and off the Freie Universität would not have been the same without Chris, Camille, Mathilde, Marie, Matthias, Henrik and Vincent de B. Max, Vinno, Christian, thanks for a warm welcome and a wonderful place to live. Likewise, Cambridge would have been a mere shadow of itself were it not for the color that Andries, Viraj, Andrea and Sara were able to bring to those long days of revision. It was also a pleasure to meet Benjamin, Omar, Wicher, Massi and especially Johnny. He will be sorely missed by many. At Hughes Hall, I was lucky enough to meet Dion, Jasper van S., Greg F., Miranda A., Xavier and Pavel anywhere between those wonderful cold morning rowing sessions and the cozy couches of Argyle Street.

Back in Amsterdam I found myself among the company of many fantastic people, new and old. Alex K., Jochem, Eva, Bernardo, Jimena, Angela, Bernat, Louise, Michael, it was a joy to meet you and learn from you. And to those who shouldered the past four years alongside me, made them more vibrant, richer and better than I could have ever imagined: Sam van L., Ido, Manus, Eva, Francesca,